THE UNIVERSITY OF QUEENSLAND

AUSTRALIA

Structural and Functional Characterisation of the Thrombopoietin Receptor and its Negative Regulator, LNK in Myeloid Malignancies

Christine Lee Mei Mei

(BSc. Hons, MRes)

S44197856

A thesis submitted for the degree of Doctor of Philosophy at

The University of Queensland in 2020

Faculty of Medicine, Diamantina Institute

Abstract

Thrombopoietin (TPO), by activating its cognate receptor, the thrombopoietin receptor (TPOR, also known as MPL), supports haematopoietic stem cell survival and expansion, megakaryocyte differentiation, as well as platelet and megakaryocyte production. LNK is an SH2-B adaptor protein that negatively regulates lymphohaematopoiesis by modulating various signalling pathways such as those mediated by TPOR. LNK can regulate downstream signalling by direct binding to the receptor and/or JAK2, a tyrosine kinase that is associated with the receptor and responsible for downstream signal transduction. In myeloproliferative neoplasms (MPNs) and leukaemia, various activating (oncogenic) mutations in TPOR and JAK2, as well as inactivating LNK mutations are frequently found. However, the mechanisms by which mutations in TPOR and LNK lead to these diseases is poorly understood. Further elucidation of the mechanism of JAK-STAT signal regulation by TPOR and LNK in normal haematopoiesis and blood cancers such as MPNs and leukaemia will be essential for understanding their role in disease and for developing novel targeted therapeutics. Particularly, the functional changes that occur in TPOR and the structural mechanisms that are used by LNK to regulate JAK-STAT signalling are key to this understanding.

This thesis employed a multi-disciplinary approach to gain a greater understanding of the mechanisms of activation and regulation of JAK-STAT and mitogen-activated protein kinases (MAPK) signalling by TPOR and LNK. Novel mutations in the transmembrane domain (TMD) of TPOR that result in constitutive signalling were characterised. Further, a peptide antagonist against the crucial signal-modulating domain (the extracellular domain-juxtamembrane (ECD-JM)/TMD) of TPOR was discovered using phage display and its functionality analysed in cell-based assays. By using single-particle tracking photoactivated localisation microscopy (sptPALM), the spatiotemporal dynamics of TPOR in live cell membranes was determined. The current study also determined the regions of LNK that may be important in contributing to inhibition of STAT and MAPK signalling, and revealed a novel role in regulating receptor levels. In addition, expression and purification of LNK for structural and biochemical assays were performed.

By employing sptPALM, the effect of cytokine stimulation on wild type TPOR and TPOR mutations (W515K and Box1Δ) on the lateral diffusion of TPOR were investigated. In the basal and stimulated states, TPOR exhibited bimodal mobility (fast and slow-moving receptor subpopulations). Upon ligand stimulation of TPOR or the TPOR mutant W515K that results in constitutive receptor activation, the mobility of the fast-moving subpopulation was significantly reduced and a fraction of

these receptors transitioned into the slow-moving subpopulation. This reduction in mobility may be related to the initiation or attenuation of signalling and this finding may elucidate the relationship between the mobility patterns of TPOR and different phases of cell signalling.

As part of a collaborative effort, every amino acid residue in the TPOR TMD was evaluated for their ability to result in constitutive proliferation in Ba/F3 cells in the absence of cytokine by using the deep mutational scanning approach. Four novel mutants were found to result in constitutive signalling (L498W, V501A, V501S, and L502S) indicating that these mutations may potentially drive myeloid malignancies. Indeed, some of these mutations were identified for the first time in patient samples by collaborators. In order to develop antagonists targeting constitutive active oncogenic TPOR mutants, peptides against the ECD-JM/TMD were discovered via phage display screening. The functionality of the peptides was assessed via cell-based assays using Ba/F3 TPOR WT and W515K mutant cell lines. Results suggest that peptide V may be acting as a peptide antagonist against the TPO/TPOR-mediated signalling pathway. Confirmation of peptide specificity to this pathway will allow for the peptide to be developed into a useful therapeutic agent by itself or to be used as a scaffold for the development of small molecules. This discovery may facilitate the development of improved targeted drugs to treat patients suffering from myeloid malignancies as a result of activating TPOR mutations.

In order to investigate the role of individual domains of LNK in regulating JAK2, various LNK domain deletions and point mutations were generated. All LNK expression constructs retained the SH2 domain required for JAK2 phosphorylated tyrosine binding. A novel function of the LNK proline dimerisation domain (Pro/DD) was found in mediating constitutive binding to TPOR with the LNK SH2 acting as the main anchor to bind to JAK2. These interactions prevent downstream signalling through a mechanism that has yet to be fully elucidated. The findings of the current study act as an important foundation for future work to increase the understanding regarding the structure-function of this important negative regulator of JAK2 signalling.

As the crystal structure of LNK is not currently available, there is still a lack of understanding towards its role as a negative regulator, in particular, for JAK signalling. Therefore, expression and purification of LNK for structural and biophysical studies were performed. Although LNK was able to be purified to a high level, sufficient quantities of soluble human LNK fractions that could be used for crystallisation studies were not able to be obtained. In the absence of LNK crystals, the purified protein could also be used for protein interaction studies and kinase activity assays. These investigations will allow better understanding regarding how LNK mutations may contribute to the different diseases.

Declaration by author

This thesis *is composed of my original work, and contains* no material previously published or written by another person except where due reference has been made in the text. I have clearly stated the contribution by others to jointly-authored works that I have included in my thesis.

I have clearly stated the contribution of others to my thesis as a whole, including statistical assistance, survey design, data analysis, significant technical procedures, professional editorial advice, financial support and any other original research work used or reported in my thesis. The content of my thesis is the result of work I have carried out since the commencement of my higher degree by research candidature and does not include a substantial part of work that has been submitted *to qualify for the award of any* other degree or diploma in any university or other tertiary institution. I have clearly stated which parts of my thesis, if any, have been submitted to qualify for another award.

I acknowledge that an electronic copy of my thesis must be lodged with the University Library and, subject to the policy and procedures of The University of Queensland, the thesis be made available for research and study in accordance with the Copyright Act 1968 unless a period of embargo has been approved by the Dean of the Graduate School.

I acknowledge that copyright of all material contained in my thesis resides with the copyright holder(s) of that material. Where appropriate I have obtained copyright permission from the copyright holder to reproduce material in this thesis and have sought permission from co-authors for any jointly authored works included in the thesis.

Publications included in this thesis

No publications included.

Submitted manuscripts included in this thesis

No manuscripts submitted for publication

Publications during candidature

Peer-reviewed paper

- Bridgford, J.L., Lee S.M., **Lee C.M.M.,** Guglielmelli P., Rumi E., Pietra D., Wilcox S., Chhabra Y., Rubin A.F., Cazzola M., Vannucchi A.M., Brooks A.J., Call M.E., Call M.J. (2019). Novel Drivers and Modifiers of MPL-dependent Oncogenic Transformation Identified by Deep Mutational Scanning, Blood.

Review article

- Dehkhoda, F., Medina, J.J., **Lee, C.M.M.,** Brooks, A.J. (2017). The Growth Hormone Receptor: Mechanism of Receptor Activation, Cell Signaling, and Physiological Aspects. Frontiers in Endocrinology, 9:35.

Conference presentations

Presenting author underlined

Christine M.M. Lee, Yash Chhabra, Andrew Perkins, and Andrew J. Brooks. Specific domains of LNK (SH2B3) bind and regulate TPOR stability and signalling. **Poster session presented at the 48th Annual Scientific Meeting International Society for Experimental Hematology**, Brisbane, Australia, 2019.

Christine M.M. Lee, Rob Luetterforst, Melissa J. Call, Matthew E. Call, Raphael Trenker, and Andrew J. Brooks. Development of peptides targeting constitutive active oncogenic thrombopoietin receptor (TPOR) mutants. **Poster session presented at the 2018 TRI Translational Research Symposium**, Brisbane, Australia, 2018.

Christine M.M. Lee, Rob Luetterforst, Melissa J. Call, Matthew E. Call, Raphael Trenker, and Andrew J. Brooks. Development of peptides targeting constitutive active oncogenic thrombopoietin receptor (TPOR) mutants. **Poster session presented at the 8th International Conference on Myeloproliferative Neoplasms**, Dublin, Ireland, 2018.

Christine M.M. Lee, Rob Luetterforst, Melissa J. Call, Matthew E. Call, Raphael Trenker, and Andrew J. Brooks. Development of peptides targeting constitutive active oncogenic thrombopoietin receptor (TPOR) mutants. **Poster session presented at the 8th Brisbane Cell and Developmental Biology Meeting**, Brisbane, Australia, 2017.

Christine M.M. Lee, Rob Luetterforst, Melissa J. Call, Matthew E. Call, Raphael Trenker, and Andrew J. Brooks. Development of peptides targeting constitutive active oncogenic thrombopoietin receptor (TPOR) mutants. **Poster session presented at the 8th Barossa Meeting (Cell Signalling in Cancer Medicine)**, Adelaide, Australia, 2017.

Christine M.M. Lee, Rob Luetterforst, Melissa J. Call, Matthew E. Call, Raphael Trenker, and Andrew J. Brooks. Development of peptides targeting constitutive active oncogenic thrombopoietin receptor (TPOR) mutants. **Poster session presented at the 8th International Postgraduate Symposium in Biomedical Sciences**, Brisbane, Australia, 2017.

Christine M.M. Lee, Rob Luetterforst, Melissa J. Call, Matthew E. Call, Raphael Trenker, and Andrew J. Brooks. Development of peptides targeting constitutive active oncogenic thrombopoietin receptor (TPOR) mutants. **Poster session presented at Combio conference**, Brisbane, Australia, 2016.

Contributions by others to the thesis

Contributor	**Statement of Contribution**
Andrew Brooks (principal supervisor)	Conception and design of projects, interpretation of research data
Yash Chhabra (associate supervisor)	Analysis and interpretation of signalling and co-immunoprecipitation (co-IP) data, conception and design of co-IP, making of some stable cell lines, assisting in some parts of signalling experiments
Nela Durisic	SptPALM training and analysis; chapter review
Rob Luetterforst	Robotic cell seeding, INCA cell counting
Steffi Cheung	Protein quality assessments and crystallisation, buffer condition optimisation

Statement of parts of the thesis submitted to qualify for the award of another degree

No works submitted towards another degree have been included in this thesis.

Research Involving Human or Animal Subjects

No animal or human subjects were involved in this research

Acknowledgements

First and foremost, I would like to thank my supervisor, Andrew Brooks, for his willingness to take me in as part of his lab. I always appreciate that you have been supportive, encouraging, and having confidence in me despite many experiments that went awry. I am also thankful for your understanding whenever I made countless mistakes. Thank you for providing many ideas and bringing me out of the dark when I am stuck, and for your endurance of reviewing such a long thesis!

I wish to express my gratitude to Yash, whom I call 'mama', for taking care of me inside and outside of the lab. You have been like a 'laboratory' mother to me. Thanks for pushing me to get me out of my comfort zone (something that I really needed) and for showering me with plenty of ideas to keep my PhD running. I am always grateful that you have believed in me and for highlighting my strengths. That really encourages me! I sincerely want to thank my two other associate supervisors, Dr Johan Medina and Professor Andrew Perkins for their advice and invaluable inputs.

I am also thankful to Kelin and Mabel for being in my lab life. Labs have been so much more fun with you girls around who kept me company till the late nights. Singing, laughing, and chatting in the lab with you both really made me enjoy my late-night experiments. Thank you for your encouragement even during my milestone and PhD journey.

I am indebted to Livia for all your valuable input and your knowledge. You were the first person who sat next to me when I started my PhD and I really enjoyed our time together in the lab. Thanks for listening to my frustrations and complains, and for putting up with my funny choice of music.

I would also like to appreciate all my other lab members whose name I have not mentioned. You are all as essential in making my PhD such joy despite all the struggles. Thank you all for your help and encouragements.

I also would like to acknowledge the financial support from the University of Queensland International Tuition Scholarship and Hardy Brothers Scholarship for Research in Blood Cancer.

I would sincerely like to thank my life group members, UQ5 and UQ6 (especially Abelyn, Tiffany, and Sandy) for being there to encourage me when I want to give up in this journey. Thanks, Joyce, my closest friend, although we are miles and miles apart, you are always there to listen to me and encourage me to not give up in finding a cure for cancer patients. I am also thankful to all the random people I have met in my life, telling me that this world needs more people like me, to help eradicate cancer.

Lastly, a big thank you to mum and dad for being so understanding and supportive, and for allowing me to pursue my passion. Thank you for visiting me yearly and making my life easier by helping me with different chores. A very big appreciation to my hubby who always knows the right words to say to encourage me to not give up when I am feeling low, and for such understanding and support to pursue my dream although we had to be apart for many years since my undergraduate. You have always brought out the best in me.

All praise be to God for placing such a wild dream in my heart to find a cure for cancer, and for miraculously bringing me to do this PhD and finishing the race and more to come.

I would like to dedicate this thesis in loving memory of my dad who passed away midway during the course of my PhD.

Financial support

This research was supported by the National Health and Medical Research Council (NHMRC), University of Queensland Research Higher Degree Scholarship, and University of Queensland Diamantina Institute Living Stipend Scholarship (Hardy Brothers Scholarship).

Keywords

thrombopoietin receptor, SH2B3, LNK, myeloproliferative neoplasm, leukaemia, signal transduction, JAK-STAT, structure, sptPALM

Australian and New Zealand Standard Research Classifications (ANZSRC)

ANZSRC code: 060111, Signal Transduction, 50%

ANZSRC code: 060110, Receptors and Membrane Biology, 40%

ANZSRC code: 060199, Biochemistry and Cell Biology not elsewhere classified, 10%

Fields of Research (FoR) Classification

FoR code: 0601, Biochemistry and Cell Biology, 100%

Dedications

To God who made all this possible, my late dad, my loving mum, and ever-supportive hubby.

“For I know the plans I have for you,” declares the Lord,

“plans to prosper you and not to harm you, plans to give you hope and a future.”

Jeremiah 29:11

Table of Contents

List of Figures

List of Tables

List of Abbreviations

AGRF	Australian Genome Research Facility
AMKL	acute megakaryoblastic leukaemia
AML	acute myeloid leukaemia
ANOVA	analysis of variance
AP2	adaptor protein 2
APS	adaptor protein with PH and SH2 domain
ATP	adenosine triphosphate
BCA	bicinchoninic acid
BHK	baby hamster kidney
BSA	bovine serum albumin
CALR	calreticulin
CAMT	congenital amegakaryocytic thrombocytopaenia
CBL	casitas b-lineage lymphoma
CCPs	clathrin-coated pits
CD	circular dichroism
CEL	chronic eosinophilic leukaemia
CFP	cyan fluorescent protein
CFU-MK	colony-forming unit megakaryocyte
CHO	chinese hamster ovary
Cit	citrine
CMC	critical micelle concentration
CML	chronic myeloid leukaemia
CMV	cytomegalovirus
CNL	chronic neutrophilic leukaemia
COase	cholesterol oxidase
Co-IP	co-immunoprecipitation
CPEC	circular polymerase extension cloning
CRHD	cytokine receptor homology domain
cryoEM	electron cryo-microscopy
CTD	c-terminal domain
CV	column volume

D	diffusion coefficient
DC-MSS	divide-and-conquer moment scaling spectrum
DDM	n-dodecyl-β-D-maltopyranoside
DLS	dynamic light scattering
DM	n-decyl-β-D-maltopyranoside
DMEM	dulbecco's modified eagle medium
DMS	deep mutational scanning
DSF	differential scanning fluorimetry
DTT	dithiothreitol
EC_{50}	effective concentration 50
ECD	extracellular domain
ECL	enhanced chemiluminescent
EDTA	ethylenediaminetetraacetic acid
EGFR	epidermal growth factor receptor
ELISA	enzyme-linked immunosorbent assay
EphB2R	ephrin type-b receptor 2
EPO	erythropoietin
EPOR	erythropoietin receptor
ER	endoplasmic reticulum
ERK	extracellular-signal-regulated kinase
ET	essential thrombocythaemia
FACS	fluorescence-activated cell sorting
FBN III	fibronectin III
FBS	foetal bovine serum
FERM	band 4.1, ezrin/radixin/moesin
FET	familial essential thrombocythaemia
FL	full-length
FLT3	fms-like tyrosine kinase 3
FRET	fluorescence resonance energy transfer
G-CSFR	granulocyte colony-stimulating factor receptor
GFP	green fluorescent protein
GH	growth hormone
GHR	growth hormone receptor
GM-CSF	granulocyte macrophage-colony stimulating factor

GPCR	g protein-coupled receptor
GST	glutathione-s-transferase
GW	gateway
HA	haemaglutinin
HEK293	human embryonic kidney
HeLa	Henrietta Lacks
HPCs	haematopoietic progenitor cells
HRP	horse radish peroxidase
HSC	haematopoietic stem cells
HTRF	homogeneous time resolved fluorescence
iAMP21	intrachromosomal amplification of chromosome 21
ICD	intracellular domain
IDPs	intrinsically disordered proteins
IFN	interferon
IFNAR1	interferon-alpha and beta receptor subunit 1
IFN-γ	interferon-γ
Ig	immunoglobulin
IGF	insulin growth factor
IL	interleukin
IMB	institute for molecular bioscience
INCA	in cell analyser
InsP6	inositol hexakisphosphate
IPTG	isopropyl β-d-1-thiogalactopyranoside
ITC	isothermal titration calorimetry
ITP	immune thrombocytopenic purpura
JAK	janus kinase
JH	jak homology
JM	juxtamembrane
KCl	potassium chloride
KDEL	endoplasmic reticulum retention signal
KE	kinase dead
KIR	kinase inhibitory region
LB	lysogeny broth
LDAO	n-lauryl dimethylamine n-oxide

LIFR	leukaemia inhibitory factor receptor
LTRs	long-terminal repeats
M	molar
MAPK	mitogen-activated protein kinases
MBP	maltose-binding protein
MDS	myelodysplastic syndrome
MF	myelofibrosis
Mg	magnesium
ml	millilitres
mM	millimolar
MNG	maltoside-neopentyl glycols
MOI	multiplicity of infection
MPL	myeloproliferative leukemia protein
MPLV	murine myeloproliferative leukaemia virus
MPN	myeloproliferative neoplasms
MPN-U	mpn-unclassifiable
MSD	mean squared displacement
NaCl	sodium chloride
NEB	new england biolabs
ng	nanogram
NGF	nerve growth factor
NK1R	neurokinin-1 receptor
nM	nanomolar
NMR	nuclear magnetic resonance
NTD	n-terminal domain
OG	octyl glucoside
OSM	oncostatin m
P2X7R	p2x purinoceptor 7
PBS	phosphate-buffered saline
PCR	polymerase chain reaction
PDGF	platelet-derived growth factor
PEG	polyethylene glycol
pfu	plaque forming units
PGK	phosphoglycerate kinase

PH	pleckstrin homology
pI	isoelectric point
PI3K	phosphoinositide 3-kinases
PIAS	protein inhibitor of activated stat
PIP2	phosphatidylinositol 4,5-bisphosphate
PKC	protein kinase c
PP	pyrolopyrimidine
PRLR	prolactin receptor
Pro/DD	proline dimerisation domain
PSM	proline-rich, ph and sh2 domain-containing signalling mediator
PTB	phosphotyrosine-binding
PTP1B	tyrosine-protein phosphatase non-receptor type 1
PTPN1	protein tyrosine phosphatase, non-receptor type 1
PTPs	protein phosphatases
PV	polycythaemia vera
PVDF	polyvinylidene fluoride
RAGE	receptor for advanced glycation end products
RGB	red green blue
rhTPO	recombinant human tpo
RIPA	radioimmunoprecipitation assay
RPMI	Roswell Park Memorial Institute
SAXS	small angle x-ray scattering
SCF	stem cell factor
SDS-PAGE	sodium dodecyl sulphate-polyacrylamide gel electrophoresis
SEC	size exclusion chromatography
SEM	standard error of mean
SFK	src family kinases
SH2	*src homology 2*
SHP	SH2 domain-containing phosphatase
siRNA	small interfering ribonucleic acid
SOCS	suppressor of cytokine signalling
sptPALM	single-particle tracking photoactivated localisation
STAT	signal transducer and activator of transcription

SUMO	small ubiquitin-like modifier
TAE	tris-acetate EDTA
T-ALL	T-cell acute lymphoblastic leukaemia
TBS	tris-buffered saline
TBST	tris buffered saline -tween
TCEP	tris(2-carboxyethyl)phosphine
TCR	T-cell receptor
TEMED	n,n,n'-tetra-methylethylenediamine
TEV	tobacco etch virus
TIRF	total internal reflection fluorescence
TKB	tyrosine kinase binding
TM	transmembrane
TMD	transmembrane domain
TNFR	tumour necrosis factor receptor
TPO	thrombopoietin
TPOR	thrombopoietin receptor
tr	truncation
TRH	thyrotropin-releasing hormone
TrkA	tropomyosin receptor kinase a
TSLPR	thymic stromal lymphopoietin receptor
TYK2	tyrosine kinase 2
WCL	whole cell lysate
µg	microgram

Chapter 1

Literature Review

1.1 Haematopoiesis

Haematopoiesis is the process of formation, development, and differentiation of blood cellular components (Figure 1). All blood cells arise from haematopoietic stem cells (HSCs) (pluripotent cells) that are usually maintained in a quiescent state but can self-renew and differentiate. These processes must be maintained in equilibrium to maintain the stem cell pool. The induction of proliferation and differentiation of cells of the haematopoietic system occurs with the direction of cytokines and their cognate receptors whereby different cell types express unique combinations of receptors and can respond to myriads of cytokines. Deregulation of haematopoiesis can occur due to mutations in the receptors and their signalling partners which may lead to enhanced cell growth, proliferation, and survival of HSC derived cells. As a result, myeloid malignancies such as leukaemia and MPNs can develop.

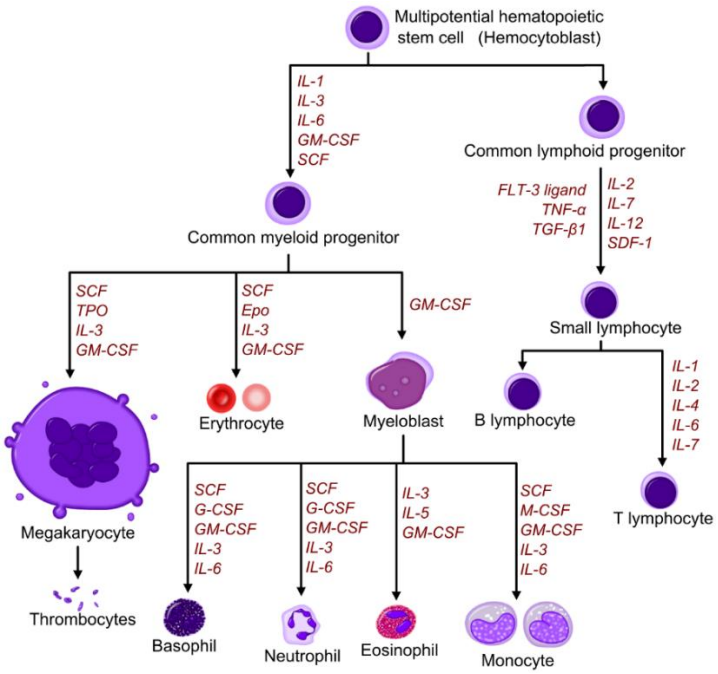

Figure 1: Haematopoiesis.

The process of differentiation of HSCs into various haematopoietic progenitor cells (HPCs) and mature blood cells. Image reproduced from Wikipedia [1].

1.2 Myeloproliferative neoplasms

MPNs are myeloid neoplasms that arise due to elevated levels of mature erythrocytes, leukocytes, and/or megakaryocytes as a result of clonal expansion. Progression of the disease can lead to acute myeloid leukaemia (AML). Although the majority of MPNs occur in adults, this disease has also been reported in children. MPNs can be divided into two major categories depending on whether the patients harbour the BCR-ABL1 fusion gene. Chronic myeloid leukaemia (CML) is classified as Philadelphia (Ph)-positive MPN whereas Ph-negative MPN includes polycythaemia vera (PV), essential thrombocythaemia (ET), myelofibrosis (MF), chronic eosinophilic leukaemia (CEL), chronic neutrophilic leukaemia (CNL), and MPN-unclassifiable (MPN-U) [2]. PV, ET, and MF are classed as classic MPNs as they are the most common. PV is distinguished by erythrocytosis, ET is characterised by thrombocytosis, whereas MF patients exhibit thrombocytosis and bone marrow fibrosis. BCR-ABL1-negative MPNs occur as a result of mutations in three main driver genes that encode proteins such as Janus Kinase 2 (JAK2) [3-17], TPOR/MPL, and calreticulin (CALR) [18]. All these proteins are involved in the TPOR signalling pathway and hence can influence thrombopoiesis and megakaryopoiesis. Driver mutations in MPNs can co-operate with mutations in other genes such as those involved in epigenetic regulation, splicing, and signalling. About 10-15% of ET/MF patients are diagnosed as triple-negative where they do not possess mutations in any of the three main driver genes of MPN [18]. These patients have mutations in the genes encoding the LNK, CBL, and other proteins [19-21]. Mutations in LNK and CBL comprise approximately 5-7% of MPN patients [22, 23]**.** These mutations may also occur with JAK2 mutation [24-28]**.** Most MPNs are sporadic but familial MPNs which contribute to approximately 7-8% of MPN cases have also been reported [29, 30]. Driver mutations in these familial MPNs arise from somatic mutations [29, 31, 32].

1.2.1 JAK2 mutations

In MPNs, JAK2 is highly mutated and this mutation is most prevalent in PV (95%) and to a lesser extent in ET and MF patients (50-60%) [3-5, 33]. JAK2 mutations have also been reported in leukaemic patients [14, 33]. Most mutations of this gene are clustered in or are adjacent to the proposed interface formed between the pseudokinase domain and the kinase domain [34], for example the commonly known $JAK2^{V617F}$ (located in the pseudokinase domain) [3-5] as well as JAK2 exon 12 mutations (located at the start of the pseudokinase domain, residues 536 to 547) such as the $JAK2^{K539L}$ mutation [35, 36]. JAK2 exon 12 mutations can co-occur with $JAK2^{V617F}$ [35, 37].

Intriguingly, the same JAK2^{V617F} mutation can result in three different diseases (PV, ET, and MF). This is hypothesised to be due to the amount of mutant allele burden present in the patients [19]. In mice, the homozygous mutation can result in PV from an ET-like phenotype [38]. A previous study found that constitutively active JAK2 mutants can preferentially associate with certain cytokine receptors with different binding affinities, and may also differently affect their tyrosine phosphorylation [39]. As a consequence, downstream signalling pathways are varyingly affected which results in the different phenotypic variations of MPN [39].

1.2.2 TPOR mutations

Activating TPOR mutations have been reported in 1-4% of ET (4, 6, 8-11) and 5-11% of MF patients [40-42]. The most common gain-of-function TPOR mutations are the W515K/L mutations [40, 43] with W515L being the most frequently reported (60-80%), and less common activating mutations include the S505N, and W515A/R mutations [40, 41, 44]. TPOR mutations such as W515K/L can co-occur with JAK2^{V617F} [40, 43]. When bone marrow cells that harbour oncogenic TPOR mutations were transplanted into mice, these mice developed a MPN-like phenotype [43].

The expression level of TPOR is downregulated in the platelets and megakaryocytes of PV and MF patients [45] regardless of driver mutations [45-48]. Besides the downregulation of receptor expression, in these patients, TPOR is vulnerable to digestion by the endoglycosidase H enzyme leading to under-glycosylation and reduced cell surface localisation [45, 49, 50]. The low levels of TPOR expression induce megakaryocyte production by the HPCs [51] which results in the thrombocytic phenotype of patients with MPNs [52, 53].

1.2.3 CALR mutations

CALR is a calcium buffering chaperone protein that contains a negatively charged C-terminal tail that can bind to calcium ions. It retains newly glycosylated proteins in the endoplasmic reticulum (ER) until these proteins have achieved a proper folding conformation [54]. CALR mutations have been described in ~25% of ET patients and 35% MF patients [18, 55]; which includes insertions and deletions. Mutated CALR proteins acquire a novel C-terminal tail as a result of the frameshift mutation [18, 55]. This truncated C-terminal tail destroys the ER retention signal (KDEL) which results in the protein localising to another area in the cell. However, only two CALR mutations are

tightly associated with MPNs, the CALRdel52 and CALRins5. These mutations confer an ET-like disease in mice [56]. Mutation in CALR may influence the progression of an ET to MF [47, 56-59]. However, the pathogenesis of CALR requires binding to TPOR [18, 47, 60]. Mutant CALR is speculated to exert its effects by locking the receptor in an active conformation [61]. Amongst all the type I and II cytokine receptors, only TPOR is able to confer constitutive activation by CALR mutants. It was shown that the mutated CALR protein only associates with TPOR and not EPOR [47] as the introduction of mutant CALR into mice only results in thrombocytosis and not erythrocytosis [47].

1.3 Type I cytokine/haematopoietin receptors

Type I cytokine receptors also known as haematopoietin receptors play important roles in haematopoiesis and immunity. They are the largest family of all cytokine receptors [62, 63] and include the growth hormone receptor (GHR), prolactin receptor (PRLR), erythropoietin receptor (EPOR), and the thrombopoietin receptor (TPOR/ c-MPL). The sequence homology amongst the members is, however, low [64]. Nevertheless, they share structural similarities (Figure 2). Type I cytokine receptors are single-pass transmembrane (TM) spanning receptors and are composed by three main structures: the ECD where the amino terminus of the receptor resides, the intracellular domain (ICD) where the carboxy terminus of the receptor resides, and the TM domain that is anchored in the hydrophobic cell membrane, separating the ECD and ICD.

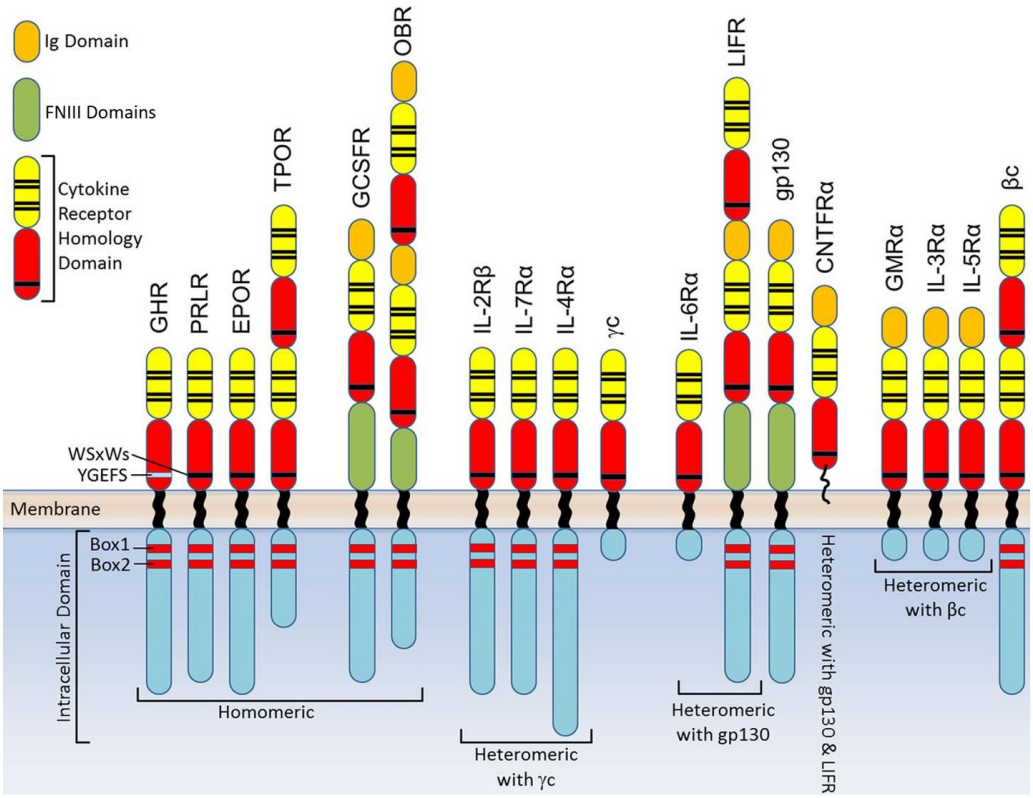

Figure 2: Haematopoietin receptors domain structure.

The figure shows the domain structures for both homomeric and heteromeric receptors (with their corresponding shared receptor unit i.e. gp130, βC, γC, and leukaemia inhibitory factor receptor (LIFR)). Figure reproduced from [65].

The ECD of type I cytokine receptors possesses at least one cytokine receptor homology domain (CRHD) which is responsible for ligand-receptor interaction. The CRHD is approximately 200 amino acids long [64, 66, 67] and consists of two fibronectin type III folds (FBN III). Similar to the immunoglobulin (Ig) domain fold, these folds are made up of β-sheets stacked together. The first FBN III fold is where four conserved cysteine residues reside, linked by disulphide bonds. These cysteine residues are important for maintaining receptor structure-function. The second FBN III fold has the conserved, consensus WSXWS motif (except for GHR where the motif is YGEFS) [64, 68] that is located at the C-terminus of the CRHD. The WSXWS is a consensus motif for C-mannosylation which is a post-translational modification where a mannose is added to a tryptophan residue via a C-C bond. This consensus sequence is important for maintaining receptor structure and expression [69] but is not involved in cytokine binding. For simple receptors such as GHR [70] and EPOR [71], one CRHD is sufficient for cytokine-binding but TPOR possesses two CRHD. Other

receptors may be equipped with additional features such as the Ig-like domain and extra FBN domains to facilitate cytokine-induced signalling [72, 73].

The CRHD also possesses a binding site (consisting mainly of loops) for the cytokine. Cytokines that bind type I receptors share a common protein structure, known as the 'four-helix bundle' consisting of four amphipathic α-helixes. The hydrophobic part of the helixes makes up the core of the bundle whereas the hydrophilic part of the helixes surrounds the core and is in contact with the aqueous environment. These helixes are arranged in an up-up-down-down topology and are connected by three loops (long-short-long) [62, 64]. Class I haematopoietic cytokines can be classified based on their helix length: short or long-chain cytokines. Short-chain cytokines are approximately 10-20 amino acids long and include interleukin (IL)-2 and IL-4, whereas long-chain cytokines are approximately 20-30 amino acids long and include the thrombopoietin (TPO), erythropoietin (EPO), growth hormone (GH), and IL-6-like cytokines [74].

The intracytoplasmic domain of type I cytokine receptors is where the Box1 and Box2 conserved motifs are located. The Box1 motif usually resides within 30 amino acid residues from the TM domain [75] and its consensus sequence is identified by proline residues that are spaced by two 'X' amino acids whereas Box2 is comprised mostly of serine and glutamic acid residues and lies approximately 35 to 60 residues downstream of the TM domain [75]. The ICD of cytokine receptors has low sequence homology apart from the Box 1 and Box 2 motifs although these motifs are also not well conserved between members of the type I cytokine receptor family. However, they are important for mediating Janus kinase (JAK) - signal transducer and activator of transcription (STAT) signalling [75, 76].

Type I cytokine receptors are either homomeric or heteromeric (Figure 2). Homomeric receptors include the GHR, PRLR, EPOR, and TPOR which have a single ligand-binding, signal-transducing subunit but require receptor homodimerisation to activate signal transduction. Heteromeric receptors, on the other hand, are comprised of at least two receptor subunits. Examples of heteromeric receptors are the granulocyte macrophage-colony stimulating factor (GM-CSF), IL-3, and IL-5 receptors that form heterodimers with the common β subunit, the IL-6, IL-11, IL-12, IL-27, oncostatin M (OSM), and LIFR that form heterodimers with the common gp130 subunit; and the IL-4, IL-7, IL-9, IL-13, and IL-15 receptors that form heterodimers with the common γ subunit. These common subunits are responsible for transducing the signal received as a result of cytokine binding.

1.4 JAK family of tyrosine kinases

Unlike many other receptor families, type I cytokine receptors do not possess intrinsic kinase activity. Hence, they require association with tyrosine kinases such as JAKs. JAKs are non-receptor tyrosine kinases that are located intracellularly. They act as signal mediators of cytokine and hormone signalling using by activating the STAT pathway that is important for modulating haematopoiesis, cell growth, cell metabolism, as well as adaptive immunity. The JAK family consists of JAK1, JAK2, JAK3, and tyrosine kinase 2 (TYK2) and its members are approximately 1150 amino acids long. JAK1, JAK2, and TYK2 are ubiquitously expressed [77, 78], whereas JAK3 is mostly expressed in haematopoietic cells and tissues [79, 80]. JAK family members possess seven homologous domains (JAK homology domain (JH) 1 to JH7) (Figure 3).

JH1 is a kinase domain that is located near the C-terminus, spanning residues 849-1124. The kinase domain crystal structures have been solved for all JAK members [81-84]. It consists of three loops, namely the activation, catalytic and nucleotide-binding loop. The Y1007 and Y1008 residues of JAK2 that are located in the activation loop and are phosphorylated upon activation. However, only the phosphorylation of Y1007 appears important for kinase activation as the mutation of Y1007 but not Y1008 to phenylalanine negatively affects kinase activity [85]. Phosphorylation of Y1007 may trigger kinase activation by the elimination of steric constraints in the inactive JAK [86]. Phosphorylated Y1007 has also been reported to bind other proteins such as suppressor of cytokine signalling 1 (SOCS1; negative regulator) [87] and acts as a substrate for protein tyrosine phosphatase, non-receptor type 1 (PTPN1) [88]. Competitive adenosine triphosphate (ATP) binding pocket inhibitors that are used clinically, target this JH1 domain.

Adjacent to JH1 is the JH2 pseudokinase domain that spans residues 545 to 808 (Figure 3). So far, the pseudokinase domain crystal structures have been solved for JAK1, JAK2, and TYK2 [34, 89, 90]. JH2 has two lobes, the N- and C-lobe [90]. The C-lobe is made up of α-helices whereas the N-lobe has five strands of β-sheets and an α-helix (αC) [90]. Interestingly, Y1007 of the constitutively active $JAK2^{V617F}$ (that resides in the pseudokinase domain) undergoes continuous phosphorylation. Unlike its name, previous findings suggested that JH2 does exhibit some level of kinase activity [91]. JH2 was found to acquire both serine and tyrosine kinase activity and it phosphorylates residues S523 (located in the Src homology 2 (SH2)-JH2 linker) and Y570 (located in the β2-β3 loop of JH2) (Figure 3), both of which are negative regulatory sites, to maintain JAK2 in a basal state in the absence of cytokine binding [92-96]. However, JH2 kinase activity is limited and this can be attributed to its structure. Although JH2 adopts a prototypical kinase fold, it binds magnesium (Mg)-ATP in an atypical manner [90]. Compared to JH1, JH2 has a shorter activation loop ending with an α-helix that

is not able to be phosphorylated, and a longer loop between the β7 and β8 strands [90]. JH2 is also deficient of certain residues in JH1 that are important for catalysis [90].

The SH2-like and band 4.1, ezrin/radixin/moesin (FERM) domains of JAK2 corresponds to JH3 to JH7 domains located at the N-terminus of each JAK [97, 98] (Figure 3). Thus far, the FERM-SH2 domain crystal structures of TYK2, JAK2, and JAK1 have been determined. The structures revealed that these domains are tightly associated with each other [99-101]. Using these domains, JAK binds to their associated receptor cytoplasmic domains (at the Box 1 and Box 2 motifs) to form the JAK-receptor complex. The FERM domain is pivotal for regulating JAK activity [102, 103]. JAK2 mutations that impair its ability to bind to the receptor have been mapped to residues in the hydrophobic core of the FERM domain and are proposed to cause a disturbance in the tightly associated FERM-SH2 structure leading to a decrease in stability of these domains.

The SH2 domains of JAKs are unusual in that they are unable to recognise phosphotyrosine residues [76, 104, 105] unlike typical SH2 domains and may act as scaffolds instead [106, 107]. It was discovered that the canonical phosphotyrosine-binding pocket in the JAK SH2 domain is inhibited by the presence of a bulky hydrophobic residue (for example, phenylalanine in JAK2) in place of a less bulky polar or hydrophobic residue [99]. An earlier study has shown that the manner in which the SH2 domain of TYK2 binds to its cognate interferon (IFN)-α and -β receptor subunit 1 (IFNAR1), is similar to how canonical SH2 domain binds to phosphotyrosine residues [108-110]. However, instead of a phosphotyrosine, TYK2 SH2 domain binds to i) a glutamate residue of the IFNAR1 and the ii) hydrophobic C-terminal region, both of which are located in the Box2 motif. A new model was proposed for the binding between JAK2 and EPOR/LEPR where a switch motif that is located N-terminal to the Box1 motif, is responsible for positioning the JAK2 FERM/SH2 as an active dimer [107]. The switch motif is not essential for JAK2 binding but is important for kinase activation, leading to downstream STAT phosphorylation [111-113]. It remains an interesting question as to how the same JAK molecule can bind to and be activated by different receptor types even though their Box1 and Box2 regions are not very well conserved. It has been demonstrated that the FERM-SH2 domains of JAK2 are structurally similar to TYK2, however, the putative receptor binding site of these two JAKs are slightly different [99]. This is probably how JAKs can confer binding specificity to their receptors.

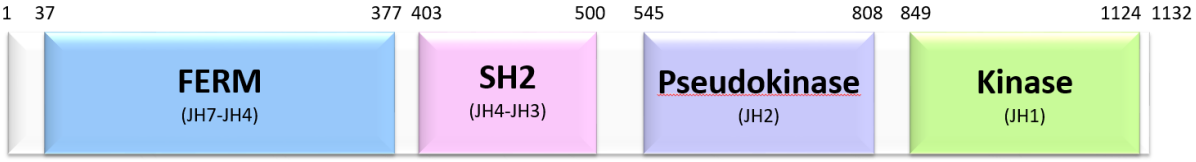

Figure 3: Domains of human JAK2.

In the JAK-receptor complex, JAKs exist as dimers. JAK2 can either form homodimers or heterodimers depending on the type of receptor that they associate with. Receptors such as TPOR, EPOR, GHR, and PRLR form homodimers. Therefore, JAK2 associates with these receptors as homodimers. On the other hand, when the receptors associate as heterodimers, for example, the IL-3 receptor, IL-5 receptor and IFN-γ receptor, JAK2 can form heterodimers with TYK2 or JAK1. The association of JAKs with their cognate receptors not only modulates signal transduction but it also aids in the membrane localisation of receptors such as EPOR and TPOR [112, 114, 115]. Besides JAKs, members of the type I cytokine receptor family can signal via Src family kinases (SFKs) using the MAPK pathway. The ability of different intracellular kinases to activate and modulate different signalling pathways via the same receptor can be explained by previous studies showing that the JAK2 and Src kinase activation can be induced by different GHR TM orientations [116]. Also, it was suggested that the levels of expression of JAK2 and Src kinase may be a determinant in whether the JAK-STAT or MAPK pathway is activated.

1.4.1 JAK2

JAK2 has been extensively studied for its role in haematopoiesis. The importance of JAK2 in haematopoiesis is demonstrated when $JAK2^{-/-}$ mice die during early embryogenesis due to the loss of definitive erythropoiesis [78, 117]. Mutations in JAK2 have been reported in MPNs where the most common mutation causing this disease is the $JAK2^{V617F}$. To investigate the pathogenic ability of $JAK2^{V617F}$, Ba/F3 cells were transduced with this mutant and they exhibited constitutive JAK-STAT signalling, excessive cell growth in the absence of cytokine and cytokine hypersensitivity in the presence of low ligand levels [5, 118]. However, $JAK2^{V617F}$ needs to associate with homodimeric class I cytokine receptors for pathogenic signalling to occur [118, 119]. In cell lines expressing EPOR, $JAK2^{V617F}$ was not able to cause cytokine-independent cell signalling and growth when its FERM domain (the domain that is responsible to bind to the receptor) was mutated [119]. Another study showed that when TPOR is reduced or diminished, neoplastic HSCs were markedly reduced [120]. Mice that harbour $JAK2^{V617F}$ but lack TPOR do not display MPN symptoms [120]. Using antisense oligonucleotides to diminish TPOR expression, a decrease in the spontaneous colony forming unit (CFU)-MK (megakaryocytes) development in PV and ET mice was observed [121]. Nevertheless, overexpression of this JAK2 mutant can confer cytokine-independent proliferation of Ba/F3 parental

cells [4, 5]. In JAK2^{V617F}, it was found that there are aromatic stacking interactions formed between V617F and the αC helix residues, F595 and F594 [90]. This interaction results in the stabilisation of the helix [90]. JAK2^{V617F} induces a reduction in the cell surface expression of TPOR so that megakaryocytes can evade cell death [122]. It also diminishes TPOR recycling capabilities and disrupts TPOR maturation via the cytoplasmic Y626 of TPOR [122].

1.4.2 Mechanism of JAK2 activation by GHR

It was simply thought that binding of the cytokine to their cognate receptors induces receptor dimerisation due to bringing the bound JAK2 close together, resulting in their autophosphorylation. Activated JAK2 will then phosphorylate the tyrosine residues of the receptor, which act as docking sites for downstream signalling molecules such as the STATs. STATs exist as pre-formed dimers [123-125] that when activated, undergo a conformational change. This change allows them to be localised to the nucleus to activate gene transcription [126-128]. However, it appears that the mechanism of JAK2 activation is more complicated than initially thought. Cytokine receptors such as GHR are pre-dimerised in the absence of cytokine-binding [129, 130]. Therefore, rather than receptor dimerisation–induced JAK2 activation, conformational changes in the receptor that trigger JAK2 activation must be the case, rather than a simple cytokine-receptor dimerisation mechanism.

A new paradigm on the mechanism of JAK2 kinase activation has been proposed [131] (Figure 4). Using GHR as a model, it was shown that cytokine-binding can trigger subunit realignment in the receptor which leads to activation of JAK2 kinase [131]. In the basal state, GHR is pre-dimerised [129], bound together via their TM helix [131]. GH binds asymmetrically and sequentially to two sites of the GHR ECD, firstly to site 1 and then to site 2 [132]. Upon binding of GH, the ECD of GHR undergoes a conformational change that causes the receptor dimer to be 'locked' together at its extracellular dimerisation domain (site 3), via hydrogen and electrostatic bonds [133]. Consequently, the electrostatic repulsion of the EED sequences at the ECD-JM domain of the receptor pair is overcome and the parallel TM helix undergoes a left-handed crossover [131] whereby its N-termini move closer together, but its C-termini separate. This results in an increase in distance between the intracellular Box1 motifs where JAK2 is bound [131] causing the pseudokinase domain of one JAK2 to 'slide' away from the kinase domain of its associated JAK2 [131] (Figure 4). The kinase domains of each JAK2 become positioned near each other, allowing *trans*-phosphorylation [131] and activation of the JAK-STAT signalling cascade to occur. A similar mechanism of JAK2 activation may be utilised by other type I cytokine receptors [131], however this has not yet been determined.

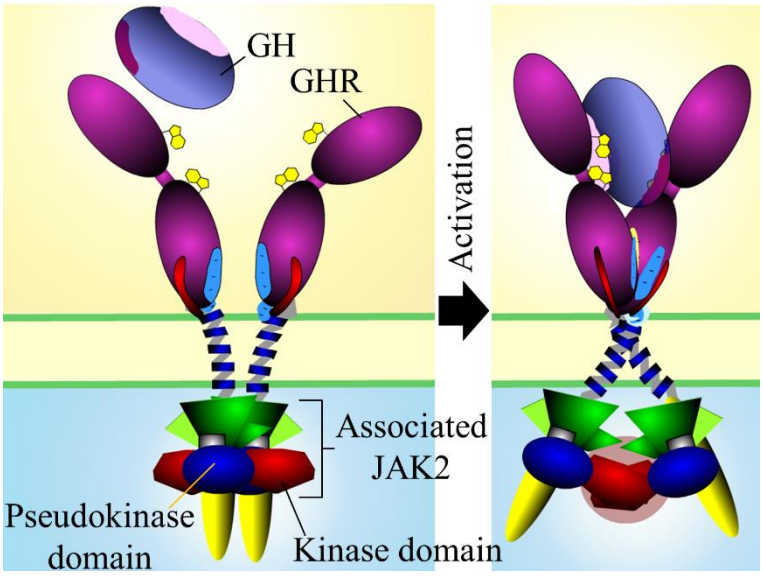

Figure 4: Model of GH-induced JAK2 activation via GHR.

GH binds asymmetrically to the GHR thereby causing a left-handed subunit rotation of the ECD. Consequently, the receptors are locked together at site 3, inducing the dimerisation of the TM N-terminus and separation of the TM C-terminus. This conformational change in the GHR induces the separation of the JAK2 JH1 from the JH2 of the corresponding JAK2. Subsequently, t*rans*-phosphorylation occurs, resulting in JAK2 activation. Figure reproduced from [131].

1.4.3 JAK2 Regulation

As JAK2 plays a crucial role in transmitting cytokine-induced signals to other downstream molecules, its tight regulation is crucial. JAK2 can be modulated by various regulatory mechanisms such as i) post-translational modification, ii) its pseudokinase domain, as well as iii) extrinsic regulators such as protein phosphatases (PTPs) and SH2 domain-containing regulatory molecules (see Section 1.6.2).

Human JAK2 possesses 49 tyrosine residues [134, 135] whereby the autophosphorylation of residues 523, 570, 1007, and 1008 acts to regulate its kinase activity. Phosphorylation of S523 and Y570 of JAK2 maintains its activity at a basal level in the absence of stimulation [92-96]. S523 is phosphorylated in-*cis* as the residue is closer to the activation site of JH2 whereas Y570 is further from this site and is phosphorylated in-*trans* by the JH2 domain of another JAK2 molecule [90]. In the absence of cytokine-binding, only S523 is constitutively phosphorylated to maintain JAK2 activity at a basal level [94] whereas Y570 is phosphorylated following cytokine binding to inhibit

JAK2 activity [93, 95]. Both S523 and Y570 residues in JAK2 are not conserved in other JAK family members and hence may represent an extra negative regulatory component of JAK2 [90].

The JH2 domain also associates and represses the kinase activity of JH1 to maintain JAK in an inactive state in the absence of stimulation [136]. There are two proposed models by which this inhibition can occur in JAKs: i) *cis*- model and ii) *trans*-model. Crystal structure studies based on TYK2 suggested the *cis* mechanism of inhibition [34]. Initially, there were three proposed hypothetical ways by which the JH1-JH2 interaction can occur within a TYK2 tyrosine kinase. Based on the distance (JH1-JH2 linker length) between the C-terminus of JH2 and N-terminus of JH1, interaction faces A, B, and C predict a distance of 67Å, 26Å, and 54Å respectively. An inhibition mechanism based on interaction face B was supported as it requires the shortest linker length that can be accomplished by the putative 14 amino acid JH1-JH2 linker. However, these findings were only based on studies of one TYK2 molecule. If the interaction between two TYK2 molecules was to be studied, it may be possible that a model similar to interaction face A may exist between these molecules. It is important to note that interaction A is the largest interaction face (1608Å^2, while interact B is 1463Å^2), however, this interaction places the C-termini of the JH2 domain and N-termini of the JH1 domain too far apart to be linked by the JH1-JH2 linker, thus could only represent a *trans*-interaction. However, *trans*-inhibition of TYK2 by an opposing TYK2 would not be expected to occur as TYK2 is not known to be activated by an opposing TYK2, rather it is activated by a different JAK family member bound to the opposing receptor subunit [137]. The interaction surface A observed in the TYK2 crystal structure may still be representative of what may occur in *trans*-inhibition with a different JAK family member. If so, this will be reminiscent of the *trans*-inhibition model of JAK2 [131]. This model proposed that the mechanism of inhibition of JAK2 occurs as a result of an interaction between the JH1 activation loop residues of one JAK2 molecule and the JH2 N-terminal lobe of another JAK2 molecule [131]. Furthermore, when a synthetic JAK2 mutant (with pseudokinase and kinase domain positions switched) was co-expressed with wild-type JAK2, it resulted in constitutive JAK2 activation [131]. However, a *cis*-inhibition model of JAK2 was also proposed [138]. Through molecular dynamics simulation, they found that the SH2-JH2 linker mediates JH1-JH2 interaction, allowing JH2 to bind to the back of JH1 kinase [138]. By doing this, JH1 is stabilised in an inactive state [138]. However, this inactive state is in conformational equilibrium with the partially active state where the JH1-JH2 domains of JAK2 are not in contact with each other [138]. In the presence of cytokine binding, conformational changes in the receptor bring the JH1 of both JAK2 close together thereby allowing phosphorylation to occur; the equilibrium subsequently shifts towards the active JAK2 conformation [138]. Nevertheless, the authors did not

consider the possibility of a *trans*-inhibition model (i.e. the pseudokinase domain of one JAK2 inhibiting another JAK2 kinase domain).

Another level of JAK2 regulation occurs after cytokine stimulation which may result in either negative or positive regulation depending on which tyrosine residues are involved. Phosphorylation of the main residues in the JH1 activation loop, Y1007 and Y1008, induces JAK2 catalytic activity. Positive regulation of JAK2 kinase activity can also occur through phosphorylation of residues Y637, Y813, Y868, Y966, and Y972. On the other hand, phosphorylation of residues Y119, Y221, Y317, Y570, and Y913 negatively regulates JAK2 [93, 95, 96, 139-141]. Extrinsic JAK2 negative regulation after cytokine-binding also occurs through the action of PTPs such as SH2 domain-containing phosphatase (SHP) 1, SHP2, and tyrosine-protein phosphatase non-receptor type 1 (PTP1B) which dephosphorylate JAK2 stimulatory sites, as well as by the action of SOCS, protein inhibitor of activated STATs (PIAS), and SH2B adaptor protein 3 (LNK/SH2B3) proteins (see Section 1.8) [136, 142-144]. Interestingly, JAK2 may also be regulated by oxidation and reduction whereby its oxidation leads to its inactivity and its reduction leads to its activity [145].

1.5 TPO and its receptor, TPOR

TPO (Figure 5), also known as megakaryocyte growth and differentiation factor (MGDF), is an acidic and strongly glycosylated cytokine. It is mostly produced in the liver [146] and to a lesser extent in the kidney, bone marrow, and spleen [146-148] whereas constitutive production of the cytokine is performed by the liver and kidney [149]. TPO binds to its cognate receptor, TPOR (Figure 5) via its N-terminus (1-153 amino acids). TPOR (635 amino acids) is encoded by the 11 exon *MPL* gene and this gene resides on chromosome 1 (p34). It is the human homologue of the *v-Mpl* that is derived from murine c-MPL that was discovered first. The murine myeloproliferative leukaemia virus (MPLV) infection results in acute myeloproliferative neoplasms in mice [150]. TPOR is expressed in haematopoietic cells such as HSCs [151], progenitor cells of the megakaryocyte lineage, megakaryocytes, platelets [152], as well as in haematopoietic tissues. Approximately 70% of HSCs express TPOR and this value decreases during differentiation [151, 153].

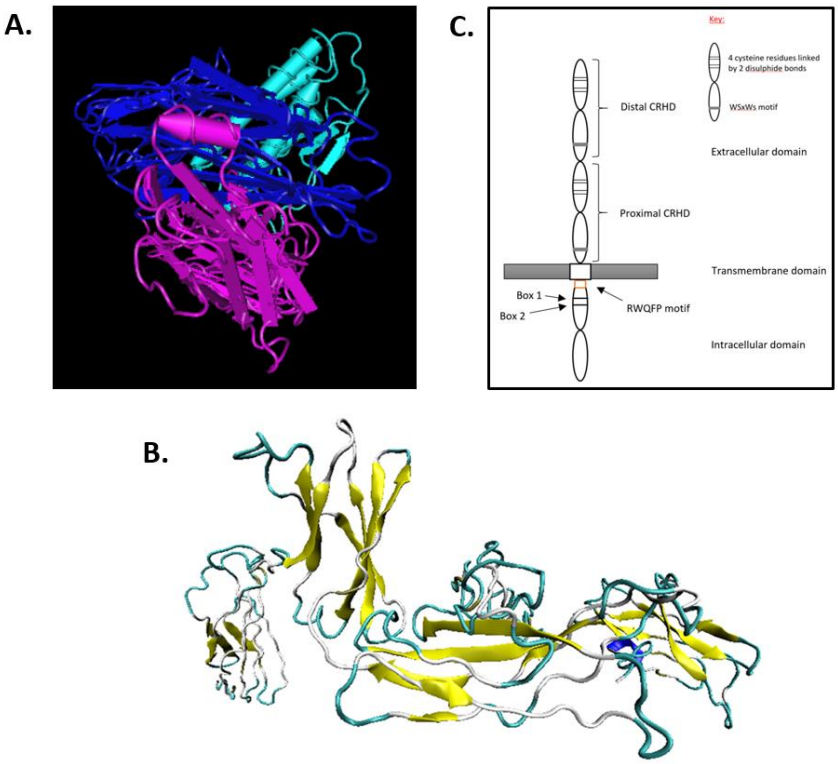

Figure 5: TPO and its cognate receptor, TPOR.

A) Crystal structure of the receptor-binding domain of human TPO (hTPO) co-crystallised with the neutralising antibody Fab. hTPO is made up of four α-helices and contains two receptor-binding sites that allow for sequential binding to the ECD of TPOR [154]. The first receptor binding in the dimer is mediated by its A and D helices whereas the second receptor binding in the dimer is conferred by its A and C helices [155]. Image reproduced from NCBI molecular graphic [156]. B) Modelled structure of TPOR ECD [157]. C) Cartoon image of TPOR showing two CRHD at the ECD and several motifs (RWQFP, Box1, Box2) at the ICD.

Compared to other receptors, TPOR is not highly expressed on the surface with approximately 25-100 receptors on a platelet [158, 159]. Circulating TPO is removed from circulation by platelets and megakaryocytes that express TPOR. The binding of TPO to the receptor results in internalisation of the TPO-TPOR complex. After TPOR is internalised, it can either be recycled back to the cell surface or degraded. However, in platelets, TPOR is not recycled but is degraded instead. Due to the negative feedback mechanism, an inverse relationship between circulating TPO and platelet levels has been observed [160]. Therefore, TPO plasma concentration depends on the level of TPOR present on thrombocytes and megakaryocytes [160]. This inversely proportional relationship helps to regulate thrombopoiesis and HSC quiescence. In the case of thrombocytosis, high levels of TPOR cause more

internalisation of the cytokine leading to reduced TPO concentration in the plasma. On the other hand, in thrombocytopaenic patients, low TPOR levels lead to reduced TPO internalisation and subsequently increase in the production of megakaryocytes and platelets.

1.5.1 TPOR isoforms

Isoforms for several cytokine receptors that arise from alternative splicing have been described whether they can positively (IL-6) [161, 162] or negatively (IL-5 or GM-CSF) [163-166] regulate signalling. Several alternative splicing isoforms of TPOR exist that vary in their biological activity. These include those with deletion of the ECD [167], a different ICD (K-isoform) [150], and those that lack the entire TMD and ICD (Mpl-tr) [168]. The K-isoform has no impact on TPO-mediated signalling as it does not bind the wild-type receptor [169]. The truncated soluble TPOR isoform, Mpl-tr, is conserved between humans and mice. This isoform retains the signal peptide but is deficient in the TM domain (and ECD-JM) [170, 171]. Regardless of the presence of signal peptide, it remains in the intracellular compartment of the cell. Interestingly, this truncated receptor can act as a dominant-negative mutant to inhibit TPOR-mediated cell proliferation by downregulating the full-length TPOR via cathepsin-like cysteine protease activity through its unique short peptide at its C-terminus tail [168].

1.5.2 Megakaryopoiesis and thrombopoiesis

Haematopoietic cells undergo lineage commitment and give rise to bipotent megakaryocyte-erythroid progenitors which in turn become megakaryocytic progenitors. These will terminally differentiate into megakaryocytes which undergo endomitosis and cytoplasmic maturation. These processes are termed megakaryopoiesis. TPO/TPOR plays an important role in the megakaryopoiesis that occurs in the bone marrow. Mice that are deficient in TPO or TPOR have markedly reduced (~85% reduction) megakaryocyte and thrombocyte numbers with no effects observed on other cell lineages [172-174]. Besides regulating megakaryocyte lineage commitment, TPO/TPOR also regulates HSC survival and proliferation [175]. However, they are not essential to regulate megakaryocyte maturation or thrombocyte generation [51, 176]. As megakaryocyte progenitors differentiate into mature megakaryocytes, they have reduced proliferative capacity. Megakaryocytes generate platelets (via a process known as thrombopoiesis) which arise from the disintegration of the pseudopial projections of mature megakaryocytes, termed as proplatelet fragmentation. The amount of

circulating platelets in the body needs to be maintained as uncontrolled or decreased production can result in thrombosis or excessive bleeding. Mice lacking the TPOR or TPO gene are thrombocytopaenic [151] as a result of markedly reduced TPO signalling leading to the reduction in mature megakaryocytes and megakaryocytic progenitors. Besides being stimulatory, TPO can exhibit inhibitory effects to maintain stem cell quiescence and cell cycle arrest in late megakaryocytes. TPO-deficient mice had markedly reduced HSCs as they age but when stimulated with TPO, there is an increase in the number of these quiescent HSCs [177, 178]. TPO can work together with other cytokines such as EPO, IL-11, and stem cell factor (SCF) to stimulate the growth of progenitor cells [179].

1.5.3 Mechanisms regulating TPOR

Unlike other cytokine receptors, TPOR has a long half-live (surface and intracellular) where surface TPOR has higher stability than that in the intracellular stores [115]. The life cycle of TPOR involves: i) the post-translational modification of immature TPOR, ii) cell surface localisation of mature TPOR, and iii) its internalisation from the cell surface. TPOR can exist in two forms, the fully glycosylated mature form (~85kDa) and the immature form with much-reduced glycosylation (~80kDa) [49, 180]. TPOR maturation and full glycosylation are essential for its cell surface expression [181]. Studies have shown that impaired glycosylation of TPOR negatively affects its function [180], leads to reduced platelet production, and reduced TPOR membrane localisation [181, 182].

Upon ligand binding, TPOR is endocytosed (internalised) and the receptor can either undergo recycling or degradation. TPOR internalisation is mediated via clathrin-mediated endocytosis [183] which is facilitated by adaptor protein 2 (AP2) complexes. AP2 facilitates TPOR endocytosis by recognising the Y^{591}RRL (Y^{78}RRL cytoplasmic numbering of mouse TPOR) motif in the receptor [183]. Mutation of Tyr to Phe in the Y^{78}RRL motif results in increased and extended signalling [184]. This motif is also important in lysosomal-mediated degradation of TPOR [183] besides the Y^{521}RRL (Y^{7}RRL cytoplasmic numbering of mouse TPOR) motif [183]. Mutation of Y78 causes an increase in cell proliferation and signalling (and duration of signalling) via JAK2, STAT5, Akt, and extracellular-signal-regulated kinase (ERK) 1/2. Interestingly, the putative AP2-recognition motif can also be found in EPOR and granulocyte colony-stimulating factor receptor (G-CSFR) [183]. The importance of the dileucine/leucine repeats (in the Box 2 motif) and Y112 (mouse TPOR cytoplasmic numbering; equivalent to human TPOR Y626) for receptor internalisation following TPO stimulation was also previously reported [185].

The ability to be recycled is unique to TPOR [185] as other type I cytokine receptors do not possess this capability. As a result of ligand binding, the mature receptor is internalised with a turnover rate of approximately 6 hours [186]. Each cycle internalises a maximum of 65-75% of mature TPOR [159, 185]. Interestingly, JAK2 and TYK2 can induce mature TPOR recycling and maintain its ability to retain TPOR cell surface localisation [187]. If recycling does not occur, the receptor will be targeted for degradation. One of the ways in which proteins are degraded is through a process known as ubiquitination although ubiquitination of target proteins may mediate different functions. Mono-ubiquitination regulates protein localisation and signalling [188] whereas poly-ubiquitination mediates proteasomal degradation. It is known that TPOR is promptly ubiquitinated after TPO induction and is then degraded by lysosomes and/or proteasomes [186]. Ubiquitination of TPOR occurs via c-CBL, an E3 ubiquitin ligase, on K553 and K573 (located in the intracytoplasmic domain). Mutation of these residues to arginine prevents receptor degradation and results in constitutive cell proliferation [186]. Upon cytokine stimulation, c-CBL is recruited and activated by phosphorylation [189, 190] which allows it to mediate the conjugation of poly-ubiquitin to TPOR.

1.5.4 Mechanism of JAK2 activation by TPOR

Previous efforts by other groups have been predominantly focussed on explaining how TPO binding leads to TPOR activation, however it is not clear as to how ligand-induced conformational change in TPOR can activate its associated JAK2 or how JAK2 JH2-JH1 interaction is relieved following activation. It is not clear as to whether JAK2 activation occurs as a result of TPOR dimerisation or that conformational change occurs in preformed TPOR dimers which leads to JAK2 activation. Currently, it is known that GHR [129], PRLR [191], IL-6R [192], and EPOR [193, 194] can exist as pre-formed dimers on the cell surface. Also, homodimeric gp130 was found to be pre-dimerised without cytokine binding but this is a transient interaction that can be stabilised by the ligand, IL-6 [195]. On the other hand, heterodimerisation between gp130 and LIFR is mediated by ligand binding [195]. For other type I cytokine receptors, their pre-dimerisation status has not yet been determined. Most importantly, there is currently no strong evidence supporting the pre-dimerisation status of TPOR. Nevertheless, as TPOR is structurally and functionally similar to EPOR, TPOR may also exist as pre-formed dimers similar to EPOR.

A recent study using split luciferase assay showed that TPOR exists in monomer-dimer equilibrium and that this equilibrium is shifted towards the formation of monomers in the inactive state [196]. This technique, however, measures the total fluorescence that is emitted from the cell and includes the fluorescence signal generated by receptors on the cell surface as well as from receptor aggregates.

Therefore, this may have masked the ratio of dimers and monomers that are present on the cell membrane. Furthermore, the receptor was C-terminal tagged with Gluc1 and Gluc2. The ICD of TPOR, like other cytokine receptor cytoplasmic domains, lacks secondary structure. Hence, tagging these molecules at the C-terminus may not allow for a clear evaluation of the occurrence of receptor dimerisation. Another study also suggests that TPOR exists as monomers in their inactive state. In this study, the authors found that the incorporation of cysteine instead of serine at position 368 (located in the putative dimerisation interface of TPOR) forced the dimerisation of TPOR via disulphide bonds and this led to constitutive signalling [197]. On the contrary, studies using complementation assay between WT and mutant TPOR have suggested that TPOR exists as pre-formed dimers prior to receptor activation [182] as WT TPOR can rescue the TPOR R102P mutant to the Golgi (R102P mutant alone can only localise in the rough ER) although it is not able to rescue this mutant to the cell membrane. The cysteine dimerisation may have locked the receptor in an induced dimeric active structure, rather than an inactive dimer.

1.5.5 TPOR-mediated signalling pathways

TPOR activation mediates the JAK-STAT, phosphoinositide 3-kinases (PI3K)/AKT, and MAPK pathways (Figure 6). In the JAK-STAT pathway, it can activate JAK2, TYK2, STAT1, STAT3, and STAT5 [184, 198-202] while the STATs induce genes involved in proliferation and survival. TPO stimulation results in phosphorylation of the receptor on residues Y112 and Y117 where they act as docking sites for STAT3 and STAT5 which subsequently undergo phosphorylation by JAK2 [184]. SHC also binds to phosphorylated Tyr112 and subsequently recruits GRB2 and SOS, leading to RAS activation. Downstream RAF, ERK1/2, p38 MAPK are recruited and activated. Stimulation of RAF also results in PI3K activation. The GAB/IRS, SHP2, p85, p110 complex is recruited N-terminal of Tyr112 following Akt phosphorylation.

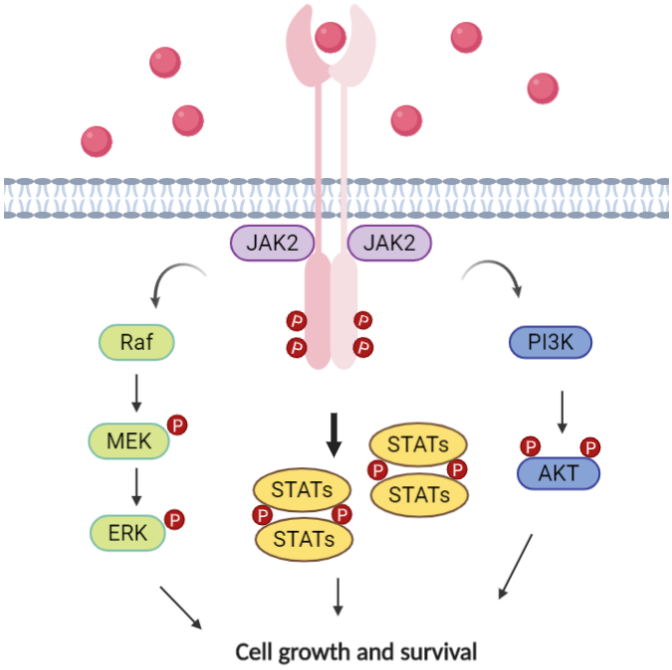

Figure 6: Figure showing a simplified diagram of the TPOR signalling pathway.

TPO binds to inactive TPOR and activates the receptor. This will initiate signal transduction through various pathways.

TPO signalling can be mediated by both JAK2 and TYK2 but only JAK2 can confer persistent JAK-STAT signalling [201]. This finding was supported by another study that showed that in the absence of JAK2, TPO-mediated signalling cannot occur, whereas in the absence of TYK2, signal transduction still occurs [203]. Furthermore, in the presence of TPO stimulation, mature megakaryocytes displayed obvious phosphorylation of JAK2 but not TYK2 [204]. JAK2 deficient foetal liver cells are defective in megakaryocyte production despite the presence of TPO [78]. Downstream signalling via the PI3K/AKT pathway regulates the cell cycle in megakaryocyte progenitors [205, 206] whereas TPOR-mediated ERK signalling is important for primary megakaryocyte endomitosis [207] and maturation [201]. In UT7 cells expressing TPOR, sustained ERK1/2 stimulation can influence megakaryocyte differentiation [201]. Activation of the MAPK pathway induced by TPO can be Shc-independent or dependent [184, 208]. When the Shc-dependent pathway is impeded, PI3K-mediated ERK activation occurs. Activation of the ERK signalling pathway can also be mediated via protein kinase c (PKC)-γ which does not require the distal phosphotyrosine of TPOR [209].

1.5.6 TPOR extracellular domain

The ECD maintains TPOR in an inactive state in the absence of stimulation. It has been suggested that the distal CRHD (CRHD-1) is particularly important for this function as deletion of CRHD-1 causes constitutive cell proliferation [210]. Furthermore, the substitution of CRHD-1 by CRHD-2 showed similar results [210]. Indeed, a mutation in CRHD-1, P106L, can stimulate cell growth in the absence of cytokine [182]. This mechanism is in place to prevent spontaneous signalling via the CRHD-2 and TMD [210]. The inhibition conferred by CRHD-1 is alleviated upon TPO binding [210]. Residues 102 to 251 of CRHD-1 are suggested to be the ligand-binding region where residues 206-251 are core residues for this binding [211]. In support of this finding, alanine-scanning mutagenesis showed that D235 and L239 residues were the most important for ligand binding as alanine substitution of these residues disrupts TPOR affinity for ligand binding [211]. In particular, residues in the F'-G' domain of CRHD-1 are suggested to potentially bind TPO [211]. This domain has been shown to play a role in ligand binding in granulocyte-colony stimulating factor (G-CSF) [212], GM-CSF [213], and IL-6 [69] receptors. Another study showed that F104 of TPOR is important for TPO association with the receptor as F104S disrupts TPOR ability to bind TPO [214]. However, unlike D235 and L239, F104 is not located in the putative F'-G' domain. Instead, it is located at the G-A' domain of TPOR ECD. This suggests that ligand binding sites can occur in regions outside of the conserved F'-G' domain and that these three residues or even other amino acid residues may play a role in forming the ligand-binding site of the receptor.

The ECD of human TPOR possesses several potential N-linked glycosylation sites such as residues 117, 178, 298, and 358 that can modulate the localisation of TPOR to the cell surface [215]. Furthermore, studies using EPOR showed that the c-mannosylation consensus motif, WSXWS, plays a role in receptor internalisation, cytokine binding, proper receptor folding as well as signal transduction [216, 217]. In TPOR, the C-mannosylation sites include tryptophan residues at positions 269 and 272 (located in the first WSXWS motif), 474, 477 (located in the second WSXWS motif), as well as 416 [218]. Consistent with EPOR data, the previous study showed that the TPOR C-mannosylated sites (except W416) are important for JAK-STAT signalling [218].

1.5.7 TPOR transmembrane domain

The N-terminal TPOR TM domain is predicted to comprise amino acid residues I492 to V495 that are connected to the hydrophobic TM region (T496-L513) by non-helical residues [219]. Mutations in the TPOR TM domain can result in spontaneous TPOR activation. A TM domain mutation, S505N, was discovered as an inherited form in familial ET [220] and then as an acquired form in ET patients [41]. It was recently discovered that the TM amino acid sequence before 499 is non-helical and that S505N can induce helix formation and strong TM helix dimerisation [196, 221]. Site-directed mutagenesis on the wild-type S505 amino residue to generate synthetic E/D/Q505 showed that these synthetic and the clinical mutation, N505 induce spontaneous receptor dimerisation [222]. The spontaneous receptor dimerisation was thought to occur via hydrogen bonding induced by strong amino acid polarity [222, 223].

However, studies by another group suggested that the N505 mutation causes spontaneous receptor activation via a different mechanism [221]. They have shown that this mutation causes TPOR TM to adopt a different conformation from the wild-type receptor via subunit rotation [221]. N505 conformation is achieved by rotating the putative inactive TPOR state by approximately 100° which results in stronger dimerisation of the TM helix with consequent spontaneous receptor activation [221]. This is reminiscent of what was proposed for the GHR in response to GH binding [131] (see Section 1.4.2). The different rotations also allow the N505 TM domain to utilise a different interface (residues L502, N505, G509, and L512) from the inactive and ligand-bound active states [221]. Nevertheless, this mutant may only induce partial receptor activation in the absence of ligand stimulation and because TPO-binding to TPOR is required for complete receptor activation [222]. This suggests that N505 can induce an intermediate TM conformation between the inactive and ligand-bound fully active states of the receptor [221]. Two types of interface clusters based on H499 (an important residue that prevents spontaneous TPOR activation) position reflect these inactive and active states, known as cluster 1 (histidine-in) and cluster 2 (histidine-out), respectively [221]. For cluster 1, TM dimer interface is formed by residues H499, L502, A506, L510, and L513 [221]. Cluster 2, on the other hand, is formed by rotating the putative inactive state by 150° which results in H499 being out of the dimeric interface [221]. In the basal state, the TM domain of TPOR is structured in a dimerised manner in a parallel left-handed fashion [221]. In contrast, another study suggested that the tryptophan in the RWQFP motif, prevents the dimerisation of the TM helix in the absence of TPO and that the TM of the wild-type TPOR is a monomer and the dimerised form exists for the mutant TPOR [224].

1.5.8 TPOR intracellular domain

Human TPOR possesses five tyrosine residues (Y521, Y542, Y591, Y626, Y631) in its intracellular domain. The TPOR TM helix extends towards the cytoplasm up to the F517 residue of the JM-ICD domain. This domain contains a unique RWQFP (human) or KWQFP (murine) amphipathic motif. The first and second residues of this motif are suggested to form a cation-π interaction, a noncovalent interaction [224] that affects protein folding, stability, and specificity. Deletion of this motif has been shown to result in constitutive activation of the receptor [225]. In particular, the tryptophan residue at position 515 plays a crucial role in regulating receptor activation. This residue maintains TPOR in an inactive state in the absence of TPO, and plays a role in TPOR activation in the presence of stimulation [224]. In the epidermal growth factor receptor (EGFR), its JM-ICD contains a phosphatidylinositol 4,5-bisphosphate (PIP2)-interacting motif (R645–R647) (located at a similar position as the RWQFP motif in TPOR) that is important for positioning its kinase domains [226]. This finding suggests that the TPOR RWQFP motif may use similar mechanisms as the EGFR PIP2-interacting motif.

The importance of conserving the tryptophan residue at position 515 is demonstrated when replacement of this residue with other aromatic amino acids (tyrosine or phenylalanine) was not able to retain the receptor in its inactive conformation [224]. A mutation in the W515 residue can drive myeloid malignancy. Although only six activating clinical TPOR W515 mutations have been currently discovered, another publication has shown that the alteration of W515 to another eleven amino acid residues (hydrophobic, charged or polar residues) was able to result in similar spontaneous activation of the JAK-STAT pathway [227]. Only the alterations of W515 to proline (W515P) or cysteine (W515C) was able to maintain the receptor in its inactive state without TPO [227]. TPOR W515P may have lost its ability to localise and anchor itself to the cell membrane for activation to occur [227]. C515 on the other hand is part of a conserved motif in birds and turtles and hence is thought not to be able to confer spontaneous receptor activation [227]. Interestingly, when amino acid residues beside W515K/L mutants were mutated to tryptophan, this was able to restore normal receptor activity [224]. This finding suggests that the five amino-acid motifs are crucial for regulating the active and inactive states of the TPOR.

Studies using K515 demonstrated that the TM of K515, but not the inactive wild-type TM, can induce TM dimerisation, with a helix tilt angle relative to the membrane normal of ~23° for the former and ~30° for the latter [224]. In support of the ability of W515 mutants to confer a different helix tilt angle from wild-type, another study found that TPOR can adopt seven different orientations [61], unlike EPOR which signals through only one dimeric orientation [228]. To investigate this, they replaced

the ECD domain of TPOR with coiled-coil dimers to orientate TPOR into various orientations with the assumption that the TM and ICD domains of TPOR are rigid [61]. It was identified that out of the seven possible orientations, one orientation does not activate TPOR and is thought to correspond to the non-ligand binding state [61]. The other six orientations were able to result in TPOR activation and may correspond to the ligand-bound state of the receptor or mutant receptor active state [61]. In agreement with these findings, another study discovered three different TM dimeric orientations of TPOR that correspond with the inactive, partially active, and fully active state of TPOR [221]. The several possible dimeric orientations that can be adopted by TPOR may explain how TPOR can exhibit a pleiotropic role in haematopoiesis (such as megakaryocytic differentiation) and how TPOR mutations can cause corresponding disease phenotypes [61].

Similar to human TPOR, the murine TPOR Box1 (cytoplasmic residues 17-20) and Box2 motifs (cytoplasmic residues 46-64) are important for JAK2 binding and activation. The intracytoplasmic TPOR residues can either be involved in JAK-STAT pathway activation or inhibition. The region between residues 69-83 after the Box2 motif, is thought to be involved in partial inhibition of cellular proliferation [184]. Mutation or truncation in this region results in augmented proliferation [184]. On the contrary, engineered truncation of 53 amino acid residues from the C-terminus of murine TPOR, designated as T53 was found to down-regulate ligand-stimulated cell proliferation [184]. This truncation resulted in the loss of the positive regulatory sites, Y616 and Y621 (equivalent to human TPOR Y626 and Y631, respectively), as well as the negative regulatory region, but may negatively impact the positive regulatory sites more than the negative regulatory sites [184]. The mouse TPOR Y616 and human TPOR Y626 residues are pivotal for SHIP protein phosphorylation, Shc activation (for MAPK signalling) [229], and the spontaneous activation of human TPOR W515A in MPN patients [230]. Human TPOR W515A-positive cell lines and mouse models harbouring Y616F, have significantly reduced pathologic signalling and dampened MPN-like phenotype [230]. Although the mouse TPOR Y616 residue mediates cell proliferation, its role is dispensable in wild-type TPOR [208]. It is, however, important for mutant TPOR pathogenesis [230]. The mouse TPOR Y621 is associated with the phosphorylation of TPOR and STAT3 [184].

It has been shown that in the case of human PRLR and GHR, their ICDs are structurally disordered but they can mediate the interaction with the inner cell membrane lipid via their ITAM (immune receptor tyrosine-based activation motifs)-like motifs [231]. This suggests another level of signal regulation and a similar mechanism may be utilised by other members of the type I cytokine receptor family such as TPOR.

In summary, the ECD, TM (H499 and S505), and ICD (^{514}RWQFP^{518} motif) co-operate to regulate TPOR activation but further studies are required to understand how conformational changes in these

domains can lead to JAK2 activation. In the case of GHR, it was discovered that in the presence of GH, the ECD and TM N-terminus come together in a receptor dimer but the TM C-terminus and ICD are pulled apart as a result of ligand-binding [131]. This relieves the inhibition of JAK2 JH2 on the JH1 domain. Elucidating the mechanism of JAK2 activation by TPOR is important to facilitate the development of improved targeted drugs to treat patients suffering from myeloid malignancies as a result of activating TPOR mutations. Furthermore, this knowledge will help to understand how TPOR mutations can cause MPNs and leukaemia.

1.5.9 TPOR activating and inactivating mutations

Mutations in TPOR can be activating or inactivating. Inactivating mutations (nonsense or missense) such as R102P and F104S can lead to congenital amegakaryocytic thrombocytopaenia (CAMT) [232-234]. In these patients, the resulting receptor may be non-functional [232, 233] or have markedly reduced function [232]. The R102P mutation results in the receptor being underglycosylated with dampened ability to bind TPO [180]. In contrast, TPOR activating mutations such as the P106L mutation cause familial essential thrombocythaemia (FET) [235]. Although R102P and P106L result in contrasting diseases, both mutations cause reduced receptor cell surface expression, unusual subcellular localisation, under-glycosylation, and an increase in circulating TPO [182]. This suggests that activating mutations such as P106L do not require proper cellular localisation, glycosylation, or surface expression to confer constitutive cell signalling and proliferation [182].

Mutations that result in constitutive TPOR activation (Figure 7) are frequently found to reside in the RWQFP motif (this motif is located at the JM-ICD and is unique to TPOR), for example, the W515L/K/A mutations. These mutations result in MPNs as they can confer cytokine-independent cell proliferation and activation of JAK-STAT, RAS/MAPK, and PI3K signal pathways which play a role in cell survival and proliferation [43, 225, 236]. TPO stimulation can, however, increase the signalling effect of the W515L mutant. Furthermore, W515L/K mutations of TPOR enhanced cell proliferation by inducing spontaneous G_1 to S phase transition [237] in the cell cycle. The cytoplasmic phosphorylated tyrosine residue 626 (putative STAT5 binding site when phosphorylated) of TPOR is crucial for the pathogenesis of W515 mutations [230]. It was previously shown that W515L with an KDEL is retained in the ER/ Golgi and is unable to cause spontaneous FDCP-1 cell proliferation and tumour growth in nude mice [238]. The W515L-KDEL mutant can bind JAK2 but is unable to induce JAK2 phosphorylation [238]. Forced dimerisation of W515L-KDEL (by substituting the S402 residue to cysteine for the formation of a disulphide-bond) allowed the mutant to localise to the cell

surface and cause constitutive activation [238]. This suggests that the binding between TPOR W515L and JAK2 occurs in the ER/ Golgi in an inactive form (either monomer or inactive dimer) and that translocation to the membrane is required for JAK2 activation and constitutive signalling to occur [238]. Other mutations that can cause constitutive receptor activation, that are located outside of the TMD include the S505N (TM domain) and T487A (JM-ECD) mutations [239]. S505N has also been reported in FET whereas the TPOR T487A mutation has only been reported in a childhood acute megakaryoblastic leukaemia (AMKL) case (without Down-syndrome) [239]. In a bone marrow transplantation experiment, the T487A mutation was sufficient to confer MPN-like symptoms in mice [239].

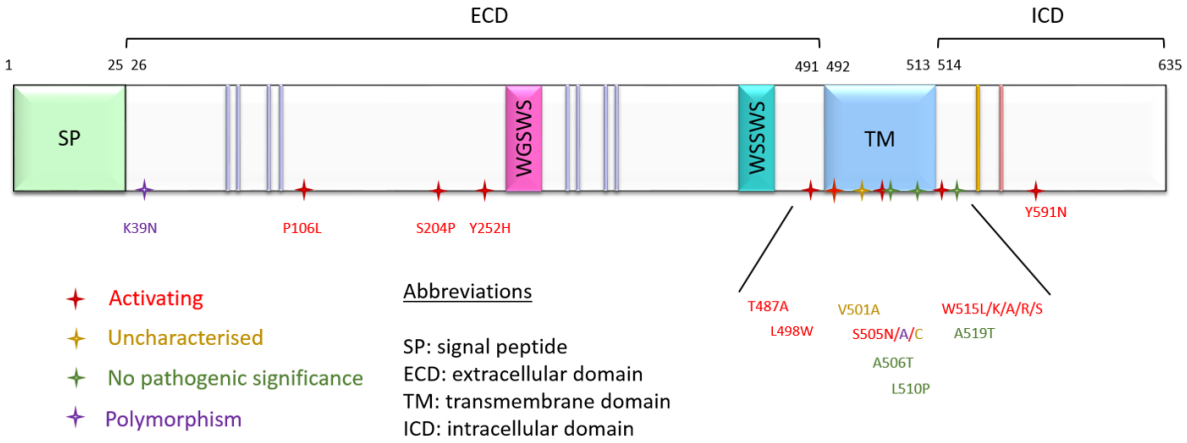

Figure 7: Clinical TPOR activating mutations and polymorphisms.

Most activating mutations reside in and around the TMD.

The W515K and T487A JM mutations are predicted to increase the tendency of TPOR to form dimers as well as to induce TPOR conformational change to the active form [40, 43, 224, 225, 240]. On the other hand, the TM S505N mutation acts by stabilising TPOR in the active dimer form [222, 241]. Interestingly, it was reported that the TPOR T487A mutation results in slower MPN development compared to the JM-ICD mutation, W515L [239]. This may suggest that the JM-ICD may play a bigger role than the JM-ECD in terms of modulating cytokine signalling, although the significance of both domains in inhibiting spontaneous signalling cannot be denied. Other *MPL* mutations such as P106L, S204P, Y591N, S505C, A506T, and L510P have also been reported.

1.5.10 Modulation of TPOR activity using agonists or antagonists

Patients that potentially require TPO agonist treatment include those with bone marrow failure, liver cirrhosis, autoimmune diseases, myelodysplastic syndrome (MDS), and those undergoing

chemotherapy/radiation. However, TPO agonists need to be used with caution particularly for MDS and chemotherapy/radiation-induced thrombocytopaenia patients as there have been reports of disease transformation to leukaemia due to the use of these agonists. Various TPO agonists have been developed and improved over the years which include mimetics (small molecules or peptides) that activate TPOR such as Eltrombopag (Promacta) and Romiplostim (Nplate), both of which have been approved by the US Food and Drug Administration (FDA). Eltrombopag (small molecule) and Romiplostim (peptide mimetic) have been developed to treat immune thrombocytopenic purpura (ITP) [242, 243]. These mimetics can induce normal thrombopoiesis in thrombocytopaenic patients. Romiplostim binds to the ECD of TPOR and induces receptor dimerisation. In contrast, Eltrombopag is structurally different from endogenous TPO and interacts with the TMD of TPOR. Therefore, Eltrombopag could potentially activate TPOR with inactivating ECD mutations. The interaction between Romiplostim or Eltrombopag with TPOR induces JAK-STAT and MAPK activation resulting in elevated platelet levels [244-246].

Treatments for MPN patients harbouring activating TPOR mutations include administration of hydroxyurea, IFN-α or JAK2 inhibitors. Ruxolitinib or also known as Jakafi works by inhibiting JAK1/JAK2 [247] and is used for the treatment of MF (*de novo* MF or post-ET/PV MF). AMKL patients with MPL mutation are not treated differently from other leukaemic patients and are administered chemotherapy drugs. As these treatments are not specific, patients develop various side effects. This highlights the need to develop more specific, targeted treatments against this receptor. However, it has to be taken into account that the absolute elimination of TPOR is unlikely to be beneficial as shown by patients with CAMT who can progress from thrombocytopaenia to pancytopaenia.

1.6 Negative regulators of JAK-STAT signalling

JAK-STAT signalling can be regulated by i) dephosphorylation of signalling molecules or receptors that mediate signalling, ii) transcriptional inhibition, iii), membrane receptor internalisation, and/or iv) degradation of signalling intermediates or receptors. These are carried out by various negative regulators that act in different stages of the pathway (discussed below). Particularly, the ones that are involved in downregulating TPO-mediated signalling include SOCS, LNK, Lyn, and phosphatases [248-251].

1.6.1 SOCS

The SOCS family of proteins is comprised of of SOCS1-SOCS7 and cytokine-induced STAT inhibitor (CIS). This family of proteins participates in the negative feedback loop of JAK-STAT signalling [252-254]. Initiation of signal transduction results in SOCS expression that is induced by STATs [253]. The SOCS family members generally possess an N-terminal domain (NTD), an SH2 domain, as well as a SOCS box domain that is located in the C-terminus. An extra region known as the kinase inhibitory region (KIR) is only present in SOCS1 and SOCS3 [84]. SOCS can work by i) blocking JAK activity directly using the KIR, ii) binding to their cognate JAKs to mediate the proteasomal degradation of the JAK-associated receptors, and/or iii) competing with STATs for binding to the receptor. Interestingly, it was discovered that when SOCS3 is not bound to JAK, its KIR is structurally disordered [255]. However, its association with JAK allows the KIR to be inserted into the substrate-binding site of JAK [81]. In turn, JAK is prevented from catalysing its substrate and this consequently results in inhibition of JAK-STAT signalling. This mechanism of inhibition is distinct from the one used by small molecule inhibitors that are used clinically. Activation of the TPO signalling pathway results in upregulation of SOCS3 whereas SOCS1 is upregulated by IFN-α, both of which functions to downregulate TPOR-mediated signalling [256].

1.6.2 PTPs

Protein phosphatases include SHP1, SHP2, PTP1B, and CD45 and they can terminate signalling by dephosphorylating receptors, JAKs, and/or STATs. The crystal structure of SHP1 and SHP2 in their closed conformation revealed that the catalytic domain is obstructed by their N-SH2 domain [257, 258]. In response to ligand binding to its SH2 domain, the crystal structure revealed a conformational change in SHP1 [259]. This change involves the dissociation of the N-SH2 domain from the catalytic domain thereby allowing phosphatase activity [259].

1.6.3 PIASs

These proteins are ubiquitously expressed and play a role in the negative feedback loop of JAK-STAT signalling. They are able to regulate signalling via their ability to small ubiquitin-like modifier

(SUMO)lyate their substrates, attracting additional co-repressors, and blocking STATs from associating with their target DNA.

1.6.4 CBL

CBL proteins are E3 ubiquitin ligases that target proteins for degradation via the proteasome or lysosome [260]. However, in some cases, CBL can positively regulate signalling [261-265]. CBL is recruited to the K553 and K573 residues in the intracytoplasmic domain of TPOR to mediate degradation [266].

1.6.5 Src family kinases

SFKs are comprised of Blk, Lck, Yes, Hck, Fgr, Src, Fyn, and Lyn that play a role in cellular migration, proliferation, and differentiation [267, 268]. In megakaryocytes, only Lyn and Fyn are activated after TPO induction [269]. Lyn can play dual functions (activating or inhibitory) but in the TPO signalling pathway, Lyn has an inhibitory function [269]. Cell proliferation was reported to be enhanced in the presence of Src kinase inhibitors (pyrolopyrimidine 1 and 2 (PP1 and PP2)) [270]. It was shown that the use of SFK inhibitors did not have an effect on the activation of JAK2 and STATs (STAT3 and STAT5) but it appeared to result in enhanced ERK activation thus showing that the TPO/TPOR signalling is limited by Lyn via ERK activation [270]. Activated Lyn can either accelerate inactivation or impede activation of ERK1/2 [270]. Auto-inhibition of SFKs occurs when its conserved C-terminal Tyr residue is phosphorylated by the C-Src kinase (CSK). When this residue is dephosphorylated or repositioned from the SH2 domain, it is activated. Residue Y112 in the intracytoplasmic domain of TPOR is indispensable for Lyn activation [270]. Lyn could be directly bound to this residue or via another phosphoprotein that relieves the binding of Lyn SH2 domain from its regulatory C-terminal Tyr residue [270].

1.7 Adaptor proteins

Most adaptor proteins do not contain intrinsic enzymatic activity but they are able to co-ordinate and regulate various signalling pathways by recruiting necessary proteins/substrates together. They can also aid in the localisation of various signalling proteins to their respective location in the cells.

Adaptor proteins themselves can be localised to the membrane (TM adaptor proteins), cell compartments such as the cytosol and ER, as well as to the cytosol (where they can be localised to the membrane when necessary). They may be ubiquitously expressed or can be expressed in specific cell types.

The ability of adaptor proteins to interact with various proteins/substrates owes to their various protein-binding modules. Generally, adaptor proteins possess an SH2 or phosphotyrosine-binding (PTB) domain that functions to bind to phosphotyrosine residues of their cognate proteins [271, 272]. They may also contain the WW and PDZ motifs that allow for protein-protein interaction to occur [273]. Moreover, adaptor proteins that contain SH3 domains are able to interact with other proteins via their proline-rich domains [274]. Still, others possess a pleckstrin homology (PH) domain that is responsible for their ability to interact with phosphatidylinositol lipids that are present in the plasma membrane or on other proteins [275]. LNK is an adaptor protein that negatively regulates TPOR-mediated signalling and will be further discussed below.

1.7.1 SH2 domain-containing adaptor proteins

LNK (~68kDa), encoded by the SH2B3 gene located on chromosome 12, is a member of a family of SH2-containing adaptor proteins that includes SH2B1 (SH2B or PSM (proline-rich, PH and SH2 domain-containing signalling mediator)) and APS (adaptor protein with PH and SH2 domain) (or SH2B2). The SH2-adaptor protein family is conserved from Drosophila melanogaster to humans. LNK is predominantly expressed in haematopoietic cells such as HSC, HPCs of the myeloid and lymphoid lineage [276], pre-B and pro-B cells, as well as in mature cells such as megakaryocytes and mast cells. LNK maintains megakaryopoiesis, erythropoiesis, and HSC quiescence and self-renewal [175, 249, 276-281]. Only LNK has been found to modulate both megakaryopoiesis and erythropoiesis whereas its family members regulate only erythropoiesis [282, 283]. Enhanced LNK expression in mice bone marrow HPCs diminished megakaryocyte proliferation and endomitosis which are induced by TPO [249]. In contrast, mice with LNK deficiency have a higher ploidy number in their megakaryocytes [249, 284] and develop MPN-like phenotype such as enlarged spleen, expansion of the HSC compartment, and increase in megakaryocyte, platelet, and leukocyte counts [276]. Interestingly, TPO and LNK play paradoxical roles in order to maintain HSC homeostasis and myeloid progenitor expansion [175]. LNK has been reported to be localised in the cytoplasm, perinuclear region, and cell membrane [285, 286].

LNK has one characterised isoform whereas SH2B1 has four isoforms denoted as α, β, γ, and δ [287-290]. SH2B1 isoforms have different C-terminus regions due to alternative mRNA splicing [289-291]. On the other hand, APS has two isoforms denoted as α and β [292]. SH2B1 and APS can act as positive or negative regulators depending on the type of cells they are expressed in and the signalling pathway that they control. Both APS and SH2B1-β upregulate the nerve growth factor (NGF)-mediated PC12 cell differentiation [293, 294]. SH2B1 is a positive regulator of insulin, insulin growth factor (IGF)-1 [295-297], and JAK-STAT signalling induced by GH [298] and leptin. APS is also a positive regulator [291, 299] of GH-induced signalling [298]. LNK is more often associated as a negative regulator (see section 1.8). This is particularly true in haematopoiesis but it plays a paradoxical role in ovarian cancer [300]. High levels of LNK has been detected in ovarian cancer and when it is overexpressed, cell death is markedly reduced [300]. Furthermore, LNK was also shown to be able to prevent endothelial cells from cell death [301]. All three family members of SH2 domain-containing adaptor proteins are able to negatively regulate EPO-mediated signalling [277, 282, 283].

1.7.2 Structure

LNK, SH2B1, and APS possess four structurally similar domains: i) N-terminal region with a) a dimerisation domain where a phenylalanine zipper can be found and b) proline-rich motifs (with a minimal consensus sequence of Pro-X-X-Pro); ii) PH domain that is important for co-localisation at cell membrane [285]; iii) SH2 domain that functions to bind phosphotyrosine residues of their target proteins; iv) C-terminal region (Figure 8). This protein family also possesses several putative serine and tyrosine phosphorylation sites. The last tyrosine residue at the C-terminal region (Y572 in human LNK protein) is conserved amongst all the family members.

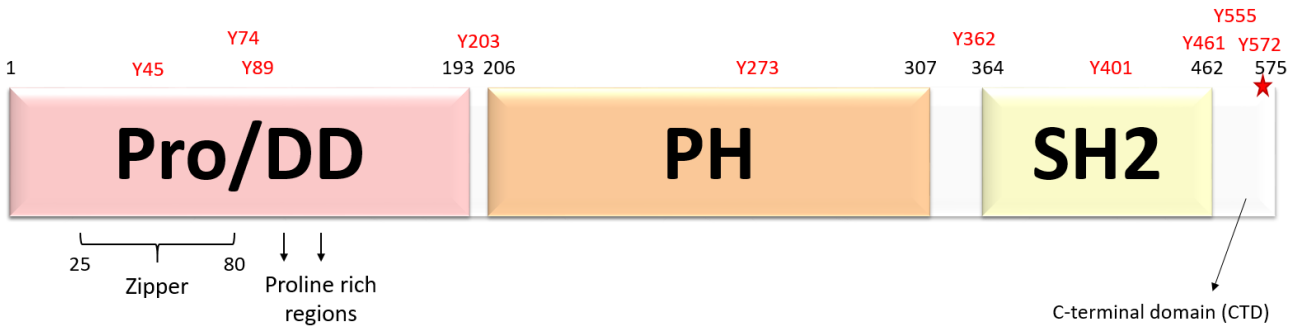

Figure 8: Domains of human LNK.

Pro/DD: Proline dimerisation domain. Red star denotes the conserved C-terminal residue at position 572.

The sequence homology amongst the family members is relatively high, approximately 72-80% [291, 302, 303]. Amongst the three main domains, the N-terminal Pro/DD domain is the most variable region among LNK family members. The phenylalanine zipper, unlike those found in SH2B1 and APS is slightly different in LNK. The zipper found in LNK has a tyrosine and a leucine residue that replace two of the phenylalanine residues present in the SH2B1/APS zipper. This difference probably contributed to the inability of LNK to heterodimerise with APS or SH2B1, as shown using a yeast model [291]. On the contrary, LNK was shown to be able to heterodimerise with SH2B1 in PC12 cells [304]. LNK homodimerisation has also been reported [281], however, this has only been demonstrated in an overexpressed system and, hence, may mask the inability/low affinity of LNK to homodimerise.

The PH and SH2 domains are partly conserved amongst the members of this family. It was discovered that the amino acid sequence of hLNK (human LNK) PH domain is 29% identical to rSH2B1 (rat SH2B1) and 35% identical to hAPS (human APS) whereas the hLNK SH2 domain is 68% identical to rSH2B1 and 65% identical to hAPS [286]. Although SH2B1, APS, and LNK may play different regulatory roles in JAK-STAT signalling, a significant percentage of sequence similarity suggests that there may be some conserved structure-function relationships between the members of this family of adaptor proteins, in particular, referring to the SH2 domain. Nevertheless, each individual member is still able to confer specificity in their own function. The SH2 domains may be monomers or form dimers. The SH2 domain of APS associates as a dimer where one SH2 domain binds to pTyr 1158 and another to pTyr 1162 of the insulin receptor, and both residues are located in the kinase activation loop [305]. Residue W475 of APS is important for this dimerisation as substitution of this residue to histidine causes disruption of the SH2 dimer [305]. It is speculated that LNK may be monomeric as it harbours a histidine residue at a similar location [305]. However, although SH2B1 possesses a tryptophan residue at a similar location to APS, its SH2 domain exists as a monomer [305].

It has been shown that SH2B1 and APS are able to undergo homo- [291, 306] and heterodimerisation [307]. The ability of these adaptor proteins to undergo dimerisation is due to the presence of a phenylalanine zipper located approximately in the middle of the dimerisation domain. The aromatic side chains of the phenylalanine residues reside in the hydrophobic core of the zipper and are bonded by stacking interactions. Modelling studies showed that the mechanism of SH2B1 homodimerisation is almost identical to APS [291]. The ability of these adaptor proteins to homodimerise suggests the creation of a heterotetrameric complex formed by two SH2B1 or APS molecules bound to their two cognate JAK2s [291]. Interestingly, it has been proposed that the heterotetrameric complexes formed by two SH2B1s/APSs with two JAK2s are able to induce JAK2 activation in the absence of

stimulation [291] whereas, in the presence of stimulation, this complex is able to enhance JAK2 signalling in the presence of receptor [291].

1.8 LNK

LNK has been suggested to act as a tumour suppressor protein [308] and this is consistent with its role as a negative regulator of lymphohaematopoiesis. LNK is expressed as a result of a negative feedback mechanism and inhibits signalling mediated by c-Kit [280, 311], c-Fms [312], and tumour necrosis factor receptor (TNFR) [313], as well as those receptors involved in the JAK-STAT pathway such as TPOR [314], EPOR [277], IL7-receptor [276, 315], and platelet-derived growth factor receptor (PDGFR) [316].

LNK affects different downstream signalling pathways. In primary erythroblasts, LNK is able to inhibit the STAT5, MAPK, and Akt pathways that are stimulated by EPO in order to downregulate the production of erythrocytes [277]. In megakaryocytes, LNK inhibits ERK1/2 signalling which is induced by TPO and subsequently reduces the responsiveness of megakaryocytes to the cytokine [284, 317]**.** Downregulation of ERK activation was also reported in stimulated cells expressing IL-3 or c-Kit receptor [276, 311]. LNK effects on activated ERK and Akt differ for different receptors. LNK prevented ERK activation in NIH3T3 cells (expressing endogenous PDGFRA and PDGFRB) that were stimulated with PDGF but without Akt activation [316]**.** In contrast, LNK reduced the activation of Akt but not ERK in c-Fms mediated signalling [312]. Interestingly, LNK was able to diminish the activation of both ERK and AKT in TPOR [249] or EPOR [277] mediated signalling pathway. For TNF, LNK intensified Akt activation but attenuated ERK activation [313]. These differences suggest that there are other LNK domains that may be involved in mediating the varying effects on different signalling pathways depending on which receptor is concerned.

Lack of LNK expression in HPCs results in increased cell growth and differentiation [280, 318] whereas megakaryocytes that are deficient in LNK expression exhibit TPO-hypersensitivity [249]. Loss-of-function of LNK can enhance the oncogenic properties caused by $JAK2^{V617F}$ in an MPN-mouse model [319]. When overexpressed, LNK is able to block constitutive cell proliferation induced by $JAK2^{V617F}$ [309, 310], mutated c-Kit [311, 320], and W515L [285]. LNK was able to down-regulate spontaneous cell proliferation in BaF/3 EPOR cells lines with JAK2 mutations such as the classic V617F and K539L [321]**.** Overexpression of LNK in Ba/F3 TPOR W515L cell lines was able to prevent spontaneous cell proliferation [321]. This inhibition of cell proliferation occurred via suppression of the JAK-STAT, MAPK, and PI3K pathway [321]. LNK overexpression also hampers

the growth of Ba/F3 cells expressing the PDGFR [316]. On the other hand, the R392E (SH2 domain mutation) LNK mutant was unable to do so [316]. LNK also inhibited the growth of 32D cells expressing fusion oncogenic proteins such as TEL-PDGFRB (associated with chronic myelomonocytic leukaemia) or FIP1L1-PDGRFA (associated with systemic mast cell disease and hypereosinophilic syndrome) [322, 323] when expressed [316].

Mice devoid of LNK exhibit elevated B cell levels, enlarged HSC compartment, and increased erythropoiesis and megakaryocytopoiesis due to lack of inhibition which subsequently leads to hyper-responsiveness to several cytokines such as EPO, SCF, and TPO [175, 249, 276, 277, 280, 284, 315]. Particularly, MAPK activation but not STATs and Akt was enhanced and lengthened in the megakaryocytes of these mice [284]. When JAK2 mutation is present in these mice lacking LNK, it was observed that the pool of myeloid progenitor cells was enlarged [324]. The degree of LNK expression was also shown to affect patient prognosis such as in B-ALL [325]. It was found that adult B-ALL that expressed the $IL7R^{high}SH2B3^{low}$ phenotype (overexpression of IL7R but the suppressed expression of LNK) is linked to high-risk ALL, resulting in a decrease of the number disease-free survival patients and increased tendency of relapse [326]. Another subtype of B-ALL, iAMP21 (Intrachromosomal amplification of chromosome 21), is associated with the loss of LNK [327]**.** This loss may be linked to leukaemia progression due to uncontrolled signalling [327]. Patients harbouring this subtype of B-ALL are associated with poor prognosis and susceptibility to relapse [327]. In contrast, increased expression of LNK has been described in the HSCs and platelets of MPN patients, particularly in patients harbouring the $JAK2^{V617F}$ mutation that may be due to the sustained negative feedback mechanism .

1.8.1 Negative regulation of c-Kit signalling

LNK plays a role in regulating B-cell production [315, 328] as LNK-deficient mice demonstrated hypersensitivity to SCF and consequently displayed elevated levels of pre- and pro-B cells [315]. The ICD-JM of c-Kit plays an important role to prevent receptor activation. When c-Kit binds to its ligand, SCF, two residues are transphosphorylated in human c-Kit, Y568 and Y570. Phosphorylation of these residues relieves the autoinhibition of the JM domain of the receptor [329]. These phosphorylated residues can also act as docking sites for various positive and negative regulators. The pY568 residue, in particular, has been shown to bind to PTPs such as SHP1 and SHP2 [330] as well as LNK (via its SH2 domain) [276, 281, 311, 318, 320, 331]. APS also binds to Y568 and Y935 of c-Kit [331]. The

binding of either of these regulators leads to attenuation of SCF-mediated c-Kit signalling [311] [330] in primary mast and progenitor cells.

1.8.2 Negative regulation of PDGFR signalling

The binding of the PDGF ligand to its receptor, PDGFR induces autophosphorylation of the tyrosine residues in the JM-ICD kinase domain where LNK binds to one of the phosphorylated residues. LNK can also bind to inactive PDGFRs although ligand stimulation increased LNK binding to the receptor [331]. This result suggests that LNK can constitutively bind to PDGFR [316]. On the other hand, LNK R392E mutant (SH2 function disruption) maintained the receptor binding property but this was significantly reduced [316]. LNK SH2 domain is however more important for binding to oncogenic FIP1L1-PDGFRA fusion protein than to WT PDGFRA or PDGFRB [316].

1.8.3 Negative regulation of fms-like tyrosine kinase 3(FLT3) signalling

Binding of ligand to FLT3 results in the phosphorylation of the ICD tyrosine residues 572, 591, and 919 (conserved residue) which serve as binding sites for LNK [332]. The binding of LNK to these residues via its SH2 domain results in its activation [332]. Both the WT FLT3 receptor and constitutively activated ITD-mutated FLT3 receptor can phosphorylate LNK [332]. LNK activation results in subsequent inhibition of the STAT5, ERK1/2, and PI3K/Akt signalling, as well as reduced cell proliferation of cells expressing WT or FLT3 mutants [332].

1.8.4 Negative regulation of JAK-STAT signalling

In the JAK-STAT signalling pathway, LNK negatively inhibits downstream signalling of TPOR, EPOR [249, 277, 324], IL7R [333], and others. Hence, disruption of LNK function can result in cytokine hypersensitivity to EPO and TPO [277, 284] with subsequent erythrocytosis and thrombocytosis, respectively. It has been suggested that LNK associates with JAK2 in haematopoietic stem/progenitor cells whereas it associates with JAK3 in B cell lineage cells [333]. By associating with JAK3/IL7R, LNK regulates pro-B and pre-B progenitor cell homeostasis [333]. Besides normal

signalling through the JAK2 pathway [278, 314], LNK can also dampen aberrant signalling by inhibiting $JAK2^{V617F}$ [278].

1.8.5 Proposed mechanism of inhibition for LNK

Although the role of LNK as a negative regulator of cytokine signalling has been well-documented, it is still unclear as to how it is able to modulate JAK-STAT signalling, although, a few mechanisms have been proposed.

1.8.5.1 LNK as a competitive inhibitor

When overexpressed or in the presence of cytokine stimulation, JAK2 is autophosphorylated particularly at Y813 which is located in the consensus YXXL motif in the pseudokinase-kinase linker [278, 334]. Interestingly, it was demonstrated that Y813 of JAK2 can also be phosphorylated in the absence of stimulation albeit at a slower rate [291]. This phosphorylated residue has been shown to be a docking site for SH2B1, APS, and LNK where they bind via their SH2 domains [291, 299, 334]. The corresponding phosphorylated tyrosine residue in JAK3, Y785, is also a binding site for the SH2B1-β adaptor protein. After docking to the pY813 on JAK2, the SH2 domain-containing adaptor protein family member is in turn phosphorylated by JAK2 [278, 282, 286-288, 293, 335-340]. Phosphorylation activates the adaptor proteins thereby allowing them to either enhance or inhibit downstream signalling. It has been shown that docking to pY813 allows SH2B1-β to amplify JAK2 and STAT5B activity. Due to the ability of all members to bind to pY813, they may compete against LNK for binding. It is currently unknown as to what factors determine which adaptor protein binds to JAK2 at a particular time and how binding to the same residue can trigger different responses i.e. signal activation or inhibition. It was proposed that LNK can compete for binding to the c-Kit receptor where it binds to the JM-ICD region to prevent positive regulators from binding [280, 311].

1.8.5.2 LNK binds via other domains besides the SH2

Although pY813 acts as an important binding site for these adaptor proteins, there may be other JAK2-binding sites unique to the particular adaptor protein that may facilitate positive or negative

regulation of signal transduction. SH2B1, APS, and LNK have also been reported to bind inactive JAK2. SH2B1-β can bind to unstimulated JAK2 via one or more sites located in its N-terminal region (amino acids 269-555 that includes the PH domain, PH-SH2 linker and a small part of the SH2 domain) albeit with a lower affinity [341]. The ability of SH2B1-β to bind to these lower affinity sites makes it able to recruit more SH2B1-β that surrounds JAK2 as proposed [341]. The recruitment of SH2B1-β may prevent abnormal JAK2 activation [341]. On the other hand, when JAK2 is activated, the presence of a high concentration of SH2B1-β surrounding JAK2 will allow its rapid binding to JAK2 phosphotyrosine residues and consequent enhanced JAK2 signalling [341].

LNK has been shown to bind to another JAK2 site, the pY613 residue (minor binding site) that is located in the pseudokinase domain [278]. Other low-affinity interaction(s) with inactive JAK2 not mediated by LNK SH2 domain may probably serve to stop abnormal JAK2 signalling [299, 309, 341]. Studies suggest that the LNK NTD may facilitate weak interactions with inactive JAK2 [309]. However, it is not clear as to which residues are involved in this interaction. LNK can also bind to mutant proteins such as $JAK2^{V617F}$ [278, 285, 309] and TPOR W515L via its SH2 domain and NTD where LNK NTD binds stronger to $JAK2^{V617F}$ than wild-type JAK2 [309]. The LNK PH domain was also suggested to be able to bind to inactive JAK2 through a weak interaction [310] but the residues that are involved in this interaction remain to be elucidated. In EPOR-mediated signalling, only SH2 appears essential for LNK function and not PH or the conserved C-terminal tyrosine residue [277].

1.8.5.3 LNK expression levels

JAK2 may have a differential binding affinity for SH2B1, APS, and LNK, or a preferential binding of a particular adaptor protein may be influenced by its respective expression levels. Interestingly, low levels of SH2B1/APS have been reported to cause an increase in JAK2 activation [291]. This has been proposed to be caused by the ability of SH2B1/APS to bring its associated JAK2s in closer proximity to each other. In contrast, high-level expression of these adaptor molecules resulted in a paradoxical effect where JAK2 activity is abrogated [291]. Thus, this suggests that depending on the relative levels of SH2B1 or APS, they are able to either positively or negatively regulate JAK2 kinase activity [291]. This effect may also be translatable to LNK.

1.8.5.4 LNK possesses a novel structure

There are limited studies on the structural changes that occur as LNK binds JAK2. This is due in part because of the lack of any LNK domains or full-length crystal structures. Nevertheless, LNK binding may induce a conformational change in activated JAK2, thereby resulting in inhibition of JAK2 kinase activity. Binding of LNK SH2 domain to regions around the pseudokinase domain of activated JAK2 may induce the pseudokinase domain to return to its original position where autoinhibition of JAK2 is restored. Other novel mechanisms of structural changes in JAK2 that are induced by LNK may also occur. It was recently discovered that SOCS3, a JAK2 inhibitor, inhibits JAK2 via its KIR. The KIR obstructs the substrate-binding site of JAK2 to prevent JAK2 from interacting with and phosphorylating its substrate [81]. It remains a possibility that LNK may contain an undiscovered mechanism that is similar to the KIR of SOCS3. A higher binding affinity was observed between LNK and $JAK2^{V617F}$ compared to wild-type JAK, which may be due to high levels of phosphorylation [6, 309, 310, 342].

1.8.5.5 LNK regulates its inhibition via other proteins

LNK can bind to ubiquitin ligases such as CBL [309, 343] which may facilitate degradation of its associated receptor/JAK [344]. Activation of the insulin receptor recruits APS, where its phosphorylated C-terminal tyrosine residue binds CBL [344]. The tyrosine kinase binding (TKB) domain of CBL binds to the (RA(V/I)XNQpY(S/T)) sequence in APS (pTyr613) [345-347] which is also highly conserved in LNK and SH2B1 [348]. This binding allows APS to inhibit signalling [282, 349].

1.8.6 LNK mutations in myeloid malignancies

Germline and somatic LNK mutations have been reported in patients affected by familial and sporadic MPNs [23, 350] (5-7%) [23], MDS (3-5%) [25, 351-353], early T-cell acute lymphoblastic leukaemia (T-ALL) (5%) [354], B-cell acute lymphoblastic leukaemia/lymphoma (B-ALL), and post-AML MPNs (10%). The frequency of the occurrence of LNK mutations is typically low, particularly in chronic-phase MPN patients. In T- and B-cell ALL, LNK mutations are usually frameshift or deletion mutations whereas, in MPNs, missense mutations are usually found [350]. This suggests that a more

severe loss of LNK function is needed to cause lymphoid malignancies [350]. LNK mutations can also occur during transformation to leukaemia [350].

The role of LNK mutations as a driver or co-operating mutation is debatable. It has been previously reported that LNK loss-of-function occurs in ET and MF patients but is not able to confer MPN pathogenesis alone [353, 355]. LNK mutations can be present concomitantly with driver mutations such as those in JAK2, TPOR, and CALR as well as with other genes such as CBL and TET2. However, the frequency of occurrence of LNK mutations in patients with or without the $JAK2^{V617F}$ mutation is similar [24]. It is not known whether these mutations occurred in the same or different clonal population, which might have different effects on the phenotype of the disease [24]. Mice lacking both TP53 and LNK gene develop B-ALL suggesting that TP53 can also work hand in hand with LNK in this disease [333]. The co-existence of LNK mutations with other driver mutations suggests its possible role as a co-operating mutation to cause MPN. On the other hand, a germline LNK mutation was reported in a triple-negative PV patient which may suggest LNK mutations can act as driver mutations, however, the association of this germline mutation with the disease was not clear [356]. A study has reported the presence of a LNK mutation in two $JAK2^{V617F}$-negative MPN patients [353]. Furthermore, mice harbouring a homologous LNK mutation were susceptible to myeloproliferative diseases [276]. These studies suggest that a more severe homozygous LNK mutation can drive MPN pathogenesis although other findings suggest that the heterozygous C613G loss-of-function mutation alone was able to induce MPN [353]. Moreover, the frequent occurrence of LNK heterozygous PH mutations in MPN patients suggests that the loss of one allele is sufficient to lead to haematologic malignancies. This evidence suggests that LNK mutants may not only be secondary mutations as previously thought but that they can drive MPN pathogenesis in these patients. Indeed, LNK knockout mice exhibit excessive HSC proliferation with enhanced self-renewal property [276, 278].

Currently, LNK mutations that have been associated with myeloid malignancies are primarily point mutations affecting the PH domain. Because of this, the PH domain was regarded as a ‘hot spot’ [25]. Clinical PH domain point mutations include E208Q [353], A215V [25], G220V, G220R, A223V, D234N, and G229S [24] and those reported in MPN patients were mostly heterozygous [24, 353]. This suggests that loss-of-function of one LNK allele may be sufficient to drive MPN pathogenesis. Further evidence to support this haploinsufficiency model was demonstrated using murine models. $LNK^{-/+}$ mouse models exhibit an intermediate, less severe MPN-like feature compared to $LNK^{-/-}$ mouse models. A ‘dosage effect’ is apparent where the loss of both alleles results in a more severe phenotype compared to the loss of one allele [276]. PH domain point mutants resulted in partial disruption of LNK function. It was observed that PH domain LNK mutants, compared to wild-type,

have reduced inhibition on STAT5 phosphorylation and cell growth [277, 353, 355, 357]. The partial disruption of LNK activity could be due to the reduced ability of the mutant proteins to localise to the cell surface and bind JAK2, with a consequent reduction in inhibition of JAK-STAT signalling [353]. In contrast, another study showed that PH domain mutants, similar to wild-types, were able to localise to both the cytoplasm and cell surface [355]. These mutants also retained their JAK2 binding ability [355]. However, a LNK mutant with synthetic deletion of the PH domain has abolished cell surface localisation ability [285]. It may be possible that the degree of retained LNK inhibitory function depends on the severity of the mutation type (i.e. missense mutations might have a lesser impact on LNK function compared to whole PH domain deletion).

Clinical LNK SH2 mutations such as Q423X, have also been reported in MPNs [352]. Unlike PH domain point mutants, SH2 mutations cause a more severe disruption of LNK function [249, 277, 278, 285, 353, 355]. This may be due to the decreased ability of LNK to associate with JAK2. The effect of SH2 domain mutation has been studied using a synthetic R392E mutant and it was found that this mutant abolished SH2 domain function. Ba/F3-TPOR cells harbouring this mutant exhibit increased cell proliferation [285] and loss of inhibition on JAK-STAT signalling [353] which may be attributed to the loss of JAK2 binding [355]. LNK mutations affecting both the PH and SH2 domains have also been reported, the E208X [25] and DEL (603-607delGCGCT;613 C>G) [353] mutation which result in truncation of these domains. Studies have shown that a synthetic truncation mutant that lacks the PH domain is unable to localise to the cell surface [285] and will most likely result in abolished LNK function.

Mutations in the LNK C-terminal domain (CTD) have also been reported. Clinical mutations found in the CTD region include R551W and I568T [352] but their pathogenic significance is unknown. Although CTD mutations have been discovered, there have not been reported any mutations of the conserved LNK C-terminus residue at position 572. To investigate the possible effects of Y572 mutation on LNK inhibitory function, the murine equivalent Y536 was mutated to phenylalanine [249]. This mutation did not affect murine LNK inhibitory function [277] on cell proliferation [249] nor JAK2 binding [278]. This Y536 residue has also shown to play no significant role in TPO-mediated signalling, although the function of its human counterpart, Y572, has not been investigated [249, 311]. In the EPOR-mediated pathway, this tyrosine residue is essential but not necessary for EPO-induced erythroblast survival and cell growth [277]. However, deletion of the C-terminal tail of the murine LNK only affected its function partially [281]. Overall, SH2 mutations appear to cause a more severe phenotype compared to PH or CTD mutations. Although various LNK mutations have been reported, it is currently unknown as to how these mutations affect LNK function and drive myeloid malignancies.

LNK polymorphisms have also been reported and these may play a role in contributing to the different clinical phenotypes observed in patients and may confer a predisposition to MPN development [356]. The position 262W (c.784T>C) nonsynonymous polymorphism (located in the PH domain) has a strong relation with the occurrence of $JAK2^{V617F}$ in MPN patients [358]. This suggests that LNK mutations can predispose patients to progress to MPNs or leukaemia [358]. The p.262W polymorphism is often related to MPN patients whereas the p.262R polymorphism is more related to CML [356]. This observation suggests that polymorphisms in LNK can play a role in causing clinical phenotypic variations by affecting the differentiation of malignant cells in the bone marrow [356]. The R262W polymorphism is also linked to increased risk of autoimmune diseases [359], myocardial infarction, and hypertension.

It was proposed that mutant LNK can exhibit a dominant-negative effect. This may be possible because most LNK mutations affect either the PH and/or SH2 domain. Therefore, functional NTD is retained. Mutant proteins that are not able to translocate to the cell surface may form a complex with wild-type LNK via homophilic interactions between the NTD [281], sequestering the complex in the cytoplasm and preventing LNK interaction with its target kinases and downstream signalling proteins [281]. A previous mouse study showed that co-expression of LNK R364E mutant (R392E in humans) with endogenous LNK facilitates the engraftment of HSCs and progenitor cells [281] suggesting that mutant LNK is able to confer a dominant-negative phenotype. Furthermore, NTD deletion of R364E/C-terminal tail deletion mutant abolished its dominant-negative effect [281] demonstrating the importance of NTD for this effect. On the contrary, another study showed that there was no observed growth advantage (in terms of colony formation) when PH domain point mutants expressed in murine bone marrow cells that also express endogenous wild-type LNK [355]. Moreover, these mutants retained the ability to suppress the growth of $LNK^{-/-}$ bone marrow cells although this suppression was slightly lower compared to the one observed in wild-type LNK [355]. However, it is unclear as to why this difference exists. These findings may in part explain why LNK R392E mutants cause a more severe disruption of LNK function than PH domain point mutants. In addition, LNK R364E has been observed to still be able to bind JAK2, phospho-JAK2, EPOR, and phospho-EPOR when stimulated by EPO although the phosphorylation of LNK and its ability to inhibit EPOR signalling were abolished [277]. On the other hand, LNK R364E was not able to bind phospho-JAK2 in the context of TPOR signalling [278]. In support of this finding, the R364E mutation was found to completely abolish the ability of LNK to interact with phosphorylated c-Kit [281].

1.8.7 LNK mutations in non-haematopoietic diseases/disorders

Besides myeloid malignancies, LNK mutations have also been associated with non-haematopoietic diseases and disorders. LNK is an important modulator of inflammation [312, 313, 316, 360] where polymorphisms in the LNK gene have been shown to be linked to autoimmune disorders such as celiac disease and type I diabetes. LNK has also been implicated in vascular disease [359] as it negatively regulates the TNF signalling pathway via downregulation of the ERK and PI3K [313]. Reduced LNK regulation in dendritic cells contributes to increased inflammatory response via IFN-γ that is produced by T cells [361]. LNK is also an important player in post-myocardial infarction inflammation and fibrosis [362], as well as hypertension [363]. Furthermore, LNK can regulate integrin signalling in platelets and endothelial cells that are involved in regulating cell adhesion and migration for the formation of blood clots.

1.8.8 LNK as a therapeutic agent

Interestingly, delivery of WT LNK with octa-arginine (cell-penetrating peptide) modification (WT Lnk R8) resulted in inhibition of leukaemic cell proliferation [364]. WT Lnk R8 can suppress the growth of M-MOK leukaemic cells but not of non-haematopoietic cells, by inducing cell death via apoptosis [364]. WT Lnk R8 binds to JAK2 and suppresses the activation of the JAK-STAT and ERK pathway that is induced by TPO in M-MOK cells [364]. WT Lnk R8 also inhibits megakaryopoieisis which is stimulated by TPO [364]. This peptide is also capable of inhibiting cell growth in signalling pathways regulated by JAK2 such as IL-3 and GM-CSF [364]. However, as the effect of the peptide is quite broad, this may lead to side effects such as thrombocytopaenia [364].

Research Aims

The overarching aim of this project is to deepen our understanding on how JAK-STAT signalling is regulated by the TPOR (encoded by *MPL*) and its negative regulator, LNK in normal haematopoiesis and blood cancers (myeloproliferative neoplasms and leukaemia). The aims that have been set out below seek to define the functional changes that occur in the receptor in order to mediate JAK-STAT activation and to shed light on the structural mechanisms that are used by LNK to downregulate this signalling. Improved understanding of these mechanisms will reveal novel avenues for drug development (to inhibit TPOR or specifically JAK2) and improve current treatment strategies for haematological malignancies such as MPNs and certain types of leukaemia caused by various TPOR and LNK mutations (e.g. W515K, T487A, and S505N in TPOR, and E395K and R425P in LNK).

Aim 1. (A): To analyse the effects of various TPOR TMD activating mutants on receptor function. For the purpose of the cell-based assays set out in aim 1 (B), stably-transduced Ba/F3 cells harbouring the clinical mutations (W515K, T487A, S505N) that lie in the TMD and surrounding (juxtamembrane) regions will be generated. The functionality of these mutants will be confirmed by analysis of their signalling and proliferative capabilities. Furthermore, stably-transduced Ba/F3 cells that harbour various engineered mutations at the important TMD domain of TPOR will be generated to investigate the specific parts of the domain that are important in regulating TPOR structure-function.

Aim 1. (B): To identify peptide antagonists against the ECD-JM/ TMD of TPOR using phage display. Clinically available treatments for MPN patients harbouring activating TPOR mutants still rely on JAK2 inhibitors that are not specific *i.e.* they do not target TPOR and in addition, they also inhibit other JAKs and resulting downstream signalling, which are vital for physiological functions. This fact clearly represents a gap in current treatment modalities for these patients and encourages the need for the development of better targeted treatments. This study will seek to discover suitable peptide antagonists against the crucial signal-modulating TPOR domain, the ECD linker/TMD. This aim will involve the search for candidate peptides *via* phage display and these peptides will be screened for functionality using cell-based assays.

Aim 2: To investigate the effect of cytokine stimulation and mutations on the molecular dynamics of the transmembrane receptor, TPOR in the plasma membrane using sptPALM. The majority of TPOR understanding is based on biochemical works with little or no relation to the spatiotemporal patterns of TPOR and its activity. Specifically, the lateral diffusion/mobility of the W515K and Box1 mutation in comparison to WT TPOR will be examined on the surface of live cells. This aim seeks to investigate if the constitutively active TPOR W515K and Box1 mutants mediate their effect on signalling via modulating their rates of lateral diffusion by tracking single molecules. Cytokine stimulation with thrombopoietin (TPO) will further provide critical information to better understand this effect.

Aim 3. (A): To fully characterise the region of LNK that interacts with and regulates JAK2 and/or TPOR activity in co-operation with its SH2 domain. It has been well established that LNK associates with phosphorylated JAK2 (pY613 and 813) via its SH2 domain [278] and that other LNK domains may associate with JAK2 in its inactive state [309, 310]. Nevertheless, there is a lack of information to explain the detailed mechanisms on how LNK inhibits JAK2/TPOR. This aim seeks to elucidate whether other LNK domain interactions with JAK2/TPOR are crucial for their inhibitory effect, i.e. the ability of other LNK domains to affect SH2 domain binding to JAK2/TPOR, and their effects on downstream signalling. By elucidating these domain interactions, novel mechanisms for JAK2/TPOR inhibition will be revealed.

Aim 3. (B): Expression and purification of LNK for structural and biochemical assays. Hitherto, the crystal structure of LNK has not been solved and this remains one of the main reasons contributing to the lack of understanding of LNK inhibitory function. The crystal structure will reveal functional sites of LNK and also predict exactly which sites of LNK are associated with JAK2. Therefore, solving the crystal structure of full-length LNK is one of my important aims, although if obtaining LNK crystals becomes difficult, the soluble protein will be used for interaction studies and kinase activity assays. The goal of this aim is also to facilitate understanding regarding the role of the important domains identified in Aim 2(A), although this will be better addressed by obtaining interacting LNK-JAK2 crystals. Furthermore, the outcome of this aim will allow us to predict possible conformational changes that can occur due to alterations of certain amino acid residues that lead to the inability of mutant LNK to inhibit its associated proteins. Addressing this aim will facilitate the development of novel treatments.

Chapter 2

Materials and General Methods

Cell Culture

Ba/F3 murine pro-B cells (RRID:CVCL_0161) are dependent on the cytokine IL-3 for growth. Ba/F3 parental and stably-transduced cells were maintained in RPMI (Roswell Park Memorial Institute)-1640 (Sigma) supplemented with 10% (vol/vol) foetal bovine serum (FBS) (Gibco, Thermo Fisher Scientific), 1× IL-3 (mouse recombinant 100× IL-3 produced in SF9 baculovirus cells), 1× GlutaMAX™ (Gibco, Thermo Fisher Scientific), and 1× sodium pyruvate (Gibco, Thermo Fisher Scientific). Adherent cell lines such as Lenti-X 293T, human embryonic kidney 293 (HEK293), HEK293T, and HeLa cells were maintained in DMEM (Dulbecco's Modified Eagle Medium) (Sigma) supplemented with 10% (vol/vol) FBS and 1× GlutaMAX™ (Gibco, Thermo Fisher Scientific). HeLa cells were generously provided by Dr Eloïse Dray (UT Health San Antonio). All cell culture flasks were supplied by Corning® Costar® (Sigma-Aldrich). Puromycin and Hygromycin B were purchased from Gibco (Thermo Fisher Scientific) and AG Scientific, respectively.

Circular Polymerase Extension Cloning (CPEC)

Polymerase chain reaction (PCR) was performed to generate fragments of DNA with overlapping complementary ends suitable for CPEC based on the method previously described [131]. For each CPEC assembly, 200 ng of the largest DNA fragment and equimolar ratio of other fragments were added to the Phusion HF reaction according to the manufacturer's instructions (New England Biolabs, NEB). CPEC was performed using a thermo cycler (Eppendorf) with cycling conditions at 98°C for 30 seconds (one cycle), 20 cycles of {98°C for 10 seconds, 70°C for 30 seconds, and 72°C for 23 seconds/kilobase pair final construct size}, and 4°C for 5 minutes (one cycle). CPEC products were transformed into either DH5α or Stbl3 *E. coli* cells.

Gateway (GW) Cloning

Gateway reaction (BP and LR reaction) was performed according to the manufacturer's instructions (Thermo Fisher Scientific). For each BP reaction, 70 ng/kilobase pair of purified PCR product, 75 ng of donor vector (pDONR221), and 1 µl of BP Clonase II enzyme mix was added to the reaction. The reaction was incubated at room temperature for at least 3 hours. For each LR reaction, 4 µl of BP reaction, 140 ng of destination vector of choice, 1 µl 112mM NaCl and 1 µl of LR Clonase II enzyme mix was added to the reaction. The reaction was incubated at room temperature for 1-3 hours. DH5α or Stbl3 cells was transformed with 1 µl of either the BP or LR reaction on kanamycin (30 µg/ml) or carbenicillin (100 µg/ml)-containing LB agar plates.

Preparation of Chemically Competent *Escherichia coli (E. coli)* Cells

DH5α or Stbl3 *E. coli* cells were allowed to grow for 16 hours at 37°C with shaking at 200 RPM in LB media without antibiotics. The culture was diluted 30-40 times in LB media (no antibiotics) and allowed to grow at 37°C with shaking at 200 RPM until the culture reaches an OD_{540} of approximately 0.4-0.6. Cells were centrifuged at 4500 RPM (rotor radius: 8.4 cm) at 4°C for 5 minutes. Supernatant was removed and cells were resuspended in ice-cold 50 mM calcium chloride and left to incubate on ice for 30 minutes to an hour. The cells were centrifuged at 4500 RPM (rotor radius: 8.4 cm) at 4°C for 5 minutes and resuspended in a tenth volume of 50 mM calcium chloride containing 15% (vol/vol) glycerol. Cells were aliquoted into tubes and snap-frozen in dry ice/ethanol baths immediately. Competent cells were stored at -80°C.

Bacterial Transformation

Plasmid DNA or ligation mixture was added to chemically competent *E. coli* cells and left to incubate on ice for 30 minutes. Heat shock was performed at 42°C for 40 seconds and the cells immediately placed on ice for 2 minutes. Following, 1 ml LB medium was added to the cells and incubated at 200 RPM at 37°C for 1-2 hours to allow for expression of antibiotic resistance gene. The culture was plated on LB agar plates containing appropriate antibiotics (100 μg/ml carbenicillin or 30 μg/ml kanamycin) and allowed to incubate overnight at 37°C.

Plasmid DNA Isolation using Alkaline Lysis

Bacterial cultures were centrifuged at 14 000 RPM (rotor radius: 8.4 cm) for 1 minute and the supernatant discarded. Cells were re-suspended in resuspension buffer containing RNase A and alkaline lysis was carried out according to manufacturer's protocol (Favorgen). Plasmid concentration was determined using NanoDrop™ Lite Spectrophotometer (Thermo Fisher Scientific).

Agarose Gel Electrophoresis

SeaKem® LE Agarose (Lonza) was melted in 1x tris-acetate ethylenediaminetetraacetic acid (TAE) buffer in an appropriate amount depending on the desired final percentage of the gels. After the molten agarose was allowed to cool for 20-30 minutes, Sybr Safe DNA gel stain (Invitrogen) was

added at a 1:30 ratio. The mixture was poured into a gel cast and allowed to solidify. Before loading into gel, appropriate amounts of plasmid DNA or PCR products was added with 10x DNA loading buffer (50% dye, 50% glycerol). A 1kb DNA ladder was also loaded as a marker for size and quantification (NEB). Electrophoresis was performed at 100V in 1X TAE buffer.

DNA Sequencing

DNA sequencing was performed by the Australian Genome Research Facility (AGRF, University of Queensland, QLD, Australia). Plasmids to be sequenced was prepared as following: plasmid (600 – 1500 ng) and primer (10 pmol final concentration) in a total volume of 12 µl made up to final volume with milliQ. The primers used for sequencing are listed in Appendix Section D.

Cytokines

Recombinant human TPO were purchased from R&D Systems. Mouse recombinant IL-3 was produced using SF9 Baculovirus expression by the Protein Expression Facility at University of Queensland.

Preparation of Sodium Dodecyl Sulphate-Polyacrylamide Gel Electrophoresis (SDS-PAGE) Gels

Laemmli resolving gel was prepared by adding 40% (vol/vol) acrylamide/bis Solution, 29:1 (final concentration 8% (vol/vol)) (Bio-Rad), N,N,N’-tetra-methylethylenediamine (TEMED) (final concentration 0.05% (vol/vol)) (Sigma-Aldrich), and 10% (wt/vol) ammonium persulphate (final concentration 0.05% (vol/vol)) to the Laemmli resolving gel buffer. The mixture was transferred to the Mini-PROTEAN® casting apparatus (Bio-Rad). A layer of water was added to the unpolymerised gel to ensure a smooth interface. After polymerisation, the water was removed and the stacking gel was added (Laemmli stacking gel buffer with 40% acrylamide/bis solution (final concentration 4.5% (vol/vol)), TEMED (final concentration 0.1% (vol/vol)), and 10% ammonium persulphate (final concentration 0.06% (vol/vol)) on top of the resolving gel followed by a spacer comb.

Western Blotting

Supernatant was mixed with 3× SDS sample buffer (containing 0.1 M dithiothreitol (DTT)) and heated to 98°C for 5 minutes before the samples were run on SDS-PAGE gel at 100 V in gel tanks filled with 1x SDS running buffer. Precision Plus Protein™ Kaleidoscope™ Prestained Protein Standards (BioRad) was used as a molecular weight marker. After electrophoresis, semi-dry transfer of proteins onto PVDF membranes was performed using Trans-Blot® Turbo™ Transfer System (BioRad). After transfer to PVDF membranes and blocking in 5% (wt/vol) bovine serum albumin (BSA) (Gibco)/ tris-buffered saline–Tween (TBST), immunoblotting was performed overnight at 4°C with corresponding primary antibodies in a solution of 5% (wt/vol) BSA/TBST. Secondary mouse or rabbit antibodies conjugated to horseradish peroxidase were used to detect the corresponding primary antibodies (see Appendix Section E). Visualisation of antibody was performed by using enhanced chemiluminescent (Clarity™ Western ECL Substrate (Bio-Rad) or Immobilon Western Chemiluminescent horseradish peroxidase (HRP) Substrate (Merck Millipore)) coupled with the ChemiDoc™ Touch Gel Imaging System. Densitometric analysis of immunoblot was performed using Fiji software.

Antibodies and Enzymes

Primary antibodies were purchased from Cell Signaling Technology®, BioLegend, and Merck (Millipore) (see Appendix Section E). HRP-conjugated secondary antibodies were supplied by Cell Signaling Technology® (MA, USA). Restriction enzymes used for molecular cloning were purchased from NEB (Genesearch Ltd.).

Stripping and Re-probing of PVDF Membranes

PVDF membranes were incubated with mild stripping buffer with agitation for 10 minutes, twice. Membranes were rinsed and incubated with phosphate buffered saline (PBS) with agitation for 10 minutes, twice. Finally, the membranes were washed in TBST with agitation for 5 minutes, twice. Blots were blocked for at least 30 minutes before re-probing.

Coomassie Staining and Destaining

SDS-PAGE gels containing protein samples were incubated with coomassie stain (R-250 (final concentration 0.1% (wt/vol)), acetic acid (final concentration 10% (vol/vol)), methanol (final

concentration 40% (vol/vol)) for 30 minutes followed by de-staining solution (methanol (final concentration 20% (vol/vol)), acetic acid (final concentration 10% (vol/vol)) for 30 minutes, twice. Gel was destained overnight.

Statistical analysis

One-way and two-way analysis of variance (ANOVA) testing were used. All statistical analyses were performed using GraphPad Prism® version 7.03 software.

Buffers and Solutions

Chemicals

All chemicals and reagents used were of analytical grade and purchased from Sigma-Aldrich unless otherwise specified.

Lysogeny Broth (LB) and Agar Plates

LB medium was prepared by dissolving 10 g of bacto-tryptone, 5 g of yeast extract, and 5 g of NaCl, in 1 L final volume of milliQ water, and sterilised by autoclaving. LB agar was prepared by dissolving 15g of agar in LB medium to a 1L final volume of water, sterilising by autoclaving and cooling to 50°C before the respective antibiotics were added. The liquefied agar was poured into Petri dishes and left at room temperature to solidify and finally, stored at 4°C.

Phosphate Buffered Saline

A 1× working PBS solution was prepared by dissolving one tablet of PBS (10 mM phosphate, 2.68 mM KCl, 140 mM NaCl) (Thermo Fisher Scientific) in 500 ml of water.

20% Sodium Dodecyl Sulfate (SDS) Solution

A 20% (wt/vol) SDS solution was made by dissolving 10 g SDS in 50 ml of water.

50× TAE Buffer

A 50× concentrated stock was made by dissolving Trizma® base (final concentration 2 M), EDTA (final concentration 50 mM, pH 8), and glacial acetic acid (final concentration 1 M) to a final volume of 1 L of water. A 1× TAE buffer was prepared by diluting 50-fold of the 50× TAE buffer with water.

Laemmli resolving gel buffer

Laemmli resolving gel buffer was prepared by mixing 1:4 of 1.5 M Tris pH 8.8 and a final concentration of 0.1% (vol/vol) of 20% SDS.

Laemmli stacking gel buffer

Laemmli stacking gel buffer was prepared by mixing 1:7 of 1 M Tris pH 6.8 and a final concentration of 0.1% (vol/vol) of 20% SDS.

10× SDS running buffer

A 10× SDS running buffer was prepared by dissolving Trizma® Base (final concentration 250 mM), glycine (final concentration 1.92 M), and 40% (wt/vol) SDS (final concentration 1%) to a final volume of 1 L of water.

1× SDS running buffer

A 1× SDS running buffer was prepared by diluting 10-fold of the 10× SDS running buffer with water.

3× SDS sample buffer

A 3× SDS sample buffer was prepared by mixing Tris-HCl (final concentration 150 mM, pH 6.8), SDS (final concentration 6%), bromophenol blue (0.3% final concentration), and glycerol (final concentration 30%) to a final volume of 50 ml milliQ water.

10× DNA loading dye

A 10× DNA loading dye was prepared by mixing dye and glycerol (final concentration 50%) to a final volume of 10 ml milliQ water.

10× TBS

A 10× TBS was prepared by dissolving Tris (final concentration 200 mM) and NaCl (final concentration 1.5 M) in milliQ water, pH adjusted to 7.6, and made up to a final volume of 1 L with milliQ water.

1× TBST

A 1× TBS-Tween solution was prepared by diluting 10-fold of the 10× TBS with milliQ water and Tween-20 was added to a final concentration of 0.1%.

Mild stripping buffer

A 1x mild stripping buffer was prepared by dissolving 15 g glycine, 1 g SDS, 10 ml Tween-20 in milliQ and pH adjusted to 2.2.

Chapter 3

Analysis of TPOR TMD Activating Mutants and Development of Novel Peptides Targeting TPOR

Introduction

Oncogenic TPOR mutations that result in constitutive receptor activation and downstream signalling are frequently located in the TMD and JM regions. In MPNs, mutation in the ICD-JM at the W515 residues such as W515L/K are most commonly reported. These findings are consistent with the role of the TMD and JM regions in regulating receptor activation. On the other side of the spectrum, inactivating mutations can result in CAMT where patients present with severe thrombocytopaenia. TPOR agonists have been developed to treat thrombocytopaenic patients such as those afflicted with CAMT, ITP, MDS, bone marrow failure, liver cirrhosis, autoimmune diseases, and those undergoing chemotherapy/radiation. Several TPO agonists have been developed and of interest is Eltrombopag (Promacta), a small molecule that binds to the TMD of TPOR. The ability of Eltrombopag to bind to the TMD to exert its effects provides the rationale for developing TPOR antagonists against this region. In this chapter, the phage display screen was utilised to discover peptide antagonists targeting constitutively active TPOR mutants.

The phage display screening method was first described in 1985 which can be used to identify protein-DNA, protein-peptide, and protein-protein interactions [365]. The versatility of this method has enabled it to be utilised for many important applications such as vaccine development [366], discovery of bioactive peptides (agonists and antagonists) [367-373], drug target validation [374, 375], discovery of drug delivery agents [376, 377], and antibody epitope mapping [378]. In comparison to cDNA library screening, phage display is a high-throughput technology that is time and cost effective that enables a vast number of various oligonucleotides or peptides, ~10^{10} to be screened at any one time against a target of interest [379, 380]. The ability to screen large pools of unique oligonucleotide/peptide sequences increases the probability of discovering high affinity oligonucleotides or peptides that can bind to the target of interest. Phage display technology takes advantage of the properties of bacteriophages that have been used as a platform include T4 [381], T7 [382], and λ [383] but filamentous phages (such as fd, f1, and M13) are more commonly used [383]. Filamentous phages are small, long, and have filament-like shape. They have a basic genome arrangement [384] with genes that encode capsid proteins (pIII, pVI, pVII, pVIII, pIX), proteins that facilitate DNA replication (pII, pV, PX), and proteins for phage assembly (pI, pIV, pXI) [385]. To utilise bacteriophages for phage display, foreign DNA will be cloned into the phage gene that encodes capsid proteins. Capsid protein gene pIII and pVIII are more commonly used. When the recombinant DNA is expressed, foreign peptides will be displayed on the surface of viral particles. These

recombinant virions can then be used for in vitro (using purified protein fragments, receptors or whole cells as bait) or in vivo (murine) screening.

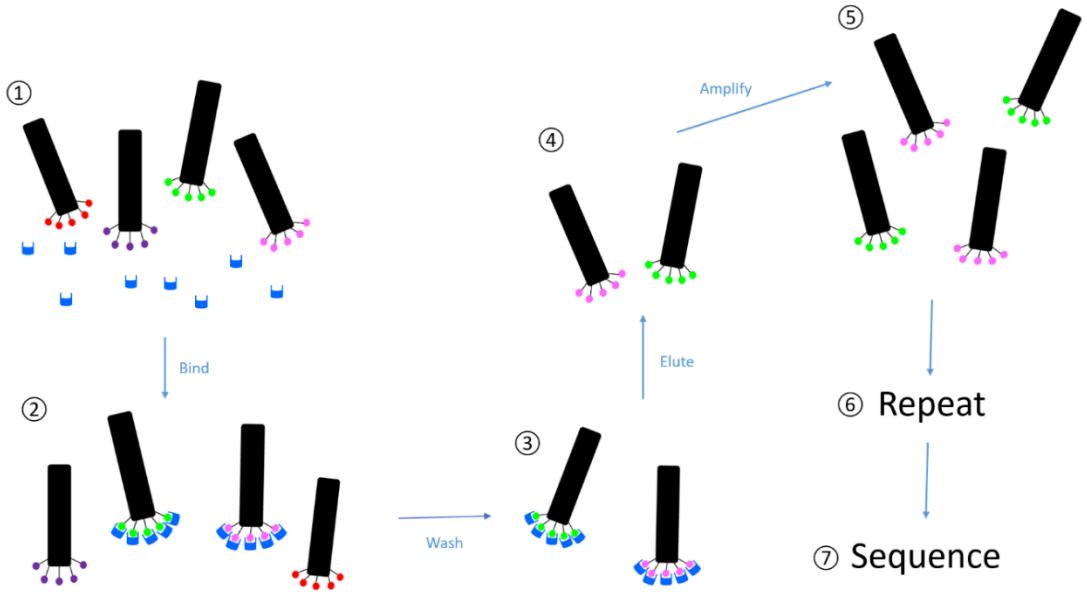

Figure 9: General flow of phage display.

Phage particles displaying the foreign peptide is allowed to bind to the target (bait) of interest. Unbound phage is washed away. Bound phage is eluted from the target and amplified via *E. coli*. Steps 1 to 5 is repeated for 2-3 times. The amplified phage is sequenced to identify high affinity displayed peptides.

The phage display general workflow (Figure 9) is as follows: i) the prey (recombinant virions) is allowed to bind to the bait (target of interest), ii) unbound phages are washed away, iii) affinity enrichment/biopanning is performed (steps i and ii are repeated several times), iv) phages bound to the bait are eluted using acidic solution, v) phage capsid gene is sequenced. The sequence of interest can then be used to synthesise lead peptides that can potentially be developed into clinical drugs.

A bioactive peptide targeting TPOR, Romiplostim (TPO agonist), has been discovered using phage display. Initially, filamentous phages were made to display random foreign peptides on the pVIII capsid protein. Then, monoclonal antibodies that bind to the ECD carboxyl-terminus of TPOR were used to immobilise the receptor [367, 386]. Biopanning was performed and the consensus sequence of the peptide (AF13948) identified from bound phage was found to not share sequence homology with TPO [368], but was able to compete with TPO for binding to TPOR. Dimerisation of the peptide by covalent linkage was able to increase its efficacy with potency similar to TPO [368]. AF13948

was then used to develop Romiplostim which has subsequently been approved clinically for the treatment of ITP [387].

Antagonists such as those against IL-6 have also been discovered by phage display [388]. Excessive production of IL-6 leads to inflammation that has been associated with diseases including Castleman's disease and rheumatoid arthritis [388]. To discover peptides that bind to IL-6, a vector containing a region of the IL-6 receptor that binds to the cytokine, was used to discover a scaffold protein using computational methods [388]. Following, certain residues at determined positions were randomised [388]. The sequences were then incorporated into the M13 phage [388]. A solution-based biopanning was performed for four to five rounds using different biotin-conjugated IL-6 as a bait [388]. Bound phage particles were eluted and the sequences were used to make synthetic peptides [388] which led to the development of PN-2921 (pegylated peptide) that has shown to be a potent antagonist and is currently in clinical trials [388].

Current treatments for MPN patients harbouring activating TPOR mutations include administration of hydroxyurea, IFN-α, or JAK2 inhibitors. Ruxolitinib or also known as Jakafi, works by inhibiting JAK1/JAK2 [247] and is used for the treatment of MF (de novo MF or post-ET/polycythaemia vera MF). As these treatments are not specific, patients developed various side effects. In particular for JAK inhibitors, these inhibit JAK activation induced by many receptors, hence, lack specificity for TPOR signalling and for specifically targeting TPOR activating mutants. This provides the rationale for specific targeting of the TPOR rather than targeting JAK activation.

Currently, two TPOR antagonists have been developed whereby one of them is known as LCP4, that inhibits myelofibrotic HSCs which expresses TPOR [389]. LCP4 is a 20-amino acid cyclic peptide that targets TPOR and acts by competitive binding to the TPOR ECD at the site where TPO binds [389]. LCP4 has been shown to deplete myelofibrotic HSCs and HPCs but does not fully eliminate these cells [389]. This peptide also results in inhibition of normal cells although it more effectively affects malignant cells [389]. The other TPOR antagonist that has been developed is a small molecule inhibitor, an analogue of 3-(4-piperidinyl) indole [390]. However, this antagonist is not specific to TPOR and can also target other monoamine receptors such as EPOR [390]. This inhibitor shows no difference in inhibition between TPOR WT and W515L [390]. This highlights the need and rationale to develop more specific, targeted treatments against TPOR (i.e. by targeting the ECD linker/ TM). Oncogenic mutations in the TMD-JM of several receptors besides TPOR have been reported which includes the IL7RA and thymic stromal lymphopoietin receptor (TSLPR). In TPOR, these activating mutations include the T487A, L498W, S505N, and W515L/K/A/R/S whereas in TSLPR the TMD F232 residue was mutated to cysteine. Oncogenic mutations in IL7 receptor-α (IL7RA) are caused by

in-frame insertions or deletions in the TMD [391, 392], or insertion of a cysteine residue in the ECD-JM [392, 393]. Poor sequence conservation of the TMD and JM regions between these receptors (Figure 10) demonstrates the suitability of targeting this region as more specific targets to a single receptor can be found. The aim of this chapter is to quantify the signalling strength of activating mutations in the TMD region of TPOR and develop peptides targeting WT TPOR and constitutive active oncogenic mutants.

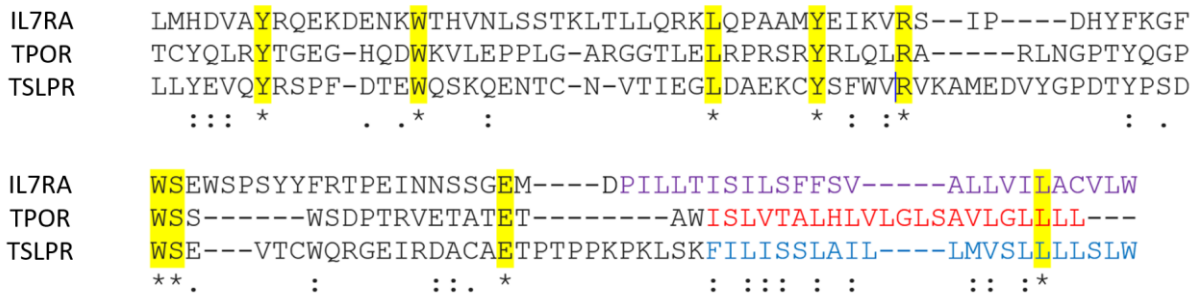

Figure 10: Poor sequence conservation of the ECD-JM and TMD regions of IL7RA, TPOR, and TSLPR.

Conserved residues are indicated by * and highlighted in yellow. Purple, red, and blue fonts indicate the TMD regions of the IL7RA, TPOR, and TSLPR, respectively.

Materials and Methods

DNA Constructs

WT hTPOR in pLV411 lentiviral vector (generously provided by ARVEC) was shuttled into pDONR221 donor vector and a HA-tag was added to the N-terminus of hTPOR after the signal peptide via CPEC. Various primers (see Appendix Section C) were designed to generate hTPOR with point mutations (W515K, S505N, T487A) via PCR mediated site-directed mutagenesis (Table 1) using the pDONR221 HA-tagged WT hTPOR as a template. *att*B sites were added to the N-terminal HA-tagged hTPOR constructs via PCR. Constructs were subsequently shuttled into the pMX-GW-mPGKpro-puroR/green fluorescent protein (GFP) destination vector by Gateway cloning (Figure 11). Primers were used to generate a Box1 mutant (this motif was mutated from PxxP to AAAA) of hTPOR via PCR mediated site-directed mutagenesis and CPEC (see Chapter 2) using pDONR221 HA-tagged WT hTPOR, and subsequently shuttled into pMX-GW-mPGKpro-puroR/GFP destination vector via Gateway cloning. All constructs were verified by DNA sequencing performed by AGRF Brisbane.

Table 1: PCR cycling conditions used.

Double-stranded DNA was denatured to single-stranded DNA and primers were allowed to anneal. PCR was performed with KOD DNA polymerase (Merck Millipore).

Cycling Steps		Temperature	Time
Polymerase activation		95 °C	2 minutes
Denaturation	35 cycles	95 °C	20 seconds
Annealing		63 °C	10 seconds
Extension		70 °C	25 seconds/kilobase pair
Hold		15 °C	∞

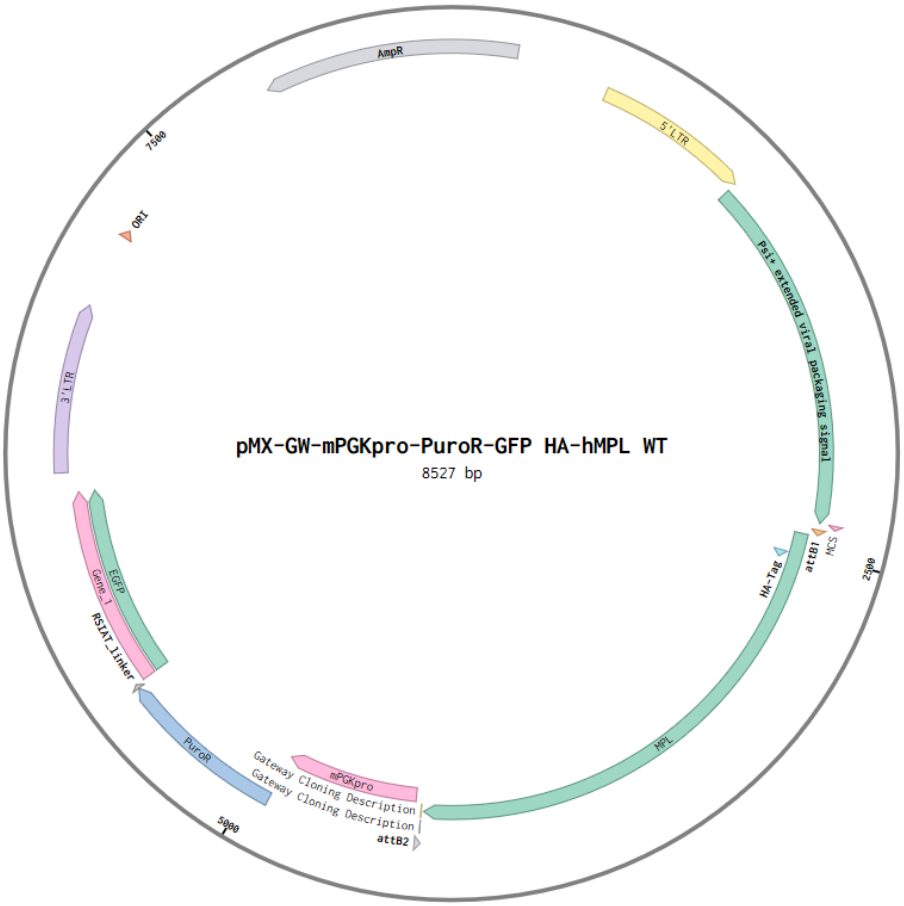

Figure 11: Representative vector map of the pMX-GW-mPGKpro-puroR/GFP HA-hTPOR vector constructs.

An HA-tag was present at the N-terminus of the *hMPL* gene.

Retroviral Transduction and Generation of Stably-Transduced Ba/F3 Cell Lines

PLAT-E cells were seeded (1.7×10^5 cells/well) into 6-well cell culture plates and cultured overnight in DMEM supplemented with 10% FBS at 37°C in a humidified 5% CO_2 incubator. Cells were transiently transfected with 3 µg plasmid DNA (pMX-GW-mPGKpro-puroR/GFP HA-tagged TPOR constructs) using Lipofectamine 2000 according to manufacturer's instructions (Invitrogen, Thermo Fisher Scientific). After 24 hours incubation at 37°C, media was replaced with fresh DMEM supplemented with 10% FBS for 48 hours. Parental Ba/F3 cells (2×10^5 cells per infection) were infected with ecotropic retroviral supernatants generated in PLAT-E cells and incubated at 37°C for 1-2 hours before an equal volume of RPMI-1640 (supplemented with 10% FBS and 2× IL-3) was added. After 3 days, puromycin selection was performed by re-suspending cells in a final concentration of 1 µg/ml puromycin (Gibco, Life Technologies, Thermo Fisher Scientific) in RPMI-1640 (supplemented with 10% FBS) and left for 3-5 days before cells were expanded to T25 cell culture flasks.

TPOR Signalling Assay using Ba/F3 TPOR Retroviral Transduced Cells

Retroviral transduced Ba/F3 TPOR WT and mutants were cultured to near end of log-phase growth (~$1\text{-}3 \times 10^6$ cells/ml) in RPMI-1640 supplemented with 10% FBS and 1 × IL-3 at 37°C in a humidified 5% CO_2 incubator. Cells were starved in RPMI-1640 supplemented with 0.5% FBS (no IL-3) for 12-16 hours. Cells were then stimulated with 50 ng/ml recombinant human (rhTPO) (R & D Systems) or PBS for 30 minutes at 37°C. Cells were subsequently washed with cold-PBS and lysed in 50-100 µl ice-cold radioimmunoprecipitation assay (RIPA) buffer (50 mM Tris pH7.5, 150 mM NaCl, 5 mM EDTA, 0.5% Triton X-100) containing 2 mM sodium orthovanadate (Sigma), 30 mM sodium fluoride (Sigma), 10 mM sodium pyrophosphate (Sigma), and 1x complete protease inhibitor cocktail (Roche Applied Science). Protein concentration was determined using the Pierce Bicinchoninic (BCA) Protein Assay Kit (Thermo Fisher Scientific). Supernatant was mixed with 3x SDS sample buffer (containing 0.1 M DTT) and heated to 98°C for 5 minutes before the samples were run on SDS-PAGE gel and subjected to western analysis using the appropriate antibodies (see Appendix Section E).

Lentiviral Transduction and Generation of Stably-Transduced HEK293 Cell Lines

Lentiviral transduction and generation of stably-transduced HEK293 cell lines were performed by Dr Yash Chhabra. Lenti-X 293T cells were seeded (1.9×10^5 cells/well) into 6-well cell culture plates and cultured overnight in DMEM supplemented with 10% FBS at 37°C in a humidified 5% CO_2 incubator. Cells were transiently transfected with 1 µg pCMV (cytomegalovirus)-VSV-G, 2.5 µg pVPac-Gag-Pol, and 3 µg pQCXIP HA-tagged hTPOR constructs using Lipofectamine 2000 according to manufacturer's instructions (Invitrogen, Thermo Fisher Scientific). After 15 hours incubation at 37°C, media was replaced with fresh DMEM supplemented with 10% FBS for 48 hours. Parental HEK293 cells (3.5×10^5 cells per infection) were infected with lentiviral supernatants filtered with a 0.2 µm PVDF Millex-GV filter unit (Millipore) that was generated in Lenti-X 293T cells. After 2-3 days, puromycin selection was performed by adding to the cells to a final concentration of 1 µg/ml puromycin (Gibco, Life Technologies, Thermo Fisher Scientific) in DMEM (supplemented with 10% FBS) and left for 3-5 days before cells were expanded to T25 cell culture flasks.

TPOR Signalling Assay using HEK293 TPOR Stably-Transduced Cells

Stably-transduced TPOR HEK293 cells were seeded (0.7×10^6 cells/well) into T25 cell culture flasks and cultured overnight in DMEM supplemented with 10% FBS at 37°C in a humidified 5% CO_2 incubator. Cells were starved in DMEM supplemented with 0.5% FBS for 12-16 hours. Cells were then stimulated with 50 ng/ml rhTPO (R & D Systems) or PBS for 10 minutes at 37°C. Cells were subsequently washed with cold-PBS and lysed in 100 µl ice-cold RIPA buffer. Protein concentration was determined using the Pierce BCA Protein Assay Kit (Thermo Fisher Scientific). Supernatant was mixed with 3x SDS sample buffer (containing 0.1 M DTT) and heated to 98°C for 5 minutes before the samples were run on SDS-PAGE gel and subjected to western analysis using the appropriate antibodies (see Appendix Section E).

TPO Dose Response Assays

Retroviral transduced Ba/F3 TPOR WT and mutants were seeded (3×10^3 cells/ well) into 384-well plates in IL-3-free and phenol red-free RPMI-1640 medium (with 10% FBS, 1× Glutamax, 1× sodium pyruvate, 1:200 penicillin-streptomycin). Increasing concentrations of rhTPO (R & D Systems) (0, 1.25, 3.7, 11.1, 33.3, 100, and 300 ng/ml) were added to the respective wells and live cells were

evaluated from day 0 to day 6 after seeding using the IN Cell Analyser (GE Healthcare Life Sciences) determined by GFP-positivity using the FITC channel (GFP expression of cells).

Flow Cytometry Analysis

Retroviral transduced Ba/F3 TPOR WT and mutant cells were tested for cell surface expression of TPOR by flow cytometry. Approximately 1×10^6 cells were washed twice to remove excess culture media, resuspended in 80 µl PBS (2% FBS) containing anti-HA primary antibody (BioLegend) (1:100 dilution) raised against the HA-tag that was engineered to the N-terminus of the receptor, and incubated for 2 hours at 4°C. Cells were washed twice, resuspended in 80 µl PBS (2% FBS) containing Alexa Fluor 647 secondary antibody, goat anti-mouse (Thermo Fisher Scientific) (1:500 dilution), and incubated for 40 minutes (in the dark) at 4°C. Cells were washed twice to remove unbound antibody, resuspended in 500 µl PBS (2% FBS), and analysed by flow cytometry (BD LSRFortessa X20, Becton Dickinson). Ten thousand gated events were collected for each sample and analysed using FlowJo software.

Phage Display Screening Assay

A peptide encoding the ECD linker of the human TPOR (^{480}PTRVETATETAW^{491}) was synthesized by Peptide2.0 company. This oligonucleotide was biotinylated at its N-terminal domain. Peptide targets were also obtained from LifeTein representing part of the ECD and TM region (^{480}PTRVETATETAWISLVTALH^{499}). Underlined amino acid sequences indicate the predicted transmembrane region of TPOR. Phage display was used to select TPOR extracellular linker/ TM binding phage particles from a 7-mer or 12-mer library (Ph.D.-7 or 12 Peptide Library Kit; NEB) comprising up to 10^{11} theoretical sequences. Before panning, various negative selections were performed for library selection using the solution-phase panning method. Negative selection of plate plastic adherent was performed by diluting 10 µl phage library in 0.1% TBST and this mixture was added to a well of a 96-well tissue culture plate. This was incubated with agitation for 30 minutes at room temperature. For tube plastic adherent negative selection, the supernatant library from previous selection was transferred to a microcentrifuge tube and a plastic tip added into the tube. This was incubated with rotation for 30 minutes at room temperature. For negative selection of BSA/plastic adherents, a microcentrifuge tube was added with BSA blocking solution and left rotating for 60 minutes at room temperature. The tube was rinsed 3 times with 0.1% TBST and the supernatant library from the previous step was added into the tube. This was incubated for 30 minutes at room

temperature with rotation. For biotin negative selection, 50 µl of washed, blocked streptavidin-coated paramagnetic beads (NEB) was mixed with 0.1 mM biotin in TBS and incubated for 15 minutes at room temperature with gentle agitation. Supernatant was removed and supernatant library from previous step was added to the biotin-beads and incubated for 15 minutes at room temperature with gentle agitation. Finally, negative selection of the beads were performed by mixing the supernatant library from the previous step to 50 µl of washed, blocked beads and incubated for 15 minutes at room temperature with gentle agitation. The first round of panning was performed by incubating the supernatant library from previous selection step with biotinylated target in 0.1% TBST for 20 minutes at room temperature with agitation. Target-bound phage was captured using beads by incubation for 15 minutes at room temperature with agitation. Beads were extensively washed with TBS containing 0.1% Tween-20 to remove non-binding phage. The remaining phage particles were eluted by incubation with 100 µM target, 0.1 mM biotin, glycine elution buffer, or 1x trypsin for 10-30 minutes with gentle agitation, and amplified by infecting log phase ER2738 *E. coli* cells at 250 RPM for 4.5 hours. Polyethylene glycol (PEG) precipitation was carried out using 20% PEG/2.5 M NaCl to capture the amplified phage particles. Panning was repeated as above for a total of three rounds using increasing volume of Tween-20 in each subsequent rounds (0.3% TBST for second panning; 0.5% for third panning). Target concentration was also decreased in each subsequent rounds (1 µM for first panning, 100 nM for second panning; 10 nM for third panning). Selected phage clones (from the last round of panning) were DNA sequenced.

Phage Amplification and Tittering

Eluted phage suspension (180 µl) was added to 20 ml ER2738 cell culture in early-log phase (OD_{600} 0.01–0.05). After incubation with vigorous shaking for 4.5–5 hours at 37°C, the culture was centrifuged at 12,000*g* for 10 minutes at 4°C. The supernatant was precipitated with 1/6 volume 20% PEG/2.5 M NaCl overnight at 4°C. The next day, precipitated phage was collected by centrifugation at 15,000*g* for 15 minutes at 4°C and resuspended in 200 µl TBS for tittering and the next round of panning. For tittering, 10 µl serial dilutions of phage solutions were added to 200 µl mid-log phase, OD_{600} ~0.5 ER2738 cell cultures. After incubation for 1-5 minutes, the culture was mixed with 5 ml 50°C top agar containing isopropyl β-d-1-thiogalactopyranoside (IPTG)/ X-gal and poured onto the LB agar plates immediately. After incubation of the plates overnight at 37°C, blue plaques were counted and phage titter as plaque forming units (pfu)/10 µl was calculated.

Hit Validation in Cell-based Assays

Stably-transduced Ba/F3 TPOR WT, TPOR W515K, or GHR WT were seeded (3×10^3 cells/ well) into 384-well plates in IL-3-free and phenol red-free RPMI-1640 medium (with 10% FBS, 1x Glutamax, 1x sodium pyruvate, 1:200 penicillin-streptomycin). Peptides (final concentration of 1 mM) were added to the respective wells containing cells and incubated for 30 minutes. rhTPO (R & D Systems) was added to the respective wells and live cells were evaluated from day 0 to day 6 after seeding using the IN Cell Analyser (GE Healthcare Life Sciences) determined by GFP-positivity using the FITC channel (GFP expression of cells).

Results

TPOR mutants show different constitutive signalling strengths in the absence of cytokine treatment using Ba/F3 cells

The functionality of the Ba/F3 TPOR WT and mutant (W515K, T487A, and S505N) cell lines was investigated for their ability to activate downstream signalling pathways such as JAK-STAT and ERK1/2. W515K and S505N but not T487A, showed constitutive activation of STAT3 in the absence of cytokine treatment with the W515K mutant showing a stronger constitutive signalling (Figure 12). In contrast, all mutants showed constitutive activation of ERK1/2 in the absence of cytokine treatment with the S505N mutant showing the strongest constitutive signalling, followed by W515K and T487A (Figure 12). However, W515K showed similar pERK1/2 levels in the presence and absence of TPO. In the presence of cytokine, WT and mutants were all able to respond to rhTPO stimulation as shown by the increase in STAT3 and ERK1/2 activation (Figure 12). Comparison between mutants suggest that W515K and T487A were hypersensitive to rhTPO as shown by the increase in STAT3 activation that was stronger than in WT in the presence of TPO (Figure 12). Receptor levels of the mutants were slightly increased compared to WT which may be due to the increase in expression levels or stability of the mutant receptors on the cell surface (Figure 12). Interestingly, there was a stark decrease in the mature receptor expression level of the S505N mutant compared to WT and other mutants suggesting that this mutation may impair glycosylation, trafficking, or degradation of mature receptor (Figure 12).

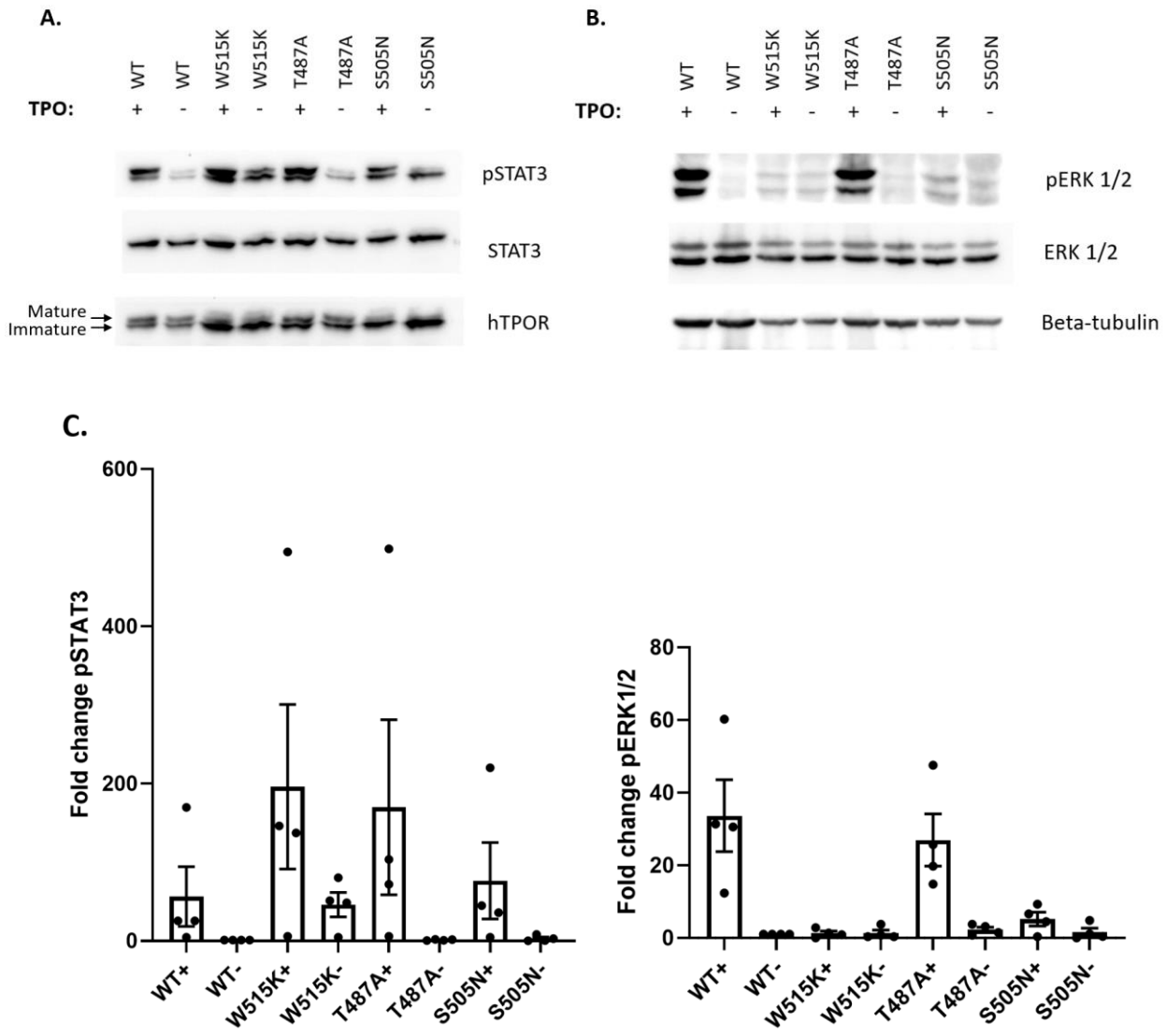

Figure 12: TPOR mutants conferred constitutive STAT3 or ERK1/2 activation in Ba/F3 cells.

Retroviral transduced Ba/F3 TPOR WT and mutant cells (W515K, T487A, S505N) were starved for 12-16 hours in RPMI-1640 media containing 0.5% FBS and no IL-3. Prior to cell harvesting, cells were stimulated accordingly with 50 ng/ml rhTPO for 30 minutes. Total protein was subjected to SDS-PAGE and immunoblotted with indicated antibodies. GAPDH was used as a loading control. A) and B) Two separate transductions. C) Graph of relative pSTAT3 and pERK levels of 4 independent experiments generated using densitometry data. For a complete list of densitometry data for replicates, see Appendix Section B. Image representative of n=4 experiments.

TPOR WT and mutants (except Box1Δ) express similar surface levels of mature receptors in BaF3 cells

The receptor surface expression of Ba/F3 TPOR WT and mutant (W515K, T487A, S505N, and Box1Δ) cell lines were compared in order to investigate if the increase in cell signalling was due to the increase in receptor expression levels on the cell surface. Immunoblot analysis (Figure 13 B) showed that there was slight variation between the mature receptor levels amongst the mutant receptors, except for Box1Δ which showed a dramatic loss of the mature receptor form. As the mature receptor levels observed on Western analysis only suggests glycosylation status and does not fully reflect the presence of receptors at the cell surface, FACS performed on non-permeabilised cells was utilised for this investigation. A two-step staining procedure was used where the primary antibody, anti-HA was used against the HA-tag present at the receptor N-terminus (after signal peptide) which was detected using the Alexa Fluor 647 secondary antibody (far-red dye). Similar surface expression was observed for WT and mutant receptors, except for Box1Δ which showed a reduced signal for surface receptors (Figure 13 A). As the Box1 motif is essential for the binding of JAK2 which acts as a chaperone to transport the receptor to the cell surface [115], mutation of this motif resulted in markedly reduced receptor expression at the cell membrane. This result was supported by the inability of the Box1Δ to signal via STAT3 and ERK1/2 even in the presence of TPO stimulation due to the absence of JAK2 binding (Figure 14).

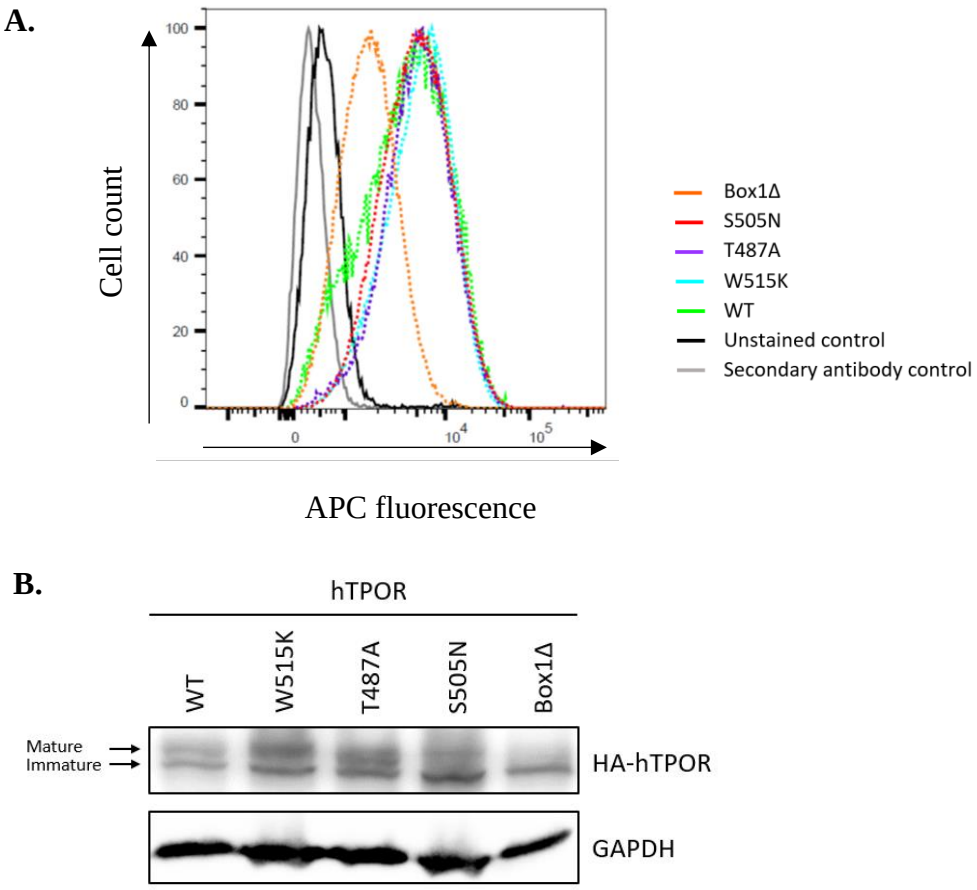

Figure 13: TPOR WT and mutants (except Box1Δ) express similar amounts of mature surface receptors.

(A) Flow cytometric analysis of surface HA-TPOR expression levels of stably transduced Ba/F3 TPOR WT and mutant cells. Cell surface expression of receptors was detected using anti-HA and AF647 anti–mouse IgG secondary antibody. Cells were not serum starved. (B) Western analysis of TPOR expression levels. Stably transduced Ba/F3 TPOR WT and mutant cells were starved for 7-8 hours in RPMI-1640 media containing no FBS and no IL-3. No TPO stimulation was performed. Total protein was subjected to SDS-PAGE and immunoblotted with indicated antibodies. GAPDH was used as a loading control. (A & B) N=1 experiment.

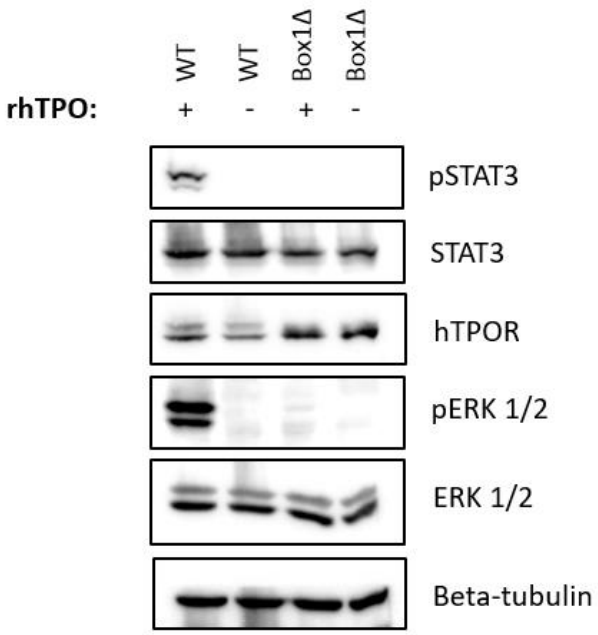

Figure 14: Box1Δ TPOR mutant does not signal via STAT3 or ERK1/2 in Ba/F3 cells.

Retroviral transduced Ba/F3 TPOR WT and Box1Δ were starved for 12-16 hours in RPMI-1640 media containing 0.5% FBS and no IL-3. Prior to cell harvesting, cells were stimulated accordingly with 50 ng/ml rhTPO for 30 minutes. Total protein was subjected to SDS-PAGE and immunoblotted with indicated antibodies. β-tubulin was used as a loading control. N=1 experiment.

TPOR W515K confers cytokine-independent cell proliferation whereas TPOR S505N confers partial cytokine-independent cell proliferation

The functionality of the Ba/F3 TPOR WT and mutant (W515K, T487A, and S505N) cell lines was investigated for their ability to proliferate in the presence and absence of TPO as activation of JAK-STAT signalling correlates with proliferation in Ba/F3 cells. WT and all mutants responded to increasing TPO concentrations used (0.0001 ng/ml to 300 ng/ml) (Figure 15). Using these polyclonal populations of cells, the TPO effective concentration (EC_{50}) was determined (Figure 15 B) and this information was used for the cell-based screening assay of peptide antagonists identified below.

A.

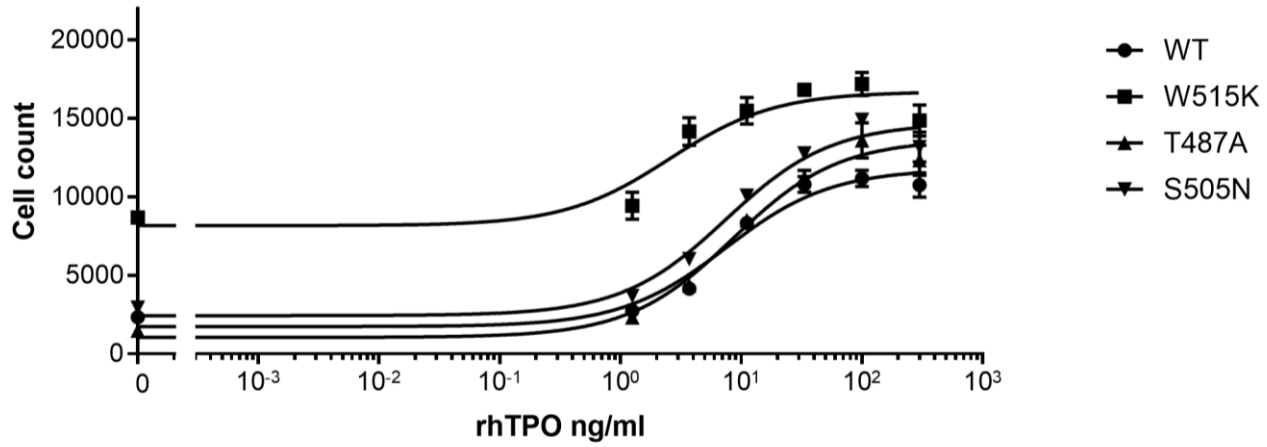

B.

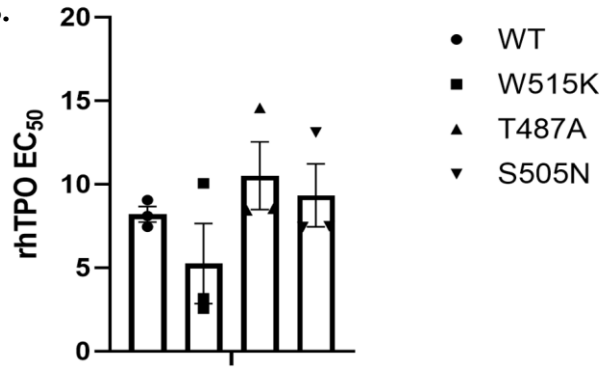

Cell lines	rhTPO EC_{50} (ng/ ml) Day 2
WT	8.2
W515K	5.3
T487A	10.5
S505N	9.3

Figure 15: Ba/F3 TPOR WT and mutants respond to increasing TPO concentrations.

Stably transduced Ba/F3 TPOR WT and mutant cells in log growth were plated at a density of 3 × 10^3 cells/ well in 384-well plates in IL-3-free and phenol-red free RPMI-1640 media (no starving condition). Increasing rhTPO concentrations were used: 0, 1.25, 3.7, 11.1, 33.3, 100, and 300 ng/ ml. Viable cells were assayed based on GFP expression from day 0 to day 6 after seeding. (A) Proliferation assay results from day 2. Results and standard error of mean represent the mean of four readings of a single experiment. Image representative of n=3 experiments. (B) rhTPO EC_{50} data from day 2 of the mean of three experimental replicates were plotted as bar charts. Statistical analysis was performed in GraphPad Prism software using student's 2-tailed unpaired t-test. All data were presented as mean ± SEM. No statistically significant difference were observed when comparing the rhTPO EC_{50} between WT and mutants. For replicates, see Appendix Section B.

The ability of Ba/F3 TPOR WT and mutant (W515K, T487A, and S505N) cell lines to confer cytokine-independent cell proliferation was investigated. Consistent with the Western analysis results (Figure 12), only the W515K and S505N mutants were able to proliferate/survive in the absence of cytokine where W515K conferred a stronger phenotype (Figure 16).

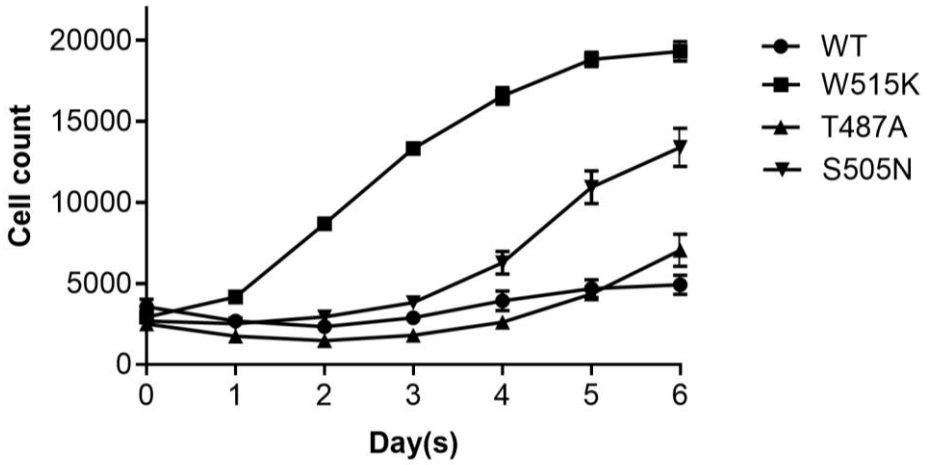

Figure 16: Ba/F3 TPOR mutants W515K and S505N show significant proliferation in the absence of cytokine, but not T487A.

T487A. Retroviral transduced Ba/F3 TPOR WT and mutant cells cultured in IL-3 until log growth were plated at a density of 3×10^3 cells/well in 384-well plates in IL-3-free, TPO free, and phenol-red free RPMI-1640 media. Viable cells were counted by image analysis of GFP expressing cells from day 0 to day 6 after seeding. Results and standard deviations represent the mean of four readings of a single experiment. For replicates, see Appendix Section B. Image representative of n=3 experiments.

Novel TPOR TMD mutations (L498W, V501A, V501S, and L502S) confer constitutive signalling

As part of a collaborative effort with group led by Melissa and Matthew Call at the WEHI (Walter and Eliza Hall Institute), this work investigated every amino acid residue in the TPOR TMD in order to evaluate their ability to result in constitutive proliferation in Ba/F3 cells in the absence of cytokine by using the deep mutational scanning (DMS) approach (Figure 17) [394].

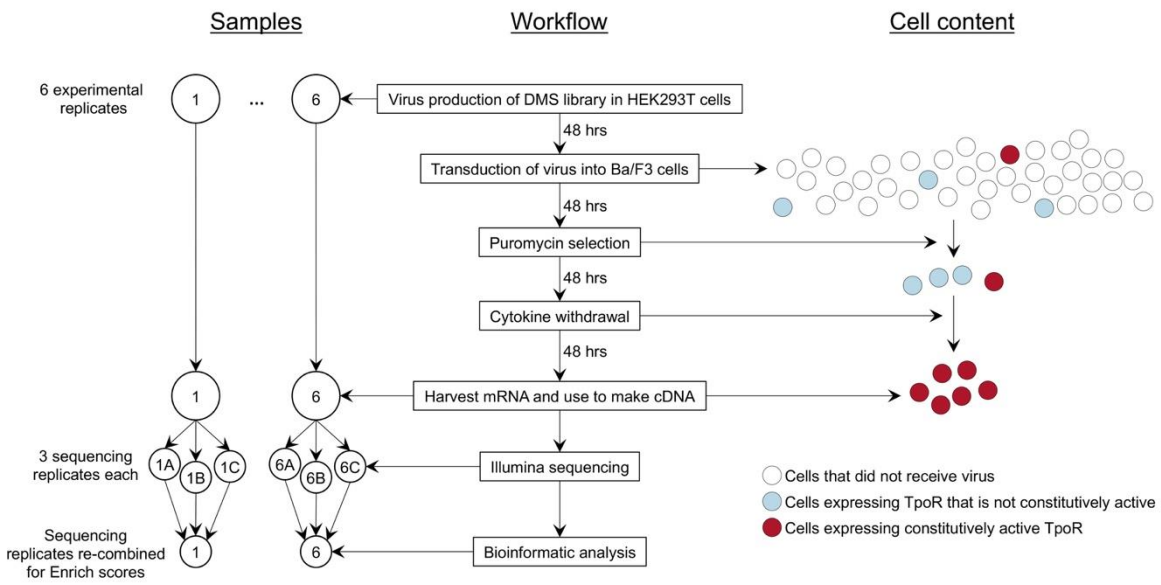

Figure 17: Deep Mutational Scanning (DMS) overview and workflow.

The DMS library was calcium phosphate transfected into HEK293T cells in order to generate virus that was used to transduced parental Ba/F3 cells. Puromycin selection (5 µg/ml) was performed for 48 hours in order to select for successfully transduced cells followed by cytokine withdrawal for 48 hours to allow for selection of constitutively active mutants. Cell lines that survived cytokine withdrawal were subjected to sequencing. Figure reproduced from [394].

Using the mutants identified to cause cytokine-independent cell proliferation, analysis of signalling was performed. Four novel mutants were found to result in constitutive STAT5 and ERK1/2 activation (L498W, V501A, V501S, and L502S) (Figure 18 A) which complemented the proliferation assays performed by the WEHI group (Figure 18 B). V501S resulted in a stronger constitutive receptor signalling compared to V501A (Figure 18 A).

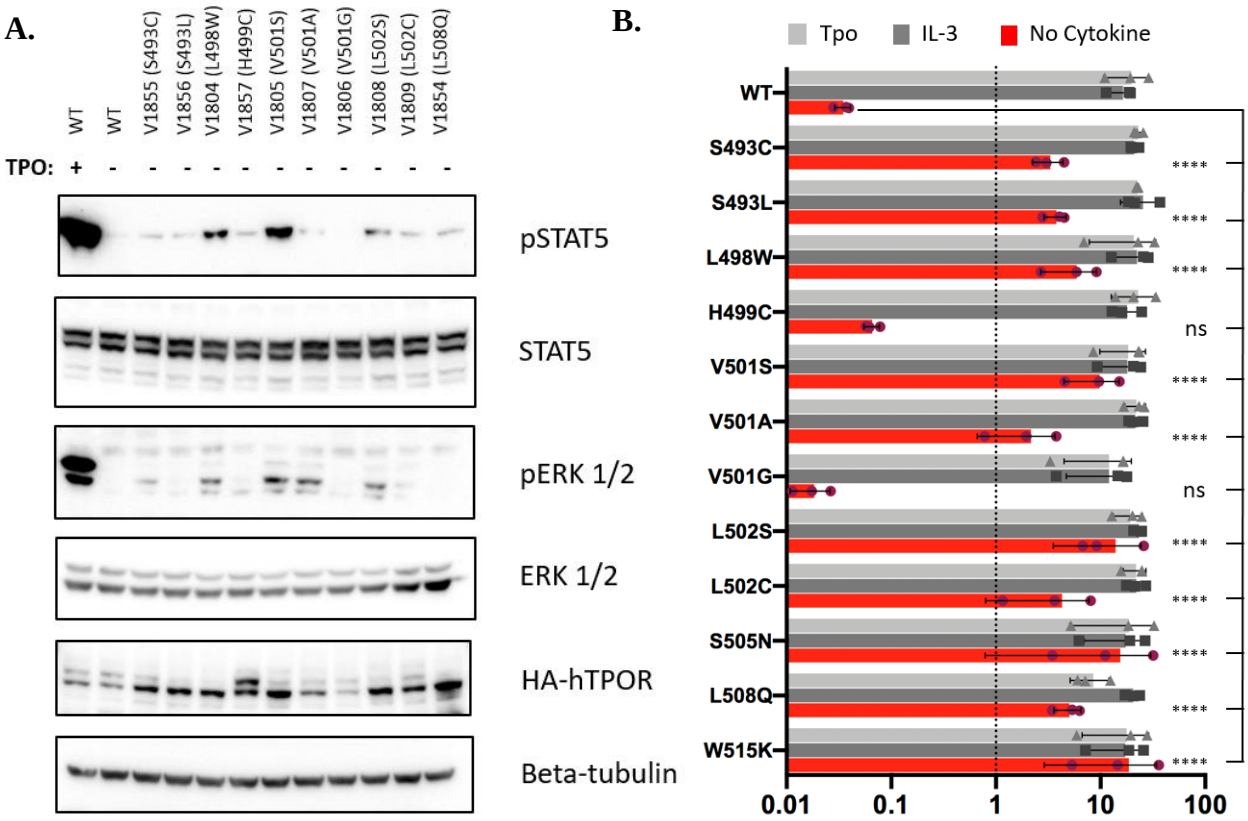

Figure 18: Four novel mutations of TPOR TMD (L498W, V501A, V501S, and L502S) conferred constitutive STAT5 and/or ERK signalling, and cell proliferation.

(A) Stably transduced Ba/F3 TPOR WT and mutant cells were starved for 6-8 hours in RPMI-1640 media containing no FBS and no IL-3. Prior to cell harvesting, cells were stimulated accordingly with 50 ng/ml rhTPO for 30 minutes. Total protein was subjected to SDS-PAGE and immunoblotted with indicated antibodies. β-tubulin was used as a loading control. Image representative of n=3 experiments. For a complete list of replicates, see Appendix Section B. (B) Figure reproduced from [394].

TPOR W515K and S505N conferred constitutive signalling in the absence of cytokine treatment in HEK293 cells

As the TPOR constructs were all based on human constructs and Ba/F3 cells are from mice, the signalling of each TPOR construct was further investigated in the human cell line HEK293. In order to confirm that the different patterns of STAT3 and ERK1/2 activation by the TPOR variants were not due to species-specific differences, a similar analysis as above was performed on retroviral-transduced HEK293 cells to express each TPOR construct. Some differences were observed when

compared with the Ba/F3 results in that while W515K was able to confer constitutive activation of STAT3, S505N and T487A do not (Figure 19). The low total STAT3 levels may have masked the weak constitutive activity of the S505N (Figure 19). Similar to the Ba/F3 results, W515K and S505N showed constitutive ERK1/2 activation but the T487A showed no or only very weak activation (Figure 19). In the presence of cytokine, WT and mutants were able to respond to rhTPO as shown by the increase in STAT5, STAT3, and ERK1/2 activation signals (Figure 19). However, the mutants did not appear to be cytokine-hypersensitive in this cell line (Figure 19) as shown by the similar levels of activation compared to WT in the presence of stimulation. A stark difference was observed upon ligand stimulation where ERK1/2 was similarly activated across all mutants but in BaF/3, a strong activation was observed for T487A (Figure 12 and Figure 19).

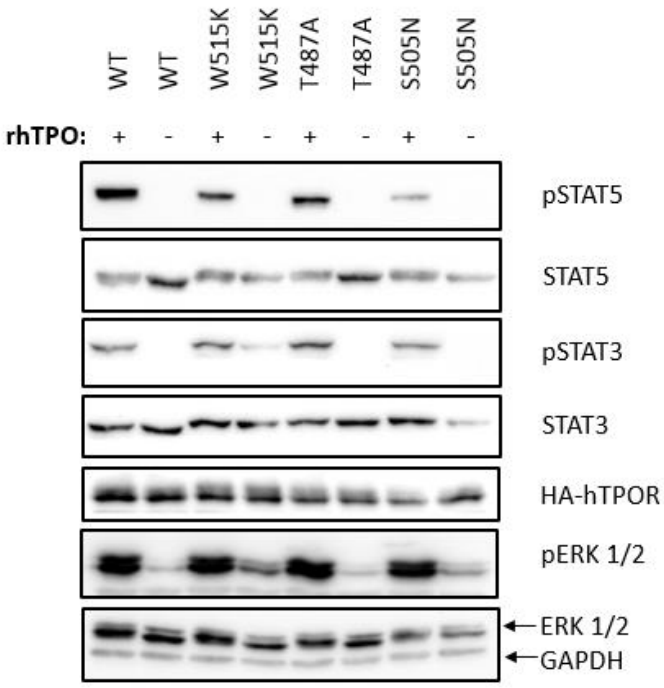

Figure 19: W515K and S505N conferred constitutive STAT3 or ERK1/2 activation in HEK293 cells.

Retroviral-transduced HEK293 TPOR WT and mutant cells (W515K, T487A, S505N) were starved for 12-16 hours in DMEM media containing 0.5% FBS. Prior to cell harvesting, cells were stimulated accordingly with 50 ng/ml rhTPO for 10 minutes. Total protein was subjected to SDS-PAGE and immunoblotted with indicated antibodies. GAPDH was used as a loading control. Image representative of n=3 experiments.

12-mer phage display peptide library yield 3 consensus peptide motifs

Peptide antagonists against the crucial-signal modulating domain (ECD linker/TMD) of TPOR were discovered using the commercial 12-mer phage display peptide library kit (NEB). Panning procedures were carried out using solution-phase panning. Three panning procedures were performed for each target and target-bound phage DNA was subsequently sequenced. Three consensus peptide motifs were discovered using this library in a screen of ~100 sequences: peptide T (2 hits), peptide S (11 hits), and peptide V (7 hits), using the ECD linker as the target (biotin-DPTRVETATETAW) and competitive bait elution method. These sequences were sent for peptide synthesis (Biomatik) with its C-terminal amidated in order to block the negative charge resulting from the free carboxy terminus.

Peptide V may be specifically inhibiting TPOR-mediated cell proliferation in the presence of TPO

The synthesised peptides with sequences obtained from the phage display screen were tested in cell-based assays for their ability to inhibit or enhance cell proliferation of Ba/F3 TPOR WT and mutant cells. Amongst the three peptides, only peptide V appeared to confer an effect. Peptide V was able to inhibit TPOR WT (at high dose TPO) and W515K (at low and high dose TPO) but not W515K cultured in the absence of cytokine or presence of IL-3 (Figure 20). Furthermore, this peptide did not affect the growth of Ba/F3 GHR WT cells (Figure 20).

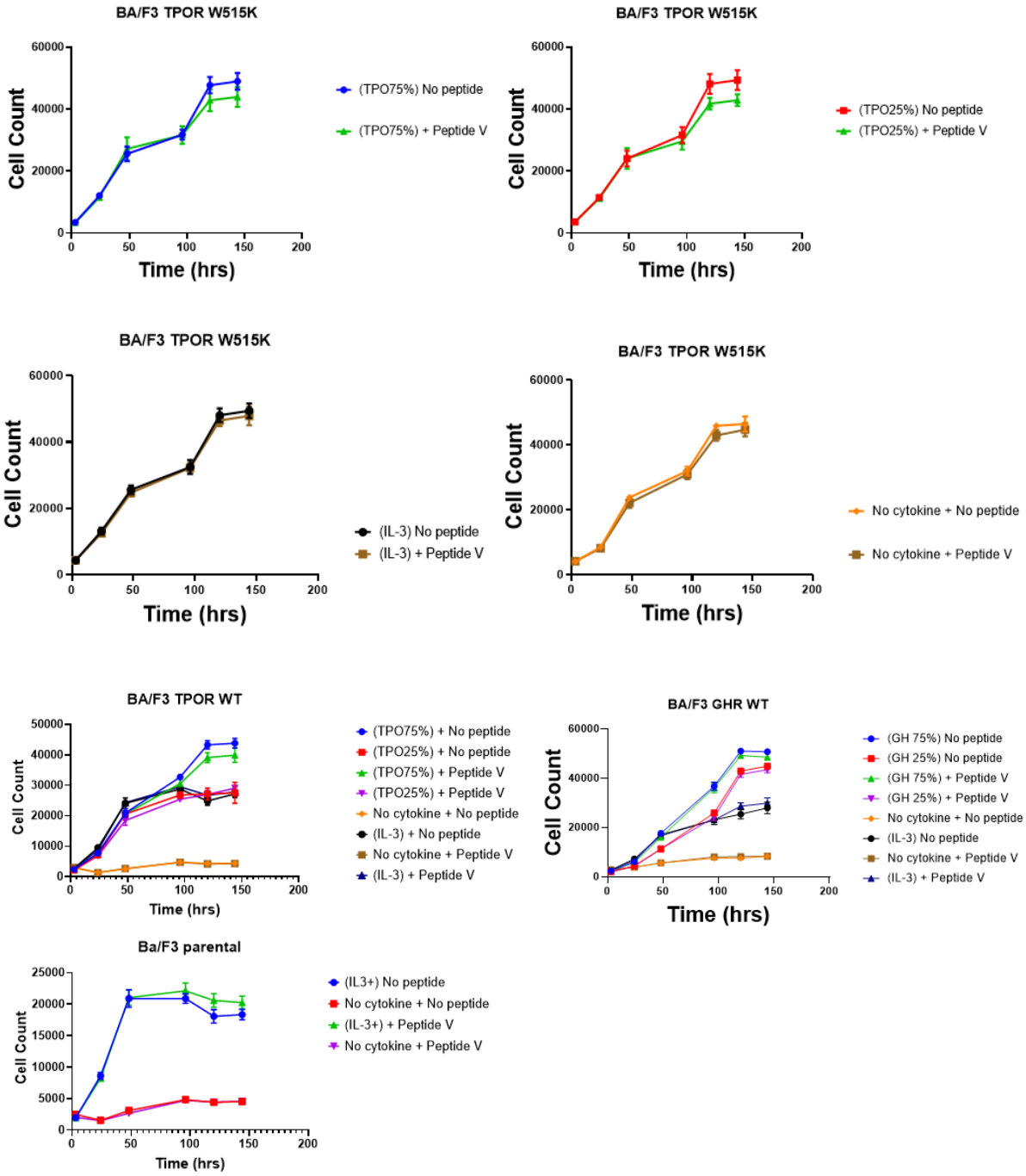
BA/F3 TPOR W515K
Cell Count
Time (hrs)
(TPO75%) No peptide
(TPO75%) + Peptide V
BA/F3 TPOR W515K
Cell Count
Time (hrs)
(TPO25%) No peptide
(TPO25%) + Peptide V
BA/F3 TPOR W515K
Cell Count
Time (hrs)
(IL-3) No peptide
(IL-3) + Peptide V
BA/F3 TPOR W515K
Cell Count
Time (hrs)
No cytokine + No peptide
No cytokine + Peptide V
BA/F3 TPOR WT
Cell Count
Time (hrs)
(TPO75%) + No peptide
(TPO25%) + No peptide
(TPO75%) + Peptide V
(TPO25%) + Peptide V
No cytokine + No peptide
(IL-3) + No peptide
No cytokine + Peptide V
(IL-3) + Peptide V
BA/F3 GHR WT
Cell Count
Time (hrs)
(GH 75%) No peptide
(GH 25%) No peptide
(GH 75%) + Peptide V
(GH 25%) + Peptide V
No cytokine + No peptide
(IL-3) No peptide
No cytokine + Peptide V
(IL-3) + Peptide V
Ba/F3 parental
Cell Count
Time (hrs)
(IL3+) No peptide
No cytokine + No peptide
(IL-3+) + Peptide V
No cytokine + Peptide V

Cell lines (Ba/F3)	Cytokine	Final concentration/well
GFP	IL-3	None or 0.5%
TPOR WT	TPO	None, 5.4 ng/ml (low), or 16.1 ng/ml (high)
TPOR W515K	TPO	None, 2.9 ng/ml (low), or 8.7 ng/ml (high)
GHR WT	GH	None, 1 ng/ml (low), or 3 ng/ml (high)

Figure 20: Peptide V specifically inhibits TPOR-mediated signalling in the presence of TPO.

Retroviral transduced Ba/F3 cell lines in log growth were plated at a density of 3×10^3 cells/well in 384-well plates in IL-3-free and phenol-red free RPMI-1640 media (no starving condition). Peptide V was added (final concentration of 1mM) to respective wells and incubated with the cells for 30 minutes. Cells were treated with plain media (phenol-red free RPMI-1640 media supplemented with 1x L-glutamine, 10% FBS, 1:200 penicillin-streptomycin, 1x sodium pyruvate) or cytokine (see Table). Viable cells were assayed based on GFP expression from day 0 to day 6 after seeding. Results and standard deviations represent the mean of four readings of a single experiment. Image representative of n=2 experiments.

Discussion

TPOR is an important regulator of megakaryocyte differentiation, platelet formation, and HSC maintenance. Clinical TPOR mutations and polymorphisms have been reported where activating mutations were documented in MPN (ET and MF) and AMKL patients. Most TPOR mutations cluster in and around the TMD which is an important region that regulates receptor activation. The current study focusses on three clinically activating point mutations found in the ECD-JM, TMD, and ICD-JM: W515K, T487A, and S505N. These mutations have been reported to result in spontaneous receptor activation leading to cytokine-independent signalling and cell proliferation [222, 239, 395]. W515K and T487A mutations have been speculated to increase the receptor tendency to form activating dimers [40, 43, 224, 225, 240] whereas the S505N is proposed to act by stabilising TPOR in the active dimer form [396, 397]. Prior to cell-based assay screening of peptide antagonists discovered using phage display, the Ba/F3 TPOR WT and mutant (W515K, T487A, S505N) cell lines were tested to confirm for their functionality. TPOR signalling in Ba/F3 and HEK293 cells was shown to produce different signalling outcomes particularly via the ERK1/2 pathway that may be attributed to used species and cell lines' differences, where Ba/F3 is a haematopoietic mouse cell line whereas

HEK293 is a non-haematopoieitic tumorigenic human cell line that may possibly arise from the adrenal gland [398]. Discussion of results will be based on Ba/F3 signalling experimental results as their growth is dependent on JAK-STAT signalling by stimulation with IL-3 or an introduced alternative activation of JAK-STAT signalling. Based on the Ba/F3 results, only the W515K and S505N mutants conferred significant cytokine-independent cell signalling and proliferation, whereas T487A conferred very weak activation. The ability of W515K to cause constitutive activation was consistent with previous studies [239, 395] confirming the inhibitory role of the JM-ICD amphipathic motif in maintaining receptor inactivity in the absence of cytokine stimulation [224, 225]. This mutation resulted in a stronger signalling than the S505N which confirmed that the S505N mutant is a partially constitutive activating mutation that does not allow the cells to proliferate but only survive in the absence of cytokine [222]. However, published comparison of viability assays for the W515K and S505N have shown that the latter conferred stronger or similar cytokine-independent proliferative activity as the W515K mutant [227, 394]. In the current study, the addition of puromycin did not continue after selection. Hence, GFP expression of the cells may be low after several passages and this may account for the lower number of GFP-expressing cells that were detected by the In Cell Analyser (INCA). Nevertheless, the S505N mutation did not confer cytokine-hypersensitivity consistent with previous studies [222, 396]. The characteristics of the S505N may explain the milder phenotype of patients with hereditary thrombocytosis [220, 399, 400] harbouring this mutation [220] and the much lower prevalence of this mutation in ET patients [399, 401]. The T487A mutation has only been found in one *de novo* acute myeloid leukaemia case [239]. This mutation has not been reported in any MPN patients to date although mouse bone marrow transplantation assays showed that the T487A mutation was able to cause a serious myeloproliferative phenotype that is comparable to W515L [239]. However, the latter mutant was able to confer an MPN phenotype with a shorter latency [43]. The current study was not able to replicate the strong constitutive activation of the T487A mutant receptor that was previously documented [239] even after four separate transductions. The different vector backbone utilising a different promoter may account for the difference in observation. The previous study utilises the vector backbone with the MSCV promoter which gives higher expression than the vector backbone with the MMLV promoter that was used in this study [402]. The inability of the T487A mutation to confer strong constitutive signalling and proliferation demonstrates that the ECD linker of the TPOR may facilitate but is not crucial for receptor activation.

FACS analysis confirmed that the increase in signalling of TPOR mutants (W515K and T487A) compared to WT in the presence of TPO was not due to the increase in mature receptor expression levels but that this may be attributed to the higher inherent stability of the mutant receptors. Receptor stability could be further investigated by utilising a cycloheximide chase assay where cells are treated

with cycloheximide to inhibit protein synthesis and analysed for changes in receptor expression levels over time. In the collaborative work, a few novel constitutively active mutants were discovered: L498W, V501A, V501S, and L502S [394]. These oncogenic substitutions are dependent on the position and amino acid residues that are mutated [394]. Consistent with these results, the V501A mutation was found in MPN patients and recently reported to confer constitutive receptor activation [403]. All these mutations lie on the same face of an α-helix which may suggest that they may form structurally similar TMD dimer interfaces [61, 221] and may potentially drive myeloid malignancies.

Currently, available treatments for MPN and leukaemia patients harbouring TPOR mutations include the use of JAK inhibitors, hydroxyurea, interferon-α, and chemotherapy which are not target specific and can cause various significant side effects. Therefore, TPOR presents as an important clinical target for therapeutic inhibition. In particular, peptide antagonists against the crucial signal-modulating TPOR domain, ECD/linker TMD, were discovered via phage display and their functionality assessed using BaF3 TPOR WT and mutant cells. This discovery may facilitate the development of improved targeted drugs to treat patients suffering from myeloid malignancies such as MPNs and AMKL as a result of activating TPOR mutations. The initial trials using the commercial 7-mer peptide library kit (NEB) yielded phages that were not specific to the target of interest or were binding non-specifically to materials used in panning (such as textile, BSA, and plastic phage binders). Indeed, comparison of peptide sequences has shown that these sequences were actually binding to fabric baits [404]. Furthermore, non-specific phage binders may be amplified over specific phage binders due to their growth advantage resulting in a library that is highly over-represented in certain clones. As the same 7-mer library as the ones used for isolating phage-binding fabric baits was used in this study, the library may have a large over-representation of certain clones making it difficult to eliminate them. Hence, several negative selections were performed before the first panning procedure. These negative selections were carried out by exposing the naïve unpanned phage library to materials used in panning such as plastic tubes, plastic plates, BSA, plastic tips, biotin, and streptavidin-coated magnetic beads, in order to remove non-specific phage binders. Additionally, specific competitive elution methods were employed such as using biotin (for N-terminally tagged target) or bait elution instead of the general elution methods using glycine elution buffer or trypsin which may elute nonspecific binding phages. However, these efforts did not significantly improve the discovery of true consensus peptide motifs. An alternative 12-mer peptide library kit was utilised where the phage displays 12 amino acid long random peptide sequences which may increase binding affinity and specificity. A peptide antagonist, peptide V, was discovered via phage display using the TPOR ECD linker as bait, and it was found that this may be a potential peptide that requires further investigation. Interestingly, the peptide only inhibited the proliferation of Ba/F3 TPOR cell lines

cultured in the presence of TPO. As TPOR has been documented to be able to adopt various conformations [61, 221], TPO stimulation may induce a unique conformation which can only be affected by the peptide. However, although this peptide inhibited TPOR W515K, it also exhibited a negative effect on TPOR WT proliferation which suggests that this peptide may not be specifically inhibiting the W515K mutant receptor. Furthermore, as this mutation is located at the JM-ICD, the peptide should not specifically bind to this region. Analysis on a range of peptide concentrations on Ba/F3 TPOR WT and W515K cells may be required in order to determine if there is a therapeutic window for the peptide that results in inhibition of the W515K receptor and not WT. As the cell-based assays were not informative as to whether the peptide can specifically bind to the respective target, an enzyme-linked immunosorbent assay (ELISA) assay may be useful to confirm target specificity. Furthermore, a scrambled peptide with the same amino acid composition may be used to determine if the small effect seen by peptide V was real and specific. An unpublished parallel study on GHR using phage display has shown two peptides that have high specificity for inhibiting GHR-mediated signalling while having a minimal effect on IL-3 signalling (Figure 21). This result strengthens the rationale for using phage display in discovering useful peptide therapeutics.

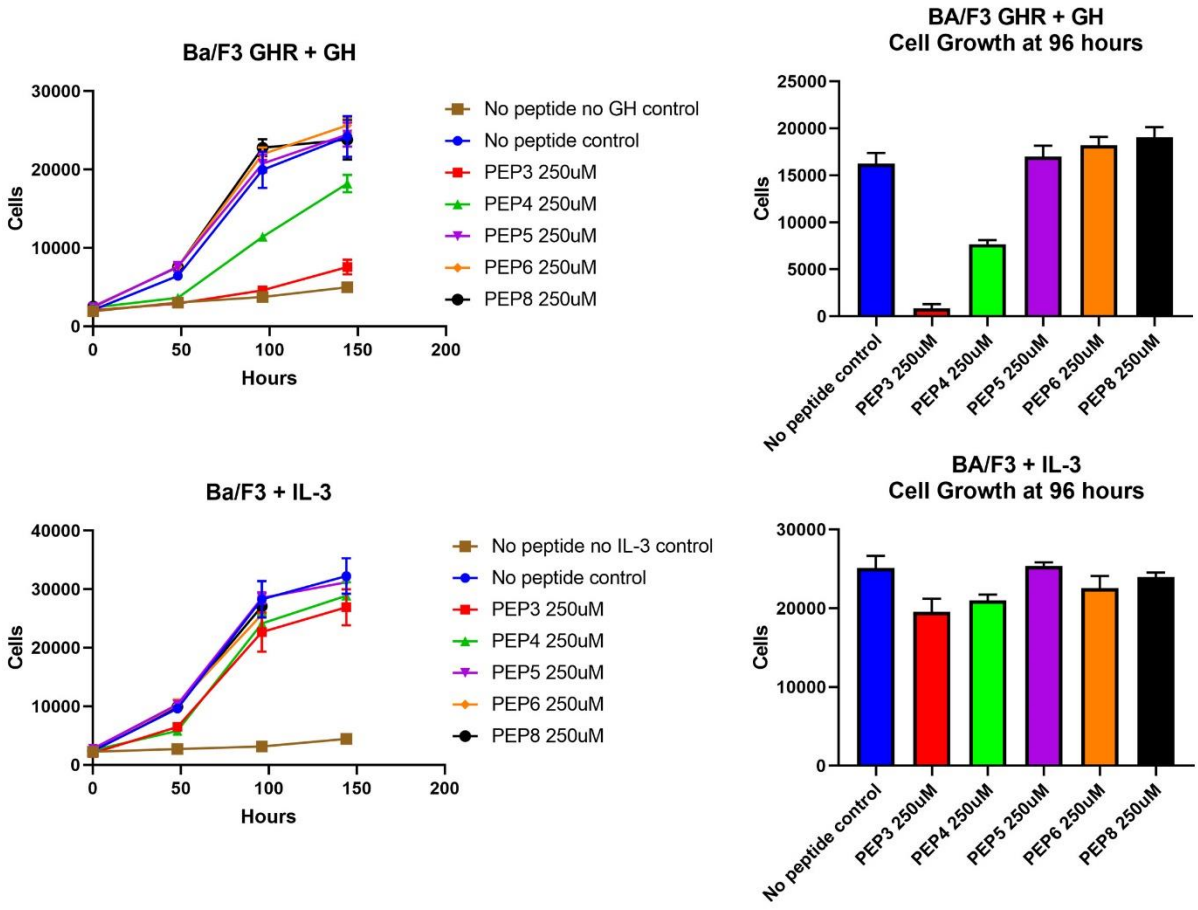

Figure 21: Peptide 3 and 4 specifically inhibit GHR-mediated signalling and not IL-3-mediated signalling in the presence of GH.

Retroviral transduced Ba/F3 cell lines in log growth were plated at a density of 3×10^3 cells/well in 384-well plates in IL-3-free and phenol-red free RPMI-1640 media (no starving condition). Peptides were added (final concentration 250 µM) to respective wells and incubated with the cells for 30 minutes. Cells were treated with plain media (phenol-red free RPMI-1640 media supplemented with 1x L-glutamine, 10% FBS, 1:200 penicillin-streptomycin) or cytokine. Viable cells were assayed based on GFP expression from day 0 to day 6 after seeding. Results and standard deviations represent the mean of four readings of a single experiment. These results were obtained by Rob Luetterforst.

Unlike small molecules and antibody therapies, peptide-based drugs are rarely found in the market as these have low bioavailability, solubility, and stability. However, for the purpose of the current study to discover antagonists that target the ECD linker/TM region, peptides are the more suitable option to be used as a therapeutic target compared to monoclonal antibodies as they can more easily target a smaller area of the protein of interest. Peptides also bind to their targets with high specificities and affinities, and have low immunogenicity and toxicity. Various modifications of peptides have been developed to enhance their efficacy which includes conjugation with PEG, termed as pegylation. The addition of PEG will prolong the half-life of peptides (by preventing proteolytic cleavage), enabling a longer pharmacological effect in the body. Pegylation also improves peptide solubility and reduces immunogenic response. Peptides may also be conjugated with phosphate ester at the amino-terminus end to improve half-life. Addition of non-natural amino acids, glycosylation, and lipidation can also improve peptide stability and/or solubility. As peptides lack avidity, covalent linkage to form peptide dimers is a possible solution in order for the peptides to bind to several targets. Generation of cyclic peptides is also of interest as these exhibit reduced toxicity, increased target specificity, and strong binding affinities to target [405, 406]. Compared to linear peptides, they are also more membrane-permeable, have increased biological activity, and are more resistant to exopeptidases and endopeptidases [407-409]. Alternatively, the peptide sequence can be used as a scaffold for the development of organic small molecules that are more stable and soluble (owing to their size and composition).

Conclusions

In summary, results from both the signalling and Ba/F3 cell proliferation assays, showed that the W515K mutant conferred constitutive signalling and was able to sustain cell proliferation even when cells were deprived of cytokine. On the other hand, the T487A mutant was either not or was weakly constitutively active, and cells expressing it may weakly survive in the absence of cytokine. Finally, the S505N mutant conferred constitutive signalling and promoted cell survival in the absence of cytokine, but may have weaker effects compared to W515K. Novel activating mutations (L498W, V501A, V501S, and L502S) were discovered where collaborators at WEHI identified for the first time some of the same mutations in patient samples. Cell-based assays using Ba/F3 TPOR WT and W515K mutant suggest that peptide V, identified by phage display screening, can be further investigated as a potential peptide antagonist against the TPO/TPOR-mediated signalling pathway. Confirmation of peptide specificity to this pathway will allow for the peptide to be developed into a useful therapeutic agent by itself or to be used as a scaffold for the development of small molecules.

Chapter 4

Investigation of the Effect of TPOR Activation upon Cell Membrane Mobility

Introduction

The majority of TPOR understanding is based on biochemical studies with little or no relation to the spatiotemporal patterns of TPOR in cell membranes and its activity. The lateral diffusion of the receptor allows interaction with other proteins/molecules in the membrane, in the cells, or outside the cells to transmit signals that are important to regulate cell proliferation, survival, and growth. These movements can be influenced by various factors including the fluidity of the phospholipid bilayer (due to variation in the composition of cholesterol in different parts of the membrane), dimerisation states of the receptor, and association with actin filaments or clathrin. The differential mobility pattern of the receptors on the plasma membrane has been shown to influence the different phases of cell signalling [410].

A cutting edge technique known as single-particle tracking photoactivated localisation microscopy (sptPALM) allows detection and tracking of particles down to a single molecule level by tagging molecules with photoconvertible or photoactivatable fluorescent tags. This technique allows for finer observation of structures such as cytoskeletal components, cellular adhesion complexes, cellular organelles, and visualisation of the plasma membrane organisation. sptPALM has also been utilised for a variety of different studies. Through this technique, it has been shown that ligand binding leads to dimerisation of IFNAR1 and IFNAR2 [411]. sptPALM also revealed different mobilities of VSVG and Gag where VSVG are free diffusing in comparison to Gag proteins that are immobile [412]. This technique also demonstrated that conformational change of p2x purinoceptor 7 (P2X7R) is responsible for influencing their mobility and confinement on the cell surface [413]. In this chapter, sptPALM was performed in conjunction with total internal reflection fluorescence (TIRF) microscopy to analyse the lateral diffusion and clustering of TPOR at the cell surface. TIRF microscopy allows for illumination of a thin portion of the sample (~ <200 nm), such as the plasma membrane, which is adjoining the glass-aqueous medium interface at a TIRF angle (Figure 22).

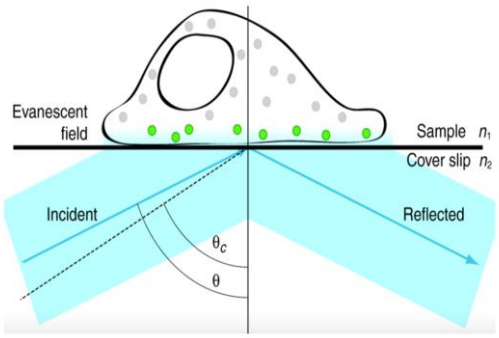

Figure 22: TIRF illumination.

The plasma membrane of a cell adjoining the glass-aqueous medium interface can be imaged at a TIRF angle. Figure reproduced from [414].

Specifically for this project, receptor constructs were tagged with a photoconvertible fluorophore, mEos2. This fluorescent protein is green in its native form and it converts to red when it is illuminated with UV light. In its green form it can be excited with 488 nm laser, while the red form can be excited using the 561 nm laser (Figure 23). In order to ensure that only a few molecules will be in their red state at any one time, a very low 405 nm laser power is used for the conversion of the fluorophore. This allows detection of isolated mEos2 molecules. The position of each mEos2 molecule can then be determined with high localisation precision (~20 nm in x and y and ~50 nm in z dimension) by fitting its image to a two-dimensional Gaussian function. This technique is superior to diffraction-limited conventional light microscopy techniques where the resolving power is very low i.e. objects smaller then ~300 nm cannot be resolved. In this study, images were first taken in green channel to find the cells that are expressing mEos2-labeled TPOR and to visualise the outline of the cells. In this channel all mEos2 molecules are fluorescent. By exposing the cells to very dim 405 nm light, we were able to convert a small subset of mEos2 molecules from green to red colour. In the red channel, these molecules were visible as well separated fluorescent puncta approximately 500 nm in size and were often moving from one frame to the other until they were bleached. These spots were imaged over thousands of frames until all molecules were converted from green to red and bleached in the red channel. The images were subsequently analysed using the Fiji TrackMate application which locates individual molecules and creates trajectories (molecule tracks) from the image series as shown in Figure 2. TPOR can exhibit various track lengths i.e. short or long trajectories (Figure 24) that could relate to receptor turnover or photobleaching [415]. Different modes of receptor diffusion can also be determined using sptPALM which includes confined/immobile, free (Brownian), and directed movements. The simplest form of the mode of diffusion in a homogenous plasma membrane is the

free Brownian motion. Confined/immobile motions can arise due to restriction of diffusion in a small area which may be due to cytoskeletal proteins residing juxtamembrane to the plasma membrane [416, 417], binding to immobile particles, or sequestering in lipid rafts. The directed motion of receptors has been thought to occur after free diffusion into the cell membrane and subsequent transport into the cell via transport vesicles that are mediated by the cytoskeleton leading to the observed directed movement. It was, however, shown that receptor directed movement can also occur on the cell membrane for example for the ephrin type-B receptor 2 (EphB2R) which in this case is cholesterol and not cytoskeleton-dependent [418].

This chapter seeks to investigate the effect of cytokine stimulation and mutations, on the molecular dynamics of the transmembrane receptor TPOR in the plasma membrane using sptPALM. This understanding may elucidate the relationship between the downstream signalling of TPOR and their mobility/clustering by tracking single molecules. sptPALM can provide invaluable information into the characteristics of TPOR in cell membranes.

A.

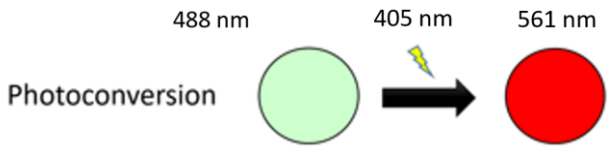

B.

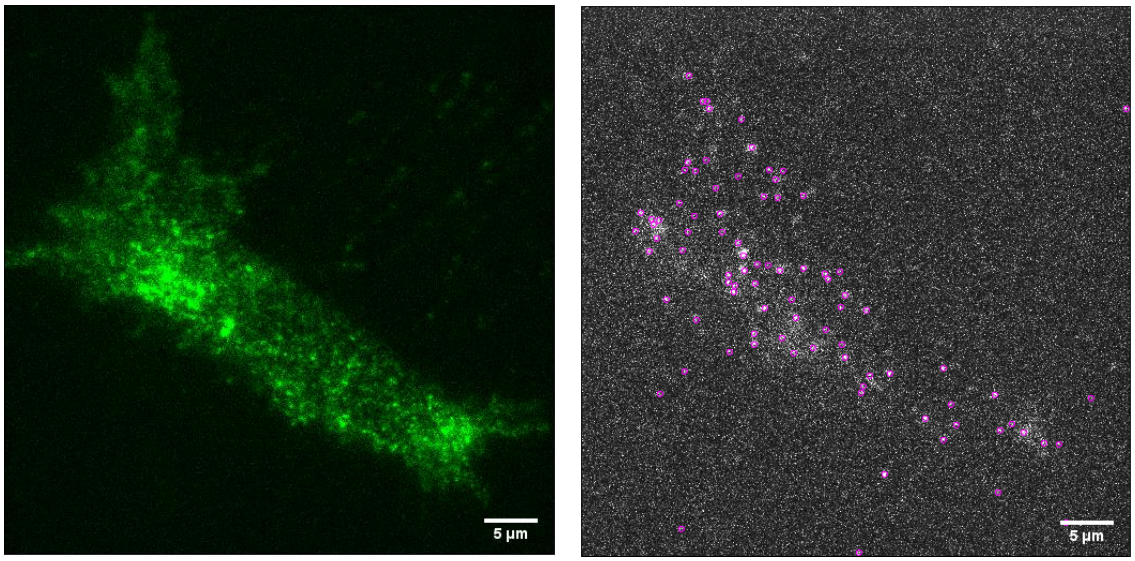

Figure 23: Properties of mEos2 fluorescent proteins.

A) Cartoon image showing photoconversion. The mEos2 photoconvertible fluorophore can be visualized using 488 nm laser in green channel (left) and with 561 nm laser in the red channel (right). The 405 nm laser is used to convert mEos2 from the green to the red-state. B) Snapshot of the mEos2

TPOR construct expressed in live HEK293 cells. Right: Same cell in the red channel (in Grays) with single mEos2 molecules in their red form. Circles around spots are showing receptor molecules detected using TrackMate (Fiji).

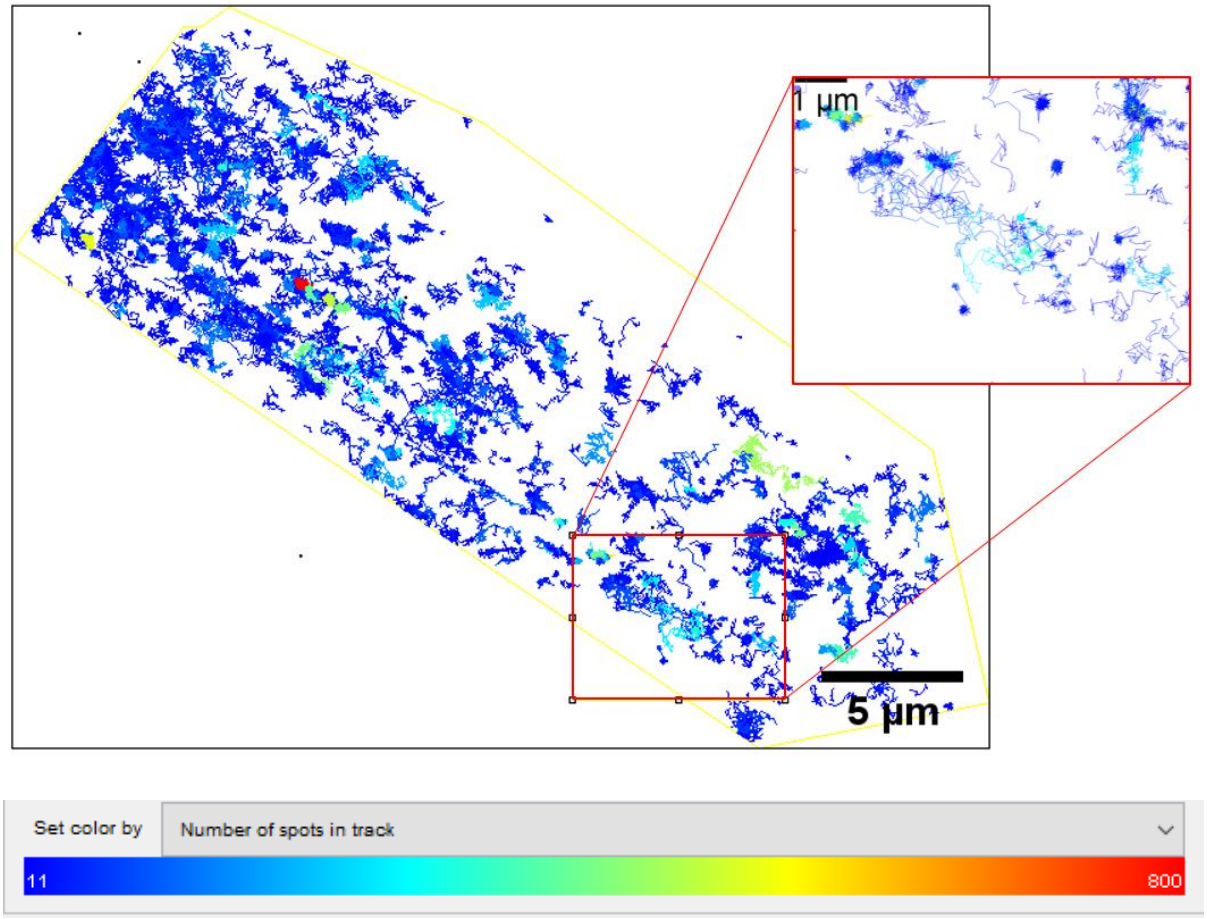

Figure 24: TPOR exhibits a variety of trajectories.

TrackMate locates receptor spots and connects the spots that reside within 0.5 microns to create trajectories. Tracks were coloured based on the number of spots (localisations). Tracks that lasts less than 10 frames were not analysed.

Materials and methods

DNA Constructs

The *mEos2* gene was added to the N- or C-terminus of the full-length HA-tagged TPOR (WT, W515K, or Box1Δ) via CPEC essentially as described in Chapter 2, with a short linker separating the receptor and fluorescent gene to provide flexibility. TPOR construct with N-terminus mEos2 was denoted mEos2-TPOR whereas those with C-terminus tag was denoted TPOR-mEos2. The plasmid backbone containing the mEos2 gene was generated and kindly provided by Farhad Dehkhoda.

Transfection

HEK293 cells were seeded (0.6×10^5 cells/dish) into 29 mm glass-bottom dishes (#1 coverslip) (Cellvis) and cultured overnight in phenol-red free DMEM supplemented with 10% FBS at 37°C in a humidified 5% CO^2 incubator. Cells were transiently transfected with 50 ng receptor (TPOR WT-mEos2, TPOR W515K-mEos2, or TPOR Box1Δ-mEos2) using 1.5 µl Attractene according to manufacturer's instructions (Qiagen). After 19-21 hours incubation at 37°C, sptPALM was performed.

Visualisation of TPOR constructs expression

HEK293 cells were seeded (0.6×10^5 cells/well) into 6-well cell culture plates and cultured overnight in DMEM supplemented with 10% FBS at 37°C in a humidified 5% CO^2 incubator. Cells were transiently transfected with 100 ng receptor (mEos2-TPOR WT, TPOR WT-mEos2, or C-terminal citrine TPOR WT) using Lipofectamine 2000 according to manufacturer's instructions (Invitrogen, Thermo Fisher Scientific). After 25 hours incubation at 37°C, receptor expression was visualised and captured using the inverted epifluorescence Olympus IX73 microscope.

sptPALM

Imaging was performed at The University of Queensland, Queensland Brain Institute's Advanced Microscopy Facility using the Elyra SIM/PALM/STORM microscope, generously supported by the Australian Government through the ARC LIEF LE130100078. sptPALM was performed using the

100× objective α Plan-Apochromat 100× 1.46 NA oil immersion lens and an EMCCD camera Andor iXon Ultra 897 (Andor Technologies). The mEos2-tagged receptors were excited using the 561 nm laser and converted with a 405 nm laser with gradually increased laser power accordingly. GFP fluorescence was detected using the 488 nm laser. Cells were imaged in TIRF angle (~66-68º) at room temperature. For each cell expressing the mEos2-tagged receptors, images were acquired at 30 ms exposures every 32 ms for 4 000 to 16 000 frames.

Data and Statistical Analysis

Data were first analysed with TrackMate, a FIJI plugin for single particle tracking [419]. We used LoG detector and Simple LAP tracker. The spot diameter was estimated to be 0.5 µm and the temporal resolution was adjusted experimentally so that molecules can move at most 0.5 µm between frames. Together with low density of single mEos2 molecules in the red channel, these analysis parameters ensured that fluorescent spots linked into a trace belong to the same molecule. The list of traces were then imported into a custom-written MatLab routine (kindly provided by Dr Nela Durisic, QBI, UQ). Instantaneous diffusion coefficient for each trace was calculated from the fit to the first four point to the mean-squared displacement (MSD) curves. Only trajectories that last for ten or more frames were used for analysis. Modes of receptor diffusion were determined using the 'divide-and-conquer moment scaling spectrum' (DC-MSS) method [420]. Only trajectories that last for 20 or more frames were analysed using moment scaling spectrum (MSS) analysis [421, 422]. Analysis of density-based receptor clustering was conducted via the SR-Tesseler software [423] using single molecule localisation list from TrackMate (Fiji) as an input file. A density factor δ of 1 and a minimum area of 0.5 was used. Within individual objects, clusters were identified with δ =1 and a minimum area of 0.02. All data were presented as mean ± SEM. Statistical analysis was performed in SigmaPlot or GraphPad Prism software using a One-way ANOVA with posthoc Tukey HSD (Honestly Significant Difference), Holm-Sidak method, Dunn's Method or student's 2-tailed unpaired t-test. All data were presented as mean ± SEM. Significance (unpaired t-test): * $P \leq 0.05$; ** $P \leq 0.01$; *** $P \leq 0.001$; **** $P \leq 0.0001$.

Results

In order to determine the role of receptor mobility/clustering in regulating downstream signalling various TPOR constructs (WT, W515K, Box1Δ) that were tagged with mEos2 were generated. It was previously shown that the TPOR W515K mutant was able to confer constitutive signalling in the absence of TPO. This observation was also confirmed in Chapter 6. This chapter investigated if there are differences in the mobility/clustering of TPOR W515K compared to WT that was able to aid its constitutive signalling. The effect of cytokine addition and their effects on the lateral diffusion/clustering of TPOR was also studied. Furthermore, JAK2 was shown to be important in associating with the receptor at its Box1 motif and plays a role in aiding the localisation of TPOR to the cell membrane. The Box1Δ TPOR mutant (with disrupted JAK2 binding) was used in the current study to determine if JAK2 plays a role in receptor mobility/clustering.

Initially, fluorescence resonance energy transfer (FRET) was planned to be utilised to gain a greater understanding of the conformational change that occurs specifically between the Box1-Box2 motifs of TPOR monomers to determine the structural rearrangements of these motifs for signal transmission. Several issues were encountered including difficulty in expressing the receptors at the cell surface, the high background of FRET images, and variability in the results obtained (see Appendix Section A for a description of the technique and more in-depth explanation regarding the issues encountered). Due to the different technical difficulties and time limitation, sptPALM was pursed to gain novel insights into the TPOR by investigating the relationship between the mobility (lateral diffusion) and clustering of TPOR, and its effect on downstream signalling.

TPOR-mEos2 constructs respond to TPO and signals downstream

The various TPOR constructs were tagged with an mEos2 photoconvertible fluorophore at its N- or C-terminus (Figure 25). Their expression was visualised using an inverted epifluorescence microscope. Results showed that constructs with an N-terminal mEos2 tag was not visualised as easily as the C-terminally tagged constructs indicating a less efficient expression of the N-terminal tagged constructs (Figure 26). As the presence of the mEos2 at the N-terminal might interfere with the localisation or insertion of the receptor into the plasma membrane, full-length TPOR that was tagged with mEos2 at its C-terminus were utilised for sptPALM analysis.

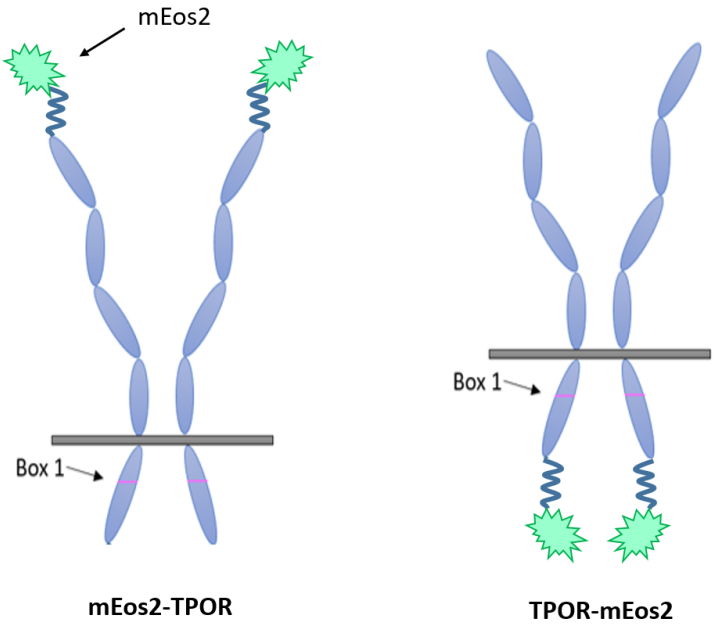

Figure 25: mEos2 was tagged at the N- or C-terminus of the full-length hTPOR.

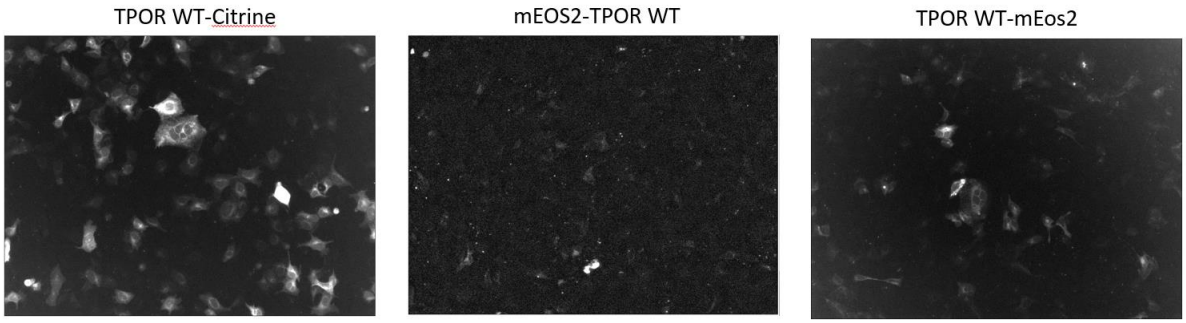

Figure 26: TPOR tagged with mEos2 at the C-terminus expressed more efficiently than N-terminally tagged receptors.

Full-length TPOR was tagged with the mEos2 fluorophore at the N- (middle) or C-terminus (right). The constructs were transfected (100 ng) and expressed in HEK293 cells. After 25 hours of transfection, receptor expression was visualised using the epifluorescence microscope. TPOR WT-Citrine acts as a positive control.

The constructs were subsequently confirmed for their functionality via their ability to confer downstream signalling to ensure that the fusion of the fluorescent gene does not interfere with the function of the receptor. TPOR WT and W515K tagged with mEos2 were able to signal upon cytokine stimulation as observed by the increase in ERK activation (Figure 27). TPOR W515K-mEos2 was

also able to signal in the absence of cytokine treatment. However, the lower constitutive activation seen in W515K tagged versus untagged may be due to the lower receptor expression. These reduced expression levels may be attributed to the different vector backbone used.

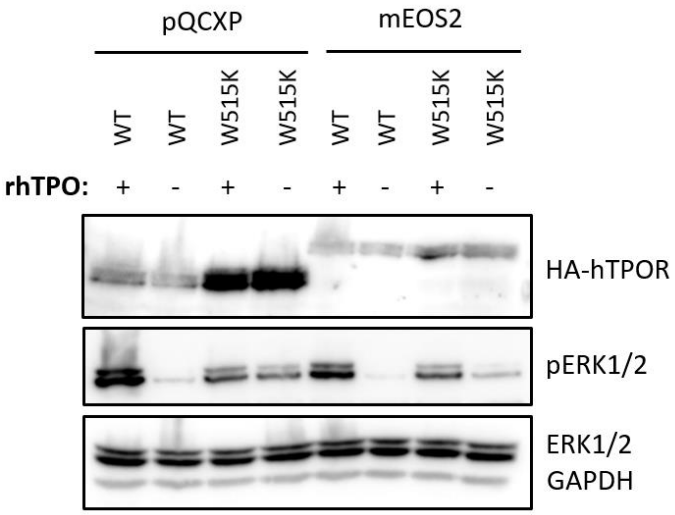

Figure 27: TPOR-mEos2 constructs respond to TPO stimulation.

HEK293 cells were transiently transfected with pQCXIP HA-hTPOR WT, pQCXIP HA-hTPOR W515K, HA-hTPOR WT-mEos2, or HA-hTPOR W515KmEos2. Cells were starved overnight and TPO (final concentration of 50 ng/ml) was added (+) for 10 minutes. Samples in the absence of TPO (-) were used for comparison. Total protein was subjected to SDS-PAGE and immunoblotted with indicated antibodies. GAPDH was used as a loading control.

TPOR exhibits bimodal mobility in the plasma membrane of HEK293 cells

Trajectories of single particle tracking TPOR diffusing on the cell surface were obtained from time-lapse series of 4 000 to 16 000 fluorescent images recorded at 32 milliseconds/frame using an Elyra PS1 PALM/STORM microscope. The recording of 4 000 frames was performed for non-stimulated cells whereas a longer recording of 16 000 frames was performed on cells stimulated with TPO to capture any difference in receptor mobility patterns upon addition of cytokine. The movement of TPOR in the plasma membrane was bimodal; many receptors were highly mobile and freely diffusing but there was also a population of slowly moving molecules. Consequently, a histogram of diffusion coefficients (Figure 28) showed two populations which were well resolved when the X-axis was shown on a Logarithmic scale. The distribution of diffusion coefficients to two Gaussians was fitted.

Fast moving population peaked at Log (D) = -0.8 and the slow moving one was centred at Log (D) = -1.5. For simplification, receptors were classified into two categories: type I (peak 1) comprised the slower diffusing receptors and type II (peak 2) comprised the highly mobile receptors with the cut-off Log (D) = -1.2.

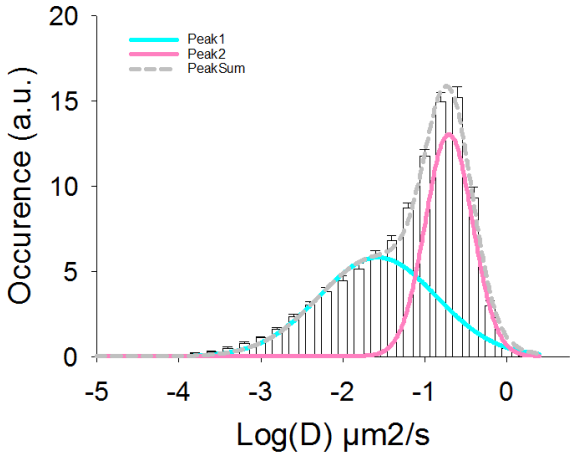

Figure 28: TPOR exhibits two mobile receptor populations, slow-diffusing (type I) and highly mobile (type II).

The diffusion coefficient D ($\mu m^2/s$) was calculated from a linear fit to the first four points of the MSD curve. Highly mobile receptors displayed an average diffusion coefficient of $10^{-0.8}$ $\mu m^2/s$ and slow-diffusing receptor populations exhibited an average diffusion coefficient of $10^{-1.5}$ $\mu m^2/s$.

Activated TPOR WT and activating W515K mutation caused a decrease in receptor mobility

In order to determine the effect of an activating ligand on TPOR mobility, the cells were stimulated with rhTPO and after 30 seconds, recording began for 16 000 frames (approximately 9 minutes of stimulation). The centre and width of the two Gaussian distributions were used to compare receptor mobility between different experiments. After addition of TPO, type II receptor population (fast-moving) of TPOR WT decreased in mobility and occurrence, in favour of the type I receptors in which the slow-moving subpopulation increased substantially (Figure 29). This is reflected in the shift of the 'centre' of peak 2 from -0.7 to -0.8, and the change in the 'width' of peak 1 from 1.4 to 1.3 and peak 2 from 0.5 to 0.6 (Figure 29). However, TPO binding did not result in the increase in occurrence of type I populations over type II. This suggests that only a small fraction of the type II subpopulations respond to TPO. Unlike TPOR WT, the W515K receptor was not affected by the addition of cytokine as the type I and type II receptor populations, in this case, did not exhibit significantly different receptor mobility (Figure 29).

In order to determine the effect of a constitutively active receptor on mobility, TPOR WT and W515K were compared. In the absence of TPO, the type II receptor population (fast-moving) of TPOR W515K decreased in mobility and occurrence compared to WT whereas the portion of type I receptors (slow-diffusing) did not differ (Figure 29). This was observed by the increase in 'centre' log (D) values and 'width' (Figure 29) of type II W515K compared to WT. In the presence of cytokine stimulation, the effect of the W515K mutant on type I and II receptor populations was not observed to be significantly different compared to WT (Figure 29).

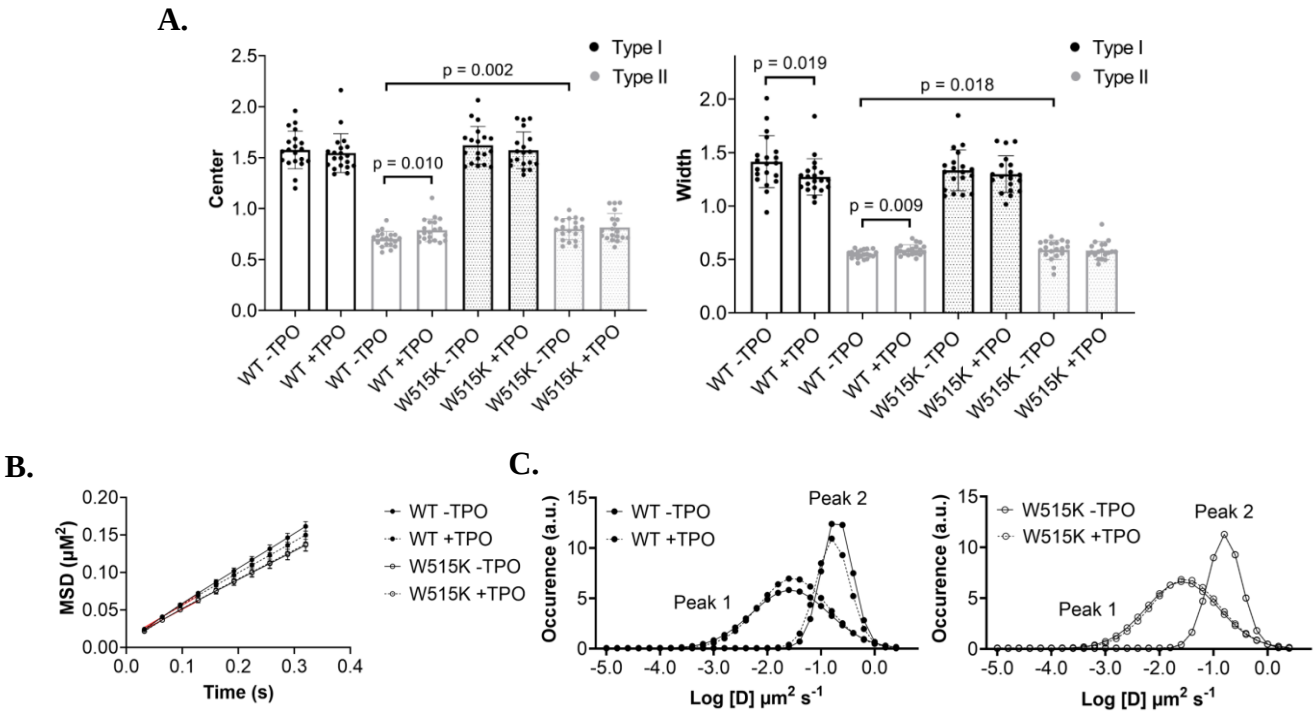

Figure 29: WT Type II receptors (in the presence of TPO) and W515K Type II receptors (in the basal state) exhibit decreased diffusivity.

A) Data were plotted as bar charts to highlight the difference in the diffusivity of TPOR WT and W515K in the basal, inactive state and the stimulated, active state. B) Diffusivity was calculated from a linear fit to the MSD of the first four recorded values (D_{1-4}) (red lines). Bar charts were obtained from histogram fits that assume the presence of two Gaussian distributions (C). Data representative of N=5 independent experiments.

JAK2 does not play a role in TPOR mobility

In order to determine the involvement of JAK2 on receptor mobility, TPOR WT and Box1Δ were compared. However, in the basal state, the effect of the Box1Δ on type I and II receptor populations was not observed to be significantly different compared to WT (Figure 30).

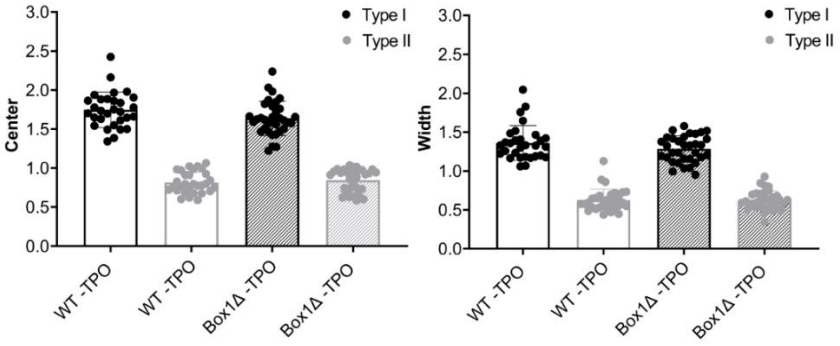

Figure 30: In the basal state, the diffusivity of WT Box1Δ TPOR did not differ.

Data were plotted as bar charts to highlight the difference in the diffusivity of TPOR WT and Box1Δ in the basal, inactive state. Data representative of N=3 independent experiments.

TPOR exhibits various modes of diffusion

The mode of diffusion of TPOR was investigated. The analysis framework used for analysing mobility patterns were determined based on the DC-MSS method from [420]. TPOR showed three distinguishable mobility regimes in the phospholipid bilayer: i) immobile/confined, ii) free Brownian diffusion, iii) and directed motion (or 'super-diffusive') (Figure 31). Receptors in the basal state, activated, or with mutation of the Box1 motif displayed all three distinct diffusion modes. Immobile and confined receptors were considered the same category as it is difficult to define the distinction between these two states. A small subset of receptors also changed their mode of diffusion (Figure 32), termed multiple diffusion states.

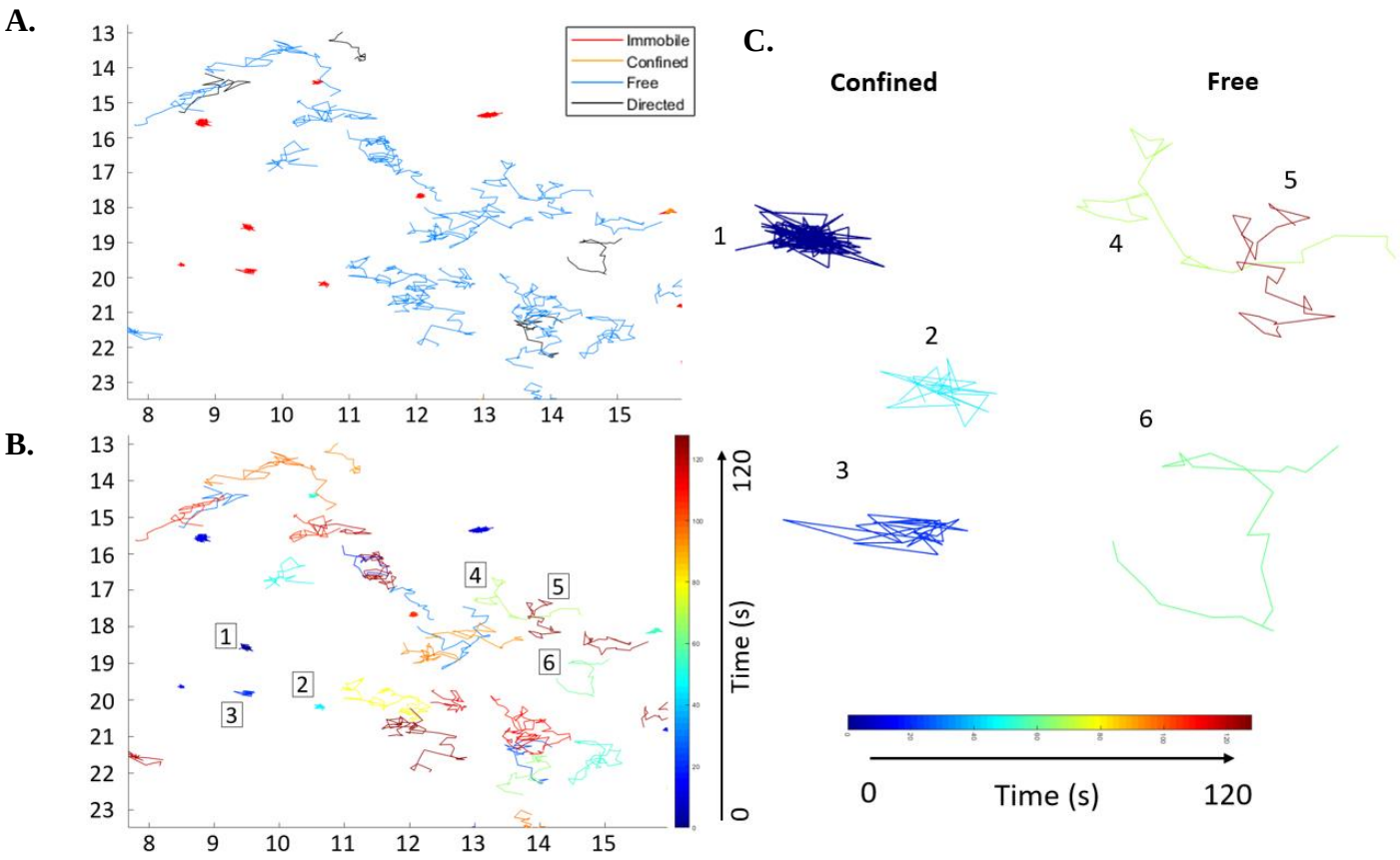

Figure 31: TPOR exhibit various modes of diffusion on the surface of HEK293 cells.

A) A representative image of TPOR trajectories in a cell. The different modes of receptor diffusion are shown in different colors: red-immobile, orange-confined, blue-free diffusion, black-directed motion). B) A representative image based on one cell of the tracks by time of appearance (0 time (dark blue) to 120 seconds (dark brown). C) Representative confined and free tracks from B) and their corresponding time of appearance. As it is difficult to accurately assign the type of motion to tracks that lasts for less than 20 frames, these tracks were not shown.

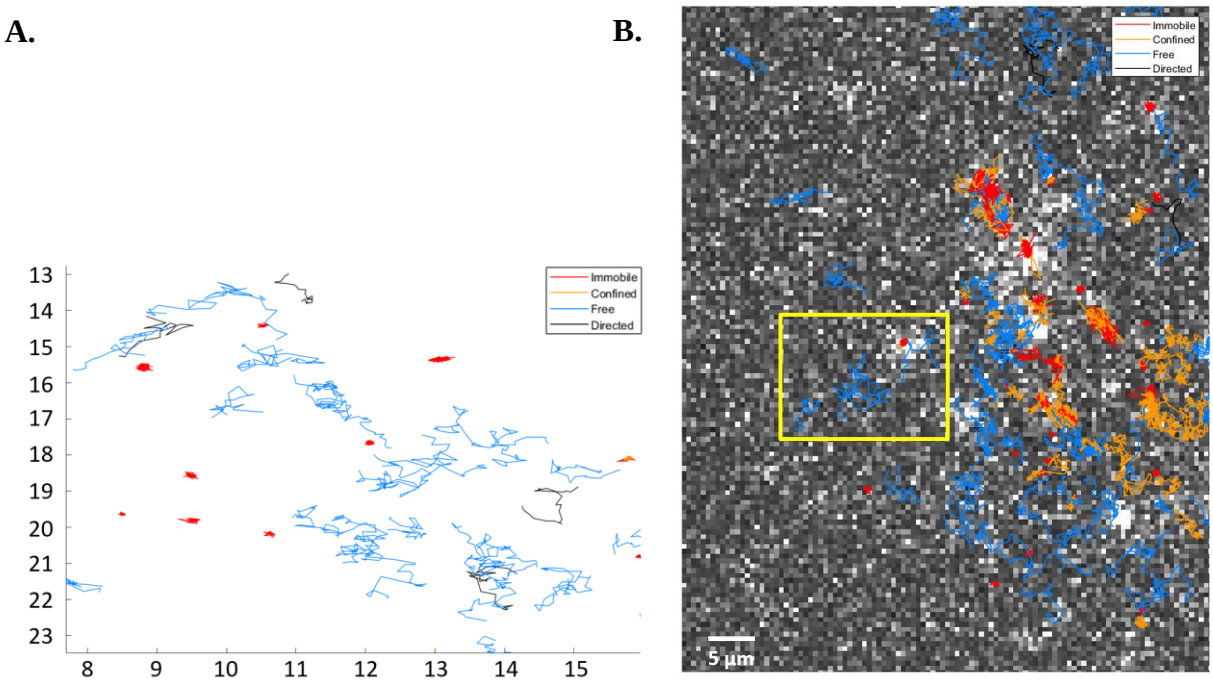

Figure 32: Track movements of TPOR can change between different diffusive states.

A) A representative image of a track that changed between freely diffusive (blue) and directed (black) states. B) A representative image of a trajectory (boxed in yellow) that changed between immobile (red) and freely diffusive (blue) states that were superimposed on a frame of a red green blue (RGB) image of receptor molecules (white blobs).

TPOR activation increased receptor confinement

The role of receptor activation on the mobility patterns of TPOR WT and W515K was investigated. TPOR is mostly present as immobile/confined followed by free-diffusing and a very low population of TPOR exhibited directed motion (Figure 33). For single-diffusive state receptors, activation of the receptor resulted in increased receptor confinement where the addition of cytokine more significantly enhanced the confinement (Figure 33). However, the comparison between the unstimulated and stimulated receptor states showed no significant difference between the numbers of free or confined molecules (Figure 33). In all cases, with or without receptor activation, the number of receptors exhibiting directed movement was less than 3.1% and hence were not included for further analysis. Receptor trajectories can exhibit multiple diffusion states with one or more changes to a different diffusion state and this contributed to less than 13% of the whole receptor population (Figure 34). However, for the ease of analysis, these are not grouped into different categories based on the number

of state changes. Ligand stimulation or the W515K mutation does not affect tracks with multiple diffusion states (Figure 34).

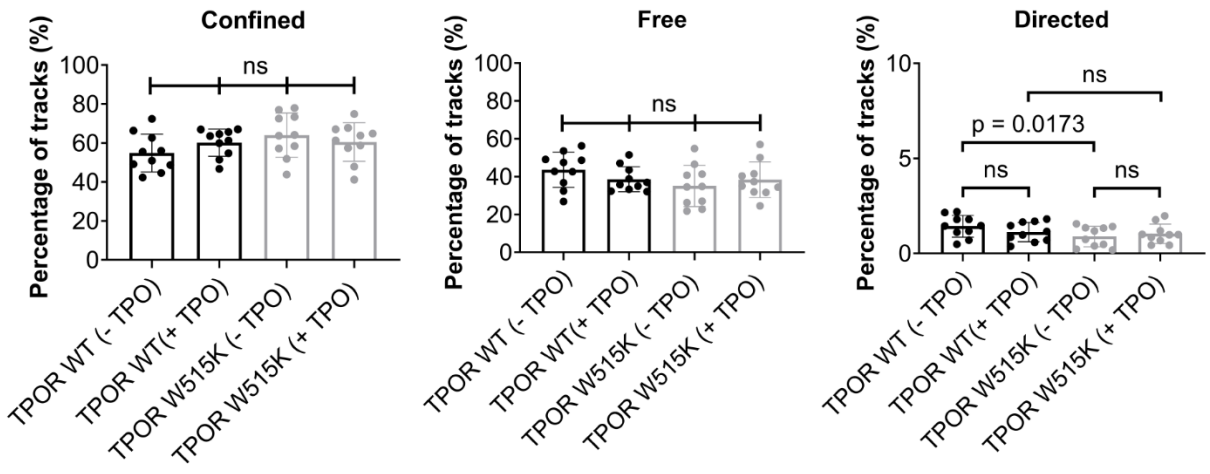

Figure 33: TPO stimulation or constitutively active receptor increases receptor confinement.

Only single-state diffusions were included in the analysis. 7782 trajectories analysed for WT-, 37580 trajectories analysed for WT+, 12090 trajectories analysed for W515K-, and 45063 trajectories analysed for W515K+. N=6 or 7 cells per condition. Data representative of N=2 independent experiments. Student's 2-tailed unpaired t-test was used for statistical analysis. Only comparisons that were statistically significant were denoted on the bar chart. WT+ C vs WT- C = ns (p = 0.3133), W515K+ C vs W515K- C = ns (p = 0.7189), W515K- C vs WT-C = ns (p = 0.5687), W515K+ C vs WT+ C = ns (p = 0.7901), WT- F vs WT- C = ns (p = 0.0964), WT+ F vs WT+ C = **** (p <0.0001), W515K- F vs W515K- C = * (p = 0.0215), W515K+ F vs W515K+ C = *** (p = 0.0004), WT+ F vs WT- F = ns (p = 0.3012), W515K+ F vs W515K- F = ns (p = 0.7274), W515K- F vs WT- F = ns (p = 0.5526), W515K+ F vs WT+ F = ns (p = 0.8138), WT+ D vs WT- D = ns (p = 0.7589), W515K+ D vs W515K- D = ns (p = 0.6449), W515K- D vs WT- D = ns (p = 0.8971), W515K+ D vs WT+ D = ns (p = 0.4225).

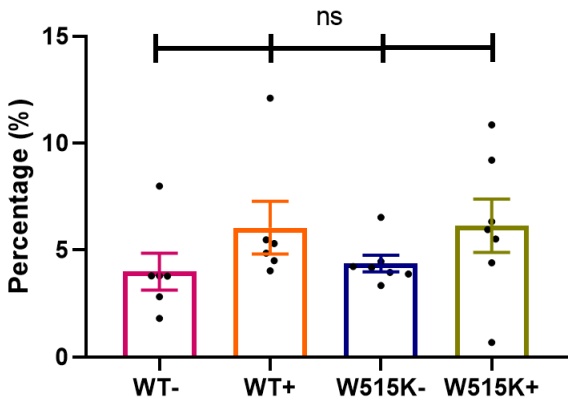

Figure 34: TPO stimulation or constitutively active receptor does not affect trajectories with multiple diffusive states.

Only multi-state diffusions were included in the analysis. Percentage of multiple-diffusive state receptors was calculated by dividing the number of receptors with multiple diffusion states with the total number of receptors (including single-state diffusions) and normalised. "-" represents no stimulation, "+" represents with 50 ng/ml TPO stimulation. 310 trajectories analysed for WT-, 2661 trajectories analysed for WT+, 578 trajectories analysed for W515K-, and 3370 trajectories analysed for W515K+. N=6 or 7 cells per condition. Student's 2-tailed unpaired t-test was used for statistical analysis. All comparisons were not statistically significant. WT+ vs WT- = ns ($p = 0.2022$), W515K+ vs W515K- = ns ($p = 0.1997$), W515K- vs WT- = ns ($p = 0.6837$), W515K+ vs WT+ = ns ($p = 0.9604$).

The effect of different receptor activation states on the diffusion coefficient of trapped (confined/immobile) and free-diffusing molecules were investigated. Receptors exhibiting Brownian free-motion have a significantly higher diffusion coefficient (faster diffusing) than trapped receptors (Figure 35). However, the diffusion coefficient of freely-diffusing or trapped receptor molecules between different receptor activation states does not significantly differ (Figure 35 B and Figure 36).

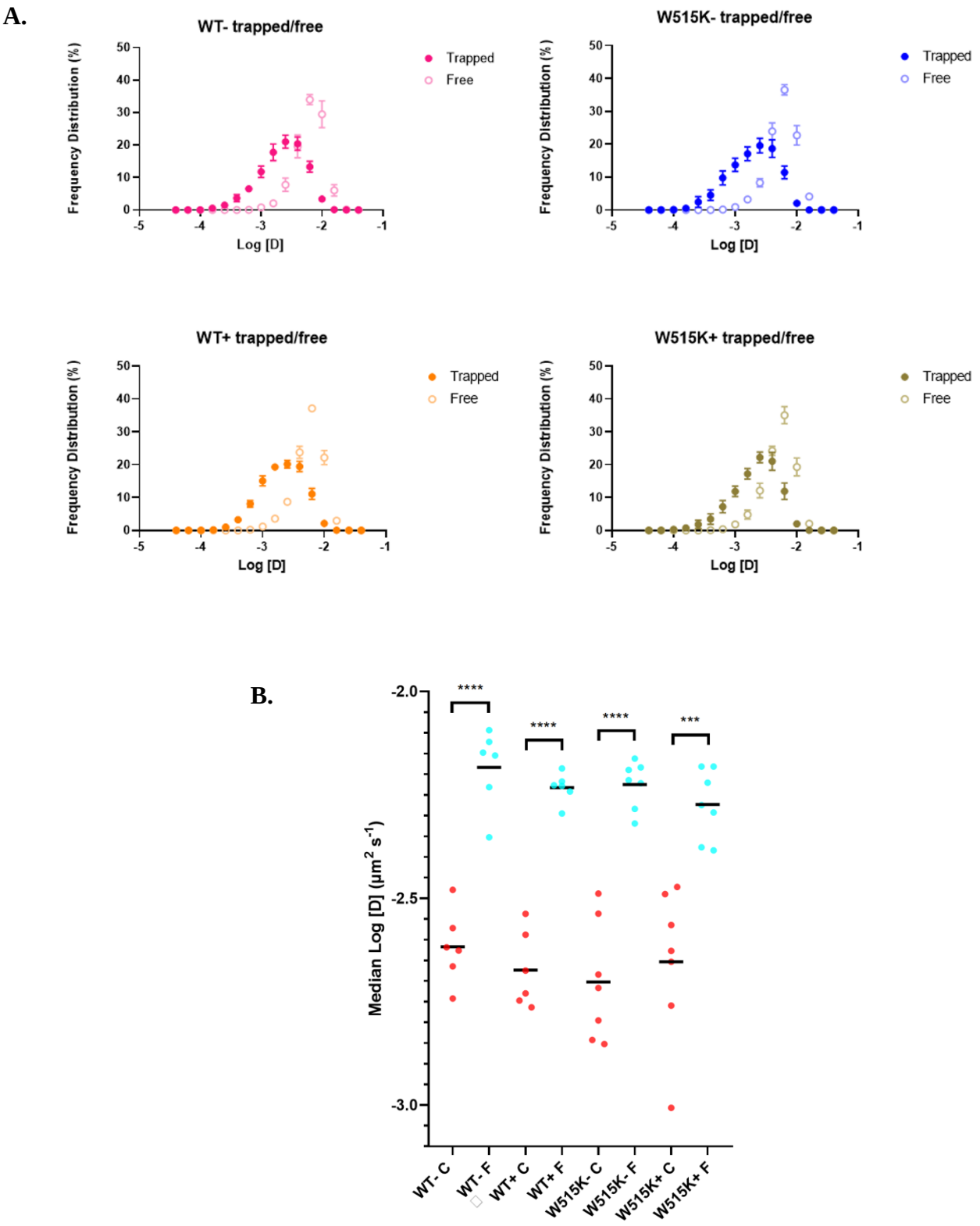

Figure 35: Free-diffusing TPOR WT and W515K molecules have a higher diffusion coefficient than trapped (confined/immobile) molecules with or without cytokine stimulation.

A) Histogram showing trapped versus free molecules for TPOR WT and W515K in the presence or absence of cytokine stimulation. B) Dot plot showing the median for trajectories. Data from each dot was obtained from a single video. Horizontal lines are means for 6-7 videos; 7782 trajectories

analysed for WT-, 37580 trajectories analysed for WT+, 12090 trajectories analysed for W515K-, and 45063 trajectories analysed for W515K+.. Only single-state diffusions were included in the analysis. "-" represents no stimulation, "+" represents with 50 ng/ml TPO stimulation. "C" denotes confined/immobile receptors and "F" represents free diffusing (Brownian) receptors. N=6 or 7 cells per condition. Data representative of N=2 independent experiments. Student's 2-tailed unpaired t-test was used for statistical analysis in B). Only comparisons that were statistically significant were denoted on the bar chart. WT- F vs WT- C = **** (p <0.0001), WT+ F vs WT+ C = **** (p <0.0001), W515K- F vs W515K- C = **** (p <0.0001), W515K+ F vs W515K+ C = *** (p = 0.0003), WT+ C vs WT- C = ns (p = 0.3042), WT+ F vs WT- F = ns (p = 0.2636), W515K+ C vs W515K- C = ns (p = 0.5895), W515K+ F vs W515K- F = ns (p = 0.2355), W515K- C vs WT-C = ns (p = 0.2344), W515K- F vs WT- F = ns (p = 0.3521), W515K+ C vs WT+ C = ns (p = 0.8130), W515K+ F vs WT+ F = ns (p = 0.3018). Log [D] units = $\mu m^2/s$.

A.

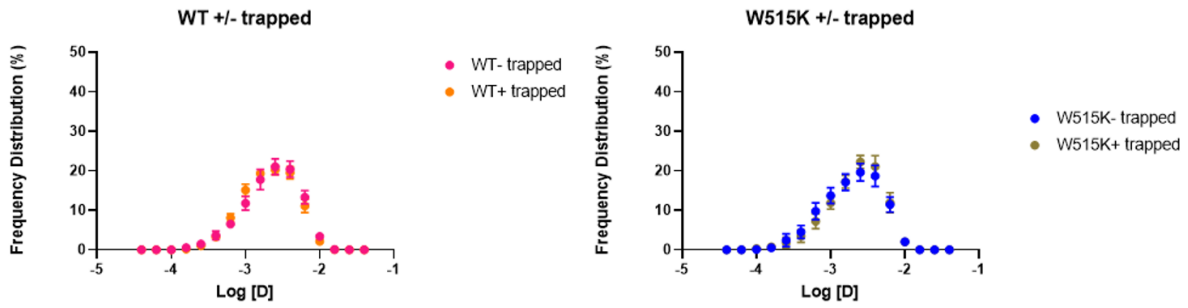

B.

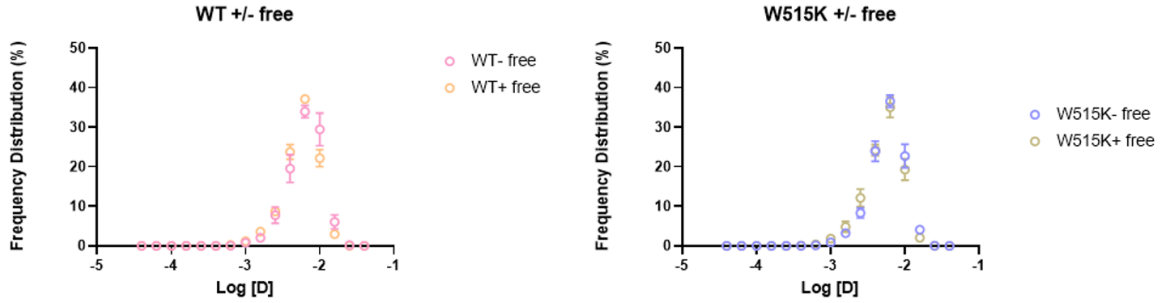

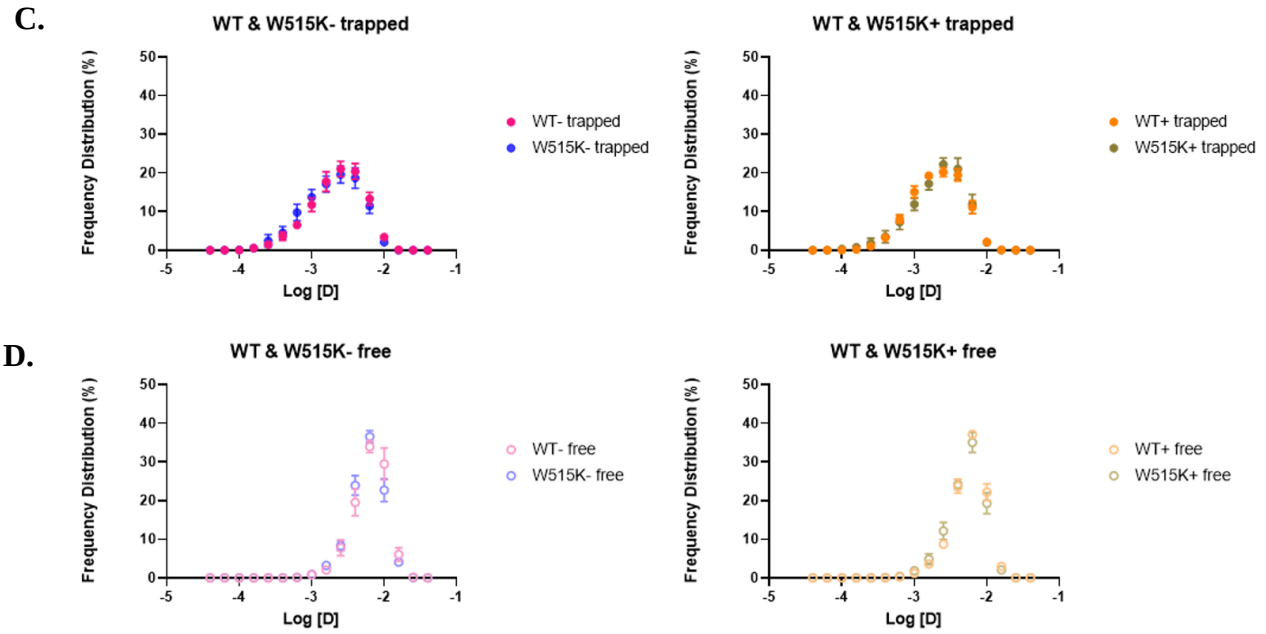

Figure 36: Cytokine stimulation or constitutive receptor activation does not affect the diffusion of the trapped (confined/immobile) or free-diffusing molecules.

A) Comparison of trapped molecules for TPOR WT or W515K in the presence and absence of cytokine stimulation. B) Comparison of free molecules for TPOR WT or W515K in the presence and absence of cytokine stimulation. C) Comparison of trapped molecules between TPOR WT and W515K in the presence (right) and absence (left) of cytokine stimulation. D) Comparison of free molecules between TPOR WT and W515K in the presence (right) and absence (left) of cytokine stimulation. Only single-state diffusions were included in the analysis. "-" represents no stimulation, "+" represents with 50 ng/ml TPO stimulation. 7782 trajectories analysed for WT-, 37580 trajectories analysed for WT+, 12090 trajectories analysed for W515K-, and 45063 trajectories analysed for W515K+. N=6 or 7 cells per condition. Data representative of N=2 independent experiments. Log [D] units = $\mu m^2/s$.

JAK2 does not play a role in TPOR mobility patterns

The role of JAK2 on the mobility patterns of TPOR WT and Box1Δ was investigated. For single-diffusion state receptors, the percentage of free-diffusing receptors is significantly lower than confined receptors for both TPOR WT and Box1Δ (Figure 37). However, the comparison between TPOR WT and Box1Δ in the basal state showed no significant difference between the amount of free or confined molecules (Figure 37). The number of receptors exhibiting directed movement was less than 2% and hence were not included in further analysis. Receptors with multiple diffusion states

contributed to less than 8% of the whole receptor population (Figure 37). Box1Δ mutation did not affect tracks with multiple diffusion states (Figure 38).

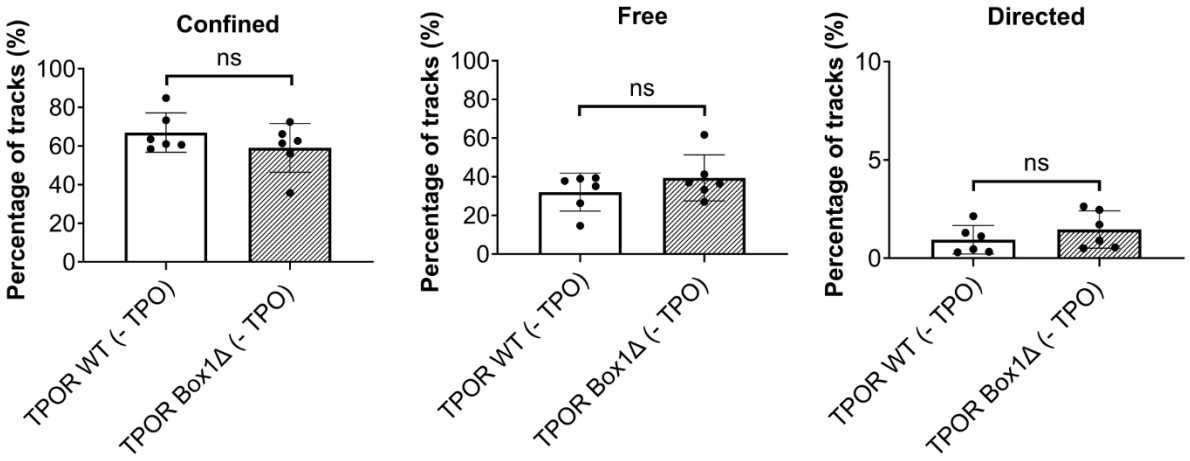

Figure 37: TPOR Box1 mutation does not affect the receptor mode of diffusion.

Only single-state diffusions were included in the analysis. Receptor populations that have directed movement are less than 2% and hence excluded from statistical analysis. 1682 trajectories were analysed for WT and 5984 trajectories were analysed for Box1Δ-. N=4 cells per condition. Data representative of N=1 experiment. Student's 2-tailed unpaired t-test was used for statistical analysis. Only comparisons that were statistically significant were denoted on the bar chart. WT- F vs WT- C = *** (p = 0.0001), Box1- F vs Box1- C = **** (<0.0001), Box1- C vs WT- C = ns (p = 0.2121), Box1- F vs WT- F = ns (p = 0.1787).

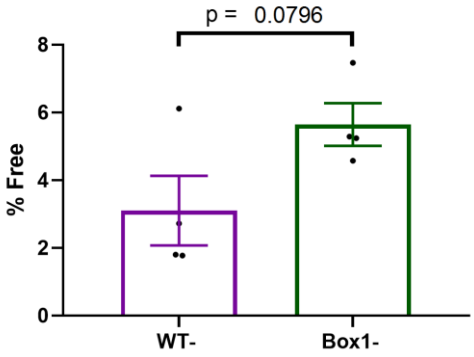

Figure 38: TPOR Box1 mutation does not affect track changes to multiple diffusive states.

Only multi-state diffusions (one or more segmentations) were included in the analysis. Percentage of multiple-diffusive state receptors was calculated by dividing by the total number of receptors (including single-state diffusions) and normalising. "-" represents no stimulation. 64 trajectories were

analysed for WT and 335 trajectories were analysed for Box1Δ-. N=4 cells per condition. Data representative of N=1 experiment. Student's 2-tailed unpaired t-test was used for statistical analysis.

The effect of the lack of JAK2 binding to TPOR using the Box1Δ on the diffusion coefficient of trapped (confined/immobile) and free-diffusing molecules was investigated. Receptors exhibiting Brownian free-motion have a significantly higher diffusion coefficient (faster diffusing) than trapped receptors (Figure 39). However, the diffusion coefficient of freely-diffusing or trapped receptor molecules in TPOR WT and Box1Δ does not significantly differ although a trend did appear apparent (Figure 39 C and Figure 40).

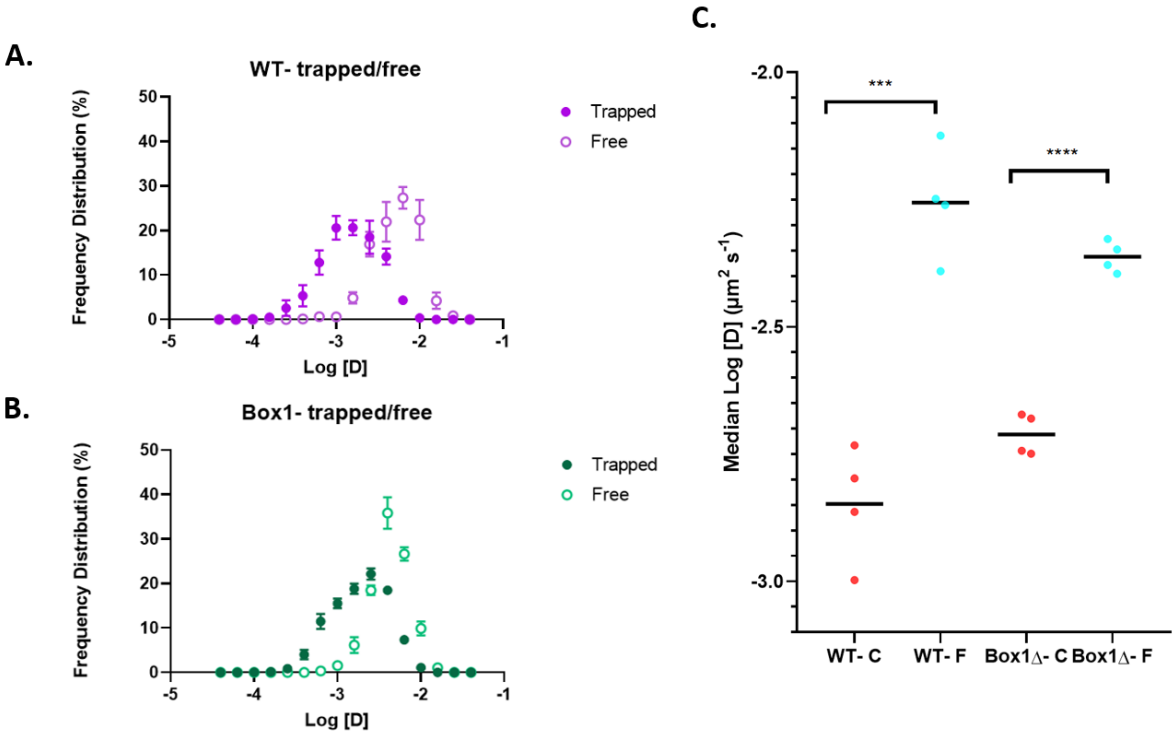

Figure 39: Free-diffusing TPOR WT and Box1Δ molecules have a higher diffusion coefficient than trapped (confined/immobile) molecules in the absence of cytokine stimulation.

A & B) Histogram showing trapped versus free molecules of TPOR WT and Box1Δ. C) Dot plots showing the median for trajectories. Data for each dot was obtained from a single video. Horizontal lines are means of 4 videos; 1682 trajectories were analysed for WT and 5984 trajectories were analysed for Box1Δ-. Only single-state diffusions were included in the analysis. "-" represents no stimulation. "C" denotes confined/immobile receptors and "F" represents free diffusing (Brownian) receptors. N=4 cells per condition. Data representative of N=1 experiment. Student's 2-tailed unpaired t-test was used for statistical analysis in C). Only comparisons that were statistically significant were denoted on the bar chart. WT- F vs WT- C = *** (p = 0.0003), Box1- F vs Box1- C

= **** (<0.0001), Box1- C vs WT- C = ns (p = 0.0636), Box1- F vs WT- F = ns (p = 0.1089). Log [D] units = $\mu m^2/s$.

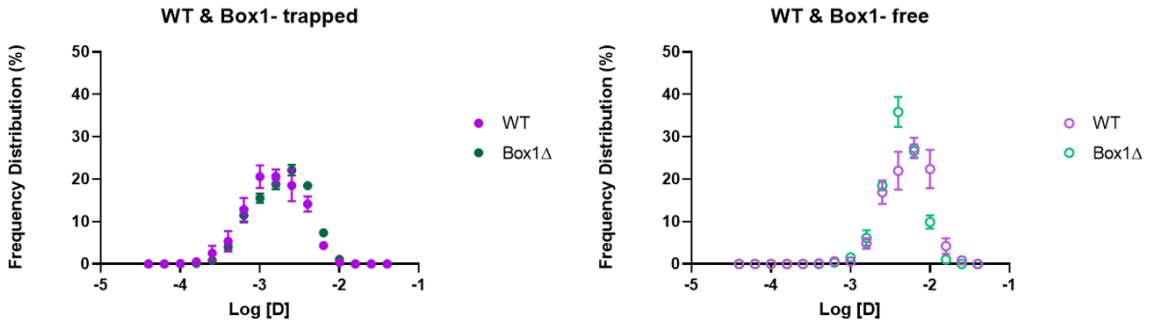

Figure 40: TPOR Box1 mutation does not affect the diffusion of the trapped (confined/immobile) or free-diffusing molecules.

Only single-state diffusions were included in the analysis. "-" represents no stimulation. Left: comparison of the diffusion coefficient of trapped TPOR WT and Box1Δ. Right: comparison of the diffusion coefficient of free TPOR WT and Box1Δ. 1682 trajectories were analysed for WT and 5984 trajectories were analysed for Box1Δ-. N=4 cells per condition. Data representative of N=1 experiment. Log [D] units = $\mu m^2/s$.

TPOR forms clusters, but clustering may not play a role in regulating signalling

As changes in receptor clustering have been shown to fine-tune signalling in some receptors, this was investigated for TPOR. TPOR can form clusters of different sizes (based on area and diameter) (Figure 41, Figure 43, and Figure 44) and it is organised in nanometer-scale small clusters in HEK293 cells (Figure 43 and Figure 44). The majority of TPOR clusters have diameters between 10 and 100 nm for both control and TPO-stimulated cells or TPOR variants (Figure 43). The number of receptors in each cluster varies between as little as 18 and as much as ~140 000 (data not shown). Confined/immobile receptors were usually located in receptor clusters whereas freely-diffusing molecules were usually situated outside of receptor clusters (Figure 42). Addition of TPO, using constitutively active W515K mutant, or mutation of the Box1 motif of TPOR did not affect the cluster diameters or areas (Figure 43 and Figure 44). However, the observation of clusters may be affected by the transient expression in HEK293 cells and may not clearly represent what occurs in haematopoietic cells with endogenous TPOR expression levels.

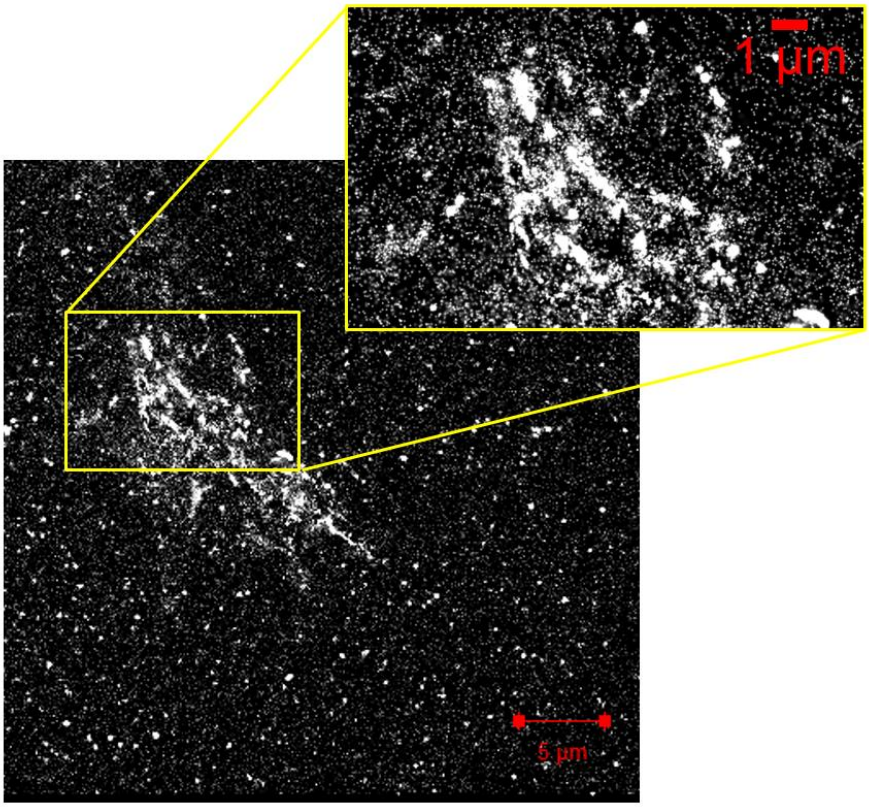

Figure 41: TPOR cluster into different cluster sizes and shapes.

A representative image of a single cell showing TPOR clusters analysed using Zen software.

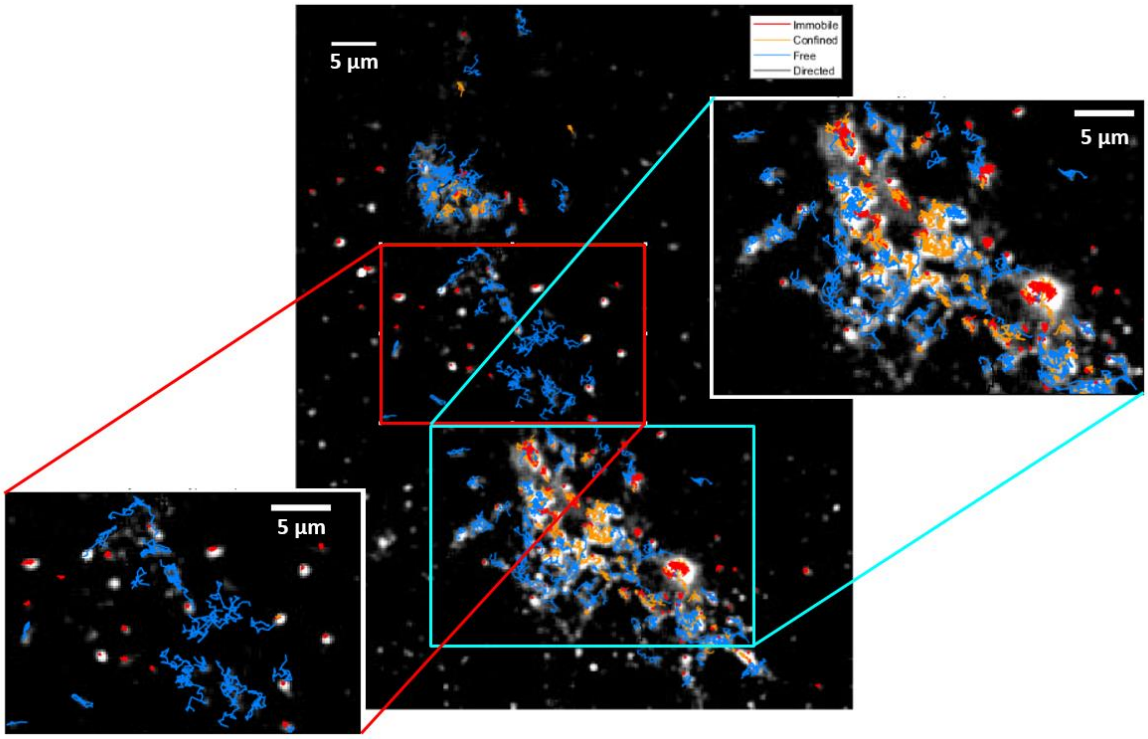

Figure 42: TPOR are clusters usually comprised of immobile/confined receptors whereas freely-diffusing receptors are usually located outside of clusters.

A representative image of trajectories (with different modes of diffusion) of a single cell that is superimposed on an RGB image of receptor clusters (white blobs) analysed using Fiji software. Track colour codes: red (immobile), orange (confined), blue (free), black (directed).

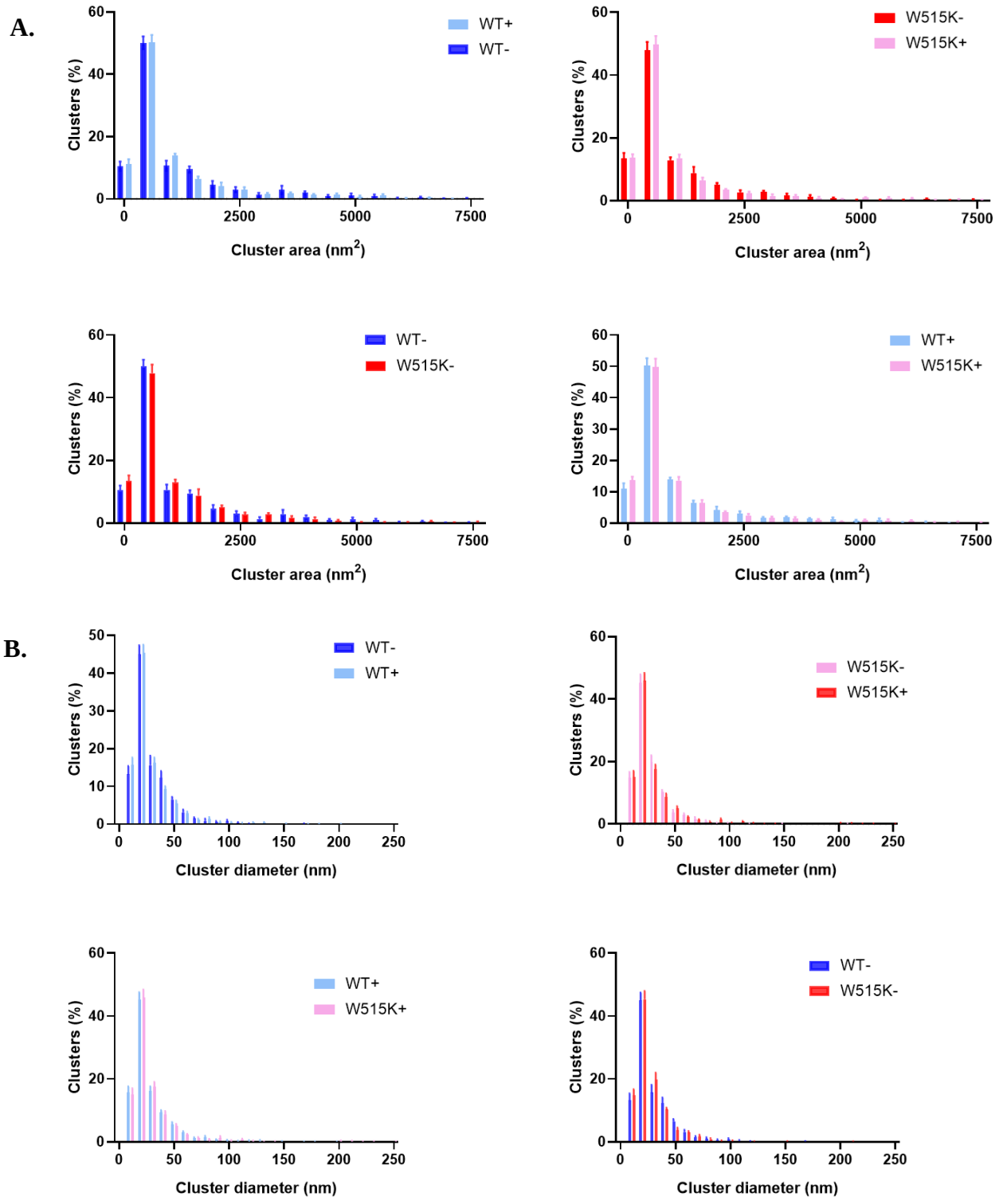

Figure 43: Receptor cluster area and diameter do not change with receptor activation due to TPO stimulation or constitutively active W515K mutant.

A) Cluster area. B) Cluster diameter. "-" represents no stimulation, "+" represents with 50 ng/ml TPO stimulation. Receptor cluster analysis based on N=6 WT TPOR cells and N=7 W515K TPOR cells. Clusters with an area of more than 7500 nm^2 were excluded as the percentage of these clusters was too insignificant and can span up to an area of 60 000 nm^2.

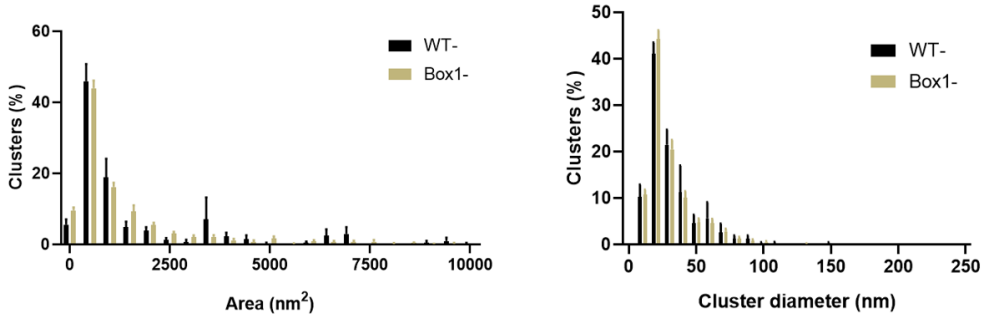

Figure 44: In the basal state, receptor cluster area and diameter do not change with the mutation of the Box1 motif.

Left: cluster area; right: cluster diameter. "-" represents no stimulation. Receptor cluster analysis based on N=8 WT TPOR cells and N=8 Box1Δ TPOR cells. Data representative of N=2 independent experiments. Clusters with area more than 10 000 nm^2 were excluded as the percentage of clusters was insignificant.

Discussion

Receptor activation can affect clustering and mobility which subsequently alters cell signalling [410, 424-427]. Currently, the understanding of the spatiotemporal patterns of TPOR and its relation to their receptor activity (i.e. downstream signalling) has been lacking. To fill this gap, the lateral diffusion and clustering of TPOR were investigated using sptPALM. For this purpose, full-length TPOR (WT, W515K, and Box1Δ) constructs tagged with the photoconvertible mEos2 fluorophore at the C-terminus were utilised. These constructs were examined for their effect in influencing TPOR spatiotemporal patterns due to constitutive receptor activation or involvement of JAK2. The effect of activation of the WT TPOR by addition of the TPO ligand on the lateral diffusion and clustering of the receptor was also determined.

The two-state model of receptor mobility pattern has been observed regarding different receptors in the plasma membrane [410, 428-431]. This model shows the existence of receptors in the highly mobile and slow diffusing states although receptors can also exist in immobile and other diffusive states. It was previously shown that the molecular weight of the receptor plays a role in influencing the diffusion coefficient of the receptor where increased weight results in a lower diffusivity and vice versa [432]. TPOR exhibited bimodal mobility: type I as the slow-diffusing receptor subpopulation and type II as the more mobile receptor subpopulation. A high fraction of TPOR exhibited the type II subpopulation. The two different receptor subpopulations may be explained by the interactions

with other proteins, recruitment to lipid rafts in the bilayer, receptor dimerisation states, as well as association with the cytoskeleton or clathrin-coated pits. Highly-mobile receptors may exist as receptor monomers [430] but there is a possibility that the presence of the highly mobile receptors may also be an artefact due to overexpression. On the other hand, the presence of slow-diffusing receptors may be due to sequestration of the receptor in lipid rafts or receptor clusters [433], undergoing pre-internalisation [434-437], interaction with cytoskeleton components [422, 438, 439], and association with other proteins.

Ligand binding has been shown to cause reduction in the lateral mobility of receptors such as tropomyosin receptor kinase A (TrkA) [430], EGFR [440], G protein-coupled receptor (GPCR) [441, 442], and insulin receptor [443]. Similarly, upon TPO stimulation or constitutive activating mutation in the absence of cytokine, the mobility of type II receptors was strongly shifted towards significantly reduced mobility upon receptor activation. In the presence of TPO, this shift resulted in two distinct effects: i) the diffusion coefficient of type II subpopulation significantly increased, and ii) a fraction of type II subpopulation shifted to type I (although this was significant only for TPO stimulation on WT and not for W515K in the absence of cytokine). These data suggest that receptor activation results in only a fraction of fast-moving subpopulation becoming slow-moving, but that the majority remained still in the fast-moving subpopulation that diffuses slightly slower. The addition of higher TPO concentration may elucidate if this partial transition from Type II to Type I was due to ligand concentration effect. It was speculated that the decrease in receptor mobility may be due to various reasons including formation of protein complexes, altered receptor conformation [444], recruitment of receptors to proteins that are involved in receptor recycling (thereby restricting movement) [185], and induction of receptor clustering [430]. Receptor clusters have been shown to allow less ligand to bind [445], although upon cytokine binding, signalling responses are enhanced in receptor clusters due to rebinding [445, 446]. In Ba/F3 cells, TPO stimulation resulted in clathrin-dependent endocytosis of TPOR [183]. AP2 facilitates TPOR endocytosis by recognising the Y^{78}RRL (cytoplasmic numbering of TPOR) motif in TPOR and leading to the formation of clathrin-coated pits (CCP) [183]. Therefore, TPO stimulation may result in the association of the receptor with CCP which subsequently contributes to the reduced receptor mobility. It has also been shown that upon ligand binding, TPOR binds to the actin cytoskeleton via Filamin A which protects the receptor from proteasomal and lysosomal-mediated degradation [447] and can also lead to decreased receptor movements. The association of TPOR with clathrin or filamin A can result in decreased receptor mobility. Lipid rafts have also been shown to restrict receptor movements [410]. The association of TPOR with lipid rafts in the cell membrane can be investigated using β-methyl cyclodextrin to deplete cholesterol. Overall, reduced receptor diffusion due to cytokine binding or constitutive receptor

activation may act to either mediate or attenuate signalling although further clarification is required to elucidate this fact. In contrast to TPOR WT, the addition of TPO did not affect the mobility of W515K. In the Western blot analysis, however, the addition of TPO increased signalling of both WT and W515K. Similarly, in the presence of TPO, the diffusion of WT and W515K did not significantly differ. This suggests that the variation in receptor mobility plays a role in regulating signalling but these movements do not appear to play a significant role in fine-tuning the extent of signalling.

Several modes of molecule diffusion have been reported which include immobile, free/Brownian, or directed movements. For mobility analysis, tracks with less than 20 frames were not included in the analysis as the DC-MSS could not define them as a distinct state [420]. All states of diffusion were present in the receptors in their basal and stimulated conditions, including those with the Box1Δ. It was observed that TPOR in its stimulated or constitutively activate state shows a statistically significant difference between free-diffusing and confined molecules with a lower percentage of the former and a higher percentage of the latter. These results suggest that the reduced mobility of the fast-diffusing receptors due to cytokine stimulation may be attributed to the increase in receptor confinement. It was also observed that there is a higher occurrence of fast-diffusing receptors compared to slow-moving receptors in the presence or absence of cytokine. As confined receptors can be fast or slow-diffusing, the increase in confinement and reduction in mobility due to cytokine stimulation may be attributed to the increase in the confined slow-diffusing TPOR population. However, the comparison between basal and activated receptors did not reveal a significant difference in the amount of free or confined receptor states. As a small sample size was analysed, this may have contributed to the non-significance observed. It was also observed that a small percentage of TPOR changed to a different diffusion state although this amount was not altered in the basal and stimulated states. The multiple-states of TPOR diffusion may be due to interaction with other proteins or due to conformational changes in the receptor [448, 449]. Larger data analysis may be needed to confirm these findings.

Receptor clusters have been shown to aid in the initiation of signal transmission and receptor internalisation for example, the ones related to the EGF receptor [426, 450-455]. On the other hand, modification in receptor clusters may regulate sensitivity to signalling. Published studies have shown that high cytokine concentrations can influence the formation of clusters but not low concentrations [456]. The results of the current study showed that receptor activation (by TPO induction or by using the W515K mutant) did not affect receptor cluster size (area and diameter) and that in the basal state, receptor clusters have already been formed. Since pre-formed TPOR dimers are present in the absence of cytokine stimulation, this suggests that TPOR clusters do not form as a result of receptor activation but that they may play a role in the activation itself. Indeed, it has been suggested that EGF receptor

clusters can be present on the membrane in the basal state [457, 458]. Similarly, T-cell receptors (TCRs) have also been shown to form preformed clusters prior to antigen binding [459-462]. It is also plausible that the pre-formed receptor clusters allow for more efficient signal regulation upon receptor activation. It was previously shown that TCR nanoclusters are more sensitive to reduced antigen levels compared to TCR monomers [461, 463, 464]. It has been shown that the binding of cytokine to receptors in clusters enhanced signalling due to rebinding [445, 446]. The findings of the current study suggest that instead of changes in cluster size, changes in receptor mobility are the driving force for regulating signalling in TPOR. However, it cannot be discarded that there is also a possibility that other factors that have yet to be determined may play a role modulating TPOR signalling. Indeed, receptor concentration and meshwork density can influence the extent of receptor clustering [465, 466]. As the current study utilises transient transfection of TPOR in HEK293 cells, receptor clustering observed in the basal state may be due to enhanced expression of the receptor. Furthermore, the addition of higher TPO concentration may significantly increase cluster size and may reflect a difference compared to what happens in the absence of cytokine stimulation. On the contrary, it has been shown that stimulation of EGFR can result in smaller receptor clusters due to recycling [467]. Despite these speculations, the small sample size that has been analysed may be insufficient to reveal any significant changes.

It was previously shown that the diffusion coefficient of EGFR increased outside of the clusters [456]. Indeed, the results of the current investigation showed that these TPOR clusters were mainly consisted of immobile/confined receptors whereas receptors exhibiting Brownian or directed movements were usually diffusing outside of these clusters. As the presence of cytokine results in increased receptor confinement and confined receptors are mostly found in clusters, it is of interest to define whether the clustering of receptors occurs as a result of the confinement or that the confinement occurred as a result of receptor clustering. Nevertheless, although cytokine stimulation resulted in increased receptor confinement, receptor cluster size was not affected. It was speculated that instead of forming bigger clusters, TPOR may form more clusters of similar size. It was previously shown that signal initiation is mediated by an increase in cluster density of the TCR-CD3 clusters [427]. Analysis of cluster density and the number of receptors that are present in each cluster might aid in understanding the role of TPOR clusters. Overall, the current study showed that immobile/confined receptors that make up the majority of receptor clusters may be the main players in regulating the signal transduction of TPOR.

JAK2 has been previously shown to stabilise TPOR at the cell surface by stabilising the glycosylated form of the receptor or by preventing proteasomal degradation of the receptor which subsequently enhances receptor recycling [115]. Currently, studies on the role of JAK2 in the spatiotemporal

patterns of type I cytokine receptors have not been published. As the Box1 motif of this family of cytokine receptors is known to be important to bind to JAK2, mutation/disruption of this motif results in markedly reduced/diminished JAK2 binding. Hence, this mutant was used to investigate the role of JAK2 in TPOR mobility and clustering. As JAK2 binds TPOR constitutively and this binding occurs even before receptor localisation to the membrane [238], it is speculated that the lack of JAK2 binding may relieve the movements of the receptor and therefore, may result in increased mobility. Hence, it was interesting to observe that in the basal state, the loss of JAK2 binding did not affect the mobility (diffusivity and mobility patterns) or clustering of TPOR. Future work including TPO stimulation may elucidate if receptor conformational changes may be involved in the role of JAK2 in TPOR mobility and clustering. A difference was observed in Figures 13 and 17 where the former showed that the percentages of confined and free molecules of TPOR WT in the basal state were not statistically different, but in the latter they showed a statistical difference. The small sample size in the latter may have contributed to the difference observed. Furthermore, results for the latter were obtained from only one experimental day whereas, for the former, results were obtained from two experimental days which may have led to a greater variation in the results. Larger sample sizes may be beneficial to investigate the reasons behind these differences.

Conclusions

In the basal and stimulated states, TPOR exhibited bimodal mobility: fast and slow-moving receptor subpopulations. Upon ligand stimulation or mutation such as W515K that causes constitutive receptor activation, the diffusivity of the fast-moving subpopulation was significantly reduced and a fraction of these receptors transitioned into the slow-moving subpopulation. This reduction in mobility may be associated with the increase in receptor confinement due to formation of protein complexes, altered receptor conformation, receptor recycling, as well as increased association with clathrin, actin cytoskeleton, or lipid rafts. Further work is required to elucidate if the reduction in receptor movement is a consequence of signal induction or attenuation. In addition, TPOR cluster size did not appear to be important in regulating signalling although the pre-formed clusters themselves may be important in mediating more efficient signal transduction due to receptor activation. Finally, JAK2 did not appear to be important in mediating TPOR mobility or clustering. The findings of the current study act as an important foundation for future work to elucidate how TPOR mobility and clustering can influence cell signalling.

Chapter 5

Specific Domains of LNK (SH2B3) Bind to TPOR and Regulate its Stability and Signalling on the Cell Surface

Introduction

LNK, also known as SH2B3, is one of the members of the SH2-domain containing adaptor proteins, which also includes SH2B1 and APS (SH2B2), that plays an important role in regulating various cytokine receptors such as c-Kit [280, 311], c-Fms [312], TNFR [313], TPOR [314]), EPOR [277], IL7-receptor [276, 315], and platelet-derived growth factor receptor (PDGFR) [316], as well as integrin receptors [284, 468]. While LNK is ubiquitously expressed, it is highly expressed in haematopoietic cells. As a result, several somatic and germline mutations in LNK have been associated with various myeloid and lymphoid malignancies. The SH2B3 gene that encodes for LNK resides on Chromosome 12q24 and the translated human LNK protein consists of 575 amino acids. Structurally, LNK comprises of three domains: i) a 70 amino acid long Pro/DD speculated to mediate homo- or hetero- dimerisation [281, 291, 306, 307], ii) a 114 amino acid long PH domain that is shown to bind to phosphoinositides in the plasma membrane [278, 285], and iii) a 99 amino acid long SH2 domain that acts as a canonical phosphotyrosine binding site.

The LNK Pro/DD domain is the least conserved amongst its family members, encoding a zipper motif that is different from its other family members. Instead of two phenylalanine residues, it comprises the tyrosine and leucine residues. These differences in the LNK Pro/DD domain may subject this domain to an alternative role whereby instead of homo- or heterodimerisation, may facilitate binding to other molecules/receptors. This proline rich region of LNK also has a consensus sequence of PXXP that acts as a potential binding site for SH3 containing proteins. A number of different, clinically relevant LNK mutations have been reported in the different LNK domains with most mutations residing in the PH domain, resulting in this region being known as a ‘hotspot’ for mutations. It was shown that mutations in this region disrupts the localisation of LNK to the membrane [285] and may therefore impair interaction with transmembrane receptors and subsequent downregulation.

The mechanism by which LNK mediates receptor downregulation is still not fully understood. It was previously shown that LNK is able to bind to active JAK2 at phosphorylated tyrosine 813 (pY813) (in the pseudokinase-kinase linker domain of JAK2) and pY613 (in the pseudokinase domain of JAK2) via its SH2 domain [278] which may suggest the formation of LNK homodimers to bind to both phosphotyrosine residues. It was proposed that upon JAK2 activation, the SH2 domain of LNK binds to phosphorylated residues of activated JAK2 in order to be phosphorylated [278]. Subsequently, LNK inhibits signalling [278]. Interestingly, other family members of LNK such as SH2B1 and APS also bind to pY813 of JAK2 although they exert different effects depending on the associated receptor (they typically enhance receptor signalling). Hence, other LNK domains may

govern specificity for its negative regulatory function on JAK2 and its interaction with the different receptors as LNK is also able to inhibit various other receptors via its SH2 domain [276, 277, 280, 311-316]. This chapter investigated if the other domains of LNK (besides SH2) are involved in inhibiting/regulating signalling of JAK2 that is associated with TPOR. By understanding this, the mechanism of LNK-mediated negative regulation may be deciphered.

Materials and Methods

DNA Constructs

Various primers (see Appendix Section C) were designed to generate hLNK with point mutations (E395K, Y572A, R392E, or R425P) via PCR mediated site-directed mutagenesis (Table 2), and domain deletions (deletion of Pro/DD, PH, CTD, or PH-SH2 linker region) via CPEC, using the N-terminal FLAG-tag WT hLNK in pcDNA3.1+ mammalian expression vector (containing the SV40ori) (Figure 45). 'AttB' sites were added to the N-terminal FLAG-tagged hLNK constructs via PCR and subsequently shuttled into the pMX-IRES-Hygro destination vector by Gateway cloning to generate FLAG-tagged hLNK constructs in pMX-IRES-Hygro vector.

Table 2: PCR cycling conditions used.

Double-stranded DNA was denatured to single-stranded DNA and primers were allowed to anneal. PCR was performed with KOD DNA polymerase (Merck Millipore).

Cycling Steps	Temperature	Time
Polymerase activation	95 °C	2 minutes
Denaturation ┐	95 °C	20 seconds
Annealing ├ 35 cycles	63 °C	10 seconds
Extension ┘	70 °C	25 seconds/kilobase pair
Hold	15 °C	∞

The coding sequences (CDS) of N-terminal HA-tagged hMPL WT or mutants (W515K, S505N, and T487A) in pMX-GW-mPGKpro-puroR/GFP vector (see Chapter 4) were shuttled into pDONR221 vector and subsequently into the pQCXP CMV/TO DEST vector (Addgene (Plasmid #17386)) [469] (Figure 46) by Gateway cloning.

The different lengths (T7, T28, T53, T69, T83, T98, T111, T116) and substitution of tyrosine (Y) to phenylalanine (F) residues (Y8F, Y29F, Y78F, Y113F, Y118F, Y113F/Y118F) (numbering is from the start of the intracellular domain) of the ICD of TPOR were made by PCR mediated site-directed mutagenesis using the HA-tagged hMPL Box1 mutant in pDONR221 plasmid (see Appendix Section C for primers used), which were subsequently shuttled into the pQCXP CMV/TO DEST vector by Gateway cloning. The number followed by 'T' represents the number of amino acids remaining in the ICD after truncation. All constructs were verified by DNA sequencing performed by the AGRF Brisbane.

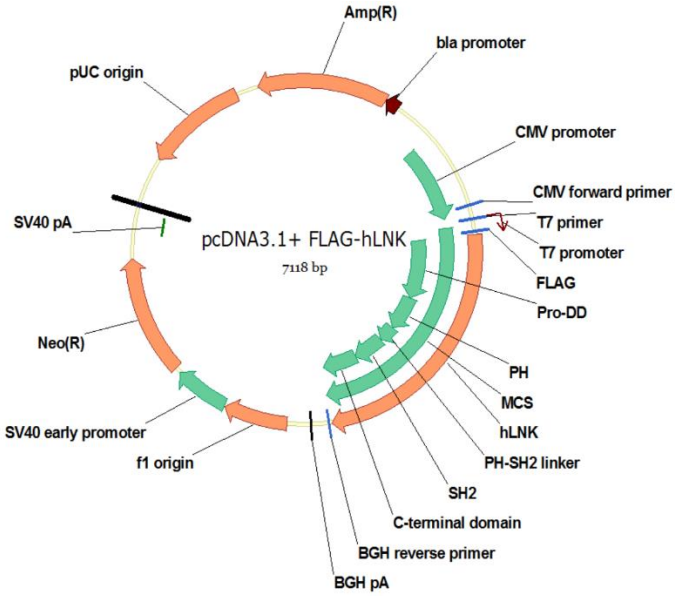

Figure 45: Representative vector map of the pcDNA3.1+ FLAG-hLNK vector constructs.

A FLAG-tag was present at the N-terminus of the *SH2B3* gene. The CMV promoter allows for high-level gene expression following transient transfection.

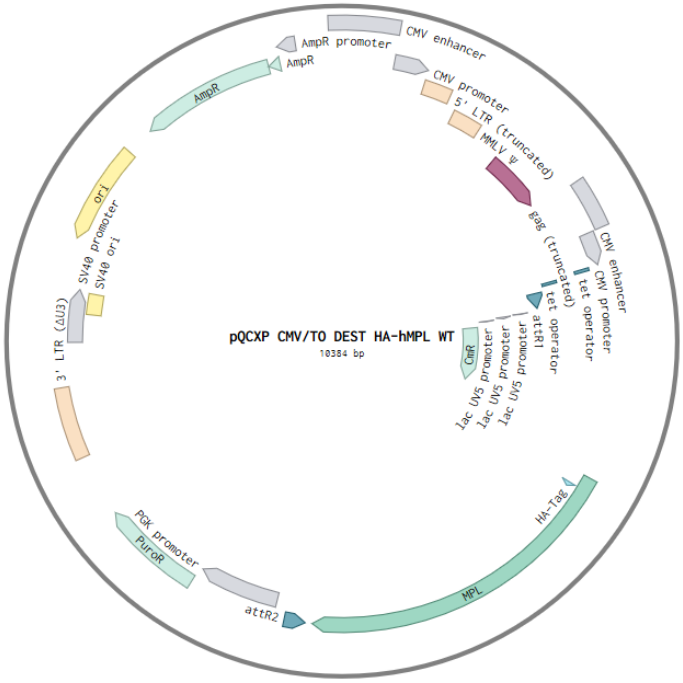

Figure 46: Representative vector map of the pQCXIP-HA-hTPOR vector constructs.

A HA-tag was present at the N-terminus of the *MPL* gene. The CMV promoter allows for high-level gene expression following transient transfection.

Murine JAK2 and kinase dead mutant (KE; K^{882E}) in pBluescriptSK was generously provided by J. N. Ihle, St. Jude Children's Research Hospital, TN, USA [86]. Each JAK2 clone was re-cloned by Dr Andrew Brooks in pEGFP-N1 (with EGFP replaced by JAK2).

Retroviral Transduction and Generation of Stably-Transduced Cell Lines

PLAT-E cells were seeded (1.7×10^5 cells/well) into 6-well cell culture plates and cultured overnight in DMEM supplemented with 10% FBS at 37°C in a humidified 5% CO_2 incubator. Cells were transiently transfected with 3 µg plasmid DNA (pMX-GW-mPGKpro-puroR/GFP HA-tagged TPOR constructs (see Chapter 4) using Lipofectamine 2000 according to manufacturer's instructions (Invitrogen, Thermo Fisher Scientific). After 24 hours incubation at 37°C, media was replaced with fresh DMEM supplemented with 10% FBS for 48 hours. Parental Ba/F3 cells (2×10^5 cells per infection) were infected with ecotropic retroviral supernatants generated in PLAT-E cells and incubated at 37°C for 1-2 hours before an equal volume of RPMI (supplemented with 10% FBS and 2× IL-3) was added. After 3 days, puromycin selection was performed by resuspending cells in a final concentration of 1 µg/ml puromycin (Gibco, Life Technologies, Thermo Fisher Scientific) in RPMI

(supplemented with 10% FBS) and left for 3-5 days before cells were expanded to T25 cell culture flasks. For cotransduction of pMX-IRES-Hygro FLAG-tagged hLNK constructs into Ba/F3 TPOR WT, W515K, or S505N cells, ecotropic retroviral supernatants were generated in PLAT-E cells and retroviral transduction was performed as before. After 3 days of transduction, hygromycin (Invitrogen, Thermo Fisher Scientific) selection was performed by resuspending cells in a final concentration of 1 mg/ml for co-transduced Ba/F3 TPOR WT or 1.5 mg/ ml for co-transduced Ba/F3 TPOR W515K or S505N in RPMI (supplemented with 10% FBS) and left for 7-10 days before cells were expanded to T25 cell culture flasks.

TPOR/LNK Signalling Assay

Lenti-X 293T cells were seeded (3×10^5 cells/well) into 6-well cell culture plates and cultured overnight in DMEM supplemented with 10% FBS at 37°C in a humidified 5% CO_2 incubator. Cells were then transiently transfected with 500 ng receptor (pQCXIP HA-tagged hTPOR WT, pQCXIP HA-tagged hGHR WT, or pQCXIP EV), 700 ng STAT3 (pBABE-STAT3 or pBABE-EV), and/or 300 ng LNK constructs (pcDNA3.1+ FLAG-tagged hLNK WT or mutants) using Lipofectamine 2000 according to manufacturer's instructions (Invitrogen, Thermo Fisher Scientific). After 24 hours incubation at 37°C, cells were starved in DMEM supplemented with 0.5% FBS for 12-16 hours. Cells were then stimulated with 50 ng/ml rhTPO (R & D Systems) or PBS for 10 minutes at 37°C. Cells were subsequently washed with cold-PBS and lysed in 40-60 µl ice-cold RIPA buffer (50 mM Tris pH7.5, 150 mM NaCl, 5 mM EDTA, 0.5% Triton X-100) containing 2 mM sodium orthovanadate (Sigma), 30 mM sodium fluoride (Sigma), 10 mM sodium pyrophosphate (Sigma), and 1x complete protease inhibitor cocktail (Roche Applied Science). Protein concentration was determined using the Pierce BCA Protein Assay Kit (Thermo Fisher Scientific). Supernatant was mixed with 3x SDS sample buffer (containing 0.1 M DTT) and heated to 98°C for 5 minutes before the samples were run on SDS-PAGE gel and subjected to western blotting analysis using the appropriate antibodies (see Appendix Section E).

Co-immunoprecipitation Assay

Lenti-X 293T cells were seeded at a density of 3.8 x 10^6 cells/T75 cell culture flask and cultured overnight in DMEM supplemented with 10% FBS at 37°C in a humidified 5% CO_2 incubator. Cells were then transiently transfected with 5 µg receptor (pQCXIP HA-tagged hTPOR WT, pQCXIP HA-tagged hGHR WT, or pQCXIP EV), 3 µg LNK constructs (pcDNA3.1+ FLAG-tagged hLNK WT or mutants), and/or 100 ng JAK2 (WT JAK2 or kinase-dead (KE) JAK2 mutant (KE mutation; dominant

negative) using Lipofectamine 2000 according to manufacturer's instructions (Invitrogen, Thermo Fisher Scientific). After 24 hours incubation at 37°C, cells were starved in DMEM supplemented with 0.5% FBS for 12-16 hours. Following, cells were stimulated with 50 ng/ml recombinant human TPO (rhTPO) (R & D Systems), recombinant human pituitary GH (100 ng/ml), or PBS for 10 minutes at 37°C. After stimulation, cells were washed once in ice-cold PBS (containing 100 µM sodium orthovanadate (Sigma)), lysed in 400 µl ice-cold extraction buffer (50 mM Tris pH7.5, 150 mM NaCl, 5 mM EDTA, 0.5% Triton X-100) containing 2 mM sodium orthovanadate (Sigma), 30 mM sodium fluoride (Sigma), 10 mM sodium pyrophosphate (Sigma), and 1x complete protease inhibitor cocktail (Roche Applied Science). Protein concentration was determined using the Pierce BCA Protein Assay Kit (Thermo Fisher Scientific). Cell lysates (3-5 mg) were pre-cleared with 40 µl of washed, blocked, 50% resuspended Protein G Sepharose^{TM} 4 Fast Flow (GE Healthcare) before incubating with their corresponding antibody for 2 hours at 4°C. After incubation, 60 µl of 50% resuspended Protein G Sepharose were added and incubated for another 1.5 hours at 4°C. The bound beads were washed twice with wash buffer (50 mM Tris pH7.5, 150 mM NaCl, 5 mM EDTA) containing 2 mM sodium orthovanadate, 30 mM sodium fluoride, 10 mM sodium pyrophosphate, and 1x complete protease inhibitor cocktail. Supernatant was removed and bound beads were mixed with 3x SDS sample buffer (containing 0.1 M DTT) and heated to 98°C for 5 minutes. Sepharose was pelleted by centrifugation at 17, 900*g* for 5 minutes before the supernatants were run on SDS-PAGE gel and subjected to western analysis using the appropriate antibodies (see Appendix Section E).

Results

Various LNK domain deletions and point mutations were generated in order to determine if the other domains of LNK (besides SH2) are involved in inhibiting/regulating signalling of JAK2 associated with TPOR. All LNK expression constructs retained the SH2 domain required for JAK2 phosphorylated tyrosine binding. Several point mutations in LNK were created in the SH2 domain (R425P, R392E, and E395K), and a single point mutation of the conserved C-terminal tyrosine residue (Y572A) was introduced (Table 3 and Figure 47). The Y572 residue was mutated to an alanine to determine if there are any phenotypic consequences that accompany the loss of this conserved tyrosine residue. Alanine is a non-bulky, hydrophobic residue and would not be expected to affect the function of the protein except for the loss of the tyrosine and its potential phosphorylation. Domain truncations of Pro/DD, PH, PH-SH2 linker, and CTD were also created (Figure 47).

Table 3: Point mutations in pcDNA3.1+ FLAG-LNK constructs generated.

Mutations	Type	Details
R425P	Clinical; uncharacterised	Causes clinical phenotype between ET and atypical CML (personal communication from Professor Andrew Perkins, Monash University)
R392E	Synthetic	Destroys the ability of the SH2 domain to bind to phosphorylated JAK2 in TPOR-mediated signalling [278]. R364E is the murine homologue
E395K	Clinical; characterised	Reported in ET patients [470]
Y572A	Synthetic	Y572 is well-conserved between the members of the SH2-domain containing adaptor proteins. Murine counterpart, Y536F, showed that this mutation does not appear to affect LNK function [249, 277]

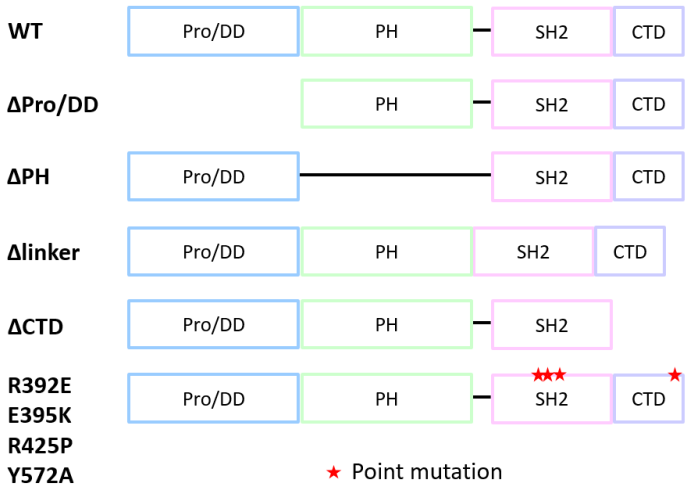

Figure 47: Illustration of pcDNA3.1+ FLAG-LNK constructs generated for this study.

Four deletion constructs were made: ΔPro/DD, ΔPH, ΔPH-SH2 linker, and ΔCTD, and four point mutations were introduced: R392E (SH2 domain), E395K (SH2 domain), R425P (SH2 domain), and Y572A (CTD domain). The Pro/DD domain spans from amino acid residue 1 to 193, the PH domain spans from amino acid residue 206 to 307, the SH2 domain spans from amino acid residue 364 to 462, and the CTD spans from amino acid residue 463 to 575.

Although it is known that the SH2 domain acts as a mediator to dock LNK to phosphorylated JAK2 at Y813, this binding provides little explanation regarding how LNK can negatively regulate this kinase. Therefore, it was hypothesised that other LNK domains may be involved in facilitating kinase inhibition by a currently unknown mechanism. In order to address this gap in knowledge, the above LNK constructs were used in signalling and co-IP assays. The outcome of these experiments showed that LNK Pro/DD domain potentially binds to TPOR and suppress TPOR-mediated signalling.

LNK Pro/DD Domain Downregulates TPOR Signalling in Co-operation with its SH2 Domain

Ba/F3-stably transduced cell lines that express TPOR-WT or clinical TPOR mutants W515K or S505N were subjected to viral transduction to introduce the various LNK constructs. However, due to various issues (outlined in Discussion section), these constructs were utilised in a transient, over expression system using Lenti-X 293T cells as these cells do not rely on cytokine receptor activation for proliferation or growth. In the current study, repeated transductions of LNK into Ba/F3 cells were performed but western analysis of LNK WT and some mutants showed little to no expression which was speculated to be due to the inhibitor effects on JAK-STAT signalling by LNK whereby cells expressing LNK are rapidly selected against during cytokine-stimulated cell proliferation. A previous study was able to observe the effects in Ba/F3 cells with LNK expression [344]. However, this was performed by transfection of these cells, therefore all data may be from transient transfection and short term analysis. In order to observe the effect of LNK on JAK-STAT signalling from TPOR in Lenti-X 293T cells, STAT3 was transfected as these cells have low endogenous STAT3 levels. STAT3 rather than STAT5 or STAT1 was utilised as STAT3 requires binding to TPOR in order to mediate signalling whereas STAT5 binding to TPOR is not essential for signalling [184]. Transfection of moderate to high amounts of STAT3 have not been shown to cause constitutive activation in a transient system, unlike JAK2 [119, 471]. This is likely due to STAT3 not possessing a kinase activity, and requiring tyrosine phosphorylation for activation. Overexpression of STAT3 was confirmed to not cause constitutive activation nor affect receptor levels (Figure 48). However, STAT3 over expression does increase sensitivity to JAK activation signals. No cell growth retardation by LNK on Lenti-X 293T cells was evident as these are non-haematopoietic cells that do not rely on JAK signalling for their growth. LNK also had no change on STAT3 protein levels (Figure 48).

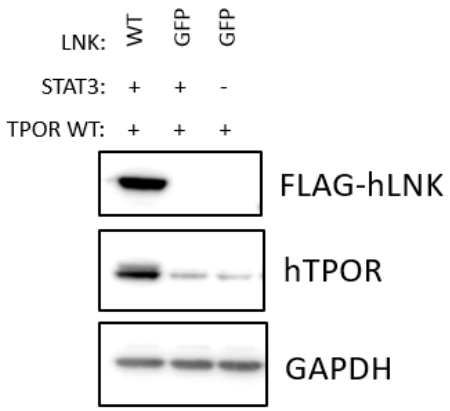

Figure 48: TPOR protein levels are increased by co-expression of LNK WT.

Lenti-X 293T cells were transiently transfected with the respective constructs: pQCXIP HA-hTPOR WT, pcDNA3.1+ FLAG-hLNK WT, pBABE-STAT3 or pBABE-empty vector (EV), and pEGFP-N1. No TPO stimulation on cells was performed. Total protein was subjected to SDS-PAGE and immunoblotted with indicated antibodies. GAPDH was used as a loading control. Image representative of n=3 experiments.

Depending on the type of mutation, LNK constructs were either able to abrogate or downregulate STAT3 and ERK activation following TPO stimulation. As expected, LNK WT reduced STAT3 and ERK signalling compared to GFP control (Figure 49). Several constructs, in a similar manner to LNK WT, were able to reduce signalling such as LNK ΔCTD (pSTAT3 and pERK), ΔPH (pERK), and Y572A (pERK) (Figure 49). On the other hand, LNK ΔPro/DD, LNK Δlinker, and SH2 domain point mutants such as R392E, E395K, and R425P showed reduced inhibition on both STAT3 and ERK signalling compared to LNK WT (Figure 49). Expression levels of the various LNK constructs were also found to differ (Figure 49). This was not unexpected as modifications in the protein sequence can alter their expression levels. Co-transfection of expression constructs for LNK WT and TPOR resulted in a higher level of the receptor detected by western analysis as opposed to GFP co-transfection with TPOR (Figure 49 and Figure 50A). However, the corresponding TPOR level with co-transfection of different LNK constructs together with TPO treatment was difficult to evaluate due to LNK-dependent ligand-mediated degradation. Therefore, a separate experiment to compare differences between the receptor levels in the absence of TPO was performed (Figure 50 A). Co-expression of TPOR with LNK WT was observed to increase receptor levels compared to GFP control (Figure 50 A). In order to determine if the increase in TPOR levels when co-expressed with LNK WT was specific to TPOR, the effect of the expression of LNK on GHR was investigated and a similar striking increase in GHR was observed when LNK WT was co-transfected with GHR (Figure 50 B).

Although a stark increase in receptor stability was observed when either TPOR or GHR was co-transfected with LNK WT, unlike GHR, all LNK constructs were able to increase TPOR levels (at different levels) (Figure 50). However, a similar trend of markedly increased receptor levels was observed when TPOR or GHR was co-expressed with LNK constructs that retained their signalling inhibition such as LNK ΔPH and LNK ΔCTD (except for E395K) (Figure 50). STAT3 transfection did not affect receptor expression, nor LNK expression, indicating no role of elevated STAT3 levels in regulating TPOR levels (Figure 48). This was not unexpected as there are no reports of STAT3 directly regulating TPOR protein levels.

A.

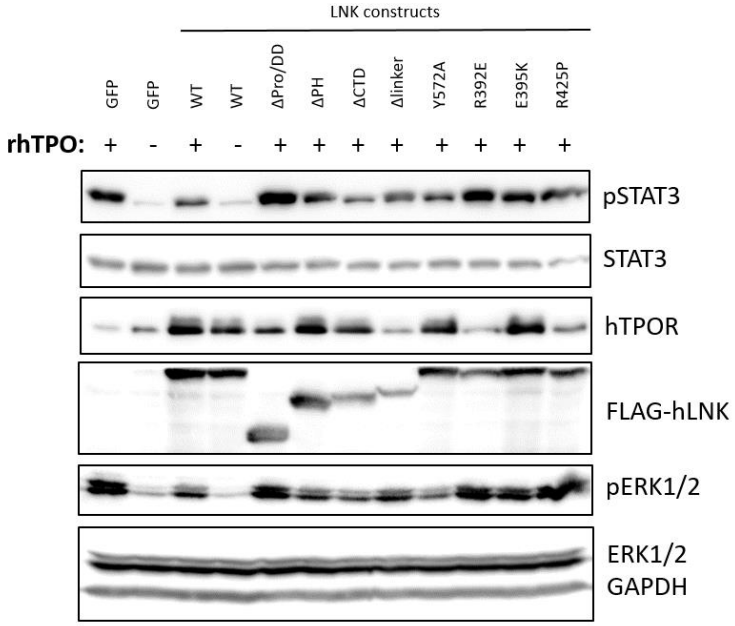

B.

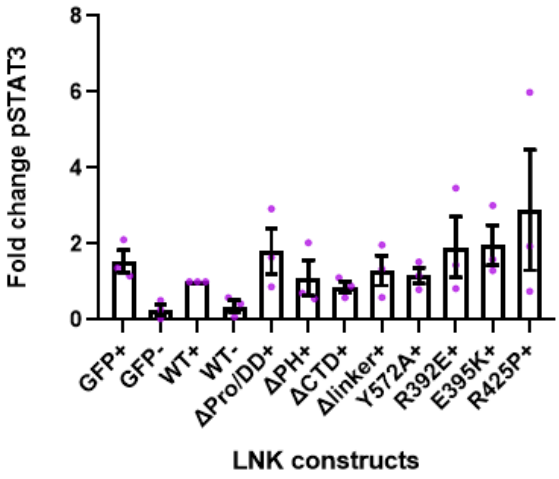

C.

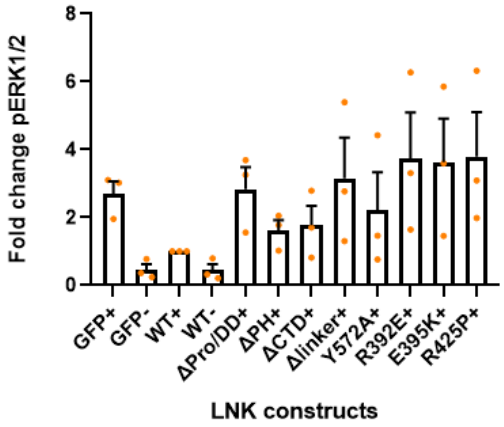

Figure 49: The ΔPro/DD and Δlinker domain deletions of LNK, and SH2 domain point mutants increased both STAT3 and ERK signalling.

Lenti-X 293T cells were transiently transfected with pQCXIP HA-hTPOR WT and pBABE-STAT3, as well as different pcDNA3.1-FLAG-hLNK constructs or pEGFP-N1. Cells were starved overnight and TPO (final concentration of 50 ng/ml) was added (+) for 10 minutes. Samples in the absence of TPO (-) were used for comparison. Total protein was subjected to SDS-PAGE and immunoblotted with indicated antibodies. GAPDH was used as a loading control. A) A representative immunoblot was shown. B & C) Graph of relative pSTAT3 and pERK levels of 3 independent experiments generated using densitometry data. For a complete list of densitometry data for replicates, see Appendix Section B. Image representative of n=3 experiments.

A.

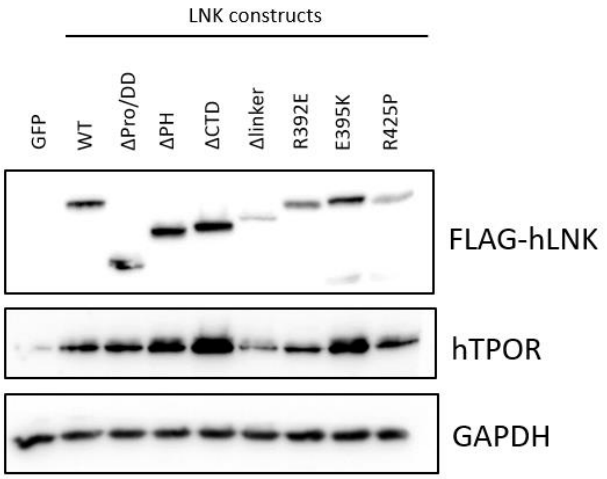

B.

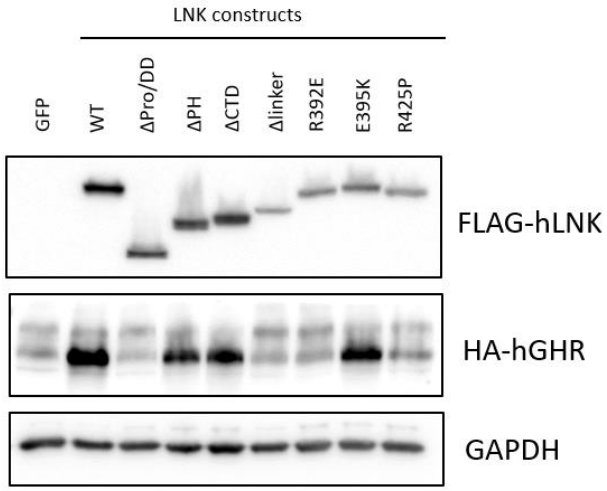

Figure 50: Co-expression of TPOR or GHR with LNK WT or non-disruptive mutations such as ΔPH and ΔCTD (except for E395K) resulted in markedly increased receptor levels in the absence of cytokine.

Lenti-X 293T cells were transiently transfected with the respective constructs: pQCXIP HA-hTPOR WT (A) or pQCXIP HA-hGHR (B) and pBABE-STAT3, as well as different pcDNA3.1-FLAG-hLNK constructs or pEGFP-N1. All transfections included STAT3. No TPO stimulation on cells was performed. Total protein was subjected to SDS-PAGE and immunoblotted with indicated antibodies. GAPDH was used as a loading control. Image representative of n=1 experiment for A and n=3 for B.

LNK associates with active JAK2 strongly, only in the presence of TPOR

The role of active JAK2 and TPOR in association with LNK was investigated by Co-IP. Initially, anti-HA antibody was used for TPOR (HA-tagged) co-immunoprecipitation during attempted optimisation of the co-IP procedure. However, the use of this antibody repeatedly showed binding to non-specific proteins. Alternatively, the anti-FLAG antibody was used to co-precipitate LNK (FLAG-tagged) and its interacting proteins, which was successful. As endogenous JAK2 is expressed at a low levels in Lenti-X 293T cells, it was necessary to transfect JAK2 as endogenous levels would be expected to be very low compared to the transfected TPOR and LNK levels, and therefore may have not allowed for full interpretation of results. For transfection, the use of 100 ng of the JAK2 WT plasmid was maintained although this amount causes overexpression of JAK2 which is known to result in constitutive activation of JAK2 [119, 471]. This JAK2 expression plasmid has a SV40ori which leads to further elevated expression in HEK293T cells. LNK WT was shown to be able to associate with the active form of JAK2 only when TPOR is present (Figure 51 and Figure 52). Receptor protein level in cells was significantly lower when only TPOR was transfected compared to when LNK was co-transfected (Figure 51) further supporting that LNK interacts with TPOR and stabilises the protein. Interestingly, little to no interaction between LNK and JAK2 WT or KE mutant was observed in the absence of TPOR (Figure 51 and Figure 52), supporting the requirement for TPOR for strong association of LNK with JAK2. LNK was still shown to associate with TPOR in the presence of exogenous JAK2 KE, however, this interaction was much less efficient compared to when JAK2 WT was transfected (Figure 51). In addition, LNK was shown to associate with TPOR in the absence of exogenous JAK2 (Figure 51 and Figure 52) although it is possible that low level endogenous JAK2 expression may be aiding the co-precipitation of TPOR by LNK. It was also evident that LNK interacted with JAK2 WT to a similar extent irrespective of TPO stimulation (Figure 52). However the lack of effect of TPO stimulation is likely due to the constitutive activation of the overexpressed JAK2.

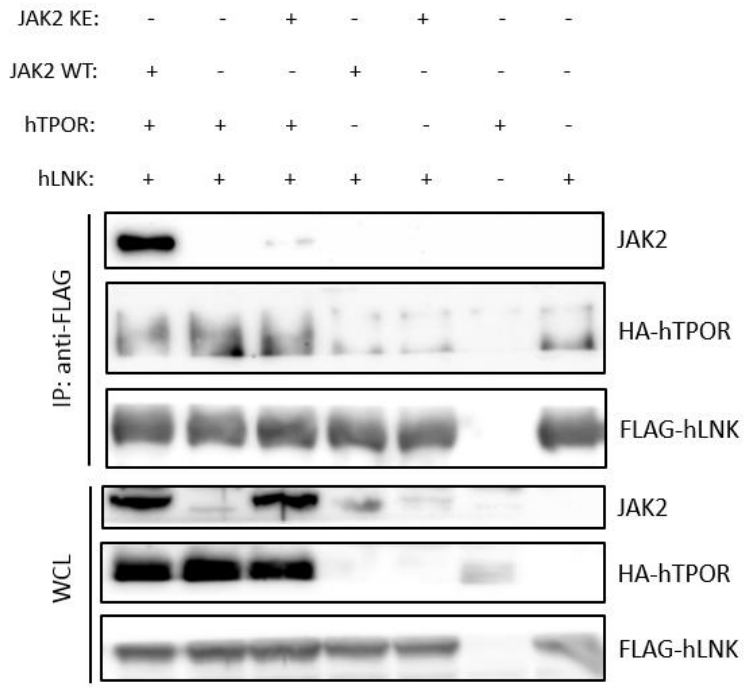

Figure 51: LNK preferentially associates with active JAK2 rather than inactive JAK2, but only in the presence of TPOR.

Lenti-X 293T cells were co-transfected with either HA-tagged hTPOR WT, FLAG-tagged hLNK WT, and/or JAK2 WT or KE. Immunoblot showing (Top) Co-IP analysis; (Bottom) Whole cell lysate (WCL). All conditions were performed without TPO stimulation. For Co-IP, protein lysates were immunoprecipitated with FLAG antibodies and blotted with antibodies specific for JAK2, HA (to detect FL-TPOR), and FLAG (to detect LNK). For WCL, total protein was subjected to SDS-PAGE and immunoblotted with indicated antibodies. Image representative of n=2 experiments.

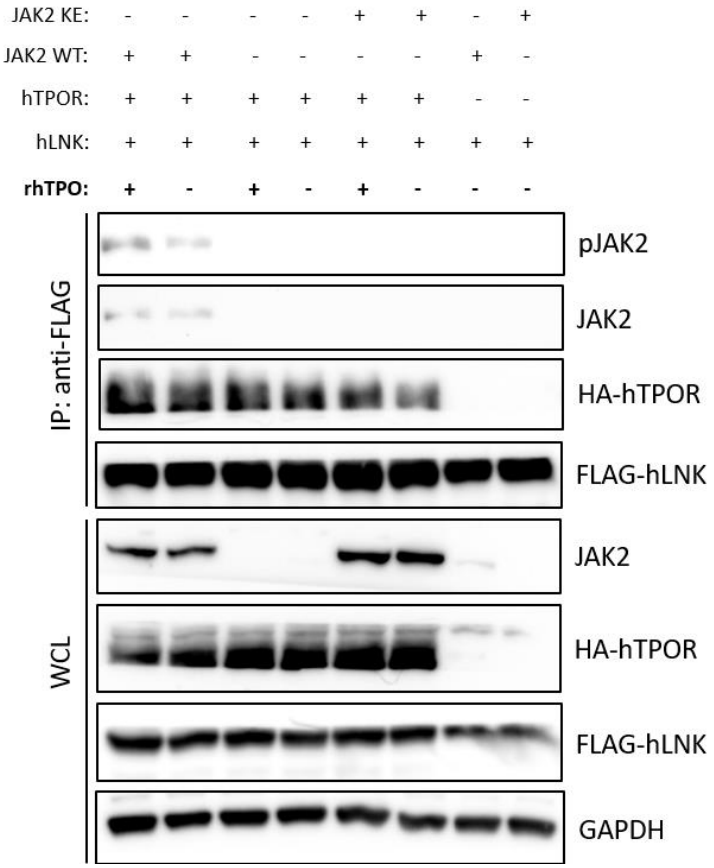

Figure 52: LNK strongly associates with JAK2 only in the presence of TPOR.

Immunoblot showing (Top) Co-IP analysis; (Bottom) WCL. Lenti-X 293T cells were co-transfected with either HA-tagged hTPOR WT, FLAG-tagged hLNK WT, and/or JAK2 WT or KE. For co-IP, protein lysates were immunoprecipitated with FLAG antibodies and blotted with antibodies specific for pJAK2 (detects phosphorylation on Tyr1007/1008), JAK2, HA (to detect FL-TPOR), and FLAG (to detect LNK). (B) For WCL, total protein was subjected to SDS-PAGE and immunoblotted with indicated antibodies. GAPDH was used as a loading control. Image representative of n=2 experiments.

LNK constitutively binds GHR and TPOR

The ability of LNK to constitutively associate with a homodimeric class I cytokine receptor (TPOR and a related family member, GHR) or require JAK2 for this interaction, was investigated. LNK was found to bind directly to GHR and not require JAK2 (Figure 53 A). This was clearly shown as GHR was co-precipitated to similar levels by LNK irrespective of JAK2 transfection (Figure 53 A). This was in stark contrast to TPOR (Figure 53 B) which showed a requirement of JAK2 overexpression for detectable TPOR co-precipitated by LNK. Interestingly, LNK preferentially interacts with the

immature rather than the mature GHR (Figure 53 A) although both precursor and glycosylated mature TPOR were detected to be precipitated by LNK (Figure 53). Overall, these results suggest that LNK binds directly to homodimeric class I cytokine receptors and that this interaction does not require JAK2.

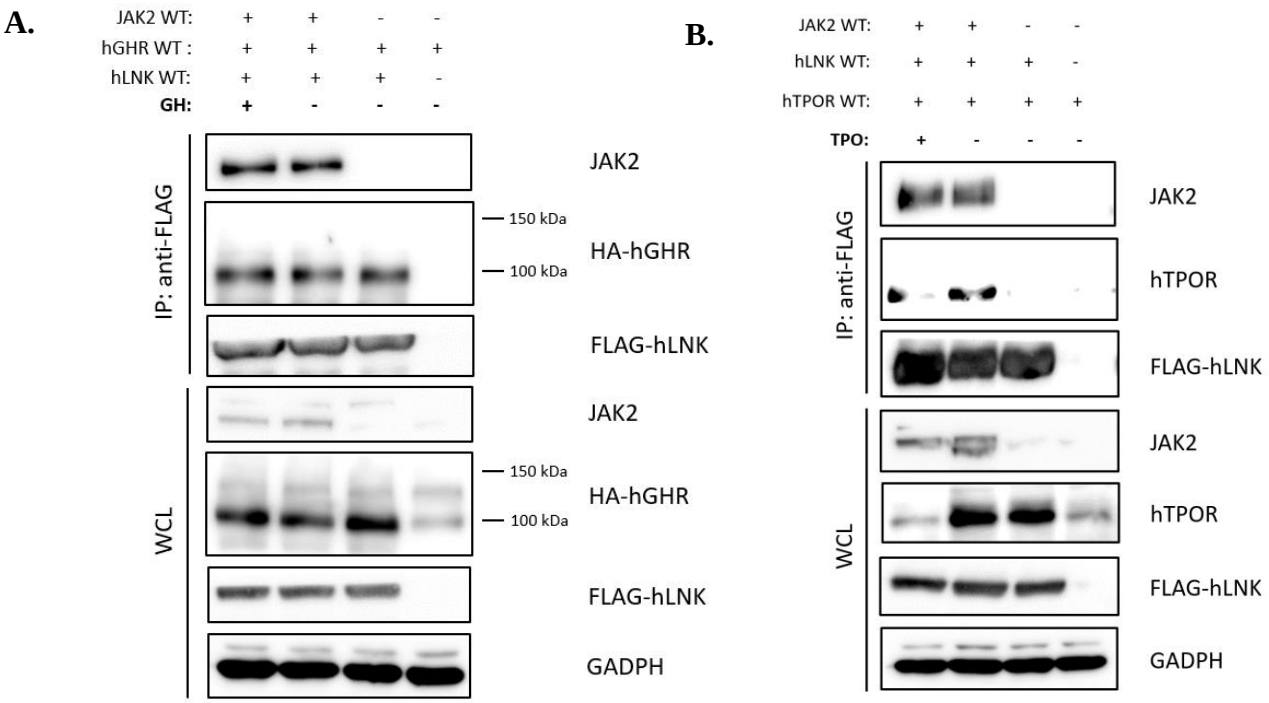

Figure 53: LNK constitutively binds to GHR and TPOR but TPOR binding requires JAK2 for efficient association.

Immunoblot showing (Top) Co-IP analysis; (Bottom) WCL. Lenti-X 293T cells were co-transfected with either HA-tagged hTPOR WT, HA-tagged hGHR WT, FLAG-tagged hLNK WT, and/or JAK2 WT. For co-IP, protein lysates were immunoprecipitated with FLAG antibodies and blotted with antibodies specific for JAK2, HA (to detect FL-hGHR), TPOR (to detect FL-hTPOR), and FLAG (to detect LNK). For WCL, total protein was subjected to SDS-PAGE and immunoblotted with indicated antibodies. GAPDH was used as a loading control. Image representative of n=2 experiments for A, n=1 experiment for B.

In order to clearly determine the role of JAK2 association with TPOR in facilitating LNK interaction with TPOR, the Box1 motif which is essential for JAK association was mutated. As the Box1 motif is the major receptor binding site of JAK2, this motif was mutated from PxxP to AAAA (Proline-X-X-Proline to Alanine-Alanine-Alanine-Alanine) in order to disrupt binding to JAK2. This disruption

of binding between receptor and JAK2 will ensure that any observed LNK binding to the receptor should be independent of JAK2. However, it remains a possibility that JAK2 may still weakly interact with the Box2 motif and interbox residues [472]. Results showed that LNK was still able to co-precipitate similar levels of TPOR Box1 mutant and WT although JAK2 association was decreased when Box1 mutant was transfected (Figure 54). The lack of STAT5 activation by TPO stimulated Box1 mutant receptor supported that there was no significant interaction of JAK2 with the mutant receptor (Figure 54). These results suggest that LNK is able to bind directly to TPOR without the requirement for JAK2.

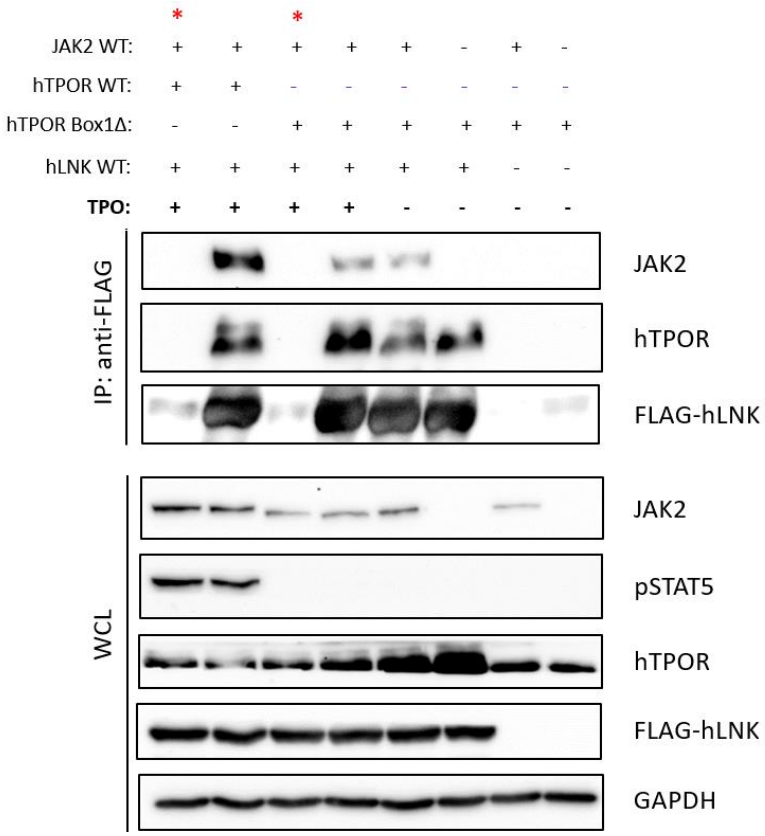

Figure 54: LNK constitutively binds to both TPOR WT and Box1 mutant.

Immunoblot showing (Top) Co-IP analysis; (Bottom) WCL. Lenti-X 293T cells were co-transfected with either HA-tagged hTPOR WT, HA-tagged hTPOR Box1 mutant, FLAG-tagged hLNK WT, and/or JAK2 WT. For co-IP, protein lysates were immunoprecipitated with FLAG antibodies and blotted with antibodies specific for JAK2, TPOR (to detect FL-hTPOR), and FLAG (to detect LNK). For WCL, total protein was subjected to SDS-PAGE and immunoblotted with indicated antibodies. GAPDH was used as a loading control. Red asterisks denote no antibody used in Co-IP. Constitutive binding to receptor is supported by figures 17 and 18.

LNK Pro/DD domain mediates association with TPOR

The role of individual domains of LNK in mediating association with JAK2 and TPOR were then investigated. Domain deletions and point mutations of LNK were used to determine whether LNK has a binding site to either JAK2 or TPOR other than its SH2 domain. LNK was shown to be able to associate with the TPOR Box1 mutant receptor suggesting that LNK does not bind to the Box1 motif and can bind receptor independently of JAK2 (Figure 55). It was observed that the expression levels of JAK2 and TPOR WT co-expressed were increased compared to when JAK2 and Box1Δ were co-expressed (data not shown). This suggested that the interaction of JAK2 with TPOR resulted in a stabilised complex. In order to overcome this issue of difference in total protein levels, an increased amount of JAK2 (three-fold) was transfected for all transfections with the Box1 mutant receptor in order to equalise the expression levels. The most striking observation was the markedly reduced association of receptor with LNK ΔPro/DD compared to LNK WT although JAK2 binding was still maintained (Figure 55). In contrast, JAK2 binding with LNK Δlinker was abolished but a strong level of TPOR interaction was retained. Similarly, LNK SH2 domain mutants (except for E395K) showed reduced binding to JAK2 but maintained a significant level of TPOR binding. The LNK Y572A mutation does not affect binding to both TPOR and JAK2, hence it maintained the same binding capabilities as WT. Following, the same experimental conditions with the inclusion of cytokine was performed to determine if the interaction between LNK mutants and JAK2/TPOR would change. This assay showed similar results as to without TPO stimulation (Figure 56), however with overexpression of JAK2, there was likely no significant increase in pJAK2 levels upon TPO stimulation as shown previously (Figure 52).

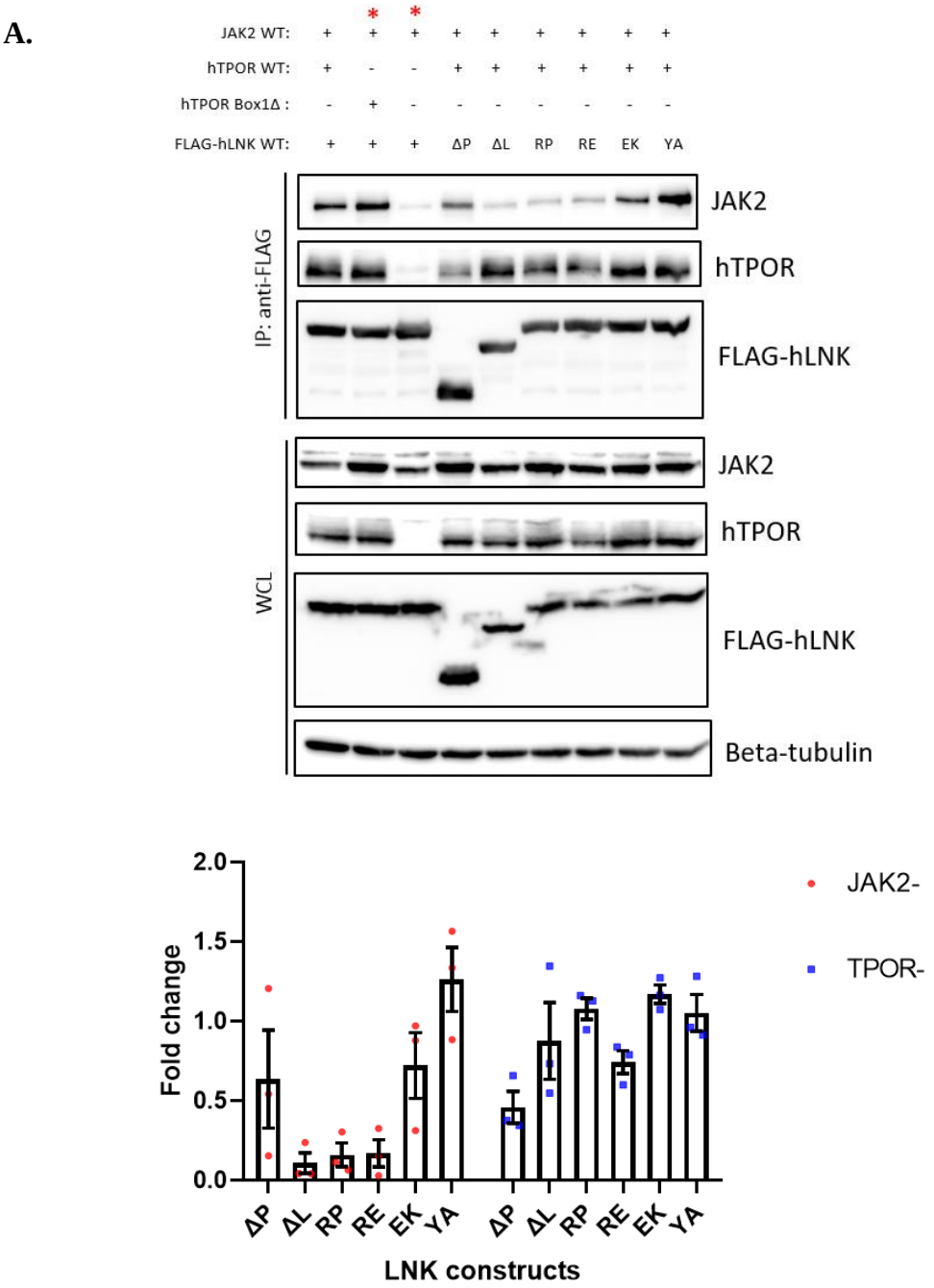

Figure 55: LNK domain deletions and point mutations show altered affinity to JAK2 or TPOR.

A) Immunoblot showing (Top) Co-IP analysis; (Bottom) WCL. Lenti-X 293T cells were co-transfected with either HA-tagged hTPOR WT, HA-tagged hTPOR Box1 mutant, FLAG-tagged hLNK WT or mutants, and/or JAK2 WT. All conditions were performed without TPO stimulation. For co-IP, protein lysates were immunoprecipitated with FLAG antibodies and blotted with antibodies specific for JAK2, TPOR (to detect FL-hTPOR), and FLAG (to detect LNK). For WCL, total protein was subjected to SDS-PAGE and immunoblotted with indicated antibodies. β-tubulin was used as a loading control. Red asterisks denote 3x JAK2 concentration used. ΔP represents ΔPro/DD, ΔL represents Δlinker, RP represents R425P, RE represent R392E, EK represents E395K,

and YA represents Y572A. B) Graph of relative JAK2 and TPOR levels of 3 independent experiments generated using densitometry data. For a complete list of densitometry data for replicates, see Appendix Section B (Figure 90). Image representative of n=3 experiments.

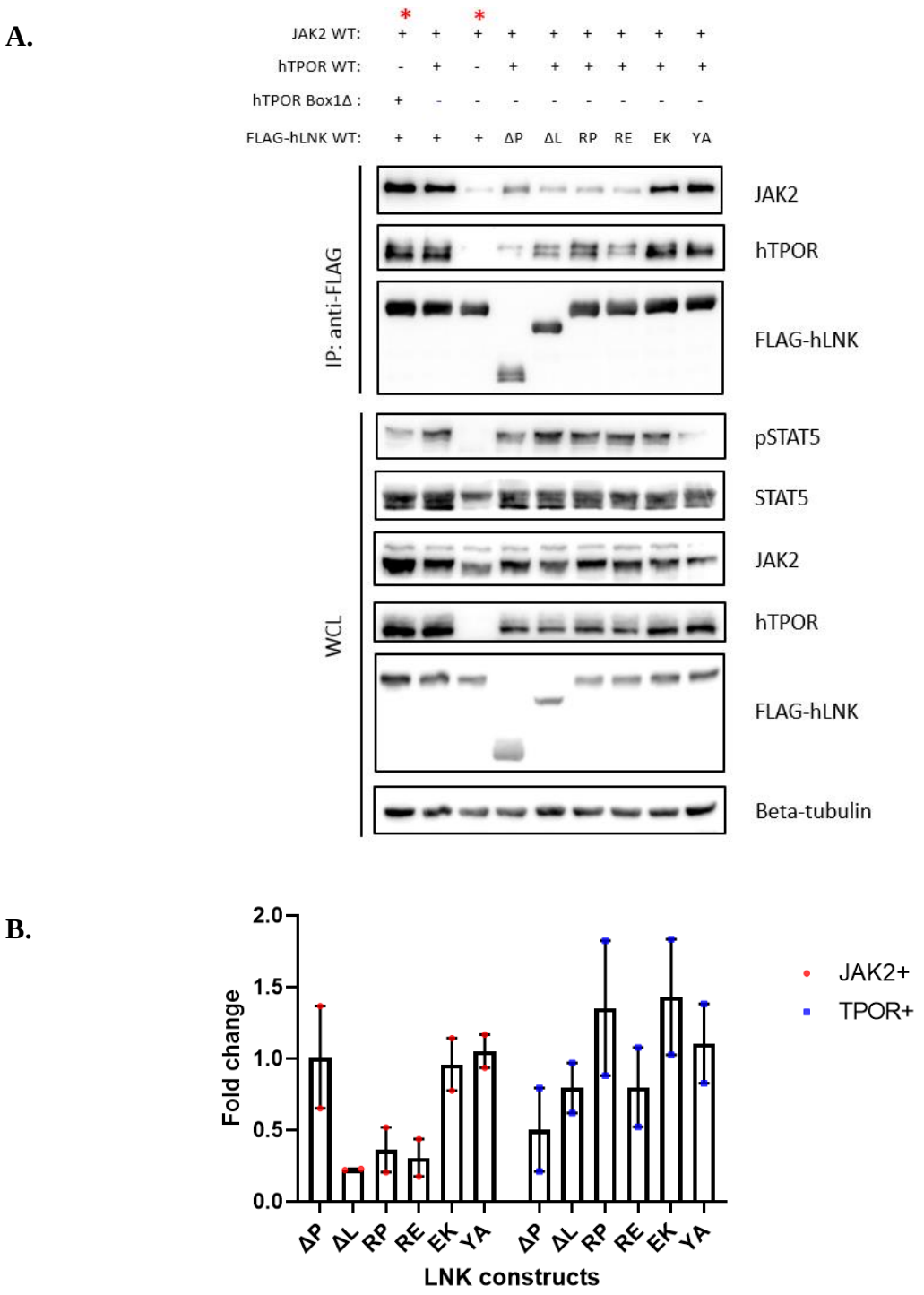

Figure 56: Addition of TPO does not alter LNK mutant binding affinities to TPOR or JAK2.

Immunoblot showing (Top) Co-IP analysis; (Bottom) WCL. Lenti-X 293T cells were co-transfected with either HA-tagged hTPOR WT, HA-tagged hTPOR Box1 mutant, FLAG-tagged hLNK WT or

mutants, and/or JAK2 WT. All conditions were performed with TPO stimulation. For co-IP, protein lysates were immunoprecipitated with FLAG antibodies and blotted with antibodies specific for JAK2, TPOR (to detect FL-hTPOR), and FLAG (to detect LNK). For WCL, total protein was subjected to SDS-PAGE and immunoblotted with indicated antibodies. β-tubulin was used as a loading control. Red asterisks denote 3x JAK2 concentration used. ΔP represents ΔPro/DD, ΔL represents Δlinker, RP represents R425P, RE represent R392E, EK represents E395K, and YA represents Y572A. B) Graph of relative JAK2 and TPOR levels of 2 independent experiments generated using densitometry data. For a complete list of densitometry data for replicates, see Appendix Section B (Figure 91). Image representative of n=2 experiments.

All LNK mutants exhibit similar tyrosine phosphorylation levels

As LNK is known to be tyrosine phosphorylated by JAK2 [278, 473], the various LNK mutant constructs were investigated for differences in phosphotyrosine levels in the presence of TPO as these phosphorylated sites may be important for LNK function or binding to other proteins. No significant difference in the level of phosphotyrosine levels was observed across all the LNK mutants indicating that loss of tyrosine phosphorylation of LNK was not playing a role in mediating interactions with JAK2 or LNK for any of the LNK mutants (Figure 57).

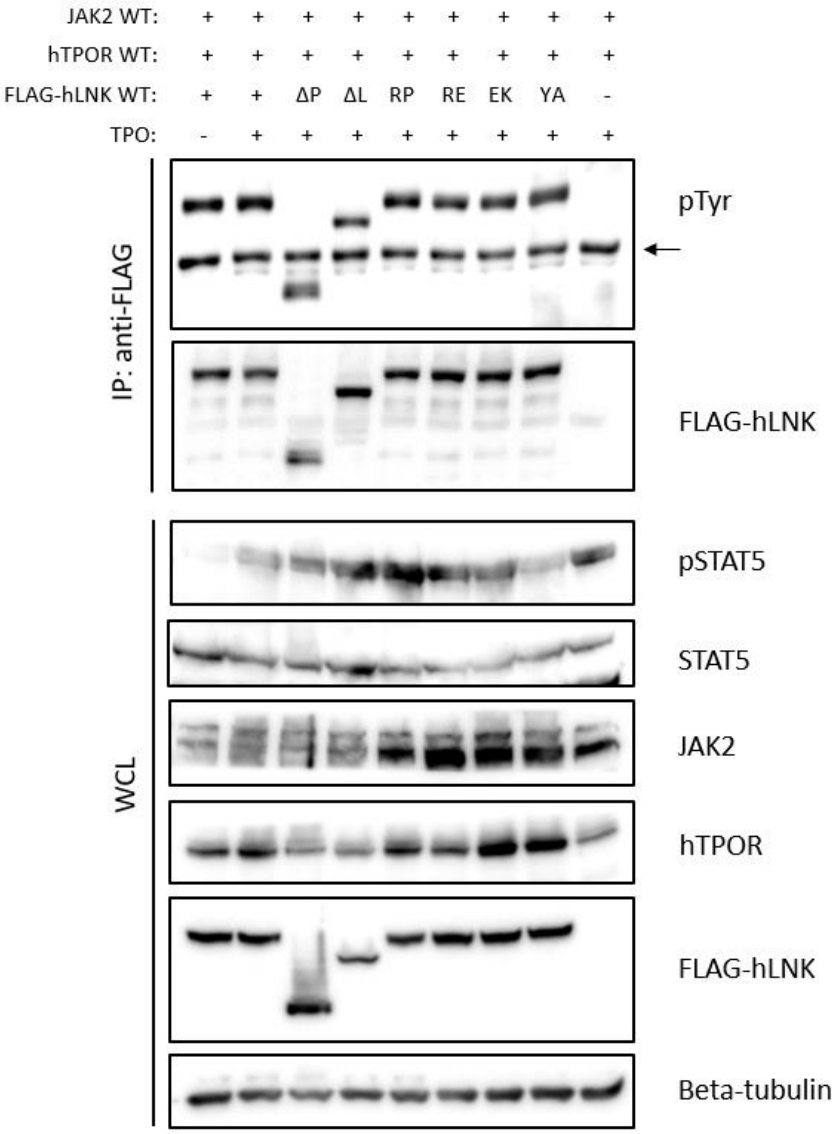

Figure 57: All LNK mutants exhibit similar tyrosine phosphorylation levels when stimulated with TPO.

Immunoblot showing (Top) IP analysis; (Bottom) WCL. Lenti-X 293T cells were co-transfected with either HA-tagged hTPOR WT, FLAG-tagged hLNK WT or mutants, and/or JAK2 WT. For IP, protein lysates were immunoprecipitated with FLAG antibodies and blotted with antibodies specific for pTyr (4G10) and FLAG (to detect LNK). For WCL, total protein was subjected to SDS-PAGE and immunoblotted with indicated antibodies. RIPA buffer was used for this assay to disrupt any interactions between LNK and other proteins in order to focus specifically on the tyrosine phosphorylation of LNK. β-tubulin was used as a loading control. ΔP represents ΔPro/DD, ΔL represents Δlinker, RP represents R425P, RE represent R392E, EK represents E395K, and YA represents Y572A. Arrow shows non-specific phospho band. Image representative of n=3 experiments.

LNK binding to TPOR involves cytoplasmic residues Y113 and Y118 of the receptor

Following the determination of the LNK Pro/DD domain that associates with TPOR, next the region of the TPOR responsible for interacting with LNK was investigated. In order to answer this question, various TPOR ICD truncations were generated. Each truncation was based on a previous study analysing the signalling function of regions of TPOR [184]. The tyrosine residues in the TPOR ICD were mutated to phenylalanine as this residue is structurally very similar to tyrosine, but importantly is not able to be phosphorylated. These phenylalanine substitutions will allow for the determination if any of the sites on the receptor are required to be phosphorylated for LNK binding. These constructs (Figure 58) were created in the pQCXP CMV/TO DEST backbone and all constructs contain the Box1 mutation (PxxP to AAAA). The Box1 mutation was included to ensure that any interaction observed was due to LNK binding and not JAK2-mediated binding. Results showed that mutation of any ICD tyrosine residues of TPOR to phenylalanine resulted in reduced LNK binding but double mutation of Tyr113/118 to phenylalanine resulted in abolished LNK binding (Figure 59). These results suggest that both of these tyrosine residues are particularly important for LNK association to the receptor. Co-precipitation assays with TPOR truncation constructs were challenging due to variation in expression levels and were not pursued further due to time limitation.

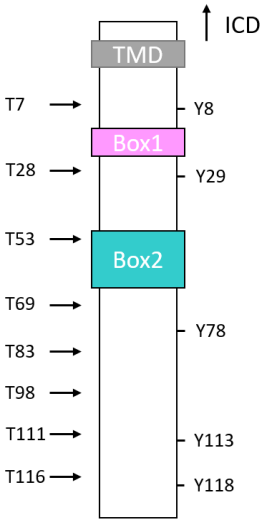

Figure 58: Illustration of the different TPOR ICD truncations and point mutations that were generated.

The number followed by 'T' represents the number of amino acids left in the ICD after truncation. All tyrosine residues 'Y' were individually mutated to phenylalanine. A dual point mutation was created for Y113/ Y118. 'TMD' represents receptor transmembrane domain. Figure was adapted from [184].

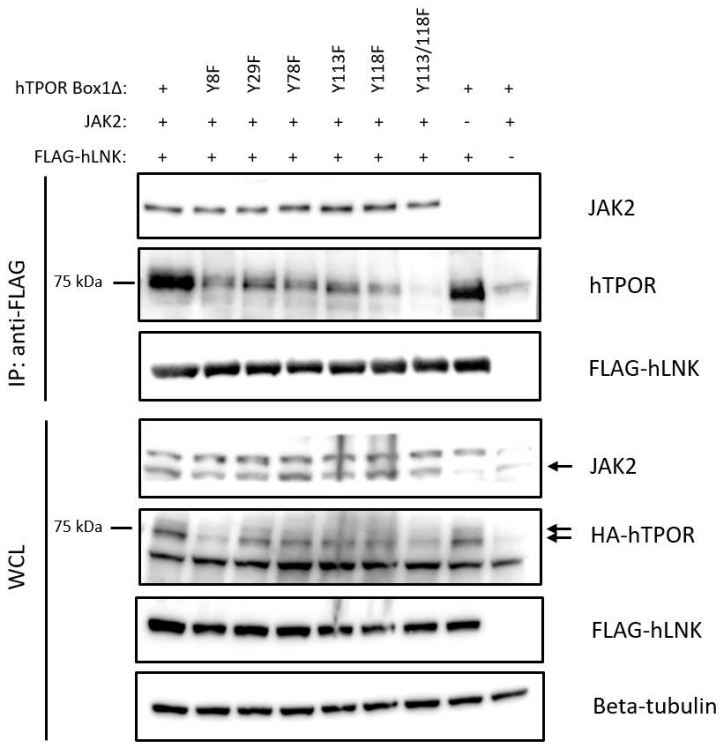

Figure 59: TPOR Y113 and Y118 residues are important for LNK association to the receptor.

Immunoblot showing (Top) IP analysis; (Bottom) WCL. Lenti-X 293T cells were co-transfected with either HA-tagged hTPOR Box1Δ and Box1Δ Tyr mutants (Y8F, Y29F, Y78F, Y113F, Y118F, Y113/118F), FLAG-tagged hLNK WT, and/or JAK2 WT. For IP, protein lysates were immunoprecipitated with antibodies specific for JAK2, TPOR (to detect FL-hTPOR), and FLAG (to detect LNK). For WCL, total protein was subjected to SDS-PAGE and immunoblotted with indicated antibodies. β-tubulin was used as a loading control. Top arrow for HA-hTPOR showing the mature glycosylated receptor band; bottom arrow for HA-hTPOR showing the immature receptor band. n=1 experiment.

LNK binding to TPOR is partially affected by the W515K and S505N mutations

The ability of TPOR TMD and JM mutants to bind to LNK was investigated. These constitutively active mutations may position the receptor in a conformation that allows for continued phosphorylation of their associated JAK2 but may reflect different degrees of phosphorylation that can affect LNK binding to JAK2 and TPOR. LNK showed reduced binding to TPOR TMD and ICD-JM mutations such as S505N and W515K (Figure 60).

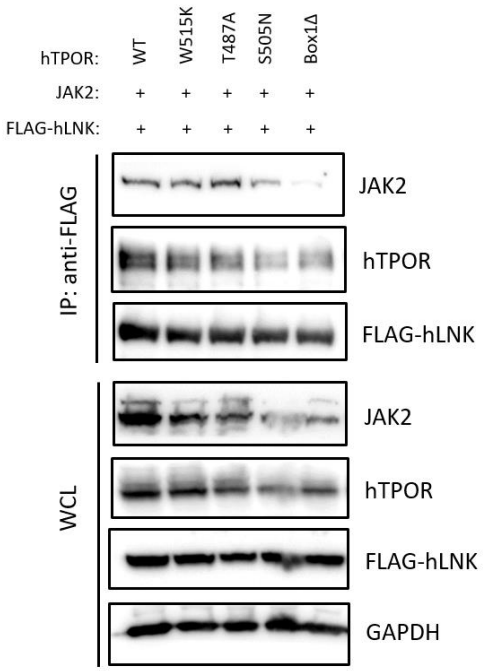

Figure 60: TPOR TMD and ICD mutations (S505N & W515K) reduce binding to LNK.

Immunoblot showing (Top) IP analysis; (Bottom) WCL. Lenti-X 293T cells were co-transfected with either HA-tagged hTPOR WT or mutants (W515K, T487A, S505N), FLAG-tagged hLNK WT, and JAK2 WT. For IP, protein lysates were immunoprecipitated with antibodies specific for JAK2, TPOR (to detect FL-hTPOR), and FLAG (to detect LNK). For WCL, total protein was subjected to SDS-PAGE and immunoblotted with indicated antibodies. GAPDH was used as a loading control. Image representative of n=2 experiments.

Discussion

LNK is an important negative regulator of JAK2 activation and mutations in LNK that impair this regulatory function are found in MPNs. The mechanism of LNK regulation of JAK is currently poorly understood. In order to address this lack of understanding, various LNK constructs with domain truncations and clinical/synthetic point mutations that retained their SH2 domain were generated. These constructs were tested and compared to LNK WT for their ability to bind TPOR and JAK2, and to determine if the different mutations can negatively regulate downstream signalling. Initially, the various LNK domain deletions and mutations (all of which retained the SH2 domain) were co-transduced into Ba/F3 TPOR WT or W515K cells. The purpose of co-transducing the different LNK constructs into both the Ba/F3 TPOR WT and W515K (or S505N initially) was to test the effects on constitutively active cells (those expressing TPOR W515K) and on those cells that are induced (those

expressing TPOR WT), using cell proliferation and signalling assays as a readout. However, several issues were encountered to achieve stable expression of LNK constructs in Ba/F3 cells. Certain constructs, in particular LNK WT, showed weak expression that was lost after culturing the cells for a short period of time (see Appendix Section B Figure 94 and Figure 95). Ba/F3 cells even while cultured in TPO or IL-3 containing media, will activate JAK (which is inhibited by LNK) which plays a pivotal role in providing the growth signals. Therefore, cells that were able to proliferate would only be those that have developed a mechanism to overcome JAK2 inhibition by LNK. This inhibition of cell growth has also been previously reported [249], but was highlighted in a study where it was found necessary to transduce the BCR-ABL oncogene in order to express LNK WT in 32D cells to allow growth while expressing LNK [342, 474]. LNK, however, when experimentally introduced, does not affect the growth of non-haematopoietic cells [249], which is consistent with its expression in cells of the megakaryocytic lineage (megakaryocyte progenitors to platelets). In the current study, constitutively active TPOR mutants did not prevent this growth inhibition (see Appendix Section B Figure 93). A previous study also showed that stably-transduced Ba/F3 expressing TPOR W515L which is a constitutively active mutant construct, were more sensitive to the growth inhibitory effects of transfected LNK than those cells expressing TPOR WT [285]. The difference in observation regarding the ability of the cells to overcome growth inhibition with the use of BCR-ABL instead of constitutively active TPOR is likely due to the ability of BCR-ABL to directly activate STATs without utilising JAKs [475]. The growth inhibitory effect of LNK was also evident in HEL cells which express the $JAK2^{V617F}$ mutant [309]. When these cells were transduced to express exogenous LNK, it was observed that the levels of LNK were significantly lowered after approximately four weeks of culture, and cell growth as well as the JAK-STAT and ERK/ MAPK signalling were no longer significantly repressed [309]. This observation is consistent with the findings in the current study but the effect occurred in a shorter time frame (less than 4 weeks) (see Appendix Section B Figure 92-Figure 95). The proliferation rate of Ba/F3 TPOR WT or W515K/S505N cells that were co-transduced with LNK WT (minimal expression on Western analysis) (Appendix Section B Figure 94 and Figure 95) seemed to be at a comparable level or even slightly elevated compared with cells that were not made to express LNK WT (see Appendix Section B Figure 92 and Figure 93). The increase in proliferation rate of these cells may be due to the utilisation of some mechanism to overcome LNK inhibition of growth. Even if the different LNK constructs were able to be expressed, their expression levels differed (see Appendix Section B Figure 94 and Figure 95). Due to the difficulties in generating stable Ba/F3 cell lines expressing different LNK constructs at comparable levels, an alternative was sought utilising transient transfection of Lenti-X 293T cells (non-haematopoietic) [249] to investigate signalling mediated by LNK.

Various LNK domain deletions (ΔPro/DD, ΔPH, ΔPH-SH2 linker, ΔCTD) and point mutations in the SH2 domain (R425P, R392E, E395K) as well as C-terminal domain, Y572A, were generated in order to determine if the other domains of LNK (besides SH2) are involved in inhibiting/regulating signalling of JAK2 associated with TPOR. All LNK expression constructs retained the SH2 domain required for JAK2 phosphorylated tyrosine binding. Domain truncations such as LNK ΔPro/DD and LNK Δlinker, and SH2 domain point mutants reduced or abolished LNK capability to inhibit downstream signalling as observed by the increase in STAT3 and ERK1/2 activation. As the Pro/DD domain is thought to mediate dimerisation via the zipper region, it is plausible that the deletion of this domain (LNK ΔPro/DD) may have abolished the ability of LNK to form homo-dimers. As a result, this prevented the formation of the complex that is required to bind and inhibit JAK2 signalling. This may occur concurrently with its SH2 domain acting as a main anchor to bind to JAK2. It has been shown that the LNK family members, SH2B1 and APS, can hetero-dimerise and associate with their two cognate JAKs [291]. Accordingly, LNK homo-dimerisation has also been reported in an overexpressed system [281]. Alternatively, it is also possible that this domain is involved in interacting with the receptor and plays a role in impeding further activation of downstream pathways. The current study has revealed a novel function of the LNK Pro/DD domain. This domain appears to play an important role in binding to TPOR whilst maintaining JAK2 interaction via the SH2 domain. Supporting this notion, it was previously shown that the related family member, APS is able to bind to a related receptor, EPOR, at its ICD [282]. On the contrary, another study showed that a similar region in LNK transiently associates with inactive JAK2 instead of TPOR [278, 309, 310, 355]. In this study, a Co-IP of glutathione-S-transferase (GST)-tagged Pro/DD-PH construct containing no SH2 domain was performed in UT7 cells expressing TPOR. It is plausible that TPOR-mediated JAK2 binding might have occurred. Based on the current results, it is likely that the LNK Pro/DD domain is another site that works in close association with the SH2 domain to bind the receptor and JAK2, respectively, and regulate TPOR-mediated signalling. Alternatively, LNK SH2 binds both TPOR and LNK independently, and forms dimers via the Pro/DD which strengthens the binding as a complex.

The importance of the LNK SH2 domain in binding and inhibiting JAK2 has been well established. This finding is well supported by the results of this study that showed all three point mutations in this domain (clinical mutants E395K and R425P, and synthetic R392E mutant) resulted in enhanced signalling and disrupted JAK2 binding capability (except for E395K). These results characterise and confirm the novel R425P mutation as oncogenic due to its role in increased signalling, and therefore, enhanced cell growth and proliferation. This explains the MPN/leukaemic clinical phenotype observed in patients harbouring the R425P mutation. The enhanced ERK1/2 activation in a transient transfection system caused by the E395K mutant was previously reported [476]. However, unlike the

other two mutations, the E395K mutant retained binding capabilities to both JAK2 and TPOR, although binding to JAK2 capability was slightly reduced compared to LNK WT. It is possible that this residue may not be directly binding JAK2 but that this amino acid or negative charge at this position may be important for regulating LNK function. The ability of this mutant to bind strongly to JAK2 may explain why TPOR expression was stabilised at the cell surface compared to the R392E and R425P mutant. A functional assay using a stably-transduced haematopoietic cell line of this mutation may be required to confirm the reduced inhibition on signalling and ensure that this was the consequence of the mutation and not of the cell type. The R392E synthetic mutation in SH2 domain has been reported to cause disruption of LNK function that is more severe than the one observed in the missense mutations in the PH domain [249, 277]. This is in complete agreement with the current data showing that SH2 domain point mutations resulted in severe functional disruption of LNK compared to ΔPH, further supporting the notion that the SH2 domain is the main regulatory site. Deletion of the PH-SH2 linker region (LNK Δlinker) also showed some effect on LNK inhibitory function. Due to the proximity to the SH2 domain, the Δlinker may have affected the conformation of the SH2 domain thereby causing ineffective LNK binding to JAK2 (with maintained TPOR binding) as observed in this study, resulting in elevated pSTAT3 and pERK1/2 levels. This observation confirms the notion that LNK can indeed bind directly to TPOR and that this binding occurs between the Pro/DD and PH domain.

LNK contains a PH domain that is responsible for lipid interaction with the inner cell membrane containing phosphoinositides [278, 285]. Deletion of the PH from LNK did not show any strong change in LNK function. A similar effect was observed for the deletion of the LNK C-terminal domain. Previous studies have suggested that the PH domain of LNK is involved in a weak interaction with inactive JAK2 and constitutively active $JAK2^{V617F}$ [310], and that this domain is crucial for LNK localisation to the cell membrane [285]. LNK PH domain missense mutations have also been shown to impair its cell surface localisation leading to reduced interaction with JAK2 and reduced inhibition of signalling [353]. The findings of the current study give support to this observation as LNK ΔPH was observed to increase STAT3 but not ERK1/2 signalling compared to LNK WT. It is plausible that in a transient high expression system, LNK does not require the PH domain to anchor to the membrane to enhance interaction with JAK2. However, in a low expression system (endogenous LNK), the PH domain may be important for membrane anchorage in order to bring LNK in close proximity to JAK2. This is in concordance with previous reports that found that the PH domain contributes to inhibition but is not required to hinder TPOR- or EPOR-mediated cell growth or haematopoiesis [249, 277]. The Y572 residue in the C-terminal domain of LNK was also not crucial in maintaining the interaction between LNK, JAK2, and TPOR. In support of this finding, previous

studies have shown that the Y572 residue that lies in the aforementioned domain may aid, but is not essential for EPOR signalling [277] and; in the context of TPOR signalling, the murine counterpart of this residue was shown to have no functional effect [249, 311]. It was also previously described that in the context of c-KIT signalling, the PH and C-terminal domain of LNK play a minor role in contributing to the LNK inhibitory function whereas its NTD and Y536 (Y572 human equivalent) are not important for this function [311]. This is in contrast to the results of the current study where in the case of TPOR, the PH and CTD do not appear to be as important for LNK function compared to the NTD that may be a potential binding site for TPOR. LNK may regulate different receptors in a different manner, something that is yet to be fully understood.

TPOR ICD domain contains several tyrosine phosphorylation residues that serve as sites for the binding of positive or negative regulatory proteins. Co-precipitation results showed that the two distal ICD Tyr residues of TPOR, Y113 and Y118 (Y112 and Y117 murine homologue) were important for LNK association. This may be one of the mechanisms whereby these constitutively activating mutations are able to enhance signalling. These residues are also positive regulatory sites that are able to be phosphorylated and are important for the recruitment and activation of various proteins such as Shc, STAT5, STAT3, SHIP, SHP2, and Gab2. Due to the ability of these two residues to bind various proteins, LNK may either be competitively binding to TPOR or its binding to TPOR may be mediated by other proteins. Interestingly, it has been shown for the murine homologue Tyr112 that this residue is important for the pathogenesis of the W515A mutation which affects the MAPK pathway and not JAK2 activation [230]. Based on this observation, LNK may bind to other proteins that are bound to Tyr112 such as Shc which mediates the activation of the MAPK pathway. Although the binding of LNK to Shc has not been shown, the related family member, APS, has been shown to bind to this protein [335].

Although a previous study has demonstrated that LNK binds to JAK2 in the absence of receptor [285], the data presented here showed that the binding of LNK to JAK2 requires the presence of a cytokine receptor, which is consistent with another study [278]. It is plausible that the binding of JAK2 to LNK preferentially occurs at the cell membrane as an entire complex, with the receptor present to anchor JAK2 at the surface (and JAK2 present to stabilise the receptor at the surface). It is likely that LNK has a higher affinity for the JAK2-TPOR complex than for JAK2 alone. In support of the observation that LNK interacts with TPOR, it has been shown that LNK is able to co-localise with this receptor at the cell surface [285, 474]. The current investigation showed that LNK was able to associate with inactive JAK2 as previously reported [278, 309, 310, 355] but it showed higher binding affinity for active JAK2. The murine JAK2 KE construct harbours the K882E mutation in the ATP binding pocket rendering JAK2 kinase dead and unable to perform downstream signalling. However, this

mutant still retained the ability to be phosphorylated by other signalling molecules including endogenous JAK2. Therefore, it is possible that a small portion of the JAK2 KE molecules was phosphorylated at the Y813 and/or Y613 residue allowing LNK to bind to this residue. The anti-pJAK2 antibody that was used only detects phosphorylation at Tyr1007/1008 and not at Tyr613/813. Alternatively, LNK may be able to bind to kinase inactive JAK2 but with a much lower affinity than to active JAK2, and this may be mediated by a site other than the SH2 domain of LNK. The SH2-disrupted LNK mutant, R392E has been shown to bind to inactive JAK2 [310, 355] as the mutation may not have completely abolished SH2 binding ability although there were contradictory findings reported by another group [342]. The presence of a second binding site in LNK either in the N-terminal [309] or PH domain [310], that binds inactive JAK2 WT has been reported [310], although the precise location of this site remains debatable.

Previous studies have provided conflicting data on whether LNK constitutively binds to TPOR or not [285, 342]. The data presented above showed that LNK binds constitutively to TPOR and the related family member, GHR, and that JAK2 may contribute to TPOR-LNK interaction but is not required for TPOR binding. This was confirmed using the TPOR Box1 mutant and supported by previous finding that state that binding of LNK WT to both TPOR WT and Box1 mutant receptor was comparable [342], suggesting that JAK2 presence may not be crucial for TPOR and LNK interaction. However, 32D cells (murine IL-3 dependent myeloid cell line) were used in this study [477] and these cells may express endogenous levels of TPOR [478]. Hence, it is plausible that LNK WT may be bound to endogenous TPOR (that is associated with JAK2) leading to the observation of a constitutive interaction with TPOR. A contradictory study showed that SH2-disrupted LNK R392E mutant does not bind to TPOR [285] possibly due to abolished binding to JAK2, indicating that it does not bind directly to TPOR. This previous study also showed that the interaction between LNK WT and TPOR W515L (constitutive active TPOR mutant) was increased in the presence of TPO stimulation [285]. LNK showed preferential co-precipitation with the immature GHR rather than with the mature form although this was not the case for TPOR. This suggests that LNK may be binding JAK2 bound to the precursor GHR in the ER. Alternatively, LNK may preferentially bind to precursor GHR preventing the maturation (glycosylation) and inhibiting cell surface localisation which would further downregulate the ability of the receptor to be activated by ligand binding. In the case of TPOR, LNK may already be bound to the precursor before localising to the surface. Activation of GHR or TPOR did not show a change in the association with LNK. However, the amount of JAK2 overexpressed by these transfected cells may have caused significant constitutive activation and therefore, ligand stimulation of GHR and TPOR may not produce any significant elevation in pJAK2 levels. The

results of this study confirmed that LNK constitutively binds to both JAK2 and TPOR, but that a TPOR-JAK2 complex is not required for LNK association.

Interestingly, TPOR levels were observed to be elevated in the presence of LNK. The reduced signalling due to LNK presence may have led to the reduced receptor degradation which may explain this observation. Alternatively, as LNK WT is overexpressed in this system, the limited amount of c-CBL or SOCSs in the cells may have degraded the unbound LNK that is present, thereby leaving the remaining LNK still bound to the receptor. This results in the receptor not being degraded as much as expected. It was previously shown for the related family member, APS, that its C-terminal tyrosine residue is a binding site for the c-CBL protein and this interaction results in the attenuation of the signalling [282, 349] and LNK was also previously shown to bind c-CBL [343, 344]. Interestingly, the co-expression of LNK WT with not just TPOR, but also GHR, resulted in increased receptor expression suggesting a general mechanism of receptor stability by LNK overexpression. When co-expressed with GHR, LNK mutations that retained their signalling inhibition resulted in increased receptor levels suggesting that LNK may be eliminating low level basal signalling [122]. Interestingly, only the precursor receptor levels seemed to have increased in this regard and not the mature receptor levels. This may be attributed to a trafficking issue where LNK may be affecting JAK2 which acts as a chaperone for the receptor to localise to the surface.

The results of this chapter showed that all LNK mutant constructs displayed similar tyrosine phosphorylation levels. This suggests that the potential site of LNK phosphorylation does not lie in the mutated regions. As only certain LNK mutant constructs (based on their ability to disrupt LNK function) were tested for the assay, it may be possible that other untested constructs (ΔPH and ΔCTD) may have a similar or different tyrosine phosphorylation pattern. LNK has ten potential tyrosine phosphorylation sites (Figure 61). The PH domain contains the Tyr273, the SH2 domain contains Tyr401 and Tyr461, whereas the CTD contains Tyr555 and Tyr572. It has been suggested that only the Y572 is a putative site for LNK phosphorylation, based on data obtained testing the similar murine tyrosine residue LNK Y536. The results of the current study showed that there are other sites in LNK besides the putative Y572 residue that can be phosphorylated, at least in the context of TPOR signalling, which may act as binding sites for other regulators.

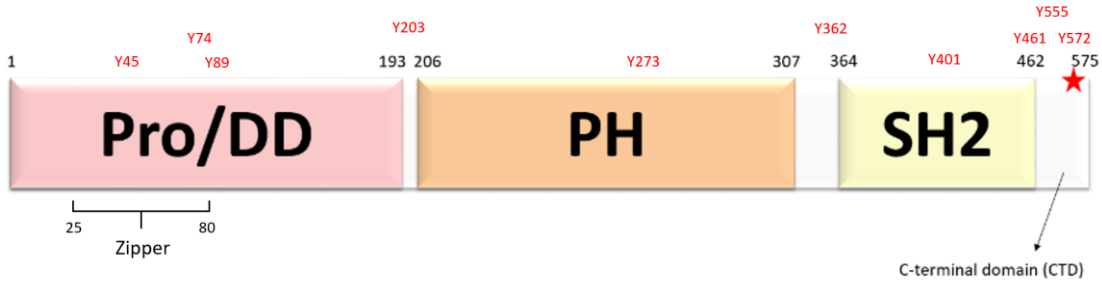

Figure 61: Domain organisation of LNK showing the location of tyrosine residues.

Position of tyrosine residues are shown in red text.

The relationship between LNK and the TPOR mutants that were investigated in this thesis (W515K, T487A, and S505N) has not been defined. This study found that LNK binds less efficiently to the W515K and S505N mutants, and may consider this as an additional mechanism that contributes to the enhanced signalling caused by these mutations. Contrary to the current study, a previous publication has shown that LNK binds to the TPOR W515L mutant better than to the WT and that this is suggested to be mediated by the SH2 domain as the R392E (with disruption of SH2 function) was unable to bind to this mutant [285]. Furthermore, the W515L mutant appeared to be more sensitive to LNK inhibition. Another point of difference was that LNK does not constitutively bind to TPOR WT although it is able to bind to W515L in the absence of cytokine and that this binding is enhanced by the presence of cytokine [285]. This is in contrary to the results of the current study, where LNK was shown to constitutively bind TPOR, and that this binding is reduced in the presence of TPOR mutations. The presence of exogenous JAK2 in the current study may account for the differences in observation. Future studies investigating the effect of LNK on the signalling properties of W515K and S505N mutations may reveal if LNK can suppress signalling of the mutants better than WT.

Conclusion

A novel function of the Pro/DD domain was found in mediating constitutive binding to TPOR possibly to the Y113 and Y118 residues with the LNK SH2 acting as a main anchor to bind to JAK2 (Figure 62 A). Alternatively, LNK may form homodimers via the Pro/DD with each unit binding to TPOR and JAK2 separately (Figure 62 B). These interactions may prevent downstream signalling through a mechanism that has yet to be fully elucidated. Several point mutations in the Pro/DD

domain have been reported in T-ALL (R43C and E78K) and acute myeloid leukaemia (R80C and I145T), and predicted to be pathogenic (based on FATHMM score) [479]. The findings of the current study act as an important foundation for future work aimed to increase the understanding regarding the structure-function of this important negative regulator of JAK2 signalling.

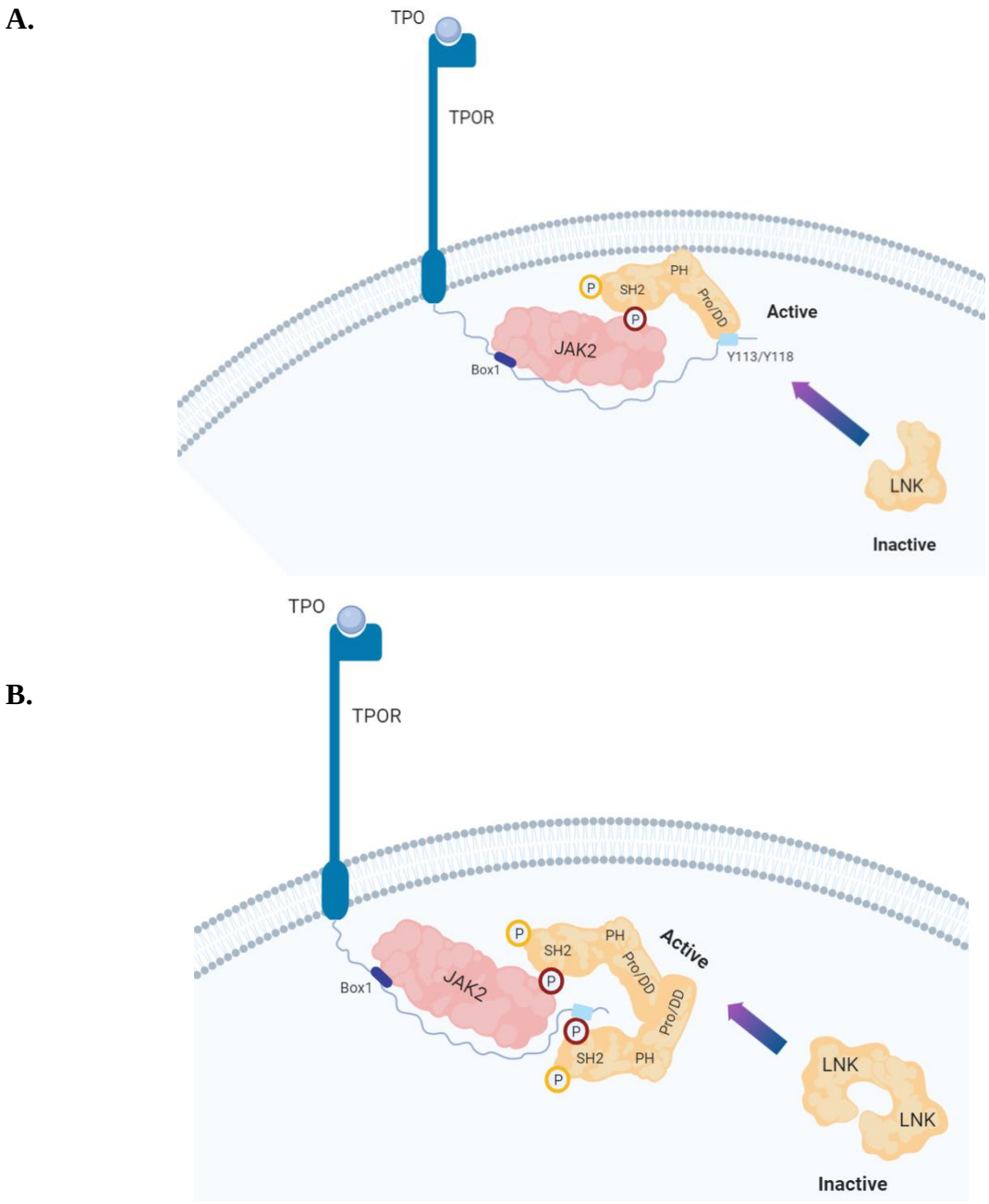

Figure 62: Proposed model for LNK interaction with TPOR and JAK2.

When receptor is present, LNK adopts a more open active conformation. A) LNK may bind to the receptor via its Pro/DD domain and to JAK2 via its SH2 domain with a strong affinity. B) LNK may form homodimers via the Pro/DD, with each unit binding to TPOR and JAK2 separately, via its SH2 domain. For the purpose of the illustration, the receptor is shown as a monomer.

Chapter 6

Protein Expression and Purification of Full-Length WT SH2B3 (LNK)

Introduction

Protein crystallisation for X-ray crystallography is a valuable technique that is used to determine protein structure. These structures are important to better understand protein function in terms of how the different domains/ amino acids interact with each other or with other proteins. This understanding will also facilitate the development of targeted drugs to enhance or inhibit protein activity. The development of targeted drugs will be useful in clinical applications to treat myriads of diseases.

In order to obtain protein for structural and biophysical studies, a suitable protein expression system needs to be employed. The bacterial expression system is one of the most common protein expression systems that is used as it is time-efficient, able to generate high yields of recombinant protein, and is relatively inexpensive compared to other expression systems [480-487]. In the case of low protein yield, codon optimisation for high expression in *E. coli* has been shown to significantly increase protein expression for many genes [488-493]. However, expression of protein in bacterial systems do not allow for many secondary structure modifications of proteins that occur in eukaryotes such as glycosylation, which may be important for the structure-function of the protein. Insect and mammalian expression systems can also be used, however these are typically much more costly and time consuming, and typically produce lower protein yields compared to bacterial expression systems, although secondary structure modifications that may be important for eukaryotic protein functions will be able to occur when expressed in higher eukaryotic cells [494, 495].

In order to obtain purified protein for structural or biophysical studies, the expressed protein will normally require purification using methods such as affinity chromatography, size exclusion chromatography (SEC), and ion exchange chromatography [496, 497]. Protein aggregation and precipitation is one of the major issues that hinder the process of obtaining soluble proteins for further characterisation. Buffer contents such as pH, salt concentration, detergents, metal ions, and other contaminants and impurities can contribute to protein aggregation. Aggregation can exist as insoluble or soluble forms, and various methods can be utilised to improve protein solubility such as incorporation of ubiquitin sequences in the constructs and/or using tags such as maltose-binding protein (MBP) and GST. Although various methods have been developed to improve protein solubility, protein aggregation remains a challenge because different proteins have varying solubility conditions and there is currently no reliable method to accurately predict the conditions for optimal solubility for each purified protein [498, 499]. Despite this, successful attainment of purified protein can be invaluable for understanding protein structure-function.

As the crystal structure of LNK is currently not currently available, there is still lack of understanding towards its role as a negative regulator i.e. how its structure contributes to its function and why LNK functions differently from its other family members. Currently, crystal structures of LNK family members have been separately solved such as the dimerisation domain of APS [306], the SH2 domain of APS in complex with the activated tyrosine kinase domain of the insulin receptor [305], the SH2 domain of SH2B1 in complex with JAK2 pTyr813 phosphopeptide [500], and the SH2 domain of SH2B1 [501]. Therefore, successful expression and purification of LNK for structural and biophysical studies would greatly enhance our knowledge and understanding of the mechanisms of how LNK regulates JAK signalling.

Materials and Methods

Expression Plasmid Constructs

The hLNK constructs for *E. coli* protein expression and purification were made in two different vector backbones using CPEC (see Chapter 2), the pHUE vector [502] (containing 6x Histidine (His)-tag followed by an ubiquitin sequence and the hLNK gene) and the pET11a vector (Novagen) (with 6x His-tag followed by a Tobacco Etch Virus (TEV) protease cleavage site inserted) (see Appendix Section C for primers used). These constructs were made to contain truncations (deletion of hydrophobic rich regions in either the N- and C-terminal regions of LNK). An *E. coli* codon optimised hLNK gene for high expression was also designed and created (ATUM). Similar constructs for the codon optimised hLNK were created in pHUE and pET11a essentially as described above using primers (see Appendix Section C for primers used) specific for the codon optimised hLNK.

Adenoviral constructs for hLNK and JAK2 JH2-JH1 mammalian protein expression and purification were generated. Sequence verified pDONR221 FLAG-hLNK WT (see Chapter 2) was shuttled into the pAD/CMV/V5-Dest adenoviral destination vector (Life Technologies) via Gateway cloning. The coding sequences for human JAK2 JH2-JH1 and 6xHis-TEV was amplified by PCR using complementary primers and joined via CPEC. The JAK2 JH2-JH1 plasmid was a gift from Associate Professor Jeff Babon (Walter and Eliza Hall Institute of Medical Research (WEHI)). The joined coding sequences of 6xHis-TEV JAK2 JH2-JH1 was amplified by PCR using primers including relevant attB sequences and were cloned into pAD/CMV/V5-DEST by Gateway cloning via pDONR221 (Life Technologies). All constructs were verified by DNA sequencing. Gateway cloning of pDONR221 FLAG-hLNK WT and pDORN221 6xHis-TEV JAK2 JH2-JH1 into pAD/CMV/V5-DEST was performed by preparing an LR reaction mix based on the manufacturer's method: 75 ng

pDONR221 constructs, 100 ng pAD/CMV/V5-Dest vector, 0.5 µl 112 mM NaCl, 1.6 µl TE (Tris-EDTA) buffer, and 1 µl LR clonase II enzyme. The components were incubated for 1-3 hours before being used for bacterial transformation.

Expression of human LNK in E. coli

BL21-Gold (DE3) *E. coli* cells (Agilent Technologies) were used to express the various LNK constructs in pHUE and pET11. Each plasmid was transformed into BL21-Gold (DE3) competent *E. coli* cells for high-level protein expression on ampicillin plates (100 µg/ ml) and incubated overnight at 37°C. Single colonies for each construct were then grown in LB to log phase with vigorous shaking (220 RPM) at 37°C. An aliquot of the pre-induction sample was centrifuged for 1 minute at 17,900*g*. After collection of the pre-induction sample, IPTG induction was added to a final concentration of 1 mM to induce expression for 2.5 hours with vigorous shaking (220 RPM) at 37°C. An aliquot of post-induction sample was collected as per the pre-induction sample and cell pellets were resuspended 1:9 with 20% SDS and heated to 95°C for 15 minutes. Samples were subsequently analysed by SDS-PAGE and western analysis (described in Chapter 2).

Adenovirus Production

The pAD/CMV/FLAG-hLNK WT and pAD/CMV/6xHis-TEV JAK2 JH2-JH1 constructs were transformed into Stbl3 *E. coli* cells and confirmed through restriction digest. The purified plasmids were then digested with *Pac1* enzyme (New England Biolabs, R0547S) to linearise and remove the bacterial backbone from the sequence in a reaction containing 10 µg plasmid, 40 U of PacI enzyme, 2 µl of the enzyme 10× CutSmart® buffer, and H_2O to a total volume of 20 µl and incubated for 3 hours at 37°C. Digestion products were confirmed by electrophoresis of 750 µg of the digest on a 0.9% agarose gel. The remaining product was purified by phenol/chloroform extraction and ethanol precipitation, and used to make adenovirus. The pAD/ CMV/GFP control plasmid (*Pac1* digested, phenol/chloroform extracted, and ethanol precipitated) was used to create a control virus.

HEK293 cells (see Chapter 2) were seeded at density of 1.3×10^6 cells/flask in $25cm^2$ cell culture flasks and incubated overnight until 60-70% confluence was reached. Cells were then transfected with 5 µg of digested and purified recombinant adenoviral plasmid (pAD/CMV/GFP control, pAD/CMV/FLAG-hLNK, or pAD/CMV/6xHis-TEV JAK2 JH2-JH1) using Lipofectamine 2000 (Invitrogen, Thermo Fisher Scientific) according to the manufacturer's instructions. Transfected cells were monitored for cytopathic effect and collected 7–10 days after transfection until the majority of

cells showed morphology changes indicating significant virus production within the cells. Cell were collected by dislodging from the flask by agitation, and centrifuged at 300*g* for 5 minutes. Supernatant was removed so that the final volume was approximately 10-15 ml. Adenovirus was released from cells by three cycles of freeze/thaw and virus titer was determined.

Adenovirus Titration by Expression Test

HeLa cells were seeded with 0.5×10^6 cells/well in a 6-well culture plate and incubated overnight at 37°C in a humidified 5% CO_2 incubator until 70-80% confluence was reached. Increasing volumes of virus was used to infect cells in respective wells (no infection, 10 µl, 20 µl, 30 µl, 40 µl, or 50 µl). Cells were monitored after 48 hours for morphological changes. Subsequently, the cells were washed once with ice-cold PBS and detached using PBS (containing 1 mM EDTA), and centrifuged. The cell pellets were resuspended and lysed using lysis buffer pH 7.4 (50 mM Tris HCl, 500 mM NaCl, 1 mM EDTA, 15% glycerol, 1% Triton X-100, 1x protease inhibitor) and centrifuged for 20 minutes at 12, 000*g*. Supernatant was transferred to a fresh tube and 10 µl of supernatant was mixed with 3x SDS sample buffer (containing 0.1 M DTT) and heated to 98°C for 5 minutes before the samples were run on SDS-PAGE gel. Western analysis was performed and a suitable amount of virus to be used for subsequent experiments were predicted based on the virus titer that caused the least cell death but achieve highest protein expression.

Adenoviral Expression of human LNK and human JAK2 JH2-JH1 in Mammalian Cells

HeLa cells were seeded with 3×10^6 cells/175 cm^2 cell culture flask and incubated for 48 hours. Based on the 'adenovirus titration by expression test' section, appropriate amounts of HEK293 lysate from adenoviral production of LNK were used to infect a 70-80% confluent cell culture flask of HeLa cells. For co-infection of HEK293 lysate from adenoviral production of JAK2 JH2-JH1, this was performed 4-5 hours after initial infection. After 24 hours of incubation at 37°C in a humidified 5% CO_2 incubator, the cells were washed twice with PBS and fresh DMEM (containing 10% FBS) was added containing 2 mM sodium butyrate to enhance protein expression and incubated again for a further 24 hours. Cells were washed once with ice-cold PBS and detached using PBS (containing 1 mM EDTA), and centrifuge. The cell pellets were resuspended and lysed using lysis buffer pH 7.4 (50 mM Tris HCl, 500 mM NaCl, 1 mM EDTA, 15% glycerol, 1% Triton X-100, 1x protease inhibitor) and centrifuged for 20 minutes at 12, 000*g*. Supernatant was transferred to a fresh tube and 10 µl of supernatant was mixed with 3x SDS sample buffer (containing 0.1 M DTT) and heated to

98°C for 5 minutes before the samples were run on SDS-PAGE gel. Coomassie staining and western analysis were performed to analyse recombinant FLAG-hLNK and 6xHis-TEV JAK2 JH2-JH1 protein expression. Remaining supernatant was used for affinity purification.

Small-scale Affinity Purification of FLAG-tagged Recombinant human LNK (or with His-tagged human JAK2 JH2-JH1)

Supernatant from cleared lysate from adenoviral expression of human LNK (or with human JAK2 JH2-JH1) in HeLa cells was made to a final volume of 1 ml with lysis buffer (50 mM Tris HCl, pH 7.6, 300 mM NaCl ,1 mM EDTA, 10% glycerol, 1% Triton X-100 (Sigma), 1× EDTA-free complete protease inhibitor ((Roche Applied Science)) and incubated with 100 µl of a 50% slurry of anti-DYKDDDDK G1 Affinity Resin (GenScript) for 2 hours on a tube rotator at 4°C. Affinity resin was then pelleted by centrifugation at 6, 000*g* for 30 seconds. Resin was then washed three times with TBS (50 mM Tris-HCl, pH 7.6, 300 mM NaCl, 10% glycerol). Supernatant was removed and the resin was re-suspended in either 3x SDS sample buffer (containing 0.1M DTT) followed by heating to 98°C for 5 minutes. Centrifugation was performed at 12, 000*g* for 5 minutes before the eluate was subjected to SDS-PAGE followed by Coomassie staining or western analysis to investigate the efficiency of the purification.

Affinity Purification of FLAG-tagged Recombinant human LNK (or with His-tagged human JAK2 JH2-JH1)

An increased scale of protein production was performed (8-20 times larger than small-scale). Supernatant from cleared lysate from adenoviral expression of human LNK (or with human JAK2 JH2-JH1) in HeLa cells was made to a final volume of ~9 ml with lysis buffer (see Table 3) and incubated in a 2:1 ratio of lysates to resin (with 2× EDTA-free complete protease inhibitor ((Roche Applied Science) and DNase I (Roche)) added) for 2 hours on a tube rotator at 4°C. In certain assays, 2mM activated sodium orthovanadate and JAK2 phosphopeptide (synthesised by Peptide2.0) (at a ratio of 3:1 peptide to protein) was added. The sample-resin mix was then transferred to a pre-wet column and allowed to flow by gravity at room temperature. The column was washed with 10-20 bed volumes of TBS wash buffer pH 7.6 (see Table 3). FLAG-tagged proteins were eluted with 1 column volume (CV) of elution buffer (see Table 3) which was added into the column containing 5 ml resin and left to incubate for 30 minutes. The eluate was collected and subjected to SDS-PAGE followed

by Coomassie staining and western analysis to investigate the efficiency of the purification. Protein concentration was estimated by running known concentrations of BSA on the SDS-PAGE.

Table 4: Composition of buffers used for cell lysis, affinity column washes, and elution of protein from the column.

1x Lysis Buffer (TBS pH 7.6)	
Reagents	**Concentration**
Detergent (OG or Triton X-100)	20 mM OG or 1% Triton X-100
Tris	50 mM
NaCl	300 mM, 500 mM, or 1 M
EDTA	1 mM
Glycerol	10% or 15%
Protease inhibitor	1x
Activated sodium orthovanadate	None or final 2 mM
Tris(2-carboxyethyl)phosphine (TCEP)/ DTT	None or 5 mM

1x Wash Buffer (TBS pH 7.6)	
Reagents	**Concentration**
Detergent (OG or Triton X-100)	5 mM, 10 mM, or 20 mM OG, or 1% Triton X-100
Tris	50 mM
NaCl	300 mM or 1 M
Glycerol	10%
Protease inhibitor	None or 1x
Activated sodium orthovanadate	None or final 2 mM

500 µg/ml FLAG (LifeTein, USA) Elution Buffer (pH 7.6 or 8.6)	
Reagents	**Concentration**
Detergent (OG or Triton X-100)	5 mM, 10 mM, or 20 mM OG, or 1% Triton X-100
Tris	50 mM
NaCl	300 mM or 500 mM
Glycerol	10% or 15%

Protease inhibitor	None or 1x
JAK2 phosphopeptide	None or 3:1 ratio of peptide to protein
TCEP	Final 5 mM

1x Arginine-HCl Elution Buffer (pH 4)	
Reagents	**Concentration**
Detergent (OG)	20 mM
Arginine	200 mM
NaCl	1 M
Glycerol	10%
Protease inhibitor	1x
TCEP	Final 5 mM

Size Exclusion Chromatography

Affinity purified FLAG-tagged hLNK fractions collected following elution with FLAG peptide were further purified by SEC on an ÄKTA purifier using a Superdex 200 10/300 GL column (GE Healthcare). The column was pre-equilibrated with 2 column volumes of TBS or sodium citrate solution (see Table 4). After equilibration, fractions containing the protein of interest were loaded into the injection ring (~800µl per injection). SEC chromatogram results (UV absorbance at 280 nm (mAU) against elution volume (ml)) were examined and purified protein was further analysed by SDS-PAGE followed by Commassie staining and western analysis.

Table 5: Composition of buffers used for SEC.

1x SEC Buffer (TBS pH 7.6 or 8.6)	
Reagents	**Concentration**
Detergent (OG or Triton X-100)	5 mM OG or 1% Triton X-100
Tris	50 mM
NaCl	300 mM or 500 mM
Glycerol	10% or 15%
TCEP	Final 1 mM

1x SEC Buffer (Sodium Citrate pH 4)	
Reagents	**Concentration**
Detergent (OG)	20 mM
Sodium citrate	10 mM
EDTA	1 mM
NaCl	1 M
Glycerol	10%
TCEP	Final 1 mM

Results

Creation of LNK constructs for protein expression in E. coli

The human *SH2B3* gene was cloned into two different vector backbones, the pET11a vector (with 6x His-tag inserted) (Figure 63 A) and pHUE vector (containing 6x Histidine (His)-tag followed by an ubiquitin sequence) (Figure 63 B) in order to exploit the benefits of recombinant protein expression in *E. coli*. A 6x His-tag was present in all constructs to facilitate purification of the proteins via affinity chromatography. These constructs (Figure 64) were also modified in various ways in an attempt to improve protein expression and solubility, such as incorporating ubiquitin sequences (also increases protein yield) and truncating the N- and C-terminal regions of LNK that contained hydrophobic rich sequences. Some constructs also included a TEV protease cleavage site after the 6x His-tag, to allow the His-tag to be cleaved using a TEV protease that recognises the ENLYFQG sequence (enzyme cleaves at Q^G). Cleavage of this tag may also be able to improve the purification of the protein. Furthermore, presence of the His-tag may also obstruct protein crystallisation and solubility. These constructs were all generated using CPEC and have been confirmed by restriction digest and DNA sequencing.

A

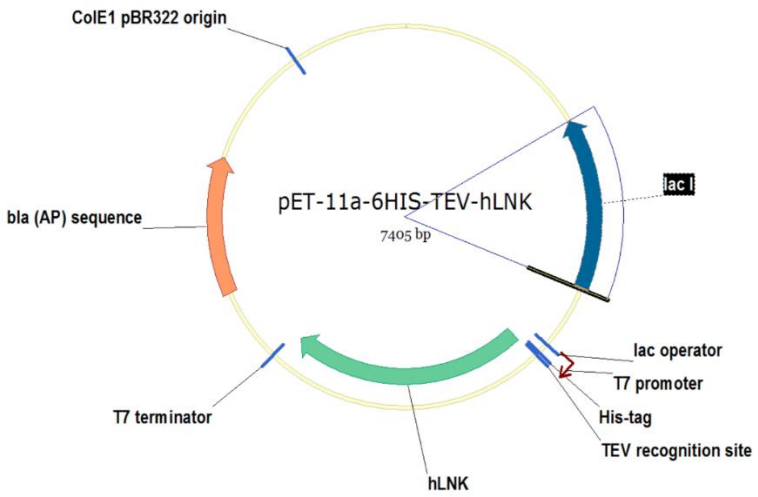

B

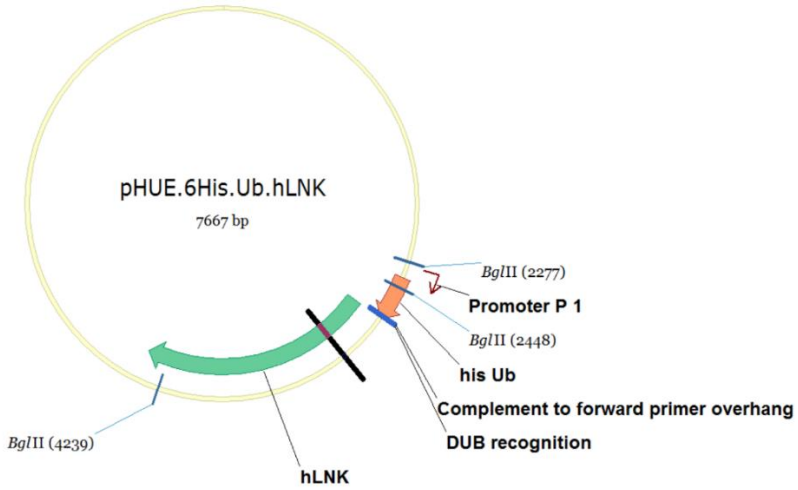

Figure 63: Representative vector map of the pET11a (A) and pHUE (B) LNK vector constructs.

A 6x His-tag is present at the N-terminus of the *SH2B3* gene to facilitate protein purification. (A) The pET11a-6HIS-TEV-hLNK vector series contains the TEV protease cleavage site after the 6x His-tag. (B) The pHUE.6His.Ub.hLNK vector contains the ubiquitin gene after the 6x His-tag. Both vectors possess the ampicillin resistance gene for bacterial cell selection. The expression of recombinant protein is initiated from the T7 promoter.

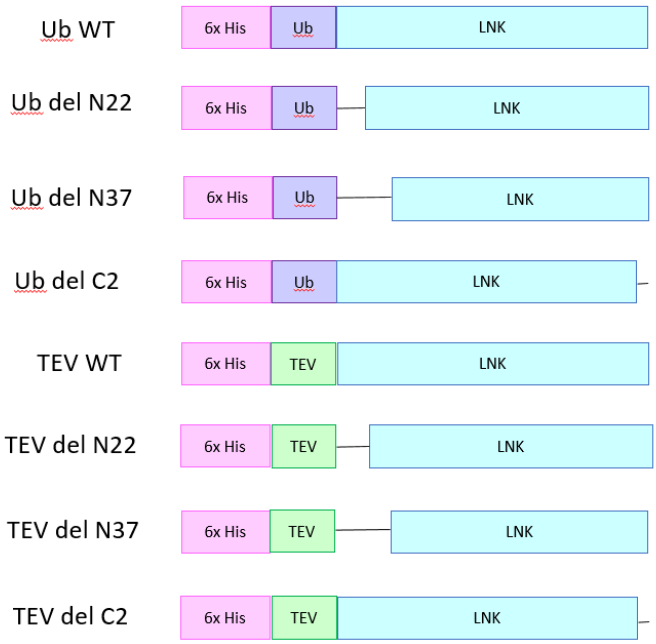

Figure 64: Illustration of the various hLNK constructs created for protein expression and purification.

All constructs possess a 6x His-tag followed by an ubiquitin or TEV protease cleavage site. The His-tag will facilitate protein purification via affinity chromatography. Numbers denote the number of amino acids that have been deleted either from the N-terminus (N22, N37) or from the C-terminus (C2) of the LNK gene.

Small scale expression of human LNK in E. coli

The hLNK constructs for expression in *E. coli* were tested in small scale induction for protein expression. Initially, each of the pHUE and pET11a hLNK plasmids were transformed into BL21-Gold (DE3) competent *E. coli* cells for high-level protein expression. Single colonies for each construct were then grown in LB to log phase (OD_{600} of 0.5 – 0.6) where IPTG induction was performed. In the absence of lactose, the lac repressor that is transcribed from the *lacI* gene present in both the DE3 lysogen (in *E. coli* genome) and plasmid binds to the lac operon. In the presence of IPTG, the lac repressors dissociate from both lac operons. This allows the *E. coli* RNA polymerase to initiate transcription of the T7 RNA polymerase from the T7 gene under the control of the lacUV5 promoter. Subsequently, the T7 RNA polymerase transcribes the target gene in the plasmid under the control of the T7lac promoter. This allows for expression of the recombinant protein that can be detected by SDS-PAGE with Coomassie staining and/or western analysis. Analysis of induced

recombinant protein expression by SDS-PAGE with Coomassie staining was unable to identify induced protein with expected protein sizes ranging from 61-72 kDa for any of the constructs (Figure 65 A). However recombinant protein expression for all constructs could be confirmed using western analysis with the anti-His antibody to detect the His-tag at the N-terminus of the LNK gene (Figure 65 B). This result showed that there is indeed recombinant protein expression but that the level of expression was below detection within the *E. coli* lysate but was able to be detected by the more sensitive and specific Western analysis method (low-femtogram-level sensitivity). In order to improve expression of human LNK in *E. coli* a gene sequence was designed and created for optimised expression in *E. coli* [503].

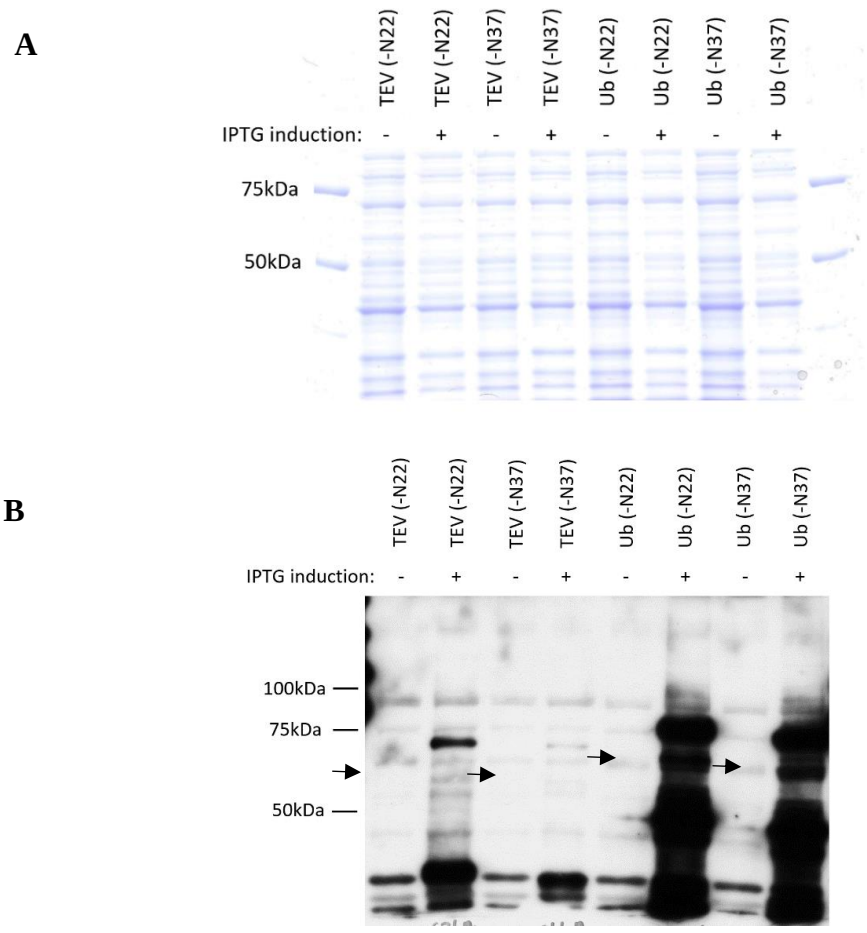

Figure 65: Protein expression of truncated LNK N-terminal domain constructs in E. coli after 1mM IPTG induction visualised by (A) Coomassie stained SDS-PAGE and (B) Western analysis.

BL21-Gold (DE3) cells were transformed with hLNK expression constructs in pHUE or pET11a vector on ampicillin plates and incubated overnight at 37°C. Single colonies for each construct were grown to log phase (OD_{600} of 0.5 – 0.6) at 37°C. An aliquot of the pre-induction sample was collected

followed by induction with IPTG (final concentration 1 mM) for 2.5 hours at 37°C. An aliquot of post-induction sample was collected and cell pellets were resuspended with 20% SDS and heated to 95°C for 15 minutes. Samples were subsequently analysed by SDS-PAGE and western analysis. Anti-His antibody was used to detect His-tagged proteins. 'TEV' denotes constructs in the pET11a vector and 'Ub' denotes constructs in the pHUE vector. Numbering followed by '-N' denotes the number of amino acids that was truncated from the N-terminus of the protein. Arrows show expected size of induced protein products.

Protein expression of codon optimised human LNK in E. coli

Since *E. coli* expression of the human *SH2B3* gene (which encodes LNK) was found to be not suitable for high level protein expression, a codon optimised sequence of the gene for high expression in *E. coli* was designed and created in an attempt to achieve suitable expression of the human LNK protein. The same modifications were made to the codon optimised gene as were previously described for the original LNK coding sequence (Figure 66) in order to increase the solubility and expression of the translated protein. Analysis of induced expression of the optimised hLNK constructs showed that they were still not able to achieve a suitable protein expression level as Coomassie staining of SDS-PAGE did not indicate any protein expression was induced (data not shown) while western analysis showed weakly detected bands at the expected sizes for each protein (Figure 67).

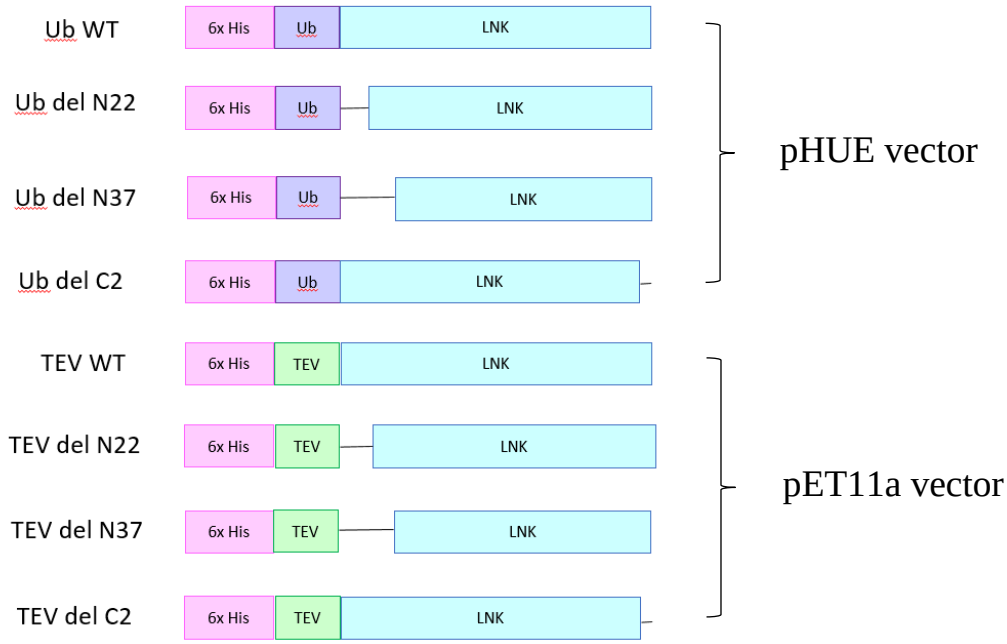

Figure 66: E. coli codon optimised LNK constructs for protein expression and purification.

All constructs possess a 6x His-tag followed by an ubiquitin or TEV protease cleavage site. His-tag was included for the purpose of protein purification via affinity chromatography. Numbers denote the number of amino acids that have been deleted either from the N-terminus (N22, N37) or from the C-terminus (C2) of the *SH2B3* gene.

A.

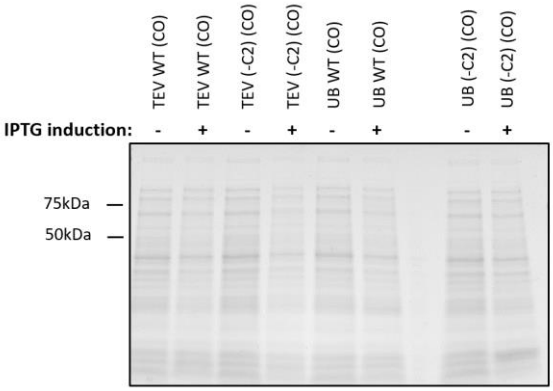

B.

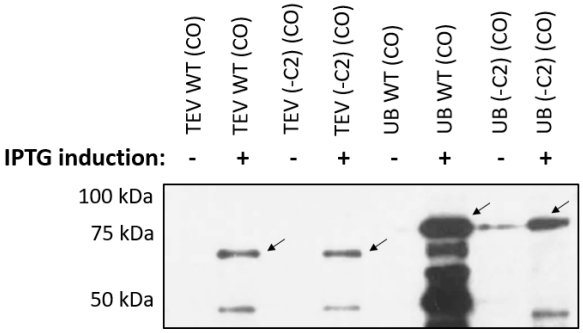

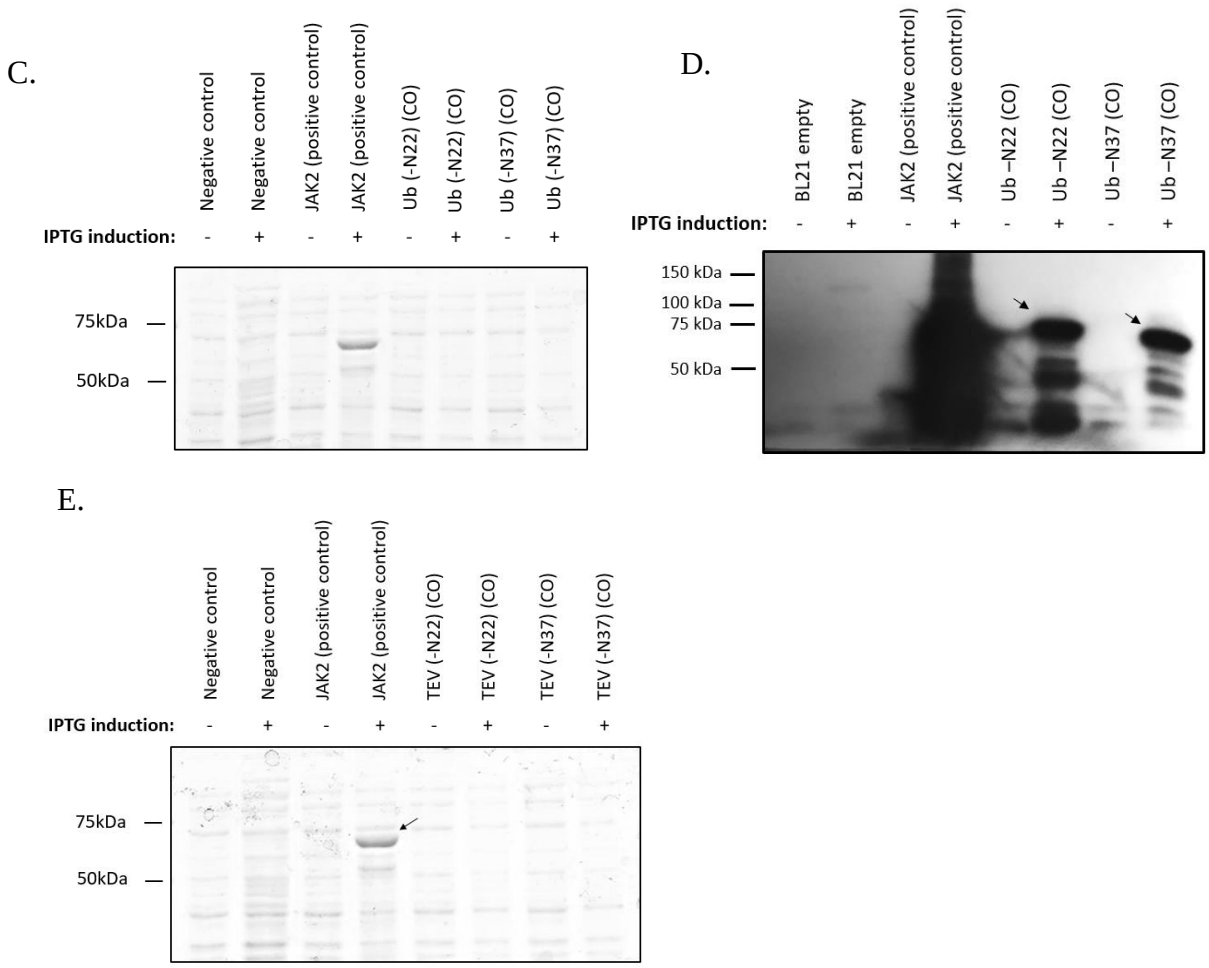

Figure 67: Protein expression of codon optimised LNK constructs in E. coli.

BL21-Gold (DE3) cells were transformed with codon optimised hLNK expression constructs in pHUE or pET11a vector on ampicillin plates and incubated overnight at 37°C. Single colonies for each construct were grown to log phase (OD_{600} of 0.5 – 0.6) at 37°C. An aliquot of the pre-induction sample was collected followed by induction with IPTG (final concentration 1 mM) for 2.5 hours at 37°C. An aliquot of post-induction sample was collected and cell pellets were resuspended with 20% SDS and heated to 95°C for 15 minutes. Samples were subsequently analysed by SDS-PAGE and western analysis. Anti-His antibody was used to detect His-tagged proteins. 'TEV' denotes constructs in the pET11a vector and 'UB' denotes constructs in the pHUE vector. Numbering followed by '-C' denotes the number of amino acids that was truncated from the C-terminus of the protein. **(A, C, E)** Coomassie-stained SDS-PAGE **(B & D)** Whole cell lysate western analysis using anti-His antibody. Arrows show the expected size of the constructs: TEV WT (CO) (64.8 kDa), TEV (-N22) (CO) (62.91 kDa), TEV (-N37) (CO) (61.28 kDa), TEV (-C2) (CO) (64.5 kDa), Ub WT (CO) (74 kDa), Ub (-N22) (CO) (71.87 kDa), Ub (-N37) (CO) (70.24 kDa), and Ub (-C2) (CO) (73.6 kDa).

Protein expression of human LNK in mammalian cells

As expression of various human LNK constructs in *E. coli* were found to all give very low expression levels, protein expression of hLNK was tested in a mammalian system. The hLNK gene (with an N-terminal FLAG-tag) was cloned into an adenovirus vector (pAD/CMV/V5) whereby hLNK is under the control CMV promoter to give constitutive high expression [504]. This plasmid was used to make adenovirus type 5 by transfecting HEK293 cells and the resulting adenovirus was harvested from these cells and was used to infect HeLa cells for two days. Analysis of proteins from virus infected HeLa cells compared to uninfected HeLa cells by Coomassie stained SDS-PAGE showed a significant induction of protein expression at the expected size of LNK (Figure 68 A). This band was confirmed to be LNK by western analysis (Figure 68 B). One of the advantages of using the mammalian system to express a mammalian protein over the *E. coli* system for protein expression is that the proteins can attain their *in situ* modifications and correct folding due to the presence of chaperones [505-508]. However, the negatives to mammalian expression systems include that they are typically costlier and commonly difficult to obtain high levels of expression in mammalian cells compared to using bacterial protein production systems.

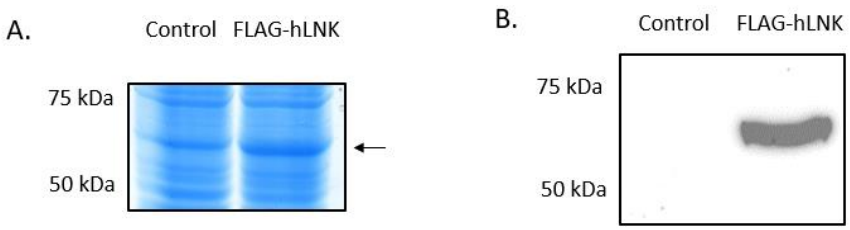

Figure 68: Adenovirus expression of FLAG-hLNK protein in HeLa cells.

HeLa cells (8×10^6 cells) were infected with adenovirus carrying the FLAG-hLNK gene and harvested 2 days after infection. **(A)** Coomassie stained SDS-PAGE of whole cell lysate. Arrow shows expected size of of FLAG-hLNK WT (64 kDa); **(B)** Whole cell lysate western analysis using anti-FLAG antibody.

Purification of FLAG-tagged human LNK by affinity chromatography

A protein expression and purification workflow using a mammalian system was developed to express and purify human LNK (Figure 69). After confirming the expression of the LNK protein, a small-scale purification using FLAG resin (anti-DYKDDDDK monoclonal antibodies coupled to agarose matrix resin) was performed. This small-scale purification was initially performed using an immunoprecipitation-based method to determine whether the expressed FLAG-tagged LNK can bind the FLAG resin effectively.

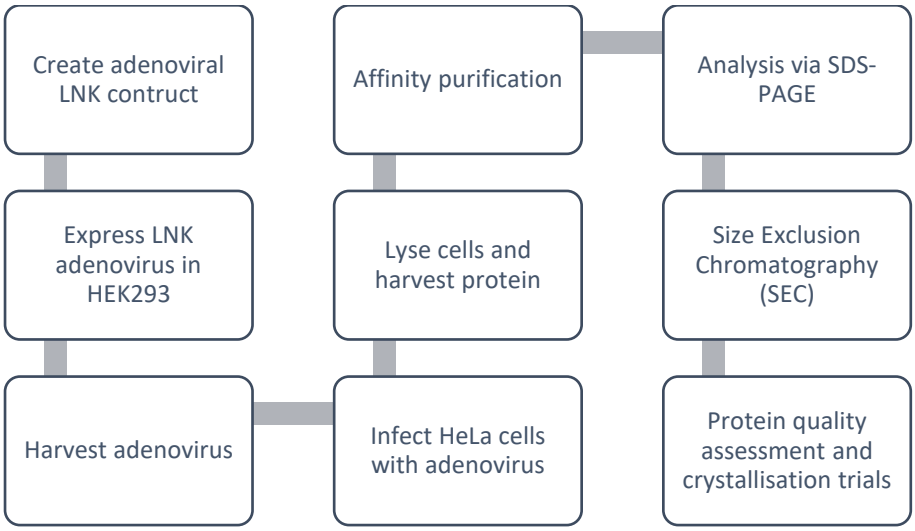

Figure 69: Workflow of LNK protein expression and purification.

Protein purification via immunoprecipitation showed that LNK was able to be purified to a high level (Figure 70). Two non-specific bands of smaller molecular weight than LNK were also observed on SDS-PAGE for proteins specifically bound to the anti-FLAG resin (Figure 70 A). The same size non-specific bands were also observed in the control sample (Figure 70 A). It was speculated that the lowest band (~50 kDa) is likely from the denatured heavy chain of the antibody that was released from the resin when the slurry was mixed with SDS sample buffer containing DTT prior to SDS-PAGE. This was expected to occur when eluting protein via this method. The other significant non-specific band was possibly a non-specific protein produced by HeLa cells that has some affinity to the monoclonal antibody on the resin. Increasing the number and stringency of washes could potentially reduce or eliminate binding of this non-specific protein from the FLAG resin. Size exclusion and/or ion exchange chromatography may also help in removing the non-specific protein. Degradation of LNK also appeared minimal, which should allow for efficient protein purification.

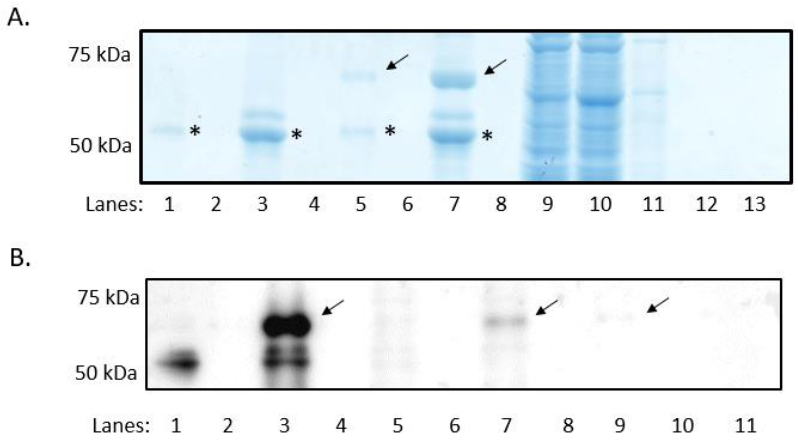

Figure 70: Purification of FLAG-hLNK protein using an immunoprecipitation-based method.

(A) Coomassie stained SDS-PAGE; **(B)** Western analysis. HeLa cells (8×10^6 cells) were infected with FLAG-hLNK adenovirus and harvested 2 days after infection. FLAG-hLNK was purified according to the manufacturer's protocol (GenScript). Whole cell lysate was added to the washed resin and mixed using a rotator for 2 hours at 4°C. The resin-sample was centrifuged at 6,000*g* for 30 seconds and washed thrice. Bound proteins were eluted using 6x SDS sample buffer (containing 0.1M DTT). Arrows show the expected size of FLAG-hLNK WT (64 kDa). **(A)** Lane 1 shows purification of control samples (total cell lysate from HeLa cells with no infection) (1 µl loaded on the gel); lane 3 shows purification of control samples (15 µl loaded on the gel); lane 5 shows purification of FLAG-hLNK samples (total cell lysate from HeLa cells infected with FLAG-hLNK adenovirus) (1 µl loaded on the gel); lane 7 shows purification of FLAG-hLNK samples (15 µl loaded on the gel); lane 9 shows the flow-through from control samples; lane 10 shows FLAG-hLNK flow-through; lane 11 shows first wash of FLAG-hLNK samples after flow-through; lane 12 shows second wash of FLAG-hLNK samples after flow-through; lane 13 shows third wash of FLAG-hLNK samples after flow-through. **(B)** Lane 1 shows purification of control samples; lane 3 shows purification of FLAG-hLNK samples; lane 5 shows the flow-through from control samples; lane 7 shows FLAG-hLNK flow-through; lane 9 shows first wash of FLAG-hLNK samples after flow-through; lane 10 shows second wash of FLAG-hLNK samples after flow-through; lane 11 shows third wash of FLAG-hLNK samples after flow-through. Denatured heavy chain of antibody is marked by asterisks (*).

Subsequent protein purification was performed using column chromatography in order to improve resin washes. A caveat of using the immunoprecipitation method is that non-specific proteins are more difficult to be removed due to lack of a continuous washing. Using the column method will also help in removing precipitated proteins. For this column chromatography, concentrated FLAG peptide was used for elution to competitively elute the FLAG tagged LNK in order to achieve high

purification efficiency rather than other methods such as alkaline buffer, acidic buffer, neutral elution buffer (~pH 7), elution with SDS and DTT buffer). However, the initial small scale test did not reveal LNK detection by Coomassie stained SDS-PAGE (Figure 71 A), although western analysis showed the presence of the FLAG-hLNK protein in the eluate (Figure 71 B) and also in the flow-through and washes (Figure 71 B). This suggested that there may be insufficient time for the protein to bind to the resin using this column method. More LNK protein was observed in the first elution (without incubation with resin) than in the elution after 60 minutes incubation with resin (Figure 71 B). This result suggests that the FLAG peptide was efficient in eluting the FLAG-tagged protein in such a short time. As a much higher volume of elution buffer was used compared to the initial purification test with elution using SDS sample buffer with DTT, this likely contributed to the undetectable protein band in Coomassie due to the purified protein being too dilute.

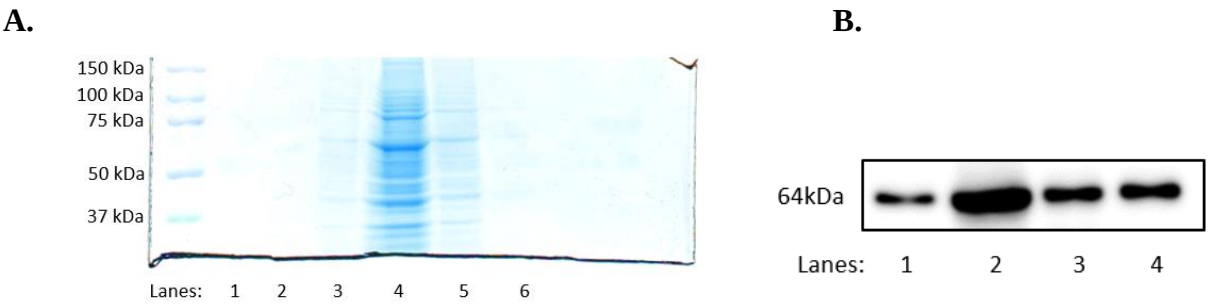

Figure 71: Small scale test of FLAG-hLNK protein purification by affinity column chromatography.

(A) Coomassie stained SDS-PAGE; **(B)** Western analysis. HeLa cells (8×10^6 cells) were infected with FLAG-hLNK adenovirus and harvested 2 days after infection. FLAG-hLNK was purified according to the manufacturer's protocol. Regenerated FLAG resin was first added to the column. Samples were then loaded and the column was washed several times. 500 µg/ml of the FLAG peptide elution buffer was then added into the column (competitive elution) and the eluate was immediately collected together with the second wash step (first elution). Another 500 µg/ml of the FLAG peptide elution buffer was added into the column and left to incubate for an hour at room temperature. After incubation, the eluate was collected (second elution). **(A)** Lane 1 shows second elution of FLAG-hLNK samples (8 µl loaded on the gel); lane 2 shows second elution of FLAG-hLNK samples (30 µl loaded on the gel); lane 4 shows FLAG-hLNK flow-through; lane 5 shows first wash of FLAG-hLNK samples after flow-through; lane 6 shows second wash of FLAG-hLNK samples after flow-through and first elution. **(B)** Lane 1 shows second elution of FLAG-hLNK samples; lane 2 showsFLAG-hLNK flow-through; lane 3 shows first wash of FLAG-hLNK samples after flow-through; lane 4 shows second wash of FLAG-hLNK samples after flow-through and first elution.

In order to enhance protein purification efficiency, a combination of batch binding and column purification was tested. The batch binding method was utilised for protein capture by the resin to allow the FLAG tagged LNK to have a longer contact time with the resin (2 hours at 4°C on a tube rotator). The lower temperature used may also increase binding efficiency. After the binding step, the bound resin was then loaded into the column and washes were performed in the column. FLAG peptides were then used to elute the bound protein, however purified LNK was still not able to be detected on Coomassie stained SDS-PAGE (Figure 72 A). Following this purification procedure, some of the beads were subsequently denatured in SDS sample buffer (containing DTT) to determine if LNK had been successfully eluted or if a large amount of the protein was still bound to the resin. A very weak band was visible by Coomassie stained SDS-PAGE at the molecular weight for LNK (Figure 72 A), however this result was not unexpected as this elution method is much harsher than using the FLAG peptide with a much more concentrated amount of protein run on the gel. In this purification test, non-regenerated resin was used. Therefore, some of FLAG peptide used for previous elution may still have been bound to the resin resulting in reduced capture of FLAG-tagged LNK.

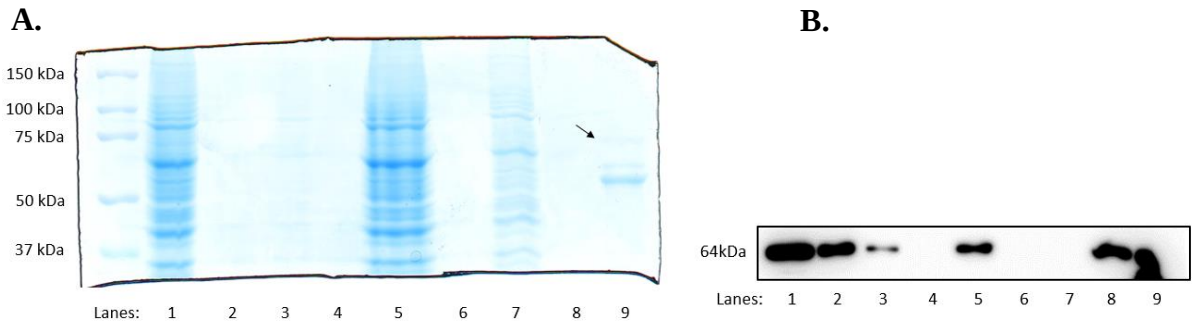

Figure 72: Small-scale batch binding and column affinity chromatography of FLAG-hLNK protein.

(A) Coomassie stained SDS-PAGE; **(B)** Western analysis. HeLa cells (8×10^6 cells) were infected with FLAG-hLNK adenovirus and harvested 2 days after infection. FLAG-hLNK was purified according to the manufacturer's protocol. Samples were added to the washed non-regenerated resin and mixed using a rotator for 2 hours at 4°C. The resin-sample were then loaded into the column and the column was washed several times. One column volume of 500 µg/ml FLAG peptide elution buffer was added into the column and left to incubate for an hour at room temperature. After incubation, the eluate was collected (first elution). Another 500 µg/ml of the FLAG peptide elution buffer was added into the column and the eluate collected immediately (second elution). **(A)** Lane 1 shows whole cell lysate; lane 2 shows first elution of FLAG-hLNK samples (4 µl loaded on the gel); lane 3 shows first

elution of FLAG-hLNK samples (30 µl loaded on the gel); lane 4 shows second elution of FLAG-hLNK samples; lane 5 shows FLAG-hLNK flow-through; lane 7 shows first wash of FLAG-hLNK samples after flow-through; lane 8 shows second wash of FLAG-hLNK samples after flow-through; lane 9 shows elution using SDS sample buffer added to beads after the purification procedure. **(B)** Lane 1 shows whole cell lysate; lane 2 shows first elution of FLAG-hLNK samples; lane 3 shows second elution of FLAG-hLNK samples; lane 5 shows first wash of FLAG-hLNK samples after flow-through; lane 6 shows second wash of FLAG-hLNK samples after flow-through; lane 7 shows third wash of FLAG-hLNK samples after flow-through; lane 8 shows FLAG-hLNK sample flow-through; lane 9 shows elution using SDS sample buffer added to beads after the purification procedure.

Larger scale protein purification methods of LNK focused on using batch binding (with regenerated resin) followed by column chromatography. This method was able to successfully purify LNK (data not shown). Furthermore, after several optimisations of the purification method and by performing large-scale protein expression, high protein yield and purity of LNK was achieved (Figure 73). The fraction eluted purified LNK were subsequently subjected to SEC for further purification and to determine how the FLAG-hLNK protein behaves in an aqueous environment.

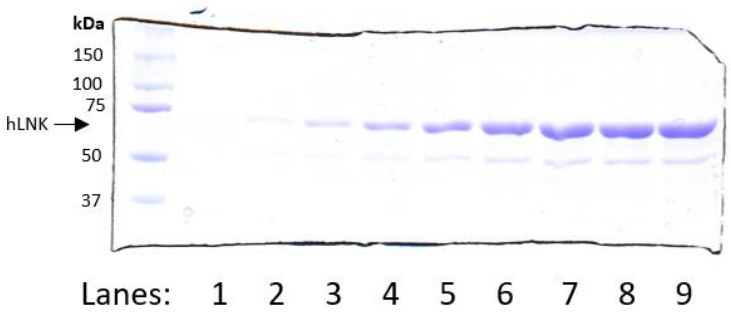

Figure 73: Purification of FLAG-hLNK protein using batch binding followed by large-scale column chromatography.

Twenty 175 cm^2 cell culture flasks of HeLa cells (8×10^6 cells/flask) were infected with FLAG-hLNK adenovirus and harvested 2 days after infection. FLAG-hLNK protein was purified according to the manufacturer's protocol. Samples were added to the washed regenerated resin and mixed using a rotator for 2 hours at 4°C. The resin-samples were then loaded unto the column and the column was washed several times. One column volume of 500 µg/ml of the FLAG peptide elution buffer was added into the column and one column volume of eluate was collected (first elution).The FLAG peptides were left to incubate for 30 minutes at room temperature. After incubation, another column volume of eluate was collected (second elution). For each elution, ten fractions of 500 µl/ fraction

were collected. Coomassie stained SDS-PAGE above shows first (lanes 1-7) and second elution fractions (lanes 8 & 9).

Size-exclusion chromatography (SEC) of purified human LNK

The scale of protein expression was increased in order to obtain more protein for downstream purification and crystallisation trials of LNK. Although purity of LNK via affinity chromatography was shown to be at a high level, the protein was subjected to further purification with SEC using Superdex 200 increase 10/ 300 GL column in conjunction with the ÄKTApurifier (GE Healthcare Life Sciences)) to remove any remaining impurities and FLAG peptide from the elution. The SEC was also performed to determine how the protein behaves in the aqueous environment. However, protein dilution will occur due to diffusion as it goes through the column although subsequent protein concentration can be performed by collecting elution peaks. Through SEC, we will be able to distinguish between soluble protein aggregates and their different oligomeric forms. By using a calibration plot with protein standards of known molecular weights against elution fraction volume (Figure 74), an estimation of the purified protein size can be determined and the degree of oligomerisation and aggregation can be identified. In addition, the purified protein can be separated from FLAG peptides, contaminating proteins of different sizes, and protein aggregates.

A.

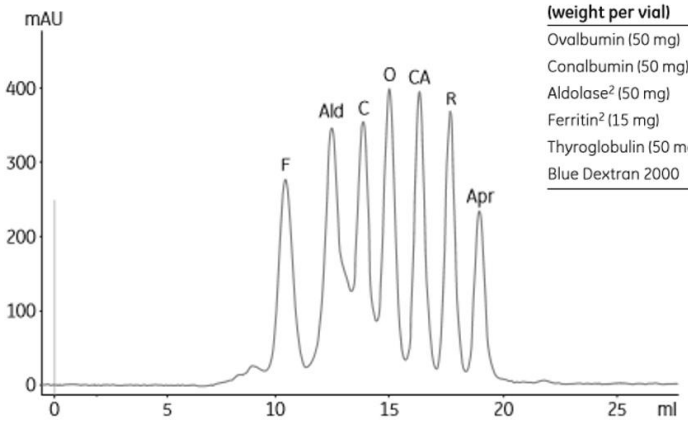

Protein (weight per vial)	Molecular weight (M_r)
Ovalbumin (50 mg)	44 000
Conalbumin (50 mg)	75 000
Aldolase[2] (50 mg)	158 000
Ferritin[2] (15 mg)	440 000
Thyroglobulin (50 mg)	669 000
Blue Dextran 2000	

B.

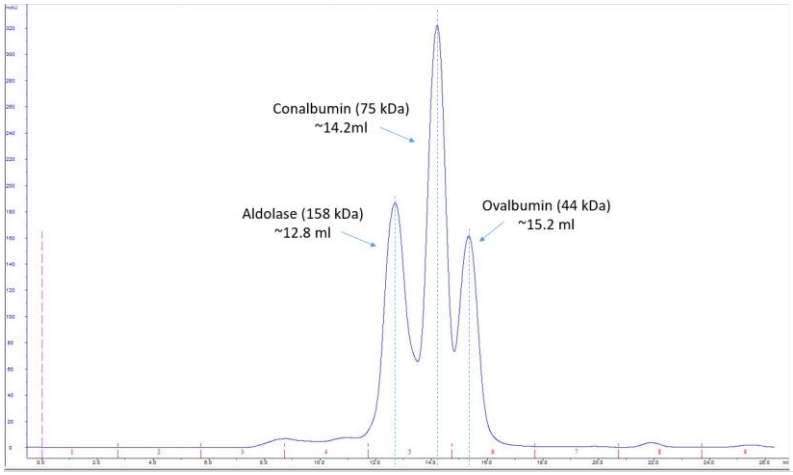

Figure 74: SEC calibration curve for protein standards.

Two different chromatograms are shown, a) based on product manual (Gel Filtration Calibration product manual (GE Healthcare)) and b) based on standard proteins in our buffer of interest. Calibration curve chromatogram is plotted using absorbance (mAU) against the elution volume (ml).

Prior to analysing the purified protein using SEC, the fractions from affinity chromatography that contained higher amounts of LNK protein (based on SDS-PAGE) were pooled and concentrated using Amicon® Ultra-15 Centrifugal Filter Units (Merck Millipore). However, protein precipitation was observed upon concentration. As contaminants remaining in the FLAG peptide eluted fractions may contribute to precipitation of the purified LNK, protein concentration prior to SEC was not performed in subsequent purifications. SEC was conducted in Tris buffer pH 8.6 (50 mM Tris, 500 mM NaCl, 15% glycerol, 1 mM TCEP) with a flow rate of 0.3 ml/min. Desired fractions were collected and analysed on SDS-PAGE. These fractions were confirmed to contain LNK by western analysis (Figure 75 A and B). LNK was also observed to exist as several oligomeric states including monomers, dimers, and oligomers based on the chromatogram (Figure 75 A). These fractions were confirmed to

be the different oligomeric states via native-PAGE western analysis (Figure 75 C) and confirmed to be LNK via SDS-PAGE and western analysis showing a single band of the expected size. The protein amount in peak 3 may be too low to be detected by western analysis or this peak may have represented a contaminating protein (Figure 75 B). Based on the calibration curve (Figure 74 B), we would expect monomeric LNK to be eluted at ~14.2 ml, dimers to be eluted at ~13 ml, and larger oligomeric forms to be eluted at a later elution.

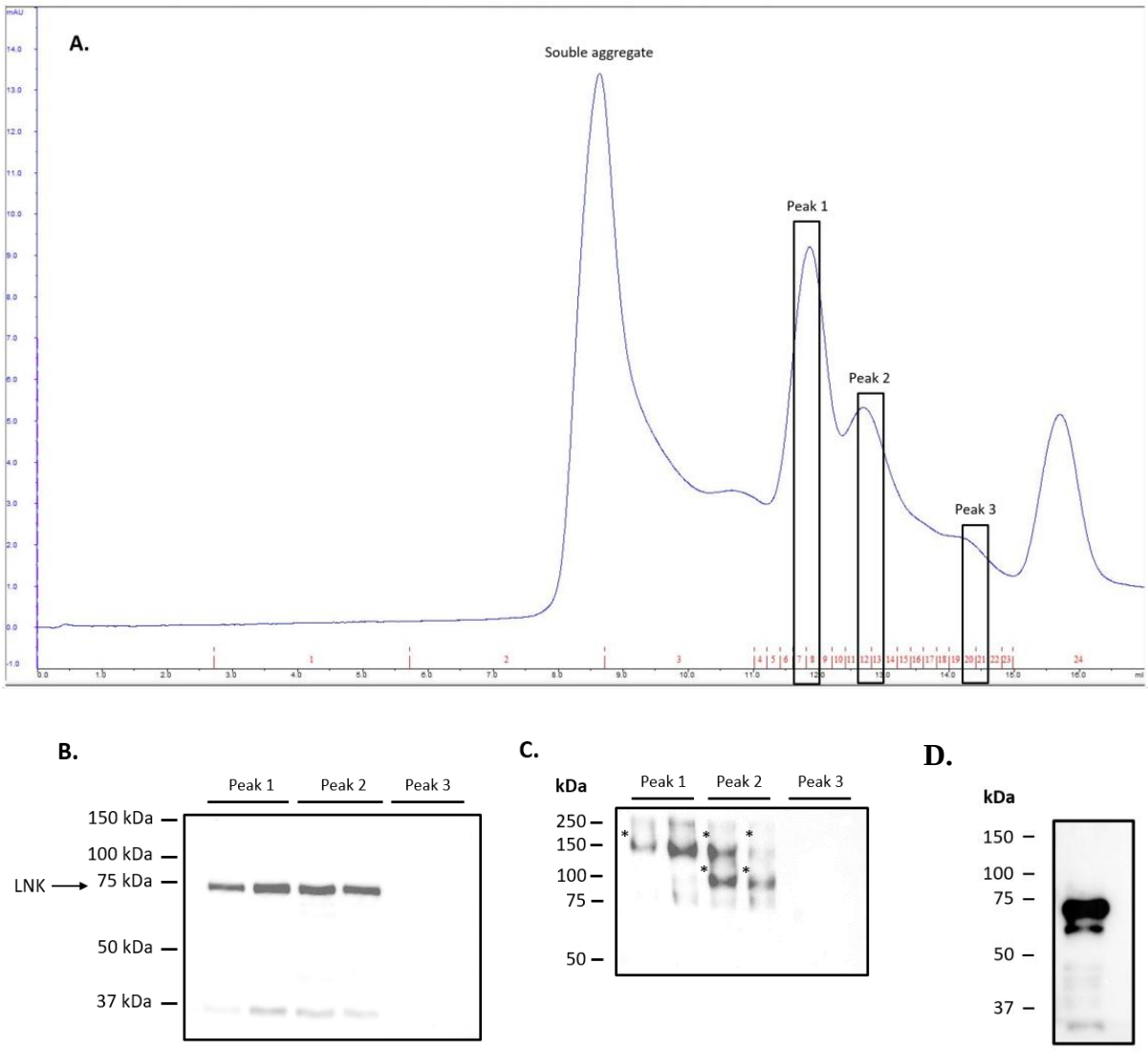

Figure 75: Purified LNK exists as different oligomeric states;

A) SEC chromatogram, B) Western analysis SDS-PAGE of peaks, C) Western analysis native-PAGE of peaks. Peak 1 is the size of oligomer (~11.8 ml), peak 2 is the size of dimer (~12.8 ml), peak 3 is the size of monomer (~14.3 ml). Soluble aggregates elute in the void volume. D) Western analysis SDS-PAGE of soluble aggregates from a separate experiment.

Although soluble LNK protein was observed in different oligomeric states via SEC, the amount of protein was insufficient for further analysis and a significant portion of protein eluted in the void volume indicating they are existing as soluble aggregates (Figure 75 A and D). Adaptation of HeLa cells to suspension culture was attempted in order to increase the scale of cell culture and hence protein production, but this was unsuccessful. Larger scale protein expression using adherent HeLa cells was subsequently performed in order to obtain more protein for further characterisation. However, the increased amount of protein led to more protein aggregation after FLAG elution (data not shown). As protein precipitation was also an issue, a range of low to high pH was used to determine if the precipitated protein was able to be re-solubilised. Precipitates appeared to solubilise when resuspended in high pH buffers such as pH 11.16 and pH 12.21 and LNK was confirmed to be present in the solubilised portion (Figure 76). Although some proteins are still able to maintain proper folding at high pH, typically, protein unfolding can occur at approximately pH 10 [509]. However, in order to prevent disruption of protein structure and function due to very high pH and due to the sensitivity of the FLAG affinity column to extreme pH (due to the antibodies present on the resin), a lower pH of 8.6 was used for the elution of the protein. Furthermore, in order to reduce aggregation, it was important to choose a pH that is further away from the isoelectric point (pI) (either more acidic or basic) as this is typically more soluble for proteins [510-512]. For LNK, the predicted pI is ~pH 6.5 and its net charge at pH 7.4 is -7.27. Therefore, in pH 8.6, LNK protein is predicted to be soluble.

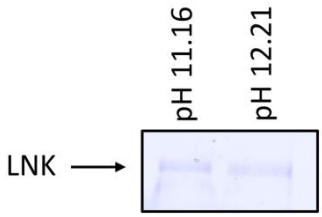

Figure 76: Precipitated LNK was able to be re-solubilised using high pH solution (pH 11.16 and 12.21) shown by Coomassie stained SDS-PAGE.

The buffer containing precipitated protein obtained after FLAG affinity purification was centrifuged at 12, 000g for 5 minutes. A range of low to high pH of TBS buffer (50 mM Tris, 500 mM NaCl, 15% glycerol) was used to solubilise each separate pellet. Solubilised protein were mixed with 3x SDS sample buffer (containing 0.1 M DTT) and heated to 98°C for 5 minutes before the samples were run on SDS-PAGE gel and Coomassie stain performed.

Besides using a higher pH in the FLAG elution buffer, the non-ionic detergent Triton X-100 was added to the wash and elution buffer to improve protein solubility and also to improve purity. Unfortunately, the presence of Triton X-100 poses several difficulties in purification, analysis, and crystallisation. Triton X-100 has a significant absorbance at 280nm which is used to monitor protein elution by SEC. This causes interference with the quantification, quality assessment, and is also known to impair the ability of proteins to crystallise [513-515] although there have been records of proteins that have been crystallised with Triton [516]. Triton X-100 also has a very low critical micelle concentration (CMC) of 0.02% and its micelle size can range from 85 to 150 kDa depending on the pH and molarity of the buffer that it is in [515]. The micelle size can also be affected by temperature [517]. The strong absorbance of Triton at this wavelength has resulted in Triton micelles Figure 37 masking the area where the protein presumably elutes [515]. Hence, it was difficult to determine if the protein of interest is indeed present based on the SEC chromatogram or if they are present, estimation of the protein concentration would not be accurate. However, running the elution fractions on SDS-PAGE may be informative regarding the presence of the protein of interest and estimation of protein concentration.

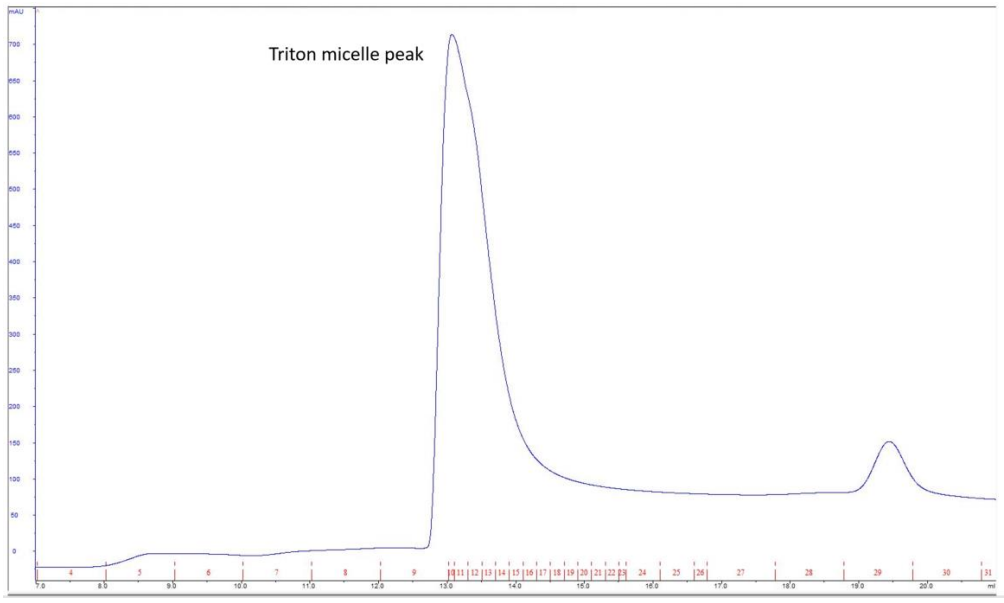

Figure 77: SEC of Triton X-100. UV trace showing Triton X-100 peak with high absorbance at 280 nm which would overlap with elution peaks for LNK.

Incubation of soluble aggregates with 1% Triton X-100 was found to resolve the aggregates into various soluble oligomeric states (Figure 78 A) at least in the case where these proteins were in an alkaline solution, sodium carbonate-bicarbonate buffer pH 9.7. This phenomenon was not observed

in acidic pH buffers such as sodium citrate buffer pH 5, however this may have been due to the amount of protein being too low to be detected by western analysis (Figure 78 B). As the SEC was equilibrated with buffer containing Triton X-100, the UV reading dropped to below 0 (negative values) as the Triton was diluted when the samples were put through the run (Figure 78). Nevertheless, some of the observed peaks were confirmed to be LNK through SDS-PAGE. Elution at ~10.8 ml (Figure 78 A, peak 1) appeared to be the size of an oligomer with six LNK subunits whereas elution at ~13 ml appeared to be the size of a LNK homodimer (Figure 78 A; peak 3). Peak 2 may be the Triton peak (Figure 78 A). As Triton X-100 micelle size is known to change with different buffers, temperature, and pH [515, 517], this can complicate the prediction of location of the protein peak.

A.

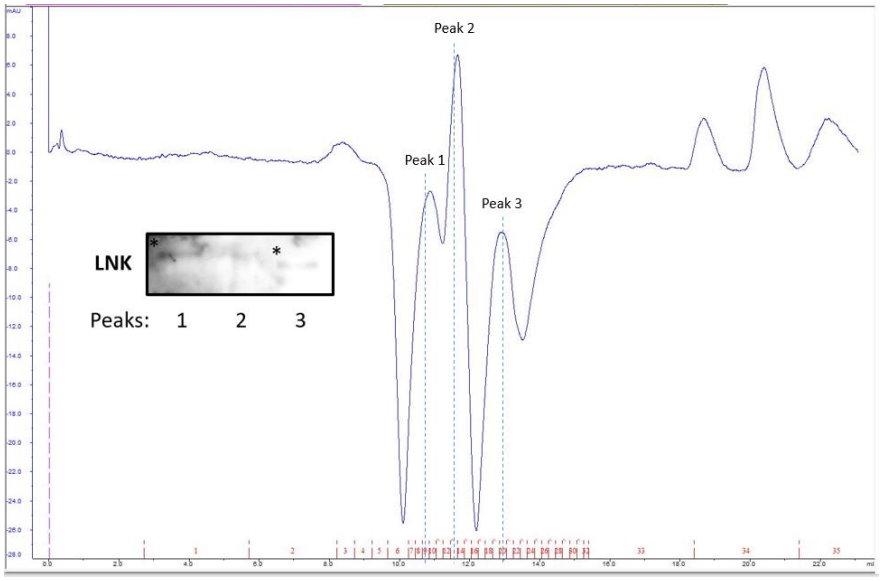

B.

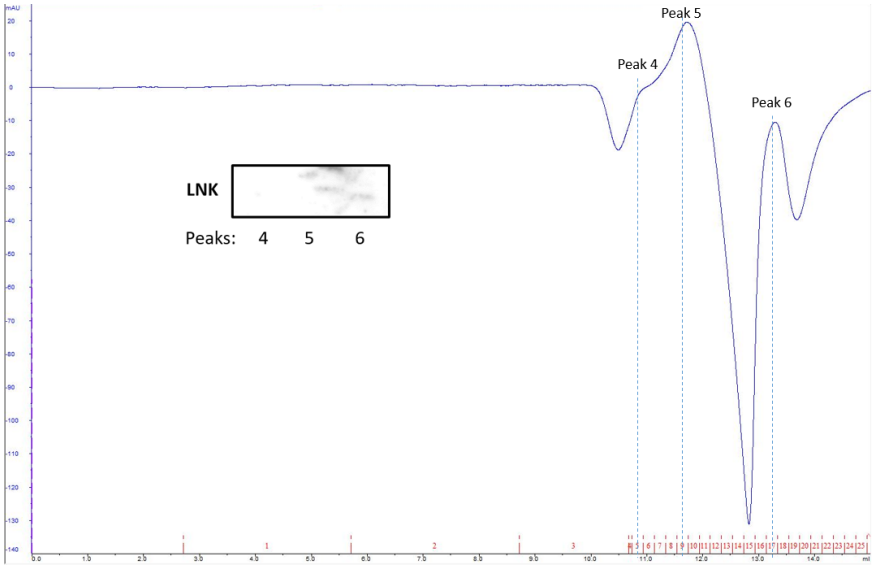

Figure 78: Addition of 1% Triton X-100 resolves soluble LNK aggregates into various oligomeric states in alkaline buffer conditions.

A) SEC UV trace of LNK protein aggregates in sodium carbonate-bicarbonate buffer pH 9.7. B) SEC UV trace of LNK protein aggregates in sodium citrate buffer pH 5. Protein aggregates were incubated with Triton-X100 (final concentration of 1%) in either sodium carbonate-bicarbonate buffer pH 9.7 or sodium citrate buffer pH 5 and allowed to incubate on ice for 30 minutes before subjecting to SEC. Peaks 1 and 3 (marked by asterisks) were confirmed by western analysis to be LNK. LNK monomer is expected to be ~64 kDa.

Protein quality assessments and crystallisation trials of human LNK

Purified full length human LNK expressed in HeLa cells and purified by FLAG affinity chromatography followed by SEC in the presence of Triton X-100, was assessed for indications of a structured protein and the ability to form protein crystals. This work was performed at Bio21 Molecular Science & Biotechnology Institute (University of Melbourne) in collaboration with the group led by Professor Michael Parker, by Dr Steffi Cheung Tung Shing. Quality assessments such as dynamic light scattering (DLS) [518-522], differential scanning fluorimetry (DSF) [523-531], and circular dichroism (CD) spectroscopy assays [532-536] were performed. DLS provides an indication of the size and size distributions of molecules and particles whereas DSF monitors protein unfolding events and hence determines the thermal stability of proteins. One of the applications of DSF is to identify a stable buffer for the target protein. CD assays can be used to determine if the protein of interest contains secondary structure i.e. whether the protein is folded.

DLS analysis of purified LNK indicated a homogeneous population (a positive sign for protein crystallisation) with a hydrodynamic diameter of ~10-20 Angstrom [537] (Figure 79 A). Aggregates usually have a larger hydrodynamic diameter. However, there was no clear indication whether the protein was properly folded or unfolded through DSF and CD spectroscopy assays due to interference from the presence of Triton (Figure 79 B and C). Despite this, crystallisation trials were initiated with 3 crystallisation screening trays for which crystals were formed after about 1 month of seeding (Figure 80). Unfortunately, despite the growth of the crystals, these did not show suitable diffraction when analysed at the Australian synchrotron research facility. Therefore, no information regarding the structure of LNK was able to be determine. Further optimisation was not possible due to insufficient protein.

A.

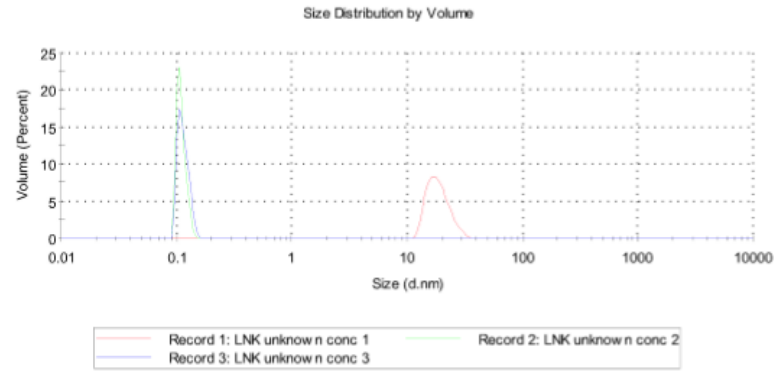

B.

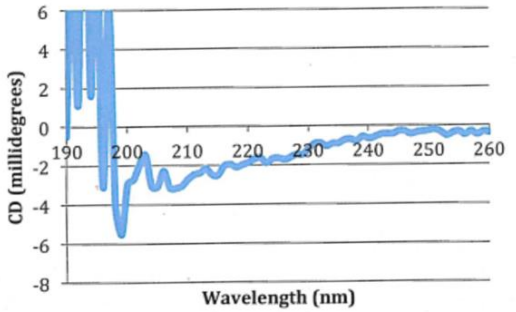

C.

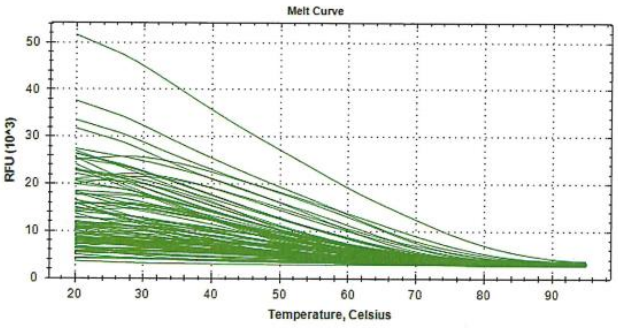

Figure 79: LNK protein quality assessment;

a) DLS, b) CD, and c) DSF. DLS indicated a homogeneous population. DSF and CD spectroscopy assay results were uninformative due to noise from Triton.

Figure 80: Example of one of the LNK protein crystals that were formed during crystallisation trials.

Optimisation trials to increase soluble fractions of LNK protein

In order to proceed with potential crystallisation studies, different conditions were tested to attempt to achieve a higher yield of soluble fractions of LNK. Due to difficulties posed with the incorporation of Triton X-100 into LNK buffers, Triton X-100 was removed from the wash used in the last half of the protocol, and from the elution buffer used for FLAG affinity chromatography. However, the absence of detergent appeared to result in severe protein aggregation as indicated on the SEC chromatogram (data not shown).

Octyl glucoside (OG) was chosen as an alternative detergent as it has a higher CMC than Triton X-100 (therefore, usage of higher concentration of detergent is made possible without the formation of micelles) and micelles are smaller in size (~25kDa) compared to LNK. Furthermore, OG has a very weak absorbance at 280nm unlike Triton X-100. Therefore, the use of OG should not affect interpretation of the SEC chromatogram and allow for more accurate estimate of the protein concentration. In addition, OG can also be removed by dialysis. The incorporation of a peptide (F^{809}TPD(phosphoY)ELLTEND^{820}) corresponding to the sequence of JAK2 comprising the phosphorylated tyrosine (pTyr 813) which is known to bind LNK [278] was employed in the purification method in an attempt to help stabilise the structure of the LNK protein [500, 538-541]. This phosphor-peptide was used at an estimated molar ratio of 3:1 (peptide to protein). Protease inhibitors were also incorporated into several steps of subsequent protein purification as rapid degradation of affinity purified LNK was apparent within a few days even at 4ºC. However, analysis of purified protein showed that the use of OG, incorporation of JAK2 phosphopeptide, and addition

of protease inhibitors into different steps of purification did not significantly improve the soluble fraction of LNK (data not shown).

Since purification using Triton X-100 appeared promising due to the previous indication of formation of LNK protein crystals, further optimistation of protein purification with Triton X-100 was tested. In order to prevent the presence of Triton X-100 to cause problems in protein quality assessment and crystallisation studies, a gradual removal of Triton X-100 after affinity purification using the Amicon® Ultra-15 Centrifugal Filter Units (Merck Millipore) was performed. However, during this process, a significant amount of protein was lost and running the remaining LNK protein through SEC further diluted the protein and no further informative results based on the SEC chromatogram could be determined (data not shown). The use low pH elution was also investigated as using buffers with pH more than one unit below or above the pI of LNK (pI 6.4) is thought to change the charge on the protein surface and increase solubility [510-512]. However, the soluble protein fractions did not significantly improve following this elution method at low pH (data not shown).

After several attempts of not being able to obtain a significant yield of soluble protein, affinity purified LNK fractions were investigated for optimal buffers (containing no Triton X-100) for protein solubility (performed by Dr Steffi Cheung Tung Shing, Bio21). However, DLS indicated that LNK was heterogeneous, with aggregates (data not shown). Also, there was no clear unfolding event using DSF which may suggest that the protein is unfolded and aggregated (data not shown). As LNK may be stabilised by binding to its partner, JAK2, combining these two proteins after expression and before carrying out affinity purification may be beneficial. This can also allow for LNK/JAK2 co-crystallisation. Alternatively, co-expression of the JAK2 JH2-JH1 domains with LNK in HeLa cells followed by affinity purification was performed. Unfortunately this attempt appeared to show very low binding of LNK to the FLAG affinity column. However, this may simply have been due to the frequent regeneration of the resin and loss of anti-FLAG antibody that is able to capture the FLAG-tagged LNK (Figure 81 A). Coomassie stained SDS-PAGE showed two bands where band 1 correlates to the expected size of LNK whereas band 2 may just be degraded LNK protein (Figure 81 A). Furthermore, the JAK2 JH2-JH1 domain did not appear to bind to LNK under the conditions used for the affinity chromatography (Figure 81 B). Due to time constraint, further optimisation of the protein expression and purification was not possible.

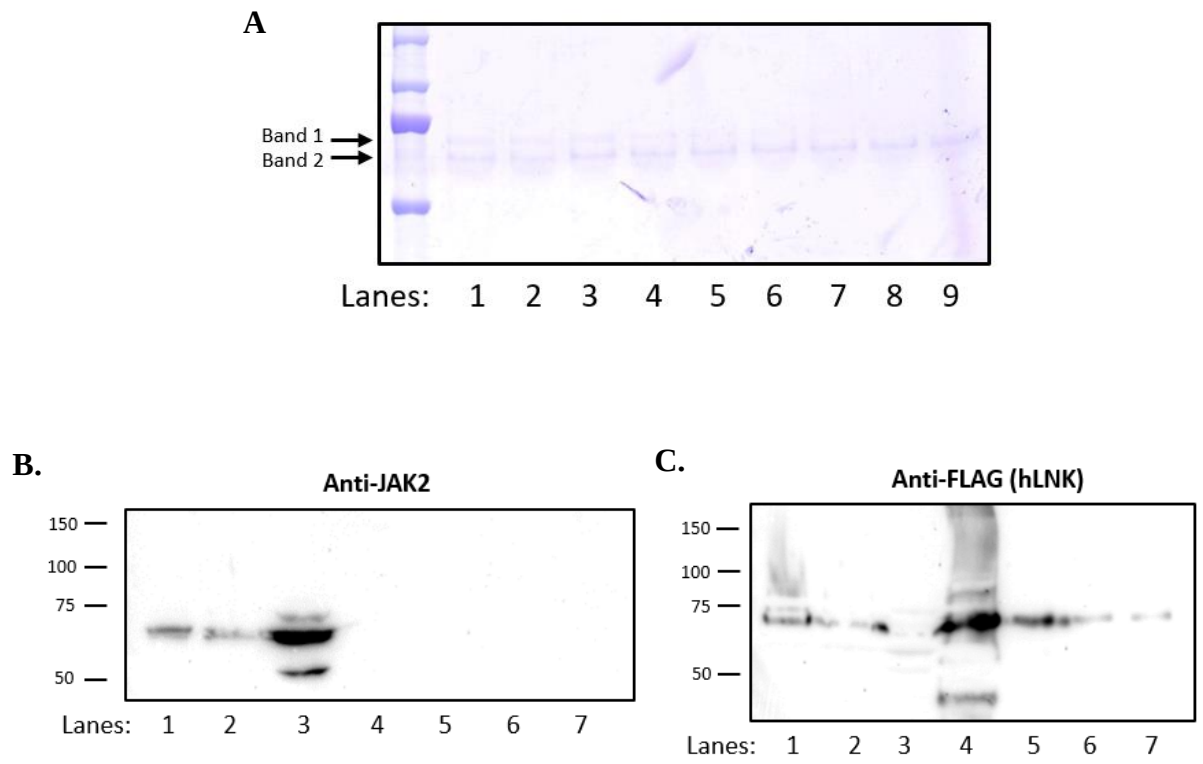

Figure 81: Reduced efficiency of FLAG resin binding to LNK protein and the inability of the co-expressed JAK2 to bind to LNK.

Twenty flasks of HeLa cells (8 x 10^6 cells/flask) were infected with FLAG-hLNK adenovirus and incubated for 4-5 hours before infecting with JAK2 JH2-JH1 adenovirus. Cells were harvested 2 days after infection. FLAG-hLNK was purified according to the manufacturer's protocol. Samples were added to the washed resin and mixed using a rotator for 2 hours at 4ºC. The resin-sample were then loaded into the column and the column was washed several times. One column volume of 500 µg/ml of the FLAG peptide elution buffer was added into the column and one column volume of eluate was collected (first elution).The FLAG peptides were incubated for 30 minutes at room temperature. After incubation, another column volume of eluate was collected (second elution). For each elution, 10 fractions of 500 µl/ fraction were collected. A) Coomassie gel shows first elution fractions (band 1: hLNK, band 2: degraded LNK). Western analysis (B & C) shows lane 1: cell lysate after lysis; lane 2: flowthrough of affinity chromatography; lane 3: cell pellet after cell lysis; lane 4: FLAG resin after column washes; lane 5: fraction 1 of first elution; lane 6: fraction 2 of first elution; lane 7: fraction 3 of first elution. Expected size of FLAG-hLNK is 64 kDa and for JAK2 JH2-JH1 is 71 kDa. Anti-JAK2 antibody was used to detect JAK2 JH2-JH1 whereas anti-FLAG was used to detect FLAG-hLNK protein.

Discussion

Currently, the crystal structure of LNK has not been solved and this is one of the main reasons that has contributed to the lack of understanding of LNK as a negative regulator of receptor signalling. To fill this gap, protein expression and purification of LNK was performed. Limited protein yield as well as solubility of the protein were the main issues, demonstrating that this was a challenging goal.

Initially, the *E. coli* expression system was used for expression of the human LNK protein. However, a suitable protein expression level was unable to be achieved even when *E. coli* codon optimisation of the LNK gene was used as it did not significantly enhance protein expression for reasons that could not be determined. Therefore, a mammalian system using adenovirus infection of the gene was attempted. The rational for using adenovirus infection is that it is more cost efficient compared to large transient transfections, it represents an efficient gene delivery system, amplification of adenoviruses is straightforward, and it provides higher protein expression compared to stable cell lines. For adenovirus infection, multiple copies of gene can be introduced into the cell for multiplicity of infection (MOI) that is greater than one whereas stable cell lines can develop promoter silencing. However, utilising adherent cell culture for protein expression was a limiting factor to the yield of protein that was able to be obtained as it was impractical to harvest very large amounts of adherent cells. Due to this limitation, alternatives for cell culture were surveyed. This included using adherent cells that have been adapted for suspension culture for high yield protein expression. However, commercially available transformed suspension cells such as Chinese Hamster Ovary (CHO) and HEK293 cells were not suitable for the adenoviral expression system although these cells are commonly used for high level protein expression. The use of adenovirus to infect HEK293 cells will generate more virus and result in a cytopathic effect that deemed this cell line unsuitable for the purpose adenoviral-mediated protein expression. Parental CHO cells on the other hand have low susceptibility for infection with adenoviruses type 5 [542]. These commercially available adapted suspension cells are also expensive and require special media which significantly adds to the cost of protein production. Hence, HeLa cells were chosen for protein expression although the infection of mammalian HeLa cells with adenovirus is not a common method for protein expression and purification. HeLa cells were used as they have efficient cell proliferation that is able to express foreign genes to a high level and are suitable and permissive for adenovirus type 5 infection. Therefore, this cell line was attempted to be adapted for suspension culture. Adaptation to suspension culture was performed by gradual serum depletion in the cell culture media and culturing the cells in flasks with gentle motion. Initially, HeLa cells were successfully adapted to culturing in 1% FBS instead of 10% FBS. Some changes in the morphology of the cells were observed where cells looked

almost spherical but still clumping to each other (data not shown). However, these cells did not survive for long. It was speculated that the short amount of time given for adaptation may have caused the death of the cells. Nevertheless, this effort was discontinued as this adaptation procedure was not time efficient and it was uncertain if there will be any significant change in the biology of the cells that might affect protein production. Therefore, adherent HeLa cells were used for the purpose of this study.

Significant problems were faced with purified LNK forming insoluble as well as soluble aggregates which subsequently reduced the yield of soluble protein for further analysis. Various methods were employed in an attempt to improve protein aggregation which included using different detergents (OG and Triton X-100), pH buffers, and salt concentrations. Rapid degradation of affinity purified LNK was also identified as a significant issue, therefore protease inhibitors were added into each step before affinity purification and SEC was subsequently performed in a short timeframe after affinity purification. A JAK2 phosphopeptide was also used in different stages of the LNK purification in order to help with low protein expression, protein stability, and improve the likelihood of crystallisation. This JAK2 phosphopeptide has been successfully used in small angle X-ray scattering (SAXS) assay to solve the structure of recombinant purified SOCS3 SH2 domain in complex with the gp130 phosphopeptide [538]. However, all efforts of the various optimisation methods that were performed did not significantly improve purified LNK solubility.

The most successful purification of LNK was with the incorporation of the detergent, Triton X-100. As LNK contains a PH domain that binds to the cell membrane containing phosphoinositides [278, 285], this domain is suspected to have a hydrophobic surface and therefore non-ionic detergents such as Triton X-100 and OG may help in preventing the protein from sticking together and forming aggregates (thereby improving solubility). A secondary structure prediction of LNK using Phyre2 predicted that this protein may be highly disordered (69% disordered) (Figure 82 B). A surface charge potential analysis also found that LNK is only moderately charged at the surface at pH 6.4 (Figure 82 A). These properties of LNK may explain why LNK requires a detergent such as Triton X-100 to remain soluble and reduce the formation of large protein aggregates. The ability of Triton X-100 to resolve the soluble aggregates into soluble oligomeric states also supports the notion that Triton X-100 does help to prevent or disrupt LNK protein aggregation. Other mechanisms to enhance protein solubility besides using detergent is to include solubility tags, deleting hydrophobic regions of the protein, and expressing only the important domains of the protein e.g. the Pro/DD. However, it was shown that the dimerisation domain from the related protein, APS by itself was found to produce some higher-order aggregates [306]. Some other alternatives may include optimisation of co-expression with JAK2, using high-throughput scans to identify suitable buffer conditions for the

protein [543-545], and using a phosphoinositide reagent such as inositolhexakisphosphate (InsP6) to mimic lipid membrane for PH domain binding. As LNK contains a PH domain that may assist in co-localisation and engage in binding to the lipid membrane of the cells, the InsP6 which is a phosphoinositide head-group mimic [546] can therefore be used to mimic the phosphoinositides present in the lipid membrane which may aid in the solubility of the LNK protein. Previously, a crystal structure of the C2 domain of class II PI3K-C2α has been solved with InsP6 [546]. Furthermore, antibody fragments (Fab, scFv, VHH, and Fv) can be added to proteins to help stability and solubility, as well as greatly enhancing protein crystallisation by expanding the hydrophilic surface area [547], and structure solving [548-551]. To improve protein yield, utilising another expression system such as the insect expression system may be beneficial [494] or alternatively using large scale bioreactors for mammalian cell culture [552].

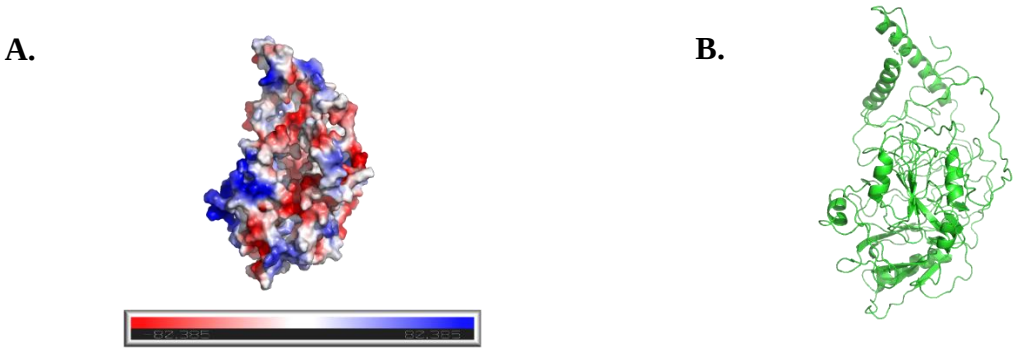

Figure 82: Secondary structure prediction of LNK using PHYRE2.

A) Electrostatic surface potential map. LNK is moderately charged at the surface. The surface potential is designated in red (−82.385) or blue (+82.385) (red for negative-charge, white for neutral, blue for positive-charge). B) Secondary structure prediction. LNK is predicted to be highly disordered (69% disordered) with limited structured regions containing α-helices and β-sheets. PHYRE2 analysis was performed by Dr Steffi Cheung Tung Shing.

Various detergents have been used for the purification and crystallisation of membrane proteins. This includes three different groups of conventional detergents: ionic, zwitterion, and non-ionic. Non-ionic detergents such as Triton X-100 and OG (alkyl glucopyranosides) were used in this study as they are non-denaturing (only disrupts lipid-lipid or lipid-protein interactions whilst maintaining protein-protein interactions) although their short alkyl chain can potentially cause protein denaturation due to the lack of hydrophobicity. Other commonly used non-ionic detergents include the n-dodecyl-β-D-maltopyranoside (DDM) (alkyl maltopyranosides) and n-decyl-β-D-maltopyranoside (DM) (alkyl

maltopyranosides), as well as the zwitterion n-lauryl dimethylamine n-oxide (LDAO) (amine oxide). Triton X-100 has a very low CMC concentration (~0.2 mM) and a variable temperature- and pH-dependent micelle size of 60 – 90 kDa [515, 517]. The presence of the aromatic ring in Triton X-100 poses difficulties in protein quantitation due to its absorbance in the UV wavelength. Triton X-100 is also heterogenous and this characteristic can compromise the need for homogeneity and purity that is needed for protein crystallisation [553]. On the other hand, OG has a much higher CMC (~20mM) and produce smaller micelles (~25 kDa) [554]. DDM has a low CMC concentration (~0.17 mM [555]) similar to Triton X-100 which allows the use of less detergent for purification, however, detergent removal would pose difficulties. Furthermore, the DDM micelles are relatively large (~65–70 kDa [556, 557]). DM has a shorter alkyl hydrophobic chain than DDM and hence results in lower protein stability and smaller micelle size (~40 kDa [556]). The CMC of DM is also much higher than DDM (~1.8 mM [555]), therefore requiring more detergent for solubilisation. The zwitterionic LDAO detergent has been shown to produce well-diffracting protein crystals [558-560] probably due to its compact micelle size (~21.5 kDa) that allows enhanced packing within crystals [557]. Also, LDAO forms elongated rather than spherical micelles [561, 562]. Advanced detergents with improved characteristics for solubility, stabilisation, and crystallisation of proteins have also been used in other studies. These include detergents with a more rigid hydrophobic alkyl chain by various modifications [563], membrane-mimicking properties (such as maltoside-neopentyl glycols (MNGs) for the human agonist β2 adrenoreceptor complex [564], addition of short alkyl chains to improve hydrophobicity (such as glucose neo-pentyl glucoside [565], steroid-based facial amphiphiles to improve crystallisation [566], and anionic calix[4]arene-based detergents to improve protein stability [567]. However, as one protein behaves differently from the other, empirical determination of suitable detergents for purification and crystallisation is required.

As with most other proteins, LNK has a combination of structured and disordered regions. LNK however, is speculated to have a propensity towards being more disordered due to the prediction of a higher proportion of regions that lack structure. This lack of structure may allow LNK to possess exceptional flexibility and plasticity in its conformation. LNK binding to other proteins may help to bring about folding that leads to a more ordered structure. It has been found that another class of proteins, which are called intrinsically disordered proteins (IDPs), are able to adopt different structures according to their binding partners [568]. This may in part explain how the flexibility of LNK allows it to bind to different receptors and JAK2 to regulate their activity. However, due to the possible flexibility of LNK, it may be difficult to be structurally analysed using X-ray crystallography. In this case, analysis of structures using nuclear magnetic resonance (NMR) with the protein in solution would be more feasible [569-574]. Furthermore, it is predicted that the lack of

structure may explain why LNK seemed to be susceptible to proteolytic cleavage. LNK also appeared to have a propensity to form dimers and tetramers which may contribute to its stability rather than monomers. The formation of these homomer may suggest some protein structure being present. It was previously shown that APS forms a heterotetrameric complex with JAK2 (APS and JAK2 dimers in complex) via its dimerisation and SH2 domain [306]. Therefore, this family of SH2-containing adaptor proteins may preferably exist as dimers or oligomers in order to retain stability and perform their function. Discovery of buffer conditions that promote the formation of the more stable dimeric form of LNK may be optimal for crystallography and other structure-function related investigations. It has been suggested that one of the alternative options to reduce proteolytic cleavage of IDPs is to perform a heat inactivation step (by boiling the lysate) after cell lysis that is able to deactivate proteases. IDPs are able to be subjected to this step as they lack tertiary structures. However, caution is needed for proteins like LNK as subjecting it to heat may distort the structured region of the protein. In this case, CD assays can be used to monitor if the protein still retained its native conformation [535].

In the absence of human LNK protein crystals, the purified protein could be subjected to structure solving using SAXS and electron cryo-microscopy (cryoEM). SAXS has been used to gain structural information on a wide range of molecule sizes (few kilodaltons to gigadaltons) and is applicable for characterisation of structurally ordered or disordered proteins, although with low resolution compared to X-ray crystallography or NMR spectroscopy. Nevertheless, SAXS provide details that complements information obtained from X-ray crystallography. Through this technique, various information regarding the protein could be gained including its oligomeric state, three-dimensional conformation, domain flexibility, as well as complex formation [575, 576]. A previously published paper have structurally characterise the expressed and purified JAK2-JH2-JH1 via SAXS [538] and this can be extended to the human LNK protein. The use of CryoEM has been limited to larger proteins above ~50 kDa for better resolution. However, it has recently been used with proteins as small as ~64 kDa (which is approximately the size of LNK monomer) [577-579] with high resolution. Nevertheless, as the purified LNK protein seemed to adopt a higher order state of dimers and tetramers, this technique may be feasible [580-584] although heterogeneity of the sample might be an issue.

Furthermore, binding interactions can be performed using the purified protein. Information regarding the binding kinetics between LNK and JAK2-JH2-JH1 can provide details regarding how rapid this interaction occurs (binding and dissociation). Subsequently, this information can be extended to screen for competitive inhibitors of this interaction. This could potentially lead to the discovery of

LNK mimetics that decreases JAK activation. The binding kinetics assay can be performed through different platforms such as Biacore [585, 586], isothermal titration calorimetry (ITC) [587-589], and homogeneous time resolved fluorescence (HTRF) [590-592]. These purified proteins could also potentially be used in kinase assays. This assay is used to measure kinase activity and hence can be exploited to determine if full-length LNK or its domains is able to inhibit JAK2 kinase activity. LNK protein harbouring important mutations can be compared to WT (under the same expression and purification conditions) to characterise impaired binding to JAK2 and to confirm which domains/residues are important for this binding.

Conclusion

Overall, sufficient quantities of soluble human LNK fractions that could be used for further quality assessments and crystallisation trials were not obtained. Due to time restraint, further optimisation was not made possible. In spite of all the challenges, defining the structure of the full-length LNK is still something worth pursuing as it will elucidate important mechanisms of regulation of JAK-STAT signalling. Solving the structure of LNK will also allow us to better understand how the function of LNK is disrupted in mutations that may contribute to the different diseases. In the absence of LNK crystals, the purified protein could also be used for protein interaction studies with other purified protein partners such as JAK2 and receptor intracellular domains. Structure analysis by NMR and Cryo-EM could also be performed as well as analysis of kinase activity with purified JAK2 JH2-JH1 domains. This analysis of expression and purification of full length human LNK in this chapter will provide a framework for future studies to build upon the understanding of how this protein should be dealt with.

Chapter 7

Final Discussion and Future Directions

Final Discussion

TPOR is expressed predominantly in haematopoietic stem and progenitor cells, megakaryocytes, and thrombocytes. Together with its ligand, TPO, the receptor regulates haematopoietic stem cell survival and expansion, megakaryocyte differentiation, as well as platelet and megakaryocyte production. TPOR is a homodimeric class I cytokine receptor and is important to regulate cell growth, differentiation, and survival via various pathways such as the JAK-STAT, MAPK, and PI3K/Akt. Clinical activating mutations of TPOR have been reported where most mutations lie in the transmembrane domain and its juxtamembrane regions. The TMD is important to regulate receptor activation and hence plays a role in modulating signalling downstream. The most common gain-of-function TPOR mutations include the W515K/L that resides in the RWQFP amphipathic motif (that is important to maintain TPOR in its basal state) which is juxtamembrane to the C-terminus of the TMD [40, 43]. Oncogenic TPOR mutations have been reported to drive the pathogenesis of myeloid malignancies such as MPNs and to a lesser extent, AMKL. These mutations are found in ~5-10% of MF patients and 1–4% of ET patients [40, 43, 593]. Predominantly, these activating mutations are due to substitutions of the W515 residue such as W515K/L/A/R. The associated non-receptor tyrosine kinase, JAK2 is constitutively bound to TPOR and mediates downstream signalling. Activating JAK2 mutations are also found in MPNs and contribute largely to the pathogenesis of this disease. Predominantly, these are the V617F substitution present in more than 95% of PV patients and 60% in ET or MF patients [4-6, 594]. JAK2 exon 12 mutations have also been reported in 2-3% of PV patients [35, 36]. Tight regulation of signalling downstream via TPOR/JAK2 is therefore clearly important in these diseases. Various extrinsic regulators of TPOR signalling pathway include the SOCS, PTPs, PIASs, and LNK. In this project, the main focus was on LNK where its mechanism of negative regulation has not yet been fully understood, although its role as a negative regulator of haematopoiesis has been well documented. Dysregulation of TPOR, JAK2, and LNK due to various activating and inactivating mutations can lead to constitutive JAK-STAT signalling and cell proliferation. Treatment options that are currently available for MPN patients have significant non-specificity to the disease-causing mutation. In the case of JAK inhibitors, these specifically inhibits JAK signalling but is not specific to the mutation. These inhibitors also target JAK signalling in a range of important cells that would be activated by a range of different cytokines. Therefore, there is a need for the development of novel therapies for these patients such as antagonists targeting oncogenic TPOR or LNK mimetics (to target JAK2). In order for these targeted therapies to be developed, further insights regarding the relationship between pathogenic signalling and the

structure-function of TPOR and LNK needs to be gained. Various aims were set out to address this in the current investigation (Figure 83).

- To discover novel mutations and compare signalling strengths of TPOR TMD-JM mutations
- To identify potential peptide antagonists against TPOR
- To understand the spatiotemporal pattern of the TPOR JM-ICD W515K mutation in comparison to TPOR WT
- To elucidate the mechanism of LNK inhibition in TPOR-mediated signalling
- To express and purify full-length LNK WT

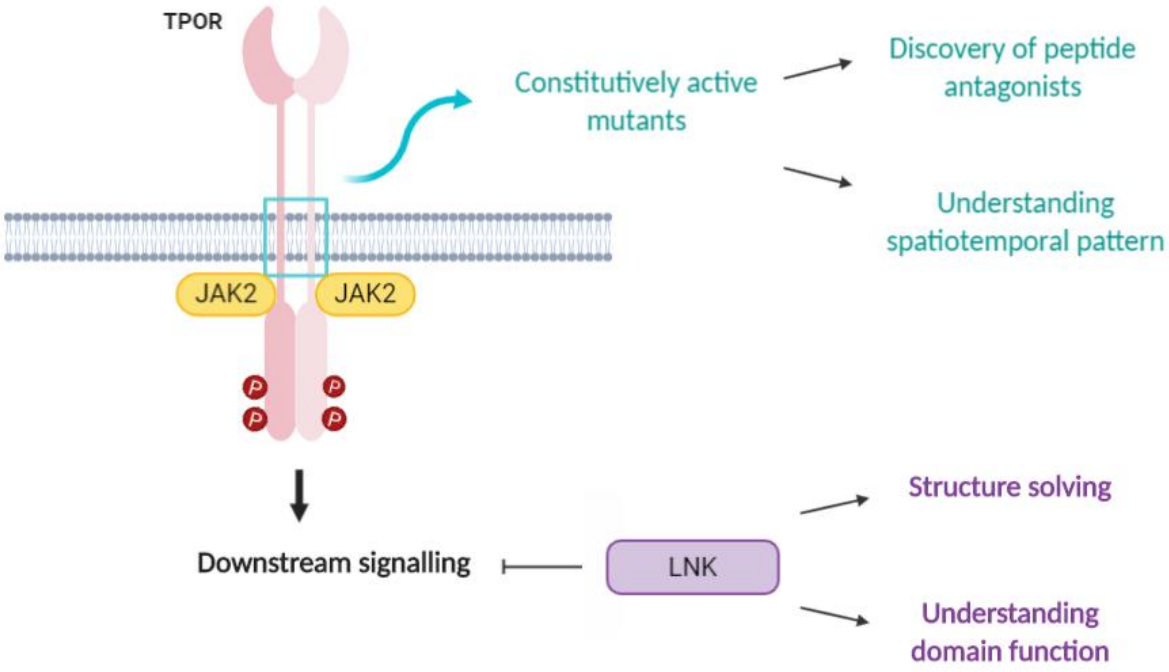

Figure 83: Diagrammatic representation of thesis aims. Figure made with BioRender.

The current investigation discovered that clinical and novel JM-TMD TPOR missense mutations confer different constitutive signalling strengths which may result in varying clinical phenotypes of MPNs. Using the clinically prevalent constitutively active W515K TPOR mutant or cytokine stimulation, sptPALM analysis showed that TPOR activation results in reduced receptor lateral diffusion that may play a role in regulating signalling. By targeting the important ECD-JM of TPOR, a peptide that antagonises TPOR-mediated signalling pathway was discovered via phage display. This peptide may act as a potential lead compound to antagonise this pathway. Investigation of the negative regulator of TPOR signalling, LNK, showed that inhibition of downstream signalling is regulated not just by the SH2 domain of LNK, but also by the proline-rich dimerisation domain. This domain was shown to be important for TPOR binding. Through the LNK protein expression and purification

analysis, it was found that LNK stability can be mediated by forming dimers or oligomers, which may be a result of the binding between the dimerisation domains.

Missense mutations are most commonly reported to have occurred in TPOR with mutations in the TMD domain frequently resulting in constitutive receptor activation. Particularly, mutations of the tryptophan residue of the RWQFP motif are frequently found. The current study investigated and compared the signalling strengths of clinical TPOR mutations that reside in the TMD and juxtamembrane regions. These clinical mutations such as W515K, T487A, and S505N have been reported to result in constitutive receptor activation which subsequently leads to constitutive downstream signalling. However, the results of the current study only partly agrees with the previous literature regarding the ability of the T487A mutant to cause constitutive activation [239]. Nevertheless, these mutations demonstrate a significant difference in their signalling capacity (cytokine-independent and dependent) which may contribute to the varying clinical phenotypes. The W515K mutation has been found in MPNs (ET and MF) and leukaemic transformation from MF, T487A has been found in one case of acute myeloid leukaemia (AML), whereas S505N has been reported in familial ET, MPNs (ET and MF), MDS, AML, as well as leukaemic transformation from ET [479]. These clinical observations also support the notion that the TMD and RWQFP motif plays a major role in keeping the receptor in its inactive state in the absence of ligand. The varying clinical phenotypes caused by the different mutations may be explained by the ability of TPOR TMD to adopt several orientations that confer its pleiotropic role in haematopoiesis [61], which when dysregulated due to mutations, can result in the different clinical phenotypes observed in patients. Furthermore, in a collaborative study (with the groups headed by Dr Melissa Call and Associate Professor Matthew Call, The Walter and Eliza Hall Institute), several novel mutations (L498W, V501A, V501S, and L502S) in the TMD that result in constitutive signalling of the JAK-STAT and MAPK pathway were identified by utilising the deep mutational scanning approach [394]. This collaborative work also showed that oncogenic TPOR mutations are dependent on the position and amino acid residues that are mutated [394]. By discovering novel TPOR mutations, this may aid in patient diagnosis and treatment strategies. Using a similar DMS approach, novel oncogenic mutations of other cytokine receptors, such as the IL7RA can also be discovered. Oncogenic mutations in IL7 receptor-α (IL7RA) have been reported in ALL that are caused by in-frame insertions or deletions in the TMD [391, 392], or insertion/substitution of a small number of amino acids introducing a cysteine residue in the ECD-JM [392, 393]. These cysteine residues allow the receptors to dimerise and confer constitutive receptor signalling even in the absence of its associated receptor subunit, the common γ-chain (γc), which usually forms a functional signalling complex. Similar mutations have also been identified in the related TSLPR [595, 596]. Another study showed that insertion of basic amino acids in the ECD-

JM, although does not result in constitutive activation, can induce cytokine hypersensitivity to IL-7 ligand in the presence of the γ-chain [597]. This mutation results in a leukaemic phenotype in mice [597]. On the other hand, TPOR mutations usually exist as missense substitutions with a lower prevalence for insertion/deletion mutations. Inframe insertion TPOR mutations in the TMD have been discovered in MPN patients whereas inframe deletion mutations in the TMD have been found in melanoma patients [479]. Interestingly, deletion frameshift mutations in W515 have been reported in MPNs [598, 599]. Analysis of inframe and deletion mutations in the TMD or JM regions of TPOR using the DMS screen may reveal a potentially new mechanism that is utilised by TPOR, similar to IL7RA. A deep mutational scanning screen of IL7RA would be beneficial to provide a better structural-functional analysis of the IL7RA TMD, but may not be clinically relevant due to the short insertions seen in clinically activating mutations. Therefore, developing a deep mutational scanning screen incorporating insertions would be important to provide greater understanding of the impact of insertions and residues in regulating IL7RA signalling.

The phage display screen to identify peptide antagonists against the important ECD/TMD region can be extended to screen for peptides against the similar region of other receptors such as IL7RA, TSLPR, and EPOR with mutations in a similar region to discover peptides that can bind to mutant receptors and not to WT ones. TSLPR mutations that are caused by chromosomal rearrangements are associated with B-ALL [595, 600, 601]. These translocations have been observed in ~60% of Down's Syndrome-ALL children and result in enhanced receptor expression [600-602]. Particularly, oncogenic mutation of residue F232 to cysteine results in receptor dimerisation and downstream signalling [595, 596]. Therefore, targeting TSLPR may be beneficial for treating ALL patients associated with mutations in this receptor. Mutations in EPOR due to chromosomal rearrangements result in the deletion of the distal part of the cytoplasmic tail which is important to bind negative regulators [603]. However, it retains important tyrosine residues C-terminal to the TMD which enable effective receptor signal transduction [603]. Hence, these EPOR mutations result in receptor stabilisation and hypersensitivity to cytokine stimulation [603]. In mouse models, these EPOR truncations have been reported to induce ALL [603]. Hence, phage display can be utilised to discover peptides that target EPOR to reduce signalling which may aid in suppressing disease burden. However, a strong inhibition of WT EPOR would be expected to result in anaemia.

Using sptPALM, comparison of the mobility of TPOR WT and W515K in the cell membrane showed that receptor activation results in reduced receptor mobility that may be linked to downstream signalling. The reason for this reduction has not yet been investigated but previous studies have shown that cholesterol contributes to the development of 'lipid rafts' that affect the mobility of membrane-

bound receptors and also downstream signalling. However, there are contradicting reports regarding the effect of cholesterol depletion on receptor mobility. Cholesterol depletion in the cell membrane resulted in reduced mobility of the thyrotropin-releasing hormone (TRH) receptor, which subsequently led to reduced cell signalling [424]. The human neurokinin-1 receptor (NK1R), a G-protein coupled receptor, also experienced reduced lateral diffusion after depletion of cholesterol with methyl-β-cyclodextrin leading to markedly reduced calcium signalling [410]. On the other hand, depletion of cholesterol has been reported to increase the mobility of GABA receptors at the extrasynaptic membrane [604] but the relationship to signalling was not investigated. An optimum amount of cholesterol is needed for the production of 'lipid rafts' in the cell membranes, for production of hormones, and cell metabolism. However, an increased amount of cholesterol can contribute to cardiovascular diseases and enhance cancer progression [605]. Statins have been used to reduce the total cholesterol level in patients with cardiovascular disease. It has been reported that cholesterol depletion in humans using statins improves cancer targeting and therefore may aid in cancer treatment [606-608]. This beneficial reduction in cholesterol levels may also be linked to the reduced formation of lipid rafts, with a subsequent reduction in receptor mobility and cell signalling, eventually preventing the progression of cancer. Furthermore, it has been reported that increased membrane cholesterol leads to increased TPOR signalling [609]. The role of lipid rafts in signalling has been shown to be contradictory depending on the type of receptor. In the case of the IL-2 receptor (IL-2R), in the basal state, the IL-2Rα is in a pre-formed complex with IL-2Rβ, and IL-2Rγ where IL-2Rα is localised to the periphery of lipid rafts whereas the IL-2Rβ and IL-2Rγ reside in the soluble membranes [610]. Upon activation, the IL-2Rα is able to bind more strongly to other signalling units of the complex and is dissociated from lipid rafts to initiate signal transduction [610]. In contrast, activation of the IL-7 receptor results in the formation of lipid rafts that allow the receptor to anchor to the cytoskeleton which subsequently stabilises the formation of a signalling complex [611].

Apart from receptor mobility, receptor clustering can also affect cell signalling. It was previously reported that ligand addition of SCF and TPO can induce receptor clustering of c-Kit and TPOR in lipid rafts [425]. It was speculated that this clustering involves both active and inactive receptors, which act in concert to enhance signalling [425]. Interestingly, this clustering is induced by opposite ligands i.e. SCF induced TPOR clustering whereas TPO induced c-Kit clustering [425] in lipid rafts. This clustering in HSCs enhances signalling downstream, particularly the PI3K–Akt–FOXO pathway and induces cell proliferation [425]. In contrary to the results of the current study, TPOR clustering has been observed even in the absence of the TPO ligand. Furthermore, cytokine stimulation did not change the cluster area or diameter. Unlike the utilisation of sptPALM for receptor cluster analysis as per current studies, previous work has used immunofluorescence for this investigation in

CD34+KSL cells [425]. Hence, the immunofluorescence technique is only able to detect major changes in clustering and accurate analysis on single clusters was not possible. For this reason, it is possible that the clustering that has been observed is a result of the concentration/ localisation of the clusters in a particular area of the cell instead. On the contrary, using sptPALM that tracks single molecules, allows minor clusters to be detected and this increases the accuracy in the analysis of clustering.

Apart from the SH2 domain, the current study found that the LNK Pro/DD domain possesses a novel function in downregulating signalling via the STAT and MAPK pathway. This domain was also shown to be important to maintain the interaction with TPOR. Based on the results of the current study, two models of interaction were proposed: i) the Pro/DD domain may be binding to TPOR whilst the SH2 binds JAK2, or ii) the Pro/DD domain mediates the formation of a functional LNK homodimer where each unit is capable of binding TPOR and JAK2 separately. As the Pro/DD domain contains the zipper region that is responsible for dimerisation, the latter proposed model may be more feasible. Furthermore, purification studies of LNK suggest that this protein preferably dimerises or oligomerises to stabilise the protein. This is consistent with the features of the dimerisation domain of APS which was found to produce higher-order aggregates and it can also form a heterotetrameric complex with JAK2 through its SH2 and dimerisation domain [291]. However, mutations in the Pro/DD are not as commonly found compared to SH2 domain point mutations and those found in patients have not yet been characterised, although the mutations were predicted to be pathogenic. It is plausible that mutations in the Pro/DD are not driver mutations and hence do not result in an obvious clinical phenotype (which may explain the rare occurrence of mutations in this domain) but they may contribute as co-operating mutations. Indeed, some studies have supported the occurrence of LNK mutations as co-operating mutations rather than driver mutations in MPNs [26, 344]. This study also revealed for the first time that LNK was able to constitutively associate with the archetypal GHR, although JAK2 did not increase the stability of this complex, unlike what happened for TPOR. These differences suggest that JAK2 helps to stabilise certain receptors and by doing so, allows LNK to exhibit its effects on different receptors, although there is no certainty whether LNK can inhibit or enhance GHR-mediated signalling.

The role of LNK serine phosphorylation has not been described in haematologic malignancies but has been described in ovarian cancer [300]. LNK possesses several serine phosphorylation sites where two serine residues have been reported to be able to be phosphorylated in humans, S103 and S150 (murine homologues are S13 and S129, respectively) [612]. The S13 murine homologue is phosphorylated by glycogen synthase kinase 3 whereas the phosphorylation of S129 is performed by protein kinase A. These phosphorylated residues act as binding sites for the 14-3-3 adaptor protein

[300, 612]. These phosphorylated serine residues are not known to interact with JAK2 in ovarian cancer cells [300]. LNK is overexpressed in ovarian cancers and its expression has been linked to an increase in the downstream signalling which promotes oncogenesis [300]. The binding of 14-3-3 was shown to negatively regulate the effects of LNK by downregulating downstream signalling [300]. However, LNK and 14-3-3 play a paradoxical role in haematopoietic cells. In these cells, 14-3-3 enhances JAK signalling by associating with LNK and preventing it from binding JAK2 to attenuate signalling [612]. In the LNK ProDD deletion mutant, four serine mutants are deleted, which includes the two serine residues that are known to play a role in binding 14-3-3. It was shown previously that mutation of these residues resulted in the localisation of LNK to the plasma membrane of HEK293T cells as the 14-3-3 was not able to sequester LNK in the cytoplasm [612]. This prevents LNK interaction with the receptor/JAK2 complex at the cell surface [612]. If this was true, LNK ΔProDD should localise to the cell surface which should result in decreased cell signalling as it can interact with the receptor/JAK2 complex. In the current study, however, an increase in cell signalling was observed with this mutant. This may be due to other important functions attributed to this domain. Immunofluorescence studies using LNK ΔProDD could reveal if its localisation to the membrane is enhanced compared to WT and this may provide further explanation regarding those differences in observation.

Although crystallisation trials of LNK were not successful, the ability to obtain high purity LNK could be beneficial for its use in other structure-function related analysis such as protein interaction studies, structure analysis, and kinase assays. The purified protein may be suitable for SAXS to investigate its oligomeric status and for structural analysis. Previous studies showed that the dimerisation domain of SH2B1 and APS can interact with each other [291]. Potential interaction sites of LNK in a complex could be determined and may complement results from the signalling and co-precipitation assays to allow for a deeper understanding regarding how it can regulate signalling. SAXS may also be performed using the Pro/DD domain and SH2 phosphopeptides of the site in TPOR that has shown potential binding to LNK in co-precipitation assays, to determine if there exist any functional interactions between them. Furthermore, the purified protein can be used to study the interaction between LNK and JAK3 which regulates IL7 receptor signalling. LNK can modulate IL-7 receptor signalling via binding to phosphorylated JAK3 [333]. Similarly, the binding kinetics between LNK and the phosphopeptide of JAK3 (pTyr785) or JAK2 (pTyr813) could be used to compare the binding and dissociation of LNK to different members of the JAK family, which may help in understanding binding affinities to different JAKs. Kinase assays could also be performed between LNK and JAK2/JAK3 to determine and compare the ability of LNK to inhibit JAK2 and JAK3 without the presence of its Pro/DD domain. Lastly, the current study used adenovirus infection

of HeLa cells for protein expression which has been shown to produce a protein with high yield and purity. This novel combination can be extended for protein expression of those proteins that may be difficult to express using a bacterial system or even yeast or insect cell expression systems.

Future Directions

It was found that ligand binding or constitutive receptor activation resulted in reduced cell membrane receptor mobility. However, it is not fully understood as to what has contributed to this reduction. This could be affected by lipid rafts, actin cytoskeleton, and receptor endocytosis. In order to fully understand this, the effect of cytoskeleton on the receptor can be investigated by using cytoskeleton-depolymerizing toxins such as Nocodazole (inhibits microtubule polymerisation) or cells can be treated with small interfering RNA (siRNA) against filamin A. Agents that cause cholesterol depletion such as methyl-β-cyclodextrin or cholesterol oxidase (COase) can be used to understand the role of cholesterol/lipid rafts in cell mobility. The role of endocytosis can be investigated by using siRNA to inhibit AP2. AP2 mediates the endocytosis of transmembrane proteins via clathrin, and the inhibition of this protein will aid in understanding if the reduction in receptor mobility is due to attenuation of signalling by internalisation. The effect of LNK on the stability of TPOR was shown in Chapter 4 and this can be extended to further studies on the ability of LNK to affect the mobility of the receptor. sptPALM using stable-transduction of LNK into HEK293 cells together with transient transfection of mEOS2-tagged TPOR can be performed to address this fact. Further on from sptPALM, step-bleaching of single molecules can also be performed to investigate the pre-dimerisation status of TPOR. This is important to further understand the mechanism of TPOR activation as a result of cytokine binding or oncogenic mutations.

In the early discovery of peptides that interact with TPOR using the 12-mer phage display library, three consensus peptide motifs were observed. However, only one peptide showed an effect, peptide V, on the proliferation of the cells. In order to discard the possibility that the other two peptides may have fallen out of solution and therefore, were not able to exhibit any effect on the cells, a precipitation condition test can be performed in order to determine if these peptides are indeed soluble and also if the observed effect is real.

The effect of peptide V should also be tested on Ba/F3 cell lines expressing other type I cytokine receptors such as PRLR and EPOR to ensure that the inhibitory effect that was observed is indeed TPOR specific. This peptide can also be further evaluated on its ability to inhibit downstream signalling to further understand which pathway has been affected and has resulted in inhibition of cell

proliferation. Besides the TPOR W515K mutant, peptide V can also be used to be tested on TPOR T487A and S505N cell lines to determine if this peptide is still able to dampen cell proliferation. If the peptide is not able to, these cell lines can be utilised to obtain specificity for the W515K mutant using T487A/S505N for negative selection. Once specificity in cell-based assays has been confirmed, the mode of interaction with the receptor can be determined. This could be performed using simulations utilising TPOR JM-TMD constructs. Further, the efficacy of the peptide may be improved by covalent linkage dimerisation or other modifications.

In the current study, the strong inhibitory effect of LNK on cell growth was observed on haematopoietic cells such as Ba/F3. Due to this inhibition of cell growth, it was difficult to further analyse the LNK mutant effect. An alternative to this, is to utilise an inducible system such as doxycycline-inducible gene expression where LNK can be expressed when desired. It will also be interesting to observe if LNK has any effects in the downstream pathway of GHR as there are currently no studies concerning this fact. It was observed in Chapter 4 that co-transfection of TPOR/GHR with LNK increased receptor expression. This effect of LNK needs to be confirmed in stable cell lines such as Ba/F3 expressing these receptors. It is, however, not certain that this is a transcriptional or a translational effect by LNK and this could be investigated by performing qPCR on RNA that is extracted from cells co-transfected with both TPOR/GHR and LNK. A further investigation could be performed to observe how TPOR levels change after LNK transfection via the cycloheximide chase assay. It will also be interesting to determine whether LNK mutants can inhibit constitutive downstream signalling of TPOR W515K and S505N or not.

Despite several optimisation trials to obtain soluble LNK protein, this task remains challenging. More optimisation methods are warranted especially the one that incorporates the use of the phosphoinositide reagent, InsP6, which may allow the membrane-binding domain of LNK, the PH domain, to bind and improve the overall protein solubility. In Chapter 5, LNK co-expression with JAK2 JH2-JH1 did not contribute to the protein solubility of LNK. However, it was also found that the JAK2 protein was not fully extracted out from the cell pellet and this contributed to the low amount of JAK2 in the solution. Furthermore, the lack of LNK binding to JAK2 suggests that the buffer conditions were not optimal for maintaining the interaction between these two proteins. These conditions need to be optimised and may hopefully improve LNK solubility. In order to further evaluate the interaction between LNK and JAK2, binding interaction studies between LNK and JAK2-JH2-JH1 can be performed. Lastly, kinase assays can be performed to compare the ability of LNK mutants to inhibit JAK2 kinase activity.

References

1. A. Rad, M.H. *Simplified hematopoiesis*. 2009 22 November 2019]; Available from: https://en.wikipedia.org/wiki/Haematopoiesis#/media/File:Hematopoiesis_simple.svg.
2. Arber, D.A., et al., *The 2016 revision to the World Health Organization classification of myeloid neoplasms and acute leukemia.* Blood, 2016. **127**(20): p. 2391-405.
3. Baxter, E.J., et al., *Acquired mutation of the tyrosine kinase JAK2 in human myeloproliferative disorders.* Lancet, 2005. **365**: p. 1054-1061.
4. James, C., et al., *A unique clonal JAK2 mutation leading to constitutive signalling causes polycythaemia vera.* Nature, 2005. **434**(7037): p. 1144-8.
5. Kralovics, R., et al., *A gain-of-function mutation of JAK2 in myeloproliferative disorders.* N Engl J Med, 2005. **352**: p. 1779-1790.
6. Levine, R.L., et al., *Activating mutation in the tyrosine kinase JAK2 in polycythemia vera, essential thrombocythemia, and myeloid metaplasia with myelofibrosis.* Cancer Cell, 2005. **7**: p. 387-397.
7. Zhao, R., et al., *Identification of an acquired JAK2 mutation in polycythemia vera.* J Biol Chem, 2005. **280**(24): p. 22788-92.
8. Kratz, C.P., et al., *Mutational screen reveals a novel JAK2 mutation, L611S, in a child with acute lymphoblastic leukemia.* Leukemia, 2006. **20**(2): p. 381-3.
9. Scott, L.M., et al., *JAK2 exon 12 mutations in polycythemia vera and idiopathic erythrocytosis.* N Engl J Med, 2007. **356**: p. 459-468.
10. Lee, J.W., et al., *The JAK2 V617F mutation in de novo acute myelogenous leukemias.* Oncogene, 2006. **25**(9): p. 1434-6.
11. Grunebach, F., et al., *Detection of a new JAK2 D620E mutation in addition to V617F in a patient with polycythemia vera.* Leukemia, 2006. **20**(12): p. 2210-1.
12. Schnittger, S., et al., *Report on two novel nucleotide exchanges in the JAK2 pseudokinase domain: D620E and E627E.* Leukemia, 2006. **20**(12): p. 2195-7.
13. Bercovich, D., et al., *Mutations of JAK2 in acute lymphoblastic leukaemias associated with Down's syndrome.* Lancet, 2008. **372**(9648): p. 1484-92.
14. Mullighan, C.G., et al., *JAK mutations in high-risk childhood acute lymphoblastic leukemia.* Proc Natl Acad Sci U S A, 2009. **106**(23): p. 9414-8.
15. Ma, W., et al., *Mutation profile of JAK2 transcripts in patients with chronic myeloproliferative neoplasias.* J Mol Diagn, 2009. **11**: p. 49-53.
16. Passamonti, F., et al., *Molecular and clinical features of the myeloproliferative neoplasm associated with JAK2 exon 12 mutations.* Blood, 2011. **117**: p. 2813-2816.
17. Ghoreschi, K., A. Laurence, and J.J. O'Shea, *Janus kinases in immune cell signaling.* Immunol Rev, 2009. **228**(1): p. 273-87.
18. Imai, M., M. Araki, and N. Komatsu, *Somatic mutations of calreticulin in myeloproliferative neoplasms.* Int J Hematol, 2017. **105**(6): p. 743-747.
19. Milosevic, J.D. and R. Kralovics, *Genetic and epigenetic alterations of myeloproliferative disorders.* Int J Hematol, 2013. **97**(2): p. 183-97.
20. Rampal, R. and R.L. Levine, *A primer on genomic and epigenomic alterations in the myeloproliferative neoplasms.* Best Pract Res Clin Haematol, 2014. **27**(2): p. 83-93.
21. Tenedini, E., et al., *Targeted cancer exome sequencing reveals recurrent mutations in myeloproliferative neoplasms.* Leukemia, 2014. **28**(5): p. 1052-9.
22. Grand, F.H., et al., *Frequent CBL mutations associated with 11q acquired uniparental disomy in myeloproliferative neoplasms.* Blood, 2009. **113**(24): p. 6182-92.
23. McMullin, M.F. and H. Cario, *LNK mutations and myeloproliferative disorders.* Am J Hematol, 2016. **91**(2): p. 248-51.
24. Pardanani, A., et al., *LNK mutation studies in blast-phase myeloproliferative neoplasms, and in chronic-phase disease with TET2, IDH, JAK2 or MPL mutations.* Leukemia, 2010. **24**(10): p. 1713-8.

25. Lasho, T.L., A. Pardanani, and A. Tefferi, *LNK mutations in JAK2 mutation-negative erythrocytosis.* N Engl J Med, 2010. **363**(12): p. 1189-90.
26. Oh, S.T., et al., *Novel mutations in the inhibitory adaptor protein LNK drive JAK-STAT signaling in patients with myeloproliferative neoplasms.* Blood, 2010. **116**(6): p. 988-92.
27. Sanada, M., et al., *Gain-of-function of mutated C-CBL tumour suppressor in myeloid neoplasms.* Nature, 2009. **460**(7257): p. 904-8.
28. Loh, M.L., et al., *Mutations in CBL occur frequently in juvenile myelomonocytic leukemia.* Blood, 2009. **114**(9): p. 1859-63.
29. Bellanne-Chantelot, C., et al., *Genetic and clinical implications of the Val617Phe JAK2 mutation in 72 families with myeloproliferative disorders.* Blood, 2006. **108**(1): p. 346-52.
30. Rumi, E., et al., *Familial chronic myeloproliferative disorders: clinical phenotype and evidence of disease anticipation.* J Clin Oncol, 2007. **25**(35): p. 5630-5.
31. Rumi, E., et al., *CALR exon 9 mutations are somatically acquired events in familial cases of essential thrombocythemia or primary myelofibrosis.* Blood, 2014. **123**(15): p. 2416-9.
32. Rumi, E., et al., *JAK2 (V617F) as an acquired somatic mutation and a secondary genetic event associated with disease progression in familial myeloproliferative disorders.* Cancer, 2006. **107**(9): p. 2206-11.
33. Godfrey, A.L. and A.R. Green, *Genotype-phenotype interactions in the myeloproliferative neoplasms.* Hematol Oncol Clin North Am, 2012. **26**(5): p. 993-1015.
34. Lupardus, P.J., et al., *Structure of the pseudokinase-kinase domains from protein kinase TYK2 reveals a mechanism for Janus kinase (JAK) autoinhibition.* Proc Natl Acad Sci U S A, 2014. **111**(22): p. 8025-30.
35. Scott, L.M., et al., *JAK2 exon 12 mutations in polycythemia vera and idiopathic erythrocytosis.* N Engl J Med, 2007. **356**(5): p. 459-68.
36. Pietra, D., et al., *Somatic mutations of JAK2 exon 12 in patients with JAK2 (V617F)-negative myeloproliferative disorders.* Blood, 2008. **111**(3): p. 1686-9.
37. Martinez-Aviles, L., et al., *JAK2 exon 12 mutations in polycythemia vera or idiopathic erythrocytosis.* Haematologica, 2007. **92**(12): p. 1717-8.
38. Li, J., et al., *JAK2V617F homozygosity drives a phenotypic switch in myeloproliferative neoplasms, but is insufficient to sustain disease.* Blood, 2014. **123**(20): p. 3139-51.
39. Yao, H., et al., *Activating JAK2 mutants reveal cytokine receptor coupling differences that impact outcomes in myeloproliferative neoplasm.* Leukemia, 2017. **31**(10): p. 2122-2131.
40. Pardanani, A.D., et al., *MPL515 mutations in myeloproliferative and other myeloid disorders: a study of 1182 patients.* Blood, 2006. **108**(10): p. 3472-6.
41. Beer, P.A., et al., *MPL mutations in myeloproliferative disorders: analysis of the PT-1 cohort.* Blood, 2008. **112**: p. 141-149.
42. Guglielmelli, P., et al., *Anaemia characterises patients with myelofibrosis harbouring Mpl mutation.* Br J Haematol, 2007. **137**(3): p. 244-7.
43. Pikman, Y., et al., *MPLW515L is a novel somatic activating mutation in myelofibrosis with myeloid metaplasia.* PLoS Med, 2006. **3**(7): p. e270.
44. Schnittger, S., et al., *Characterization of 35 new cases with four different MPLW515 mutations and essential thrombocytosis or primary myelofibrosis.* Haematologica, 2009. **94**(1): p. 141-4.
45. Moliterno, A.R., W.D. Hankins, and J.L. Spivak, *Impaired expression of the thrombopoietin receptor by platelets from patients with polycythemia vera.* N Engl J Med, 1998. **338**(9): p. 572-80.
46. Girardot, M., et al., *miR-28 is a thrombopoietin receptor targeting microRNA detected in a fraction of myeloproliferative neoplasm patient platelets.* Blood, 2010. **116**(3): p. 437-45.
47. Chachoua, I., et al., *Thrombopoietin receptor activation by myeloproliferative neoplasm associated calreticulin mutants.* Blood, 2016. **127**(10): p. 1325-35.
48. Balligand, T., et al., *Pathologic activation of thrombopoietin receptor and JAK2-STAT5 pathway by frameshift mutants of mouse calreticulin.* Leukemia, 2016. **30**(8): p. 1775-8.
49. Moliterno, A.R. and J.L. Spivak, *Posttranslational processing of the thrombopoietin receptor is impaired in polycythemia vera.* Blood, 1999. **94**(8): p. 2555-2561.

50. Tefferi, A., S.Y. Yoon, and C.Y. Li, *Immunohistochemical staining for megakaryocyte c-mpl may complement morphologic distinction between polycythemia vera and secondary erythrocytosis.* Blood, 2000. **96**(2): p. 771-2.
51. Ng, A.P., et al., *Mpl expression on megakaryocytes and platelets is dispensable for thrombopoiesis but essential to prevent myeloproliferation.* Proc Natl Acad Sci U S A, 2014. **111**(16): p. 5884-9.
52. Horikawa, Y., et al., *Markedly reduced expression of platelet c-mpl receptor in essential thrombocythemia.* Blood, 1997. **90**(10): p. 4031-8.
53. Harrison, C.N., et al., *Platelet c-mpl expression is dysregulated in patients with essential thrombocythaemia but this is not of diagnostic value.* Br J Haematol, 1999. **107**(1): p. 139-47.
54. McCaffrey, K. and I. Braakman, *Protein quality control at the endoplasmic reticulum.* Essays Biochem, 2016. **60**(2): p. 227-235.
55. Nangalia, J., et al., *Somatic CALR mutations in myeloproliferative neoplasms with nonmutated JAK2.* N Engl J Med, 2013. **369**(25): p. 2391-2405.
56. Marty, C., et al., *Calreticulin mutants in mice induce an MPL-dependent thrombocytosis with frequent progression to myelofibrosis.* Blood, 2016. **127**(10): p. 1317-24.
57. Elf, S., et al., *Mutant Calreticulin Requires Both Its Mutant C-terminus and the Thrombopoietin Receptor for Oncogenic Transformation.* Cancer Discov, 2016. **6**(4): p. 368-81.
58. Araki, M., et al., *Activation of the thrombopoietin receptor by mutant calreticulin in CALR-mutant myeloproliferative neoplasms.* Blood, 2016. **127**(10): p. 1307-16.
59. Han, L., et al., *Calreticulin-mutant proteins induce megakaryocytic signaling to transform hematopoietic cells and undergo accelerated degradation and Golgi-mediated secretion.* J Hematol Oncol, 2016. **9**(1): p. 45.
60. Rampal, R., et al., *Integrated genomic analysis illustrates the central role of JAK-STAT pathway activation in myeloproliferative neoplasm pathogenesis.* Blood, 2014. **123**(22): p. e123-33.
61. Staerk, J., et al., *Orientation-specific signalling by thrombopoietin receptor dimers.* EMBO J, 2011. **30**(21): p. 4398-413.
62. Bazan, J.F., *Haemopoietic receptors and helical cytokines.* Immunol Today, 1990. **11**(10): p. 350-4.
63. Cosman, D., *The hematopoietin receptor superfamily.* Cytokine, 1993. **5**(2): p. 95-106.
64. Bazan, J.F., *Structural design and molecular evolution of a cytokine receptor superfamily.* Proc Natl Acad Sci U S A, 1990. **87**(18): p. 6934-8.
65. Waters, M.J. and A.J. Brooks, *JAK2 activation by growth hormone and other cytokines.* Biochem J, 2015. **466**(1): p. 1-11.
66. Bravo, J. and J.K. Heath, *Receptor recognition by gp130 cytokines.* Embo j, 2000. **19**(11): p. 2399-411.
67. Boulay, J.L., J.J. O'Shea, and W.E. Paul, *Molecular phylogeny within type I cytokines and their cognate receptors.* Immunity, 2003. **19**(2): p. 159-63.
68. Bagley, C.J., et al., *The structural and functional basis of cytokine receptor activation: lessons from the common beta subunit of the granulocyte-macrophage colony-stimulating factor, interleukin-3 (IL-3), and IL-5 receptors.* Blood, 1997. **89**(5): p. 1471-82.
69. Yawata, H., et al., *Structure-function analysis of human IL-6 receptor: dissociation of amino acid residues required for IL-6-binding and for IL-6 signal transduction through gp130.* Embo j, 1993. **12**(4): p. 1705-12.
70. de Vos, A.M., M. Ultsch, and A.A. Kossiakoff, *Human growth hormone and extracellular domain of its receptor: crystal structure of the complex.* Science, 1992. **255**(5042): p. 306-12.
71. Livnah, O., et al., *Functional mimicry of a protein hormone by a peptide agonist: the EPO receptor complex at 2.8 A.* Science, 1996. **273**(5274): p. 464-71.
72. Chow, D., et al., *Structure of an extracellular gp130 cytokine receptor signaling complex.* Science, 2001. **291**(5511): p. 2150-5.
73. Boulanger, M.J., et al., *Hexameric structure and assembly of the interleukin-6/IL-6 alpha-receptor/gp130 complex.* Science, 2003. **300**(5628): p. 2101-4.
74. Rozwarski, D.A., et al., *Structural comparisons among the short-chain helical cytokines.* Structure, 1994. **2**(3): p. 159-73.
75. Murakami, M., et al., *Critical cytoplasmic region of the interleukin 6 signal transducer gp130 is conserved in the cytokine receptor family.* Proc Natl Acad Sci U S A, 1991. **88**(24): p. 11349-53.

76. Haan, C., et al., *Jaks and cytokine receptors--an intimate relationship.* Biochem Pharmacol, 2006. **72**(11): p. 1538-46.
77. Rodig, S.J., et al., *Disruption of the Jak1 gene demonstrates obligatory and nonredundant roles of the Jaks in cytokine-induced biologic responses.* Cell, 1998. **93**(3): p. 373-83.
78. Parganas, E., et al., *Jak2 is essential for signaling through a variety of cytokine receptors.* Cell, 1998. **93**(3): p. 385-95.
79. Kawamura, M., et al., *Molecular cloning of L-JAK, a Janus family protein-tyrosine kinase expressed in natural killer cells and activated leukocytes.* Proc Natl Acad Sci U S A, 1994. **91**(14): p. 6374-8.
80. Musso, T., et al., *Regulation of JAK3 expression in human monocytes: phosphorylation in response to interleukins 2, 4, and 7.* J Exp Med, 1995. **181**(4): p. 1425-31.
81. Kershaw, N.J., et al., *SOCS3 binds specific receptor-JAK complexes to control cytokine signaling by direct kinase inhibition.* Nat Struct Mol Biol, 2013. **20**(4): p. 469-76.
82. Boggon, T.J., et al., *Crystal structure of the Jak3 kinase domain in complex with a staurosporine analog.* Blood, 2005. **106**(3): p. 996-1002.
83. Chrencik, J.E., et al., *Structural and thermodynamic characterization of the TYK2 and JAK3 kinase domains in complex with CP-690550 and CMP-6.* J Mol Biol, 2010. **400**(3): p. 413-33.
84. Liau, N.P.D., et al., *The molecular basis of JAK/STAT inhibition by SOCS1.* Nat Commun, 2018. **9**(1): p. 1558.
85. Feng, J., et al. *Activation of Jak2 catalytic activity requires phosphorylation of Y1007 in the kinase activation loop*. Mol Cell Biol, 1997. **17**, 2497-501 DOI: 10.1128/MCB.17.5.2497.
86. Funakoshi-Tago, M., et al., *Jak2 FERM domain interaction with the erythropoietin receptor regulates Jak2 kinase activity.* Mol Cell Biol, 2008. **28**(5): p. 1792-801.
87. Yasukawa, H., et al., *The JAK-binding protein JAB inhibits Janus tyrosine kinase activity through binding in the activation loop.* Embo j, 1999. **18**(5): p. 1309-20.
88. Myers, M.P., et al., *TYK2 and JAK2 are substrates of protein-tyrosine phosphatase 1B.* J Biol Chem, 2001. **276**(51): p. 47771-4.
89. Toms, A.V., et al., *Structure of a pseudokinase-domain switch that controls oncogenic activation of Jak kinases.* Nat Struct Mol Biol, 2013. **20**(10): p. 1221-3.
90. Bandaranayake, R.M., et al., *Crystal structures of the JAK2 pseudokinase domain and the pathogenic mutant V617F.* Nat Struct Mol Biol, 2012. **19**(8): p. 754-9.
91. Silvennoinen, O., et al., *New insights into the structure and function of the pseudokinase domain in JAK2.* Biochem Soc Trans, 2013. **41**(4): p. 1002-7.
92. Ungureanu, D., et al., *The pseudokinase domain of JAK2 is a dual-specificity protein kinase that negatively regulates cytokine signaling.* Nat Struct Mol Biol, 2011. **18**(9): p. 971-6.
93. Argetsinger, L.S., et al., *Autophosphorylation of JAK2 on tyrosines 221 and 570 regulates its activity.* Mol Cell Biol, 2004. **24**(11): p. 4955-67.
94. Ishida-Takahashi, R., et al., *Phosphorylation of Jak2 on Ser(523) inhibits Jak2-dependent leptin receptor signaling.* Mol Cell Biol, 2006. **26**(11): p. 4063-73.
95. Feener, E.P., et al., *Tyrosine phosphorylation of Jak2 in the JH2 domain inhibits cytokine signaling.* Mol Cell Biol, 2004. **24**(11): p. 4968-78.
96. Mazurkiewicz-Munoz, A.M., et al., *Phosphorylation of JAK2 at serine 523: a negative regulator of JAK2 that is stimulated by growth hormone and epidermal growth factor.* Mol Cell Biol, 2006. **26**(11): p. 4052-62.
97. Wilks, A.F., et al., *Two novel protein-tyrosine kinases, each with a second phosphotransferase-related catalytic domain, define a new class of protein kinase.* Mol Cell Biol, 1991. **11**(4): p. 2057-65.
98. Girault, J.A., et al., *Janus kinases and focal adhesion kinases play in the 4.1 band: a superfamily of band 4.1 domains important for cell structure and signal transduction.* Mol Med, 1998. **4**(12): p. 751-69.
99. McNally, R., A.V. Toms, and M.J. Eck, *Crystal Structure of the FERM-SH2 Module of Human Jak2.* PLoS One, 2016. **11**(5): p. e0156218.
100. Wallweber, H.J., et al., *Structural basis of recognition of interferon-alpha receptor by tyrosine kinase 2.* Nat Struct Mol Biol, 2014. **21**(5): p. 443-8.

101. Ferrao, R., et al., *The Structural Basis for Class II Cytokine Receptor Recognition by JAK1.* Structure, 2016. **24**(6): p. 897-905.
102. Zhou, Y.J., et al., *Unexpected effects of FERM domain mutations on catalytic activity of Jak3: structural implication for Janus kinases.* Mol Cell, 2001. **8**(5): p. 959-69.
103. Haan, S., et al., *Dual role of the Jak1 FERM and kinase domains in cytokine receptor binding and in stimulation-dependent Jak activation.* J Immunol, 2008. **180**(2): p. 998-1007.
104. Higgins, D.G., J.D. Thompson, and T.J. Gibson, *Using CLUSTAL for multiple sequence alignments.* Methods Enzymol, 1996. **266**: p. 383-402.
105. Kampa, D. and J. Burnside, *Computational and functional analysis of the putative SH2 domain in Janus Kinases.* Biochem Biophys Res Commun, 2000. **278**(1): p. 175-82.
106. Radtke, S., et al., *The Jak1 SH2 domain does not fulfill a classical SH2 function in Jak/STAT signaling but plays a structural role for receptor interaction and up-regulation of receptor surface expression.* J Biol Chem, 2005. **280**(27): p. 25760-8.
107. Ferrao, R.D., H.J. Wallweber, and P.J. Lupardus, *Receptor-mediated dimerization of JAK2 FERM domains is required for JAK2 activation.* Elife, 2018. **7**.
108. Kuriyan, J. and D. Cowburn, *Modular peptide recognition domains in eukaryotic signaling.* Annu Rev Biophys Biomol Struct, 1997. **26**: p. 259-88.
109. Liu, B.A., et al., *SRC Homology 2 Domain Binding Sites in Insulin, IGF-1 and FGF receptor mediated signaling networks reveal an extensive potential interactome.* Cell Commun Signal, 2012. **10**(1): p. 27.
110. McNally, R. and M.J. Eck, *JAK-cytokine receptor recognition, unboxed.* Nat Struct Mol Biol, 2014. **21**(5): p. 431-3.
111. Constantinescu, S.N., et al., *The erythropoietin receptor cytosolic juxtamembrane domain contains an essential, precisely oriented, hydrophobic motif.* Mol Cell, 2001. **7**(2): p. 377-85.
112. Huang, L.J., S.N. Constantinescu, and H.F. Lodish, *The N-terminal domain of Janus kinase 2 is required for Golgi processing and cell surface expression of erythropoietin receptor.* Mol Cell, 2001. **8**(6): p. 1327-38.
113. Haan, C., P.C. Heinrich, and I. Behrmann, *Structural requirements of the interleukin-6 signal transducer gp130 for its interaction with Janus kinase 1: the receptor is crucial for kinase activation.* The Biochemical journal, 2002. **361**(Pt 1): p. 105-111.
114. Behrmann, I., et al., *Janus kinase (Jak) subcellular localization revisited: the exclusive membrane localization of endogenous Janus kinase 1 by cytokine receptor interaction uncovers the Jak.receptor complex to be equivalent to a receptor tyrosine kinase.* J Biol Chem, 2004. **279**(34): p. 35486-93.
115. Royer, Y., et al., *Janus kinases affect thrombopoietin receptor cell surface localization and stability.* J Biol Chem, 2005. **280**(29): p. 27251-61.
116. Rowlinson, S.W., et al., *An agonist-induced conformational change in the growth hormone receptor determines the choice of signalling pathway.* Nat Cell Biol, 2008. **10**(6): p. 740-7.
117. Neubauer, H., et al., *Jak2 deficiency defines an essential developmental checkpoint in definitive hematopoiesis.* Cell, 1998. **93**(3): p. 397-409.
118. Lu, X., L.J. Huang, and H.F. Lodish, *Dimerization by a cytokine receptor is necessary for constitutive activation of JAK2V617F.* J Biol Chem, 2008. **283**: p. 5258-5266.
119. Wernig, G., et al., *The Jak2V617F oncogene associated with myeloproliferative diseases requires a functional FERM domain for transformation and for expression of the Myc and Pim proto-oncogenes.* Blood, 2008. **111**(7): p. 3751-9.
120. Sangkhae, V., et al., *The thrombopoietin receptor, MPL, is critical for development of a JAK2V617F-induced myeloproliferative neoplasm.* Blood, 2014. **124**(26): p. 3956-63.
121. Li, Y., et al., *Proto-oncogene c-mpl is involved in spontaneous megakaryocytopoiesis in myeloproliferative disorders.* Br J Haematol, 1996. **92**(1): p. 60-6.
122. Pecquet, C., et al., *Thrombopoietin receptor down-modulation by JAK2 V617F: restoration of receptor levels by inhibitors of pathologic JAK2 signaling and of proteasomes.* Blood, 2012. **119**(20): p. 4625-35.
123. Braunstein, J., et al., *STATs dimerize in the absence of phosphorylation.* J Biol Chem, 2003. **278**(36): p. 34133-40.

124. Kretzschmar, A.K., et al., *Analysis of Stat3 (signal transducer and activator of transcription 3) dimerization by fluorescence resonance energy transfer in living cells.* Biochem J, 2004. **377**(Pt 2): p. 289-97.
125. Vogt, M., et al., *The role of the N-terminal domain in dimerization and nucleocytoplasmic shuttling of latent STAT3.* J Cell Sci, 2011. **124**(Pt 6): p. 900-9.
126. Schindler, C., et al., *Proteins of transcription factor ISGF-3: one gene encodes the 91-and 84-kDa ISGF-3 proteins that are activated by interferon alpha.* Proc Natl Acad Sci U S A, 1992. **89**(16): p. 7836-9.
127. Schindler, C., et al., *Interferon-dependent tyrosine phosphorylation of a latent cytoplasmic transcription factor.* Science, 1992. **257**(5071): p. 809-13.
128. Shuai, K., et al., *Activation of transcription by IFN-gamma: tyrosine phosphorylation of a 91-kD DNA binding protein.* Science, 1992. **258**(5089): p. 1808-12.
129. Gent, J., et al., *Ligand-independent growth hormone receptor dimerization occurs in the endoplasmic reticulum and is required for ubiquitin system-dependent endocytosis.* Proc Natl Acad Sci U S A, 2002. **99**(15): p. 9858-63.
130. Brown, R.J., et al., *Model for growth hormone receptor activation based on subunit rotation within a receptor dimer.* Nat Struct Mol Biol, 2005. **12**(9): p. 814-21.
131. Brooks, A.J., et al., *Mechanism of activation of protein kinase JAK2 by the growth hormone receptor.* Science, 2014. **344**(6185): p. 1249783.
132. Wells, J.A., *Binding in the growth hormone receptor complex.* Proceedings of the National Academy of Sciences of the United States of America, 1996. **93**(1): p. 1-6.
133. Chen, C., R. Brinkworth, and M.J. Waters, *The role of receptor dimerization domain residues in growth hormone signaling.* J Biol Chem, 1997. **272**(8): p. 5133-40.
134. Argetsinger, L.S., et al., *Identification of JAK2 as a growth hormone receptor-associated tyrosine kinase.* Cell, 1993. **74**(2): p. 237-44.
135. Silvennoinen, O., et al., *Structure of the murine Jak2 protein-tyrosine kinase and its role in interleukin 3 signal transduction.* Proc Natl Acad Sci U S A, 1993. **90**(18): p. 8429-33.
136. Saharinen, P. and O. Silvennoinen, *The pseudokinase domain is required for suppression of basal activity of Jak2 and Jak3 tyrosine kinases and for cytokine-inducible activation of signal transduction.* J Biol Chem, 2002. **277**(49): p. 47954-63.
137. *Heterodimerization of JAK2 with JAK1 or TYK2 Promotes Drug Persistence.* Cancer Discovery, 2012. **2**(9): p. OF10.
138. Shan, Y., et al., *Molecular basis for pseudokinase-dependent autoinhibition of JAK2 tyrosine kinase.* Nat Struct Mol Biol, 2014. **21**(7): p. 579-84.
139. Matsuda, T., et al., *Determination of the transphosphorylation sites of Jak2 kinase.* Biochem Biophys Res Commun, 2004. **325**(2): p. 586-94.
140. Robertson, S.A., et al., *Regulation of Jak2 function by phosphorylation of Tyr317 and Tyr637 during cytokine signaling.* Mol Cell Biol, 2009. **29**(12): p. 3367-78.
141. Argetsinger, L.S., et al., *Tyrosines 868, 966, and 972 in the kinase domain of JAK2 are autophosphorylated and required for maximal JAK2 kinase activity.* Mol Endocrinol, 2010. **24**(5): p. 1062-76.
142. Shuai, K. and B. Liu, *Regulation of JAK-STAT signalling in the immune system.* Nat Rev Immunol, 2003. **3**(11): p. 900-11.
143. Saharinen, P., K. Takaluoma, and O. Silvennoinen, *Regulation of the Jak2 Tyrosine Kinase by Its Pseudokinase Domain.* Molecular and Cellular Biology, 2000. **20**(10): p. 3387-3395.
144. Saharinen, P., M. Vihinen, and O. Silvennoinen, *Autoinhibition of Jak2 tyrosine kinase is dependent on specific regions in its pseudokinase domain.* Mol Biol Cell, 2003. **14**(4): p. 1448-59.
145. Duhe, R.J., et al., *Nitric oxide and thiol redox regulation of Janus kinase activity.* Proc Natl Acad Sci U S A, 1998. **95**(1): p. 126-31.
146. Qian, S., et al., *Primary role of the liver in thrombopoietin production shown by tissue-specific knockout.* Blood, 1998. **92**(6): p. 2189-91.
147. Sungaran, R., B. Markovic, and B.H. Chong, *Localization and regulation of thrombopoietin mRNA expression in human kidney, liver, bone marrow, and spleen using in situ hybridization.* Blood, 1997. **89**(1): p. 101-7.

148. Lok, S., et al., *Cloning and expression of murine thrombopoietin cDNA and stimulation of platelet production in vivo.* Nature, 1994. **369**(6481): p. 565-8.
149. Stoffel, R., A. Wiestner, and R.C. Skoda, *Thrombopoietin in thrombocytopenic mice: evidence against regulation at the mRNA level and for a direct regulatory role of platelets.* Blood, 1996. **87**(2): p. 567-73.
150. Wendling, F., et al., *MPLV: a retrovirus complex inducing an acute myeloproliferative leukemic disorder in adult mice.* Virology, 1986. **149**(2): p. 242-6.
151. Solar, G.P., et al., *Role of c-mpl in early hematopoiesis.* Blood, 1998. **92**(1): p. 4-10.
152. Debili, N., et al., *The Mpl receptor is expressed in the megakaryocytic lineage from late progenitors to platelets.* Blood, 1995. **85**(2): p. 391-401.
153. Kaushansky, K., et al., *Thrombopoietin expands erythroid, granulocyte-macrophage, and megakaryocytic progenitor cells in normal and myelosuppressed mice.* Exp Hematol, 1996. **24**(2): p. 265-9.
154. Pearce, K.H., Jr., et al., *Mutational analysis of thrombopoietin for identification of receptor and neutralizing antibody sites.* J Biol Chem, 1997. **272**(33): p. 20595-602.
155. Kuroki, R., et al., *Crystallization of the functional domain of human thrombopoietin using an antigen-binding fragment derived from neutralizing monoclonal antibody.* Acta Crystallogr D Biol Crystallogr, 2002. **58**(Pt 5): p. 856-8.
156. Feese, M.D., et al., *Structure of the receptor-binding domain of human thrombopoietin determined by complexation with a neutralizing antibody fragment.* Proc Natl Acad Sci U S A, 2004. **101**(7): p. 1816-21.
157. Singh, V.K., et al., *A Novel Peptide Thrombopoietin Mimetic Designing and Optimization Using Computational Approach.* Front Bioeng Biotechnol, 2016. **4**: p. 69.
158. Broudy, V.C., et al., *Human platelets display high-affinity receptors for thrombopoietin.* Blood, 1997. **89**(6): p. 1896-904.
159. Li, J., Y. Xia, and D.J. Kuter, *Interaction of thrombopoietin with the platelet c-mpl receptor in plasma: binding, internalization, stability and pharmacokinetics.* Br J Haematol, 1999. **106**(2): p. 345-56.
160. Kuter, D.J. and R.D. Rosenberg, *The reciprocal relationship of thrombopoietin (c-Mpl ligand) to changes in the platelet mass during busulfan-induced thrombocytopenia in the rabbit.* Blood, 1995. **85**(10): p. 2720-30.
161. Peters, M., et al., *The function of the soluble interleukin 6 (IL-6) receptor in vivo: sensitization of human soluble IL-6 receptor transgenic mice towards IL-6 and prolongation of the plasma half-life of IL-6.* J Exp Med, 1996. **183**(4): p. 1399-406.
162. Ogata, A., et al., *IL-6 triggers cell growth via the Ras-dependent mitogen-activated protein kinase cascade.* J Immunol, 1997. **159**(5): p. 2212-21.
163. Hayashida, K., et al., *Molecular cloning of a second subunit of the receptor for human granulocyte-macrophage colony-stimulating factor (GM-CSF): reconstitution of a high-affinity GM-CSF receptor.* Proc Natl Acad Sci U S A, 1990. **87**(24): p. 9655-9.
164. Tavernier, J., et al., *Molecular basis of the membrane-anchored and two soluble isoforms of the human interleukin 5 receptor alpha subunit.* Proc Natl Acad Sci U S A, 1992. **89**(15): p. 7041-5.
165. Tsuruoka, N., K. Yamashiro, and M. Tsujimoto, *Purification of soluble murine interleukin 5 (IL-5) receptor alpha expressed in Chinese hamster ovary cells and its action as an IL-5 antagonist.* Arch Biochem Biophys, 1993. **307**(1): p. 133-7.
166. Brown, C.B., et al., *In vitro characterization of the human recombinant soluble granulocyte-macrophage colony-stimulating factor receptor.* Blood, 1995. **85**(6): p. 1488-95.
167. Li, J., D.F. Sabath, and D.J. Kuter, *Cloning and functional characterization of a novel c-mpl variant expressed in human CD34 cells and platelets.* Cytokine, 2000. **12**(7): p. 835-44.
168. Coers, J., C. Ranft, and R.C. Skoda, *A truncated isoform of c-Mpl with an essential C-terminal peptide targets the full-length receptor for degradation.* J Biol Chem, 2004. **279**(35): p. 36397-404.
169. Millot, G.A., et al., *MplK, a natural variant of the thrombopoietin receptor with a truncated cytoplasmic domain, binds thrombopoietin but does not interfere with thrombopoietin-mediated cell growth.* Exp Hematol, 2002. **30**(2): p. 166-75.

170. Skoda, R.C., et al., *Murine c-mpl: a member of the hematopoietic growth factor receptor superfamily that transduces a proliferative signal.* Embo j, 1993. **12**(7): p. 2645-53.
171. Vigon, I., et al., *Characterization of the murine Mpl proto-oncogene, a member of the hematopoietic cytokine receptor family: molecular cloning, chromosomal location and evidence for a function in cell growth.* Oncogene, 1993. **8**(10): p. 2607-15.
172. Gurney, A.L., et al., *Thrombocytopenia in c-mpl-deficient mice.* Science, 1994. **265**(5177): p. 1445-7.
173. Alexander, W.S., et al., *Deficiencies in progenitor cells of multiple hematopoietic lineages and defective megakaryocytopoiesis in mice lacking the thrombopoietic receptor c-Mpl.* Blood, 1996. **87**(6): p. 2162-70.
174. de Sauvage, F.J., et al., *Physiological regulation of early and late stages of megakaryocytopoiesis by thrombopoietin.* J Exp Med, 1996. **183**(2): p. 651-6.
175. Buza-Vidas, N., et al., *Cytokines regulate postnatal hematopoietic stem cell expansion: opposing roles of thrombopoietin and LNK.* Genes Dev, 2006. **20**(15): p. 2018-23.
176. Nishimura, S., et al., *IL-1alpha induces thrombopoiesis through megakaryocyte rupture in response to acute platelet needs.* J Cell Biol, 2015. **209**(3): p. 453-66.
177. Qian, H., et al., *Critical role of thrombopoietin in maintaining adult quiescent hematopoietic stem cells.* Cell Stem Cell, 2007. **1**(6): p. 671-84.
178. Yoshihara, H., et al., *Thrombopoietin/MPL signaling regulates hematopoietic stem cell quiescence and interaction with the osteoblastic niche.* Cell Stem Cell, 2007. **1**(6): p. 685-97.
179. Broudy, V.C., N.L. Lin, and K. Kaushansky, *Thrombopoietin (c-mpl ligand) acts synergistically with erythropoietin, stem cell factor, and interleukin-11 to enhance murine megakaryocyte colony growth and increases megakaryocyte ploidy in vitro.* Blood, 1995. **85**(7): p. 1719-26.
180. Fox, N.E., et al., *Compound heterozygous c-Mpl mutations in a child with congenital amegakaryocytic thrombocytopenia: functional characterization and a review of the literature.* Exp Hematol, 2009. **37**(4): p. 495-503.
181. Moliterno, A.R., W.D. Hankins, and J.L. Spivak, *Impaired expression of the thrombopoietin receptor by platelets from patients with polycythemia vera.* New England Journal of Medicine, 1998. **338**(9): p. 572-580.
182. Stockklausner, C., et al., *The thrombopoietin receptor P106L mutation functionally separates receptor signaling activity from thrombopoietin homeostasis.* Blood, 2015. **125**(7): p. 1159-69.
183. Hitchcock, I.S., et al., *YRRL motifs in the cytoplasmic domain of the thrombopoietin receptor regulate receptor internalization and degradation.* Blood, 2008. **112**(6): p. 2222-31.
184. Drachman, J.G. and K. Kaushansky, *Dissecting the thrombopoietin receptor: functional elements of the Mpl cytoplasmic domain.* Proc Natl Acad Sci U S A, 1997. **94**(6): p. 2350-5.
185. Dahlen, D.D., V.C. Broudy, and J.G. Drachman, *Internalization of the thrombopoietin receptor is regulated by 2 cytoplasmic motifs.* Blood, 2003. **102**(1): p. 102-8.
186. Saur, S.J., et al., *Ubiquitination and degradation of the thrombopoietin receptor c-Mpl.* Blood, 2010. **115**: p. 1254-1263.
187. Royer, Y., et al., *Janus kinases affect thrombopoietin receptor cell surface localization and stability.* J Biol Chem, 2005. **280**: p. 27251-27261.
188. Sigismund, S., S. Polo, and P.P. Di Fiore, *Signaling through monoubiquitination.* Curr Top Microbiol Immunol, 2004. **286**: p. 149-85.
189. Levkowitz, G., et al., *Ubiquitin ligase activity and tyrosine phosphorylation underlie suppression of growth factor signaling by c-Cbl/Sli-1.* Mol Cell, 1999. **4**(6): p. 1029-40.
190. Waterman, H., et al., *A mutant EGF-receptor defective in ubiquitylation and endocytosis unveils a role for Grb2 in negative signaling.* Embo j, 2002. **21**(3): p. 303-13.
191. Qazi, A.M., C.H. Tsai-Morris, and M.L. Dufau, *Ligand-independent homo- and heterodimerization of human prolactin receptor variants: inhibitory action of the short forms by heterodimerization.* Mol Endocrinol, 2006. **20**(8): p. 1912-23.
192. Schuster, B., et al., *The human interleukin-6 (IL-6) receptor exists as a preformed dimer in the plasma membrane.* FEBS Lett, 2003. **538**(1-3): p. 113-6.
193. Livnah, O., et al., *Crystallographic evidence for preformed dimers of erythropoietin receptor before ligand activation.* Science, 1999. **283**(5404): p. 987-90.

194. Remy, I., I.A. Wilson, and S.W. Michnick, *Erythropoietin receptor activation by a ligand-induced conformation change.* Science, 1999. **283**(5404): p. 990-3.
195. Giese, B., et al., *Dimerization of the cytokine receptors gp130 and LIFR analysed in single cells.* J Cell Sci, 2005. **118**(Pt 21): p. 5129-40.
196. Leroy, E., et al., *His499 Regulates Dimerization and Prevents Oncogenic Activation by Asparagine Mutations of the Human Thrombopoietin Receptor.* J Biol Chem, 2016. **291**(6): p. 2974-87.
197. Alexander, W.S., D. Metcalf, and A.R. Dunn, *Point mutations within a dimer interface homology domain of c-Mpl induce constitutive receptor activity and tumorigenicity.* EMBO J, 1995. **14**: p. 5569-5578.
198. Miyakawa, Y., et al., *Recombinant thrombopoietin induces rapid protein tyrosine phosphorylation of Janus kinase 2 and Shc in human blood platelets.* Blood, 1995. **86**(1): p. 23-7.
199. Drachman, J.G., J.D. Griffin, and K. Kaushansky, *The c-Mpl ligand (thrombopoietin) stimulates tyrosine phosphorylation of Jak2, Shc, and c-Mpl.* J Biol Chem, 1995. **270**(10): p. 4979-82.
200. Miyakawa, Y., et al., *Thrombopoietin induces tyrosine phosphorylation of Stat3 and Stat5 in human blood platelets.* Blood, 1996. **87**(2): p. 439-46.
201. Rouyez, M.C., et al., *Control of thrombopoietin-induced megakaryocytic differentiation by the mitogen-activated protein kinase pathway.* Mol Cell Biol, 1997. **17**(9): p. 4991-5000.
202. Filippi, M.D., et al., *Requirement for mitogen-activated protein kinase activation in the response of embryonic stem cell-derived hematopoietic cells to thrombopoietin in vitro.* Blood, 2002. **99**(4): p. 1174-82.
203. Drachman, J.G., K.M. Millett, and K. Kaushansky, *Thrombopoietin signal transduction requires functional JAK2, not TYK2.* J Biol Chem, 1999. **274**(19): p. 13480-4.
204. Drachman, J.G., et al., *Thrombopoietin signal transduction in purified murine megakaryocytes.* Blood, 1997. **89**(2): p. 483-92.
205. Geddis, A.E., N.E. Fox, and K. Kaushansky, *Phosphatidylinositol 3-kinase is necessary but not sufficient for thrombopoietin-induced proliferation in engineered Mpl-bearing cell lines as well as in primary megakaryocytic progenitors.* J Biol Chem, 2001. **276**(37): p. 34473-9.
206. Nakao, T., et al., *PI3K/Akt/FOXO3a pathway contributes to thrombopoietin-induced proliferation of primary megakaryocytes in vitro and in vivo via modulation of p27(Kip1).* Cell Cycle, 2008. **7**(2): p. 257-66.
207. Rojnuckarin, P., J.G. Drachman, and K. Kaushansky, *Thrombopoietin-induced activation of the mitogen-activated protein kinase (MAPK) pathway in normal megakaryocytes: role in endomitosis.* Blood, 1999. **94**(4): p. 1273-82.
208. Luoh, S.M., et al., *Role of the distal half of the c-Mpl intracellular domain in control of platelet production by thrombopoietin in vivo.* Mol Cell Biol, 2000. **20**(2): p. 507-15.
209. Rojnuckarin, P., et al., *The roles of phosphatidylinositol 3-kinase and protein kinase Czeta for thrombopoietin-induced mitogen-activated protein kinase activation in primary murine megakaryocytes.* J Biol Chem, 2001. **276**(44): p. 41014-22.
210. Sabath, D.F., K. Kaushansky, and V.C. Broudy, *Deletion of the extracellular membrane-distal cytokine receptor homology module of Mpl results in constitutive cell growth and loss of thrombopoietin binding.* Blood, 1999. **94**(1): p. 365-7.
211. Chen, W.M., et al., *Identification of the residues in the extracellular domain of thrombopoietin receptor involved in the binding of thrombopoietin and a nuclear distribution protein (human NUDC).* J Biol Chem, 2010. **285**(34): p. 26697-709.
212. Layton, J.E., et al., *Identification of a ligand-binding site on the granulocyte colony-stimulating factor receptor by molecular modeling and mutagenesis.* J Biol Chem, 1997. **272**(47): p. 29735-41.
213. Rajotte, D., et al., *Crucial role of the residue R280 at the F'-G' loop of the human granulocyte/macrophage colony-stimulating factor receptor alpha chain for ligand recognition.* J Exp Med, 1997. **185**(11): p. 1939-50.
214. Fox, N.E., et al., *F104S c-Mpl responds to a transmembrane domain-binding thrombopoietin receptor agonist: proof of concept that selected receptor mutations in congenital amegakaryocytic thrombocytopenia can be stimulated with alternative thrombopoietic agents.* Exp Hematol, 2010. **38**(5): p. 384-91.

215. Albu, R.I. and S.N. Constantinescu, *Extracellular domain N-glycosylation controls human thrombopoietin receptor cell surface levels.* Front Endocrinol (Lausanne), 2011. **2**: p. 71.
216. Yoshimura, A., et al., *Mutations in the Trp-Ser-X-Trp-Ser motif of the erythropoietin receptor abolish processing, ligand binding, and activation of the receptor.* J Biol Chem, 1992. **267**(16): p. 11619-25.
217. Quelle, D.E., F.W. Quelle, and D.M. Wojchowski, *Mutations in the WSAWSE and cytosolic domains of the erythropoietin receptor affect signal transduction and ligand binding and internalization.* Mol Cell Biol, 1992. **12**(10): p. 4553-61.
218. Sasazawa, Y., et al., *C-Mannosylation of thrombopoietin receptor (c-Mpl) regulates thrombopoietin-dependent JAK-STAT signaling.* Biochem Biophys Res Commun, 2015. **468**(1-2): p. 262-8.
219. Kim, M.J., et al., *NMR structural studies of interactions of a small, nonpeptidyl Tpo mimic with the thrombopoietin receptor extracellular juxtamembrane and transmembrane domains.* J Biol Chem, 2007. **282**(19): p. 14253-61.
220. Ding, J., et al., *Familial essential thrombocythemia associated with a dominant-positive activating mutation of the c-MPL gene, which encodes for the receptor for thrombopoietin.* Blood, 2004. **103**(11): p. 4198-200.
221. Matthews, E.E., et al., *Thrombopoietin receptor activation: transmembrane helix dimerization, rotation, and allosteric modulation.* Faseb j, 2011. **25**(7): p. 2234-44.
222. Ding, J.M., et al., *The Asn505 mutation of the c-MPL gene, which causes familial essential thrombocythemia, induces autonomous homodimerization of the c-Mpl protein due to strong amino acid polarity.* Blood, 2009. **114**(15): p. 3325-3328.
223. Choma, C., et al., *Asparagine-mediated self-association of a model transmembrane helix.* Nat Struct Biol, 2000. **7**(2): p. 161-6.
224. Defour, J.P., et al., *Tryptophan at the transmembrane-cytosolic junction modulates thrombopoietin receptor dimerization and activation.* Proc Natl Acad Sci U S A, 2013. **110**(7): p. 2540-5.
225. Staerk, J., et al., *An amphipathic motif at the transmembrane-cytoplasmic junction prevents autonomous activation of the thrombopoietin receptor.* Blood, 2006. **107**(5): p. 1864-71.
226. Abd Halim, K.B., H. Koldso, and M.S. Sansom, *Interactions of the EGFR juxtamembrane domain with PIP2-containing lipid bilayers: Insights from multiscale molecular dynamics simulations.* Biochim Biophys Acta, 2015. **1850**(5): p. 1017-25.
227. Defour, J.P., et al., *Oncogenic activation of MPL/thrombopoietin receptor by 17 mutations at W515: implications for myeloproliferative neoplasms.* Leukemia, 2016. **30**(5): p. 1214-6.
228. Seubert, N., et al., *Active and inactive orientations of the transmembrane and cytosolic domains of the erythropoietin receptor dimer.* Mol Cell, 2003. **12**(5): p. 1239-50.
229. Alexander, W.S., et al., *Tyrosine-599 of the c-Mpl receptor is required for Shc phosphorylation and the induction of cellular differentiation.* Embo j, 1996. **15**(23): p. 6531-40.
230. Pecquet, C., et al., *Induction of myeloproliferative disorder and myelofibrosis by thrombopoietin receptor W515 mutants is mediated by cytosolic tyrosine 112 of the receptor.* Blood, 2010. **115**(5): p. 1037-48.
231. Haxholm, G.W., et al., *Intrinsically disordered cytoplasmic domains of two cytokine receptors mediate conserved interactions with membranes.* Biochemical Journal, 2015. **468**: p. 495-506.
232. Ballmaier, M., et al., *c-mpl mutations are the cause of congenital amegakaryocytic thrombocytopenia.* Blood, 2001. **97**(1): p. 139-46.
233. Ihara, K., et al., *Identification of mutations in the c-mpl gene in congenital amegakaryocytic thrombocytopenia.* Proceedings of the National Academy of Sciences of the United States of America, 1999. **96**(6): p. 3132-3136.
234. van den Oudenrijn, S., et al., *Mutations in the thrombopoietin receptor, Mpl, in children with congenital amegakaryocytic thrombocytopenia.* Br J Haematol, 2000. **110**(2): p. 441-8.
235. El-Harith el, H.A., et al., *Familial thrombocytosis caused by the novel germ-line mutation p.Pro106Leu in the MPL gene.* Br J Haematol, 2009. **144**(2): p. 185-94.
236. Chaligne, R., et al., *New mutations of MPL in primitive myelofibrosis: only the MPL W515 mutations promote a G1/S-phase transition.* Leukemia, 2008. **22**: p. 1557-1566.
237. Chaligne, R., et al., *New mutations of MPL in primitive myelofibrosis: only the MPL W515 mutations promote a G1/S-phase transition.* Leukemia, 2008. **22**(8): p. 1557-66.

238. Marty, C., et al., *Ligand-independent thrombopoietin mutant receptor requires cell surface localization for endogenous activity.* J Biol Chem, 2009. **284**(18): p. 11781-91.
239. Malinge, S., et al., *Activating mutations in human acute megakaryoblastic leukemia.* Blood, 2008. **112**(10): p. 4220-4226.
240. Chaligne, R., et al., *Evidence for MPL W515L/K mutations in hematopoietic stem cells in primitive myelofibrosis.* Blood, 2007. **110**(10): p. 3735-43.
241. Onishi, M., et al., *Identification of an oncogenic form of the thrombopoietin receptor MPL using retrovirus-mediated gene transfer.* Blood, 1996. **88**(4): p. 1399-406.
242. Cheng, G., et al., *Eltrombopag for management of chronic immune thrombocytopenia (RAISE): a 6-month, randomised, phase 3 study.* Lancet, 2011. **377**(9763): p. 393-402.
243. Kuter, D.J., et al., *Efficacy of romiplostim in patients with chronic immune thrombocytopenic purpura: a double-blind randomised controlled trial.* Lancet, 2008. **371**(9610): p. 395-403.
244. Imbach, P. and M. Crowther, *Thrombopoietin-Receptor Agonists for Primary Immune Thrombocytopenia.* New England Journal of Medicine, 2011. **365**(8): p. 734-741.
245. Erickson-Miller, C.L., et al., *Preclinical activity of eltrombopag (SB-497115), an oral, nonpeptide thrombopoietin receptor agonist.* Stem Cells, 2009. **27**(2): p. 424-30.
246. Erickson-Miller, C.L., et al., *Discovery and characterization of a selective, nonpeptidyl thrombopoietin receptor agonist.* Exp Hematol, 2005. **33**(1): p. 85-93.
247. Quintas-Cardama, A., et al., *Preclinical characterization of the selective JAK1/2 inhibitor INCB018424: therapeutic implications for the treatment of myeloproliferative neoplasms.* Blood, 2010. **115**(15): p. 3109-17.
248. Lannutti, B.J., et al., *Increased megakaryocytopoiesis in Lyn-deficient mice.* Oncogene, 2006. **25**(23): p. 3316-24.
249. Tong, W. and H.F. Lodish, *Lnk inhibits Tpo-mpl signaling and Tpo-mediated megakaryocytopoiesis.* J Exp Med, 2004. **200**(5): p. 569-80.
250. Wang, Q., et al., *Interferon-alpha directly represses megakaryopoiesis by inhibiting thrombopoietin-induced signaling through induction of SOCS-1.* Blood, 2000. **96**: p. 2093-2099.
251. Hitchcock, I.S., et al., *Roles of focal adhesion kinase (FAK) in megakaryopoiesis and platelet function: studies using a megakaryocyte lineage specific FAK knockout.* Blood, 2008. **111**(2): p. 596-604.
252. Endo, T.A., et al., *A new protein containing an SH2 domain that inhibits JAK kinases.* Nature, 1997. **387**(6636): p. 921-4.
253. Starr, R., et al., *A family of cytokine-inducible inhibitors of signalling.* Nature, 1997. **387**(6636): p. 917-21.
254. Naka, T., et al., *Structure and function of a new STAT-induced STAT inhibitor.* Nature, 1997. **387**(6636): p. 924-9.
255. Babon, J.J., et al., *Secondary structure assignment of mouse SOCS3 by NMR defines the domain boundaries and identifies an unstructured insertion in the SH2 domain.* Febs j, 2005. **272**(23): p. 6120-30.
256. Wang, Q., et al., *Interferon-alpha directly represses megakaryopoiesis by inhibiting thrombopoietin-induced signaling through induction of SOCS-1.* Blood, 2000. **96**(6): p. 2093-9.
257. Hof, P., et al., *Crystal structure of the tyrosine phosphatase SHP-2.* Cell, 1998. **92**(4): p. 441-50.
258. Yang, J., et al., *Crystal structure of human protein-tyrosine phosphatase SHP-1.* J Biol Chem, 2003. **278**(8): p. 6516-20.
259. Wang, W., et al., *Crystal structure of human protein tyrosine phosphatase SHP-1 in the open conformation.* J Cell Biochem, 2011. **112**(8): p. 2062-71.
260. Sanjay, A., W.C. Horne, and R. Baron, *The Cbl family: ubiquitin ligases regulating signaling by tyrosine kinases.* Sci STKE, 2001. **2001**(110): p. pe40.
261. Garcia-Guzman, M., E. Larsen, and K. Vuori, *The proto-oncogene c-Cbl is a positive regulator of Met-induced MAP kinase activation: a role for the adaptor protein Crk.* Oncogene, 2000. **19**(35): p. 4058-65.
262. Yasuda, T., et al., *Cbl-b positively regulates Btk-mediated activation of phospholipase C-gamma2 in B cells.* J Exp Med, 2002. **196**(1): p. 51-63.

263. Chiang, S.H., et al., *Insulin-stimulated GLUT4 translocation requires the CAP-dependent activation of TC10.* Nature, 2001. **410**(6831): p. 944-8.
264. Ahn, M.Y., et al., *Primary and essential role of the adaptor protein APS for recruitment of both c-Cbl and its associated protein CAP in insulin signaling.* J Biol Chem, 2004. **279**(20): p. 21526-32.
265. Standaert, M.L., et al., *Requirements for pYXXM motifs in Cbl for binding to the p85 subunit of phosphatidylinositol 3-kinase and Crk, and activation of atypical protein kinase C and glucose transport during insulin action in 3T3/L1 adipocytes.* Biochemistry, 2004. **43**(49): p. 15494-502.
266. Saur, S.J., et al., *Ubiquitination and degradation of the thrombopoietin receptor c-Mpl.* Blood, 2010. **115**(6): p. 1254-63.
267. Brown, M.T. and J.A. Cooper, *Regulation, substrates and functions of src.* Biochim Biophys Acta, 1996. **1287**(2-3): p. 121-49.
268. Thomas, S.M. and J.S. Brugge, *Cellular functions regulated by Src family kinases.* Annu Rev Cell Dev Biol, 1997. **13**: p. 513-609.
269. Lannutti, B.J., et al., *Identification and activation of Src family kinases in primary megakaryocytes.* Exp Hematol, 2003. **31**(12): p. 1268-74.
270. Lannutti, B.J. and J.G. Drachman, *Lyn tyrosine kinase regulates thrombopoietin-induced proliferation of hematopoietic cell lines and primary megakaryocytic progenitors.* Blood, 2004. **103**(10): p. 3736-43.
271. Wang, B., et al., *SH2 domain-mediated interaction of inhibitory protein tyrosine kinase Csk with protein tyrosine phosphatase-HSCF.* Mol Cell Biol, 2001. **21**(4): p. 1077-88.
272. Margolis, B., et al., *The function of PTB domain proteins.* Kidney Int, 1999. **56**(4): p. 1230-7.
273. Macias, M.J., et al., *Structure of the WW domain of a kinase-associated protein complexed with a proline-rich peptide.* Nature, 1996. **382**(6592): p. 646-9.
274. Mayer, B.J., *SH3 domains: complexity in moderation.* J Cell Sci, 2001. **114**(Pt 7): p. 1253-63.
275. Lemmon, M.A. and K.M. Ferguson, *Signal-dependent membrane targeting by pleckstrin homology (PH) domains.* Biochem J, 2000. **350 Pt 1**: p. 1-18.
276. Velazquez, L., et al., *Cytokine signaling and hematopoietic homeostasis are disrupted in Lnk-deficient mice.* J Exp Med, 2002. **195**(12): p. 1599-611.
277. Tong, W., J. Zhang, and H.F. Lodish, *Lnk inhibits erythropoiesis and Epo-dependent JAK2 activation and downstream signaling pathways.* Blood, 2005. **105**(12): p. 4604-4612.
278. Bersenev, A., et al., *Lnk controls mouse hematopoietic stem cell self-renewal and quiescence through direct interactions with JAK2.* J Clin Invest, 2008. **118**(8): p. 2832-44.
279. Ema, H., et al., *Quantification of self-renewal capacity in single hematopoietic stem cells from normal and Lnk-deficient mice.* Dev Cell, 2005. **8**(6): p. 907-14.
280. Takaki, S., et al., *Enhanced hematopoiesis by hematopoietic progenitor cells lacking intracellular adaptor protein, Lnk.* J Exp Med, 2002. **195**(2): p. 151-60.
281. Takizawa, H., et al., *Enhanced engraftment of hematopoietic stem/progenitor cells by the transient inhibition of an adaptor protein, Lnk.* Blood, 2006. **107**(7): p. 2968-75.
282. Wakioka, T., et al., *APS, an adaptor protein containing Pleckstrin homology (PH) and Src homology-2 (SH2) domains inhibits the JAK-STAT pathway in collaboration with c-Cbl.* Leukemia, 1999. **13**(5): p. 760-7.
283. Javadi, M., et al., *The SH2B1 adaptor protein associates with a proximal region of the erythropoietin receptor.* J Biol Chem, 2012. **287**(31): p. 26223-34.
284. Takizawa, H., et al., *Growth and maturation of megakaryocytes is regulated by Lnk/Sh2b3 adaptor protein through crosstalk between cytokine- and integrin-mediated signals.* Exp Hematol, 2008. **36**(7): p. 897-906.
285. Gery, S., et al., *Adaptor protein Lnk negatively regulates the mutant MPL, MPLW515L associated with myeloproliferative disorders.* Blood, 2007. **110**(9): p. 3360-4.
286. Li, Y., et al., *Cloning and characterization of human Lnk, an adaptor protein with pleckstrin homology and Src homology 2 domains that can inhibit T cell activation.* J Immunol, 2000. **164**(10): p. 5199-206.
287. Osborne, M.A., S. Dalton, and J.P. Kochan, *The yeast tribrid system--genetic detection of trans-phosphorylated ITAM-SH2-interactions.* Biotechnology (N Y), 1995. **13**(13): p. 1474-8.

288. Rui, L., et al., *Identification of SH2-Bbeta as a substrate of the tyrosine kinase JAK2 involved in growth hormone signaling.* Mol Cell Biol, 1997. **17**(11): p. 6633-44.
289. Nelms, K., et al., *Alternative splicing, gene localization, and binding of SH2-B to the insulin receptor kinase domain.* Mamm Genome, 1999. **10**(12): p. 1160-7.
290. Yousaf, N., et al., *Four PSM/SH2-B alternative splice variants and their differential roles in mitogenesis.* Journal of Biological Chemistry, 2001. **276**(44): p. 40940-40948.
291. Nishi, M., et al., *Kinase activation through dimerization by human SH2-B.* Molecular and Cellular Biology, 2005. **25**(7): p. 2607-2621.
292. Li, M., et al., *Identification of SH2B2beta as an inhibitor for SH2B1- and SH2B2alpha-promoted Janus kinase-2 activation and insulin signaling.* Endocrinology, 2007. **148**(4): p. 1615-21.
293. Qian, X., et al., *Identification and characterization of novel substrates of Trk receptors in developing neurons.* Neuron, 1998. **21**(5): p. 1017-29.
294. Rui, L., J. Herrington, and C. Carter-Su, *SH2-B is required for nerve growth factor-induced neuronal differentiation.* J Biol Chem, 1999. **274**(15): p. 10590-4.
295. Ohtsuka, S., et al., *SH2-B Is Required for Both Male and Female Reproduction.* Molecular and Cellular Biology, 2002. **22**(9): p. 3066-3077.
296. Duan, C., et al., *Disruption of the SH2-B gene causes age-dependent insulin resistance and glucose intolerance.* Mol Cell Biol, 2004. **24**(17): p. 7435-43.
297. Ren, D., et al., *Identification of SH2-B as a key regulator of leptin sensitivity, energy balance, and body weight in mice.* Cell Metab, 2005. **2**(2): p. 95-104.
298. Rui, L.Y. and C. Carter-Su, *Identification of SH2-B beta as a potent cytoplasmic activator of the tyrosine kinase Janus kinase 2.* Proceedings of the National Academy of Sciences of the United States of America, 1999. **96**(13): p. 7172-7177.
299. Kurzer, J.H., et al., *Binding of SH2-B family members within a potential negative regulatory region maintains JAK2 in an active state.* Mol Cell Biol, 2006. **26**(17): p. 6381-94.
300. Ding, L.W., et al., *LNK (SH2B3): paradoxical effects in ovarian cancer.* Oncogene, 2015. **34**(11): p. 1463-74.
301. Chatelais, M., et al., *Gene transfer of the adaptor Lnk (SH2B3) prevents porcine endothelial cell activation and apoptosis: implication for xenograft's cytoprotection.* Xenotransplantation, 2011. **18**(2): p. 108-20.
302. Ahmed, Z. and T.S. Pillay, *Adapter protein with a pleckstrin homology (PH) and an Src homology 2 (SH2) domain (APS) and SH2-B enhance insulin-receptor autophosphorylation, extracellular-signal-regulated kinase and phosphoinositide 3-kinase-dependent signalling.* Biochem J, 2003. **371**(Pt 2): p. 405-12.
303. Qian, X. and D.D. Ginty, *SH2-B and APS are multimeric adapters that augment TrkA signaling.* Mol Cell Biol, 2001. **21**(5): p. 1613-20.
304. Wang, T.C., et al., *The adaptor protein SH2B3 (Lnk) negatively regulates neurite outgrowth of PC12 cells and cortical neurons.* PLoS One, 2011. **6**(10): p. e26433.
305. Hu, J., et al., *Structural basis for recruitment of the adaptor protein APS to the activated insulin receptor.* Mol Cell, 2003. **12**(6): p. 1379-89.
306. Dhe-Paganon, S., et al., *A phenylalanine zipper mediates APS dimerization.* Nat Struct Mol Biol, 2004. **11**(10): p. 968-74.
307. Maures, T.J., J.H. Kurzer, and C. Carter-Su, *SH2B1 (SH2-B) and JAK2: a multifunctional adaptor protein and kinase made for each other.* Trends in Endocrinology and Metabolism, 2007. **18**(1): p. 38-45.
308. Perez-Garcia, A., et al., *Genetic loss of SH2B3 in acute lymphoblastic leukemia.* Blood, 2013. **122**(14): p. 2425-32.
309. Baran-Marszak, F., et al., *Expression level and differential JAK2-V617F-binding of the adaptor protein Lnk regulates JAK2-mediated signals in myeloproliferative neoplasms.* Blood, 2010. **116**(26): p. 5961-71.
310. Gery, S., et al., *Lnk inhibits myeloproliferative disorder-associated JAK2 mutant, JAK2V617F.* J Leukoc Biol, 2009. **85**(6): p. 957-65.
311. Simon, C., et al., *Lnk adaptor protein down-regulates specific Kit-induced signaling pathways in primary mast cells.* Blood, 2008. **112**(10): p. 4039-47.

312. Gueller, S., et al., *Adaptor protein Lnk inhibits c-Fms-mediated macrophage function.* J Leukoc Biol, 2010. **88**(4): p. 699-706.
313. Fitau, J., et al., *The adaptor molecule Lnk negatively regulates tumor necrosis factor-alpha-dependent VCAM-1 expression in endothelial cells through inhibition of the ERK1 and -2 pathways.* J Biol Chem, 2006. **281**(29): p. 20148-59.
314. Seita, J., et al., *Lnk negatively regulates self-renewal of hematopoietic stem cells by modifying thrombopoietin-mediated signal transduction.* Proc Natl Acad Sci U S A, 2007. **104**(7): p. 2349-54.
315. Takaki, S., et al., *Control of B cell production by the adaptor protein lnk. Definition Of a conserved family of signal-modulating proteins.* Immunity, 2000. **13**(5): p. 599-609.
316. Gueller, S., et al., *Adaptor protein Lnk binds to PDGF receptor and inhibits PDGF-dependent signaling.* Exp Hematol, 2011. **39**(5): p. 591-600.
317. Miyakawa, Y., et al., *Thrombopoietin induces phosphoinositol 3-kinase activation through SHP2, Gab, and insulin receptor substrate proteins in BAF3 cells and primary murine megakaryocytes.* J Biol Chem, 2001. **276**(4): p. 2494-502.
318. Nobuhisa, I., et al., *Regulation of hematopoietic development in the aorta-gonad-mesonephros region mediated by Lnk adaptor protein.* Mol Cell Biol, 2003. **23**(23): p. 8486-94.
319. Bersenev, A., et al., *Lnk constrains myeloproliferative diseases in mice.* J Clin Invest, 2010. **120**: p. 2058-2069.
320. Gueller, S., et al., *Adaptor protein Lnk associates with Tyr(568) in c-Kit.* Biochem J, 2008. **415**(2): p. 241-5.
321. Gery, S., et al., *Adaptor Protein Lnk Negatively Regulates Mutant MPL and JAK2 Alleles Associated with Myeloproliferative Disorders.* Blood, 2007. **110**(11): p. 1531-1531.
322. Pardanani, A., et al., *CHIC2 deletion, a surrogate for FIP1L1-PDGFRA fusion, occurs in systemic mastocytosis associated with eosinophilia and predicts response to imatinib mesylate therapy.* Blood, 2003. **102**(9): p. 3093-6.
323. Cools, J., et al., *A tyrosine kinase created by fusion of the PDGFRA and FIP1L1 genes as a therapeutic target of imatinib in idiopathic hypereosinophilic syndrome.* N Engl J Med, 2003. **348**(13): p. 1201-14.
324. Bersenev, A., et al., *Lnk constrains myeloproliferative diseases in mice.* J Clin Invest, 2010. **120**(6): p. 2058-69.
325. Yano, M., et al., *Clinical significance of SH2B3 (LNK) expression in paediatric B-cell precursor acute lymphoblastic leukaemia.* Br J Haematol, 2018. **183**(2): p. 327-330.
326. Ge, Z., et al., *Co-existence of IL7R high and SH2B3 low expression distinguishes a novel high-risk acute lymphoblastic leukemia with Ikaros dysfunction.* Oncotarget, 2016. **7**(29): p. 46014-46027.
327. Baughn, L.B., et al., *SH2B3 aberrations enriched in iAMP21 B lymphoblastic leukemia.* Cancer Genet, 2018. **226-227**: p. 30-35.
328. Iseki, M., et al., *APS, an adaptor molecule containing PH and SH2 domains, has a negative regulatory role in B cell proliferation.* Biochem Biophys Res Commun, 2005. **330**(3): p. 1005-13.
329. Chan, P.M., et al., *Autoinhibition of the kit receptor tyrosine kinase by the cytosolic juxtamembrane region.* Mol Cell Biol, 2003. **23**(9): p. 3067-78.
330. Kozlowski, M., et al., *SHP-1 binds and negatively modulates the c-Kit receptor by interaction with tyrosine 569 in the c-Kit juxtamembrane domain.* Mol Cell Biol, 1998. **18**(4): p. 2089-99.
331. Wollberg, P., et al., *The adapter protein APS associates with the multifunctional docking sites Tyr-568 and Tyr-936 in c-Kit.* Biochem J, 2003. **370**(Pt 3): p. 1033-8.
332. Lin, D.C., et al., *Adaptor protein Lnk binds to and inhibits normal and leukemic FLT3.* Blood, 2012. **120**(16): p. 3310-7.
333. Cheng, Y., et al., *LNK/SH2B3 regulates IL-7 receptor signaling in normal and malignant B-progenitors.* J Clin Invest, 2016. **126**(4): p. 1267-81.
334. Kurzer, J.H., et al., *Tyrosine 813 is a site of JAK2 autophosphorylation critical for activation of JAK2 by SH2-B beta.* Mol Cell Biol, 2004. **24**(10): p. 4557-70.
335. Yokouchi, M., et al., *Cloning and characterization of APS, an adaptor molecule containing PH and SH2 domains that is tyrosine phosphorylated upon B-cell receptor stimulation.* Oncogene, 1997. **15**(1): p. 7-15.

336. Riedel, H., et al., *PSM, an insulin-dependent, pro-rich, PH, SH2 domain containing partner of the insulin receptor.* J Biochem, 1997. **122**(6): p. 1105-13.
337. Rui, L. and C. Carter-Su, *Platelet-derived growth factor (PDGF) stimulates the association of SH2-Bbeta with PDGF receptor and phosphorylation of SH2-Bbeta.* J Biol Chem, 1998. **273**(33): p. 21239-45.
338. Kotani, K., P. Wilden, and T.S. Pillay, *SH2-Balpha is an insulin-receptor adapter protein and substrate that interacts with the activation loop of the insulin-receptor kinase.* Biochem J, 1998. **335 (Pt 1)**: p. 103-9.
339. Moodie, S.A., J. Alleman-Sposeto, and T.A. Gustafson, *Identification of the APS protein as a novel insulin receptor substrate.* J Biol Chem, 1999. **274**(16): p. 11186-93.
340. Wang, J. and H. Riedel, *Insulin-like growth factor-I receptor and insulin receptor association with a Src homology-2 domain-containing putative adapter.* J Biol Chem, 1998. **273**(6): p. 3136-9.
341. Rui, L., et al., *Differential binding to and regulation of JAK2 by the SH2 domain and N-terminal region of SH2-bbeta.* Mol Cell Biol, 2000. **20**(9): p. 3168-77.
342. Bersenev, A., et al., *Lnk Controls Hematopoietic Stem Cell Self-Renewal through Direct Interactions with JAK2 and Contributes to Oncogenic JAK2-Induced Myeloproliferative Diseases in Mice.* Blood, 2008. **112**(11): p. 329-329.
343. Lv, K., et al., *CBL family E3 ubiquitin ligases control JAK2 ubiquitination and stability in hematopoietic stem cells and myeloid malignancies.* Genes Dev, 2017. **31**(10): p. 1007-1023.
344. Koren-Michowitz, M., et al., *SH2B3 (LNK) mutations from myeloproliferative neoplasms patients have mild loss of function against wild type JAK2 and JAK2 V617F.* Br J Haematol, 2013. **161**(6): p. 811-20.
345. Liu, J., et al., *APS facilitates c-Cbl tyrosine phosphorylation and GLUT4 translocation in response to insulin in 3T3-L1 adipocytes.* Mol Cell Biol, 2002. **22**(11): p. 3599-609.
346. Ahmed, Z. and T.S. Pillay, *Functional effects of APS and SH2-B on insulin receptor signalling.* Biochem Soc Trans, 2001. **29**(Pt 4): p. 529-34.
347. Liu, J., et al., *The roles of Cbl-b and c-Cbl in insulin-stimulated glucose transport.* J Biol Chem, 2003. **278**(38): p. 36754-62.
348. Hu, J. and S.R. Hubbard, *Structural characterization of a novel Cbl phosphotyrosine recognition motif in the APS family of adapter proteins.* J Biol Chem, 2005. **280**(19): p. 18943-9.
349. Yokouchi, M., et al., *APS, an adaptor protein containing PH and SH2 domains, is associated with the PDGF receptor and c-Cbl and inhibits PDGF-induced mitogenesis.* Oncogene, 1999. **18**(3): p. 759-67.
350. Maslah, N., et al., *The role of LNK/SH2B3 genetic alterations in myeloproliferative neoplasms and other hematological disorders.* Leukemia, 2017. **31**(8): p. 1661-1670.
351. Hurtado, C., et al., *LNK can also be mutated outside PH and SH2 domains in myeloproliferative neoplasms with and without V617FJAK2 mutation.* Leuk Res, 2011. **35**(11): p. 1537-9.
352. Ha, J.S. and D.S. Jeon, *Possible new LNK mutations in myeloproliferative neoplasms.* Am J Hematol, 2011. **86**(10): p. 866-8.
353. Oh, S.T., et al., *Novel mutations in the inhibitory adaptor protein LNK drive JAK-STAT signaling in patients with myeloproliferative neoplasms.* Blood, 2010. **116**(6): p. 988-992.
354. Zhang, J., et al., *The genetic basis of early T-cell precursor acute lymphoblastic leukaemia.* Nature, 2012. **481**: p. 157-163.
355. Koren-Michowitz, M., et al., *SH2B3 (LNK) mutations from myeloproliferative neoplasms patients have mild loss of function against wild type JAK2 and JAK2 V617F.* British Journal of Haematology, 2013. **161**(6): p. 811-820.
356. Chen, Y., et al., *The Polymorphisms in LNK Gene Correlated to the Clinical Type of Myeloproliferative Neoplasms.* PLoS One, 2016. **11**(4): p. e0154183.
357. McMullin, M.F., et al., *A nonsynonymous LNK polymorphism associated with idiopathic erythrocytosis.* Am J Hematol, 2011. **86**(11): p. 962-4.
358. Lesteven, E., et al., *Association of a single-nucleotide polymorphism in the SH2B3 gene with JAK2V617F-positive myeloproliferative neoplasms.* Blood, 2014. **123**(5): p. 794-6.
359. Devalliere, J. and B. Charreau, *The adaptor Lnk (SH2B3): an emerging regulator in vascular cells and a link between immune and inflammatory signaling.* Biochem Pharmacol, 2011. **82**(10): p. 1391-402.

360. Rudd, C.E., *Lnk adaptor: novel negative regulator of B cell lymphopoiesis.* Sci STKE, 2001. **2001**(85): p. pe1.
361. Mori, T., et al., *Lnk/Sh2b3 controls the production and function of dendritic cells and regulates the induction of IFN-gamma-producing T cells.* J Immunol, 2014. **193**(4): p. 1728-36.
362. Flister, M.J., et al., *SH2B3 Is a Genetic Determinant of Cardiac Inflammation and Fibrosis.* Circ Cardiovasc Genet, 2015. **8**(2): p. 294-304.
363. Dale, B.L. and M.S. Madhur, *Linking inflammation and hypertension via LNK/SH2B3.* Curr Opin Nephrol Hypertens, 2016. **25**(2): p. 87-93.
364. Looi, C.Y., et al., *Octa-arginine mediated delivery of wild-type Lnk protein inhibits TPO-induced M-MOK megakaryoblastic leukemic cell growth by promoting apoptosis.* PLoS One, 2011. **6**(8): p. e23640.
365. Smith, G.P., *Filamentous fusion phage: novel expression vectors that display cloned antigens on the virion surface.* Science, 1985. **228**(4705): p. 1315-7.
366. De Berardinis, P. and N.L. Haigwood, *New recombinant vaccines based on the use of prokaryotic antigen-display systems.* Expert Rev Vaccines, 2004. **3**(6): p. 673-9.
367. Wrighton, N.C., et al., *Small peptides as potent mimetics of the protein hormone erythropoietin.* Science, 1996. **273**(5274): p. 458-64.
368. Cwirla, S.E., et al., *Peptide agonist of the thrombopoietin receptor as potent as the natural cytokine.* Science, 1997. **276**(5319): p. 1696-9.
369. Su, J.L., et al., *A novel peptide specifically binding to interleukin-6 receptor (gp80) inhibits angiogenesis and tumor growth.* Cancer Res, 2005. **65**(11): p. 4827-35.
370. Hetian, L., et al., *A novel peptide isolated from a phage display library inhibits tumor growth and metastasis by blocking the binding of vascular endothelial growth factor to its kinase domain receptor.* J Biol Chem, 2002. **277**(45): p. 43137-42.
371. Schooltink, H. and S. Rose-John, *Designing cytokine variants by phage-display.* Comb Chem High Throughput Screen, 2005. **8**(2): p. 173-9.
372. McConnell, S.J., et al., *Isolation of erythropoietin receptor agonist peptides using evolved phage libraries.* Biol Chem, 1998. **379**(10): p. 1279-86.
373. Tipps, M.E., et al., *Identification of novel specific allosteric modulators of the glycine receptor using phage display.* J Biol Chem, 2010. **285**(30): p. 22840-5.
374. Tao, J., et al., *Drug target validation: lethal infection blocked by inducible peptide.* Proc Natl Acad Sci U S A, 2000. **97**(2): p. 783-6.
375. Hong, H.Y., et al., *Phage display selection of peptides that home to atherosclerotic plaques: IL-4 receptor as a candidate target in atherosclerosis.* J Cell Mol Med, 2008. **12**(5b): p. 2003-14.
376. Sergeeva, A., et al., *Display technologies: application for the discovery of drug and gene delivery agents.* Adv Drug Deliv Rev, 2006. **58**(15): p. 1622-54.
377. Arap, W., et al., *Steps toward mapping the human vasculature by phage display.* Nat Med, 2002. **8**(2): p. 121-7.
378. Rowley, M.J., K. O'Connor, and L. Wijeyewickrema, *Phage display for epitope determination: a paradigm for identifying receptor-ligand interactions.* Biotechnol Annu Rev, 2004. **10**: p. 151-88.
379. Smith, G.P. and V.A. Petrenko, *Phage Display.* Chem Rev, 1997. **97**(2): p. 391-410.
380. Bratkovic, T., *Progress in phage display: evolution of the technique and its application.* Cell Mol Life Sci, 2010. **67**(5): p. 749-67.
381. Gamkrelidze, M. and K. Dabrowska, *T4 bacteriophage as a phage display platform.* Arch Microbiol, 2014. **196**(7): p. 473-9.
382. Teesalu, T., K.N. Sugahara, and E. Ruoslahti, *Mapping of vascular ZIP codes by phage display.* Methods Enzymol, 2012. **503**: p. 35-56.
383. Nicastro, J., K. Sheldon, and R.A. Slavcev, *Bacteriophage lambda display systems: developments and applications.* Appl Microbiol Biotechnol, 2014. **98**(7): p. 2853-66.
384. Rakonjac, J., et al., *Filamentous bacteriophage: biology, phage display and nanotechnology applications.* Curr Issues Mol Biol, 2011. **13**(2): p. 51-76.
385. Marvin, D.A., M.F. Symmons, and S.K. Straus, *Structure and assembly of filamentous bacteriophages.* Prog Biophys Mol Biol, 2014. **114**(2): p. 80-122.

386. Whitehorn, E.A., et al., *A generic method for expression and use of "tagged" soluble versions of cell surface receptors.* Biotechnology (N Y), 1995. **13**(11): p. 1215-9.
387. Newland, A., *Romiplostim: a breakthrough treatment for the management of immune thrombocytopenic purpura.* Eur J Haematol Suppl, 2009(71): p. 20-5.
388. Ranganath, S., et al., *Discovery and Characterization of a Potent Interleukin-6 Binding Peptide with Neutralizing Activity In Vivo.* PLoS One, 2015. **10**(11): p. e0141330.
389. Wang, X.L., et al., *A thrombopoietin receptor antagonist is capable of depleting myelofibrosis hematopoietic stem and progenitor cells.* Blood, 2016. **127**(26): p. 3398-3409.
390. Ngo, A., et al., *A Phenotypic Screen for Small-Molecule Inhibitors of Constitutively Active Mutant Thrombopoietin Receptor Implicated in Myeloproliferative Neoplasms.* Combinatorial Chemistry & High Throughput Screening, 2016. **19**(10): p. 824-833.
391. Shochat, C., et al., *Novel activating mutations lacking cysteine in type I cytokine receptors in acute lymphoblastic leukemia.* Blood, 2014. **124**(1): p. 106-10.
392. Shochat, C., et al., *Gain-of-function mutations in interleukin-7 receptor-alpha (IL7R) in childhood acute lymphoblastic leukemias.* J Exp Med, 2011. **208**(5): p. 901-8.
393. Zenatti, P.P., et al., *Oncogenic IL7R gain-of-function mutations in childhood T-cell acute lymphoblastic leukemia.* Nat Genet, 2011. **43**(10): p. 932-9.
394. Bridgford, J.L., et al., *Novel Drivers and Modifiers of MPL-dependent Oncogenic Transformation Identified by Deep Mutational Scanning.* Blood, 2019.
395. Chaligne, R., et al., *New mutations of MPL in primitive myelofibrosis: only the MPL W515 mutations promote a G(1)/S-phase transition.* Leukemia, 2008. **22**(8): p. 1557-1566.
396. Onishi, M., et al., *Identification of an oncogenic form of the thrombopoietin receptor MPL using retrovirus-mediated gene transfer.* Blood, 1996. **88**(4): p. 1399-1406.
397. Ding, J., et al., *The Asn505 mutation of the c-MPL gene, which causes familial essential thrombocythemia, induces autonomous homodimerization of the c-Mpl protein due to strong amino acid polarity.* Blood, 2009. **114**(15): p. 3325-8.
398. Stepanenko, A.A. and V.V. Dmitrenko, *HEK293 in cell biology and cancer research: phenotype, karyotype, tumorigenicity, and stress-induced genome-phenotype evolution.* Gene, 2015. **569**(2): p. 182-90.
399. Teofili, L., et al., *Markers of myeloproliferative diseases in childhood polycythemia vera and essential thrombocythemia.* J Clin Oncol, 2007. **25**(9): p. 1048-53.
400. Liu, K., et al., *Evidence for a founder effect of the MPL-S505N mutation in eight Italian pedigrees with hereditary thrombocythemia.* Haematologica, 2009. **94**(10): p. 1368-74.
401. Morrell, R., et al., *Nonfamilial, MPL S505N-Mutated Essential Thrombocythaemia.* Case Rep Hematol, 2013. **2013**: p. 729327.
402. Inc., T.B. *MSCV retrovirus system*. 2019 22 Nov 2019]; Available from: https://www.takarabio.com/products/gene-function/viral-transduction/retrovirus/vector-systems/mscv-system.
403. Defour, J.P., et al., *The S505A thrombopoietin receptor mutation in childhood hereditary thrombocytosis and essential thrombocythemia is S505N: single letter amino acid code matters.* Leukemia, 2019. **33**(2): p. 563-564.
404. (CRI), C.f.R.a.I. *Binding group: Finding novel fabric binding peptides*. Available from: http://2016.igem.org/Team:Paris_Bettencourt/Project/Binding.
405. Zorzi, A., K. Deyle, and C. Heinis, *Cyclic peptide therapeutics: past, present and future.* Curr Opin Chem Biol, 2017. **38**: p. 24-29.
406. Kang, H.K., et al., *Therapeutic Properties and Biological Benefits of Marine-Derived Anticancer Peptides.* Int J Mol Sci, 2018. **19**(3).
407. C Fromageot, a. and M. Jutisz, *Chemistry of Amino Acids, Peptides, and Proteins.* Annual Review of Biochemistry, 1953. **22**(1): p. 629-678.
408. Horton, D.A., G.T. Bourne, and M.L. Smythe, *Exploring privileged structures: the combinatorial synthesis of cyclic peptides.* Mol Divers, 2002. **5**(4): p. 289-304.
409. Joo, S.H., *Cyclic peptides as therapeutic agents and biochemical tools.* Biomolecules & therapeutics, 2012. **20**(1): p. 19-26.

410. Veya, L., J. Piguet, and H. Vogel, *Single Molecule Imaging Deciphers the Relation between Mobility and Signaling of a Prototypical G Protein-coupled Receptor in Living Cells.* J Biol Chem, 2015. **290**(46): p. 27723-35.
411. Wilmes, S., et al., *Receptor dimerization dynamics as a regulatory valve for plasticity of type I interferon signaling.* J Cell Biol, 2015. **209**(4): p. 579-93.
412. Manley, S., et al., *High-density mapping of single-molecule trajectories with photoactivated localization microscopy.* Nat Methods, 2008. **5**(2): p. 155-7.
413. Shrivastava, A.N., et al., *Dynamic micro-organization of P2X7 receptors revealed by PALM based single particle tracking.* Front Cell Neurosci, 2013. **7**: p. 232.
414. Mattheyses, A.L., S.M. Simon, and J.Z. Rappoport, *Imaging with total internal reflection fluorescence microscopy for the cell biologist.* J Cell Sci, 2010. **123**(Pt 21): p. 3621-8.
415. Rines, D.R., et al., *Live cell imaging of yeast.* Cold Spring Harb Protoc, 2011. **2011**(9).
416. Kusumi, A. and Y. Sako, *Cell surface organization by the membrane skeleton.* Curr Opin Cell Biol, 1996. **8**(4): p. 566-74.
417. Sheetz, M.P., *Membrane skeletal dynamics: role in modulation of red cell deformability, mobility of transmembrane proteins, and shape.* Semin Hematol, 1983. **20**(3): p. 175-88.
418. Taylor, R.D., et al., *Neuronal Receptors Display Cytoskeleton-Independent Directed Motion on the Plasma Membrane.* iScience, 2018. **10**: p. 234-244.
419. Tinevez, J.Y., et al., *TrackMate: An open and extensible platform for single-particle tracking.* Methods, 2017. **115**: p. 80-90.
420. Vega, A.R., et al., *Multistep Track Segmentation and Motion Classification for Transient Mobility Analysis.* Biophys J, 2018. **114**(5): p. 1018-1025.
421. Ferrari, R., A.J. Manfroi, and W.R. Young, *Strongly and weakly self-similar diffusion.* Phys. D, 2001. **154**(1-2): p. 111-137.
422. Jaqaman, K., et al., *Cytoskeletal control of CD36 diffusion promotes its receptor and signaling function.* Cell, 2011. **146**(4): p. 593-606.
423. Levet, F., et al., *SR-Tesseler: a method to segment and quantify localization-based super-resolution microscopy data.* Nat Methods, 2015. **12**(11): p. 1065-71.
424. Brejchova, J., et al., *TRH-receptor mobility and function in intact and cholesterol-depleted plasma membrane of HEK293 cells stably expressing TRH-R-eGFP.* Biochim Biophys Acta, 2015. **1848**(3): p. 781-96.
425. Yamazaki, S., et al., *Cytokine signals modulated via lipid rafts mimic niche signals and induce hibernation in hematopoietic stem cells.* EMBO J, 2006. **25**(15): p. 3515-23.
426. Ariotti, N., et al., *Epidermal growth factor receptor activation remodels the plasma membrane lipid environment to induce nanocluster formation.* Mol Cell Biol, 2010. **30**(15): p. 3795-804.
427. Pageon, S.V., et al., *Functional role of T-cell receptor nanoclusters in signal initiation and antigen discrimination.* Proc Natl Acad Sci U S A, 2016. **113**(37): p. E5454-63.
428. Triller, A. and D. Choquet, *New concepts in synaptic biology derived from single-molecule imaging.* Neuron, 2008. **59**(3): p. 359-74.
429. Serge, A., et al., *Receptor activation and homer differentially control the lateral mobility of metabotropic glutamate receptor 5 in the neuronal membrane.* J Neurosci, 2002. **22**(10): p. 3910-20.
430. Marchetti, L., et al., *Ligand signature in the membrane dynamics of single TrkA receptor molecules.* J Cell Sci, 2013. **126**(Pt 19): p. 4445-56.
431. Barak, L.S. and W.W. Webb, *Diffusion of low density lipoprotein-receptor complex on human fibroblasts.* J Cell Biol, 1982. **95**(3): p. 846-52.
432. Thoumine, O., et al., *Weak Effect of Membrane Diffusion on the Rate of Receptor Accumulation at Adhesive Contacts.* Biophysical Journal, 2005. **89**(5): p. L40-L42.
433. Allsopp, R.C., U. Lalo, and R.J. Evans, *Lipid raft association and cholesterol sensitivity of P2X1-4 receptors for ATP: chimeras and point mutants identify intracellular amino-terminal residues involved in lipid regulation of P2X1 receptors.* J Biol Chem, 2010. **285**(43): p. 32770-7.
434. Roosterman, D., et al., *Recycling and resensitization of the neurokinin 1 receptor. Influence of agonist concentration and Rab GTPases.* J Biol Chem, 2004. **279**(29): p. 30670-9.

435. Cezanne, L., et al., *Dynamic confinement of NK2 receptors in the plasma membrane. Improved FRAP analysis and biological relevance.* J Biol Chem, 2004. **279**(43): p. 45057-67.
436. Ehrlich, M., et al., *Endocytosis by random initiation and stabilization of clathrin-coated pits.* Cell, 2004. **118**(5): p. 591-605.
437. den Otter, W.K. and W.J. Briels, *The generation of curved clathrin coats from flat plaques.* Traffic, 2011. **12**(10): p. 1407-16.
438. Andrews, N.L., et al., *Actin restricts FcεRI diffusion and facilitates antigen-induced receptor immobilization.* Nature Cell Biology, 2008. **10**(8): p. 955-963.
439. Bouzigues, C., et al., *Asymmetric redistribution of GABA receptors during GABA gradient sensing by nerve growth cones analyzed by single quantum dot imaging.* Proceedings of the National Academy of Sciences, 2007. **104**(27): p. 11251-11256.
440. Chung, I., et al., *Spatial control of EGF receptor activation by reversible dimerization on living cells.* Nature, 2010. **464**(7289): p. 783-7.
441. Kasai, R.S., et al., *Full characterization of GPCR monomer-dimer dynamic equilibrium by single molecule imaging.* J Cell Biol, 2011. **192**(3): p. 463-80.
442. Lill, Y., et al., *Kinetics of the initial steps of G protein-coupled receptor-mediated cellular signaling revealed by single-molecule imaging.* Chemphyschem, 2005. **6**(8): p. 1633-40.
443. Winter, P.W., et al., *Actin-dependent clustering of insulin receptors in membrane microdomains.* Biochim Biophys Acta, 2012. **1818**(3): p. 467-73.
444. Schaaf, M.J. and J.A. Cidlowski, *Molecular determinants of glucocorticoid receptor mobility in living cells: the importance of ligand affinity.* Mol Cell Biol, 2003. **23**(6): p. 1922-34.
445. Care, B.R. and H.A. Soula, *Impact of receptor clustering on ligand binding.* BMC Syst Biol, 2011. **5**: p. 48.
446. Gopalakrishnan, M., et al., *Effects of receptor clustering on ligand dissociation kinetics: theory and simulations.* Biophys J, 2005. **89**(6): p. 3686-700.
447. Jurak, A.B., et al. *Filamin A stabilizes thrombopoietin receptor surface expression and inhibits its degradation*. in *2nd European Platelet Network (EUPLAN) Conference*. 2014.
448. Hibino, K., et al., *Single- and multiple-molecule dynamics of the signaling from H-Ras to cRaf-1 visualized on the plasma membrane of living cells.* Chemphyschem, 2003. **4**(7): p. 748-53.
449. Matsuoka, S., T. Shibata, and M. Ueda, *Asymmetric PTEN distribution regulated by spatial heterogeneity in membrane-binding state transitions.* PLoS Comput Biol, 2013. **9**(1): p. e1002862.
450. Clayton, A.H., M.L. Tavarnesi, and T.G. Johns, *Unligated epidermal growth factor receptor forms higher order oligomers within microclusters on A431 cells that are sensitive to tyrosine kinase inhibitor binding.* Biochemistry, 2007. **46**(15): p. 4589-97.
451. Hofman, E.G., et al., *Ligand-induced EGF receptor oligomerization is kinase-dependent and enhances internalization.* J Biol Chem, 2010. **285**(50): p. 39481-9.
452. Boersma, Y.L., et al., *Bispecific designed ankyrin repeat proteins (DARPins) targeting epidermal growth factor receptor inhibit A431 cell proliferation and receptor recycling.* J Biol Chem, 2011. **286**(48): p. 41273-85.
453. Friedman, L.M., et al., *Synergistic down-regulation of receptor tyrosine kinases by combinations of mAbs: implications for cancer immunotherapy.* Proc Natl Acad Sci U S A, 2005. **102**(6): p. 1915-20.
454. Spangler, J.B., et al., *Combination antibody treatment down-regulates epidermal growth factor receptor by inhibiting endosomal recycling.* Proc Natl Acad Sci U S A, 2010. **107**(30): p. 13252-7.
455. Hackel, B.J., et al., *Epidermal growth factor receptor downregulation by small heterodimeric binding proteins.* Protein Eng Des Sel, 2012. **25**(2): p. 47-57.
456. Bag, N., S. Huang, and T. Wohland, *Plasma Membrane Organization of Epidermal Growth Factor Receptor in Resting and Ligand-Bound States.* Biophys J, 2015. **109**(9): p. 1925-36.
457. Lemmon, M.A. and J. Schlessinger, *Cell signaling by receptor tyrosine kinases.* Cell, 2010. **141**(7): p. 1117-34.
458. Yang, S., et al., *Mapping ErbB receptors on breast cancer cell membranes during signal transduction.* J Cell Sci, 2007. **120**(Pt 16): p. 2763-73.
459. Lillemeier, B.F., et al., *TCR and Lat are expressed on separate protein islands on T cell membranes and concatenate during activation.* Nat Immunol, 2010. **11**(1): p. 90-6.

460. Schamel, W.W. and B. Alarcon, *Organization of the resting TCR in nanoscale oligomers.* Immunol Rev, 2013. **251**(1): p. 13-20.
461. Schamel, W.W., et al., *Coexistence of multivalent and monovalent TCRs explains high sensitivity and wide range of response.* J Exp Med, 2005. **202**(4): p. 493-503.
462. Sherman, E., et al., *Functional nanoscale organization of signaling molecules downstream of the T cell antigen receptor.* Immunity, 2011. **35**(5): p. 705-20.
463. Kumar, R., et al., *Increased sensitivity of antigen-experienced T cells through the enrichment of oligomeric T cell receptor complexes.* Immunity, 2011. **35**(3): p. 375-87.
464. Alarcon, B., et al., *T-cell antigen-receptor stoichiometry: pre-clustering for sensitivity.* EMBO Rep, 2006. **7**(5): p. 490-5.
465. Grecco, Hernán E., M. Schmick, and Philippe I.H. Bastiaens, *Signaling from the Living Plasma Membrane.* Cell, 2011. **144**(6): p. 897-909.
466. Costa, M.N., K. Radhakrishnan, and J.S. Edwards, *Monte Carlo simulations of plasma membrane corral-induced EGFR clustering.* J Biotechnol, 2011. **151**(3): p. 261-70.
467. Abulrob, A., et al., *Nanoscale imaging of epidermal growth factor receptor clustering: effects of inhibitors.* J Biol Chem, 2010. **285**(5): p. 3145-56.
468. Takizawa, H., et al., *Lnk regulates integrin alphaIIbbeta3 outside-in signaling in mouse platelets, leading to stabilization of thrombus development in vivo.* J Clin Invest, 2010. **120**(1): p. 179-90.
469. Campeau, E., et al., *A versatile viral system for expression and depletion of proteins in mammalian cells.* PLoS One, 2009. **4**(8): p. e6529.
470. Magor, G.W., et al., *Rapid Molecular Profiling of Myeloproliferative Neoplasms Using Targeted Exon Resequencing of 86 Genes Involved in JAK-STAT Signaling and Epigenetic Regulation.* J Mol Diagn, 2016. **18**(5): p. 707-718.
471. Zou, H., D. Yan, and G. Mohi, *Differential biological activity of disease-associated JAK2 mutants.* FEBS Lett, 2011. **585**(7): p. 1007-13.
472. Ferrao, R. and P.J. Lupardus, *The Janus Kinase (JAK) FERM and SH2 Domains: Bringing Specificity to JAK-Receptor Interactions.* Front Endocrinol (Lausanne), 2017. **8**: p. 71.
473. Huang, X., et al., *Cloning and characterization of Lnk, a signal transduction protein that links T-cell receptor activation signal to phospholipase C gamma 1, Grb2, and phosphatidylinositol 3-kinase.* Proc Natl Acad Sci U S A, 1995. **92**(25): p. 11618-22.
474. Jiang, J., et al., *14-3-3 regulates the LNK/JAK2 pathway in mouse hematopoietic stem and progenitor cells.* Journal of Clinical Investigation, 2012. **122**(6): p. 2079-2091.
475. Carlesso, N., D.A. Frank, and J.D. Griffin, *Tyrosyl phosphorylation and DNA binding activity of signal transducers and activators of transcription (STAT) proteins in hematopoietic cell lines transformed by Bcr/Abl.* J Exp Med, 1996. **183**(3): p. 811-20.
476. Bastarache, L., et al., *Phenotype risk scores identify patients with unrecognized Mendelian disease patterns.* Science, 2018. **359**(6381): p. 1233-1239.
477. Migliaccio, G., et al., *Isolation of pure megakaryocytic clones (32D TPO) from the murine multipotent IL-3-dependent 32D cell line.* Experimental Hematology, 2000. **28**(7): p. 77-77.
478. Amabile, G., et al., *Isolation of TPO-dependent subclones from the multipotent 32D cell line.* Blood Cells Mol Dis, 2005. **35**(2): p. 241-52.
479. Tate, J.G., et al., *COSMIC: the Catalogue Of Somatic Mutations In Cancer.* Nucleic Acids Res, 2019. **47**(D1): p. D941-D947.
480. Demain, A.L. and P. Vaishnav, *Production of recombinant proteins by microbes and higher organisms.* Biotechnol Adv, 2009. **27**(3): p. 297-306.
481. Makino, T., G. Skretas, and G. Georgiou, *Strain engineering for improved expression of recombinant proteins in bacteria.* Microb Cell Fact, 2011. **10**: p. 32.
482. Zerbs, S., A.M. Frank, and F.R. Collart, *Bacterial systems for production of heterologous proteins.* Methods Enzymol, 2009. **463**: p. 149-68.
483. Makrides, S.C., *Strategies for achieving high-level expression of genes in Escherichia coli.* Microbiol Rev, 1996. **60**(3): p. 512-38.
484. Hayat, S.M.G., et al., *Recombinant Protein Expression in Escherichia coli (E.coli): What We Need to Know.* Curr Pharm Des, 2018. **24**(6): p. 718-725.

485. Stevens, R.C., *Design of high-throughput methods of protein production for structural biology.* Structure, 2000. **8**(9): p. R177-85.
486. Jana, S. and J.K. Deb, *Strategies for efficient production of heterologous proteins in Escherichia coli.* Appl Microbiol Biotechnol, 2005. **67**(3): p. 289-98.
487. Sorensen, H.P. and K.K. Mortensen, *Advanced genetic strategies for recombinant protein expression in Escherichia coli.* J Biotechnol, 2005. **115**(2): p. 113-28.
488. Fei, D., et al., *Correction: Codon Optimization, Expression in Escherichia coli, and Immunogenicity of Recombinant Chinese Sacbrood Virus (CSBV) Structural Proteins VP1, VP2, and VP3.* PLoS One, 2015. **10**(7): p. e0134423.
489. Burgess-Brown, N.A., et al., *Codon optimization can improve expression of human genes in Escherichia coli: A multi-gene study.* Protein Expr Purif, 2008. **59**(1): p. 94-102.
490. Maertens, B., et al., *Gene optimization mechanisms: a multi-gene study reveals a high success rate of full-length human proteins expressed in Escherichia coli.* Protein Sci, 2010. **19**(7): p. 1312-26.
491. Yadava, A. and C.F. Ockenhouse, *Effect of codon optimization on expression levels of a functionally folded malaria vaccine candidate in prokaryotic and eukaryotic expression systems.* Infect Immun, 2003. **71**(9): p. 4961-9.
492. Tian, J., et al., *Predicting synonymous codon usage and optimizing the heterologous gene for expression in E. coli.* Sci Rep, 2017. **7**(1): p. 9926.
493. Zhou, Z., et al., *Codon usage is an important determinant of gene expression levels largely through its effects on transcription.* Proc Natl Acad Sci U S A, 2016. **113**(41): p. E6117-e6125.
494. Contreras-Gomez, A., et al., *Protein production using the baculovirus-insect cell expression system.* Biotechnol Prog, 2014. **30**(1): p. 1-18.
495. Khan, K.H., *Gene expression in Mammalian cells and its applications.* Adv Pharm Bull, 2013. **3**(2): p. 257-63.
496. Coskun, O., *Separation techniques: Chromatography.* North Clin Istanb, 2016. **3**(2): p. 156-160.
497. Liu, Z.Z., S.R. Wickramasinghe, and X.H. Qian, *Membrane chromatography for protein purifications from ligand design to functionalization.* Separation Science and Technology, 2017. **52**(2): p. 299-319.
498. Lebendiker, M., M. Maes, and A. Friedler, *A screening methodology for purifying proteins with aggregation problems.* Methods Mol Biol, 2015. **1258**: p. 261-81.
499. Bondos, S.E. and A. Bicknell, *Detection and prevention of protein aggregation before, during, and after purification.* Anal Biochem, 2003. **316**(2): p. 223-31.
500. Hu, J. and S.R. Hubbard, *Structural basis for phosphotyrosine recognition by the Src homology-2 domains of the adapter proteins SH2-B and APS.* J Mol Biol, 2006. **361**(1): p. 69-79.
501. McKercher, M.A., et al., *Diversity in peptide recognition by the SH2 domain of SH2B1.* Proteins, 2018. **86**(2): p. 164-176.
502. Catanzariti, A.M., et al., *An efficient system for high-level expression and easy purification of authentic recombinant proteins.* Protein Sci, 2004. **13**(5): p. 1331-9.
503. Gustafsson, C., et al., *Engineering genes for predictable protein expression.* Protein Expr Purif, 2012. **83**(1): p. 37-46.
504. Wilkinson, G.W. and A. Akrigg, *Constitutive and enhanced expression from the CMV major IE promoter in a defective adenovirus vector.* Nucleic Acids Res, 1992. **20**(9): p. 2233-9.
505. Hartl, F.U., R. Hlodan, and T. Langer, *Molecular chaperones in protein folding: the art of avoiding sticky situations.* Trends Biochem Sci, 1994. **19**(1): p. 20-5.
506. Stuart, R.A., et al., *Mitochondrial molecular chaperones: their role in protein translocation.* Trends Biochem Sci, 1994. **19**(2): p. 87-92.
507. Hendrick, J.P. and F.U. Hartl, *Molecular chaperone functions of heat-shock proteins.* Annu Rev Biochem, 1993. **62**: p. 349-84.
508. Hendrick, J.P. and F.U. Hartl, *The role of molecular chaperones in protein folding.* Faseb j, 1995. **9**(15): p. 1559-69.
509. Monahan, F.J., J.B. German, and J.E. Kinsella, *Effect of Ph and Temperature on Protein Unfolding and Thiol-Disulfide Interchange Reactions during Heat-Induced Gelation of Whey Proteins.* Journal of Agricultural and Food Chemistry, 1995. **43**(1): p. 46-52.

510. Shaw, K.L., et al., *The effect of net charge on the solubility, activity, and stability of ribonuclease Sa.* Protein Sci, 2001. **10**(6): p. 1206-15.
511. Becktel, W.J. and W.A. Baase, *Thermal denaturation of bacteriophage T4 lysozyme at neutral pH.* Biopolymers, 1987. **26**(5): p. 619-23.
512. Pace, C.N., D.V. Laurents, and R.E. Erickson, *Urea denaturation of barnase: pH dependence and characterization of the unfolded state.* Biochemistry, 1992. **31**(10): p. 2728-34.
513. Yegutkin, G.G., *Effect of increasing concentrations of nonionic detergent Triton X-100 on solubilization and structure of rat liver and adipose plasma membranes.* Membr Cell Biol, 1997. **10**(5): p. 515-20.
514. Ashani, Y. and G.N. Catravas, *Highly reactive impurities in Triton X-100 and Brij 35: partial characterization and removal.* Anal Biochem, 1980. **109**(1): p. 55-62.
515. Paradies, H.H., *Shape and size of a nonionic surfactant micelle. Triton X-100 in aqueous solution.* The Journal of Physical Chemistry, 1980. **84**(6): p. 599-607.
516. D'Angelo, I., et al., *A novel bipartite phospholipid-binding module in the neurofibromatosis type 1 protein.* EMBO Rep, 2006. **7**(2): p. 174-9.
517. Streletzky, K. and G.D.J. Phillies, *Temperature Dependence of Triton X-100 Micelle Size and Hydration.* Langmuir, 1995. **11**(1): p. 42-47.
518. Oberthuer, D., et al., *Monitoring and Scoring Counter-Diffusion Protein Crystallization Experiments in Capillaries by in situ Dynamic Light Scattering.* PLOS ONE, 2012. **7**(6): p. e33545.
519. Dierks, K., et al., *Dynamic Light Scattering in Protein Crystallization Droplets: Adaptations for Analysis and Optimization of Crystallization Processes.* Crystal Growth & Design, 2008. **8**(5): p. 1628-1634.
520. Wilson, W.W., *Light scattering as a diagnostic for protein crystal growth--a practical approach.* J Struct Biol, 2003. **142**(1): p. 56-65.
521. Ferre-D'Amare, A.R. and S.K. Burley, *Use of dynamic light scattering to assess crystallizability of macromolecules and macromolecular assemblies.* Structure, 1994. **2**(5): p. 357-9.
522. Kadima, W., et al., *Characterization of precrystallization aggregation of canavalin by dynamic light scattering.* Biophysical Journal, 1990. **57**(1): p. 125-132.
523. Vedadi, M., et al., *Biophysical characterization of recombinant proteins: a key to higher structural genomics success.* J Struct Biol, 2010. **172**(1): p. 107-19.
524. Niesen, F.H., H. Berglund, and M. Vedadi, *The use of differential scanning fluorimetry to detect ligand interactions that promote protein stability.* Nat Protoc, 2007. **2**(9): p. 2212-21.
525. Ericsson, U.B., et al., *Thermofluor-based high-throughput stability optimization of proteins for structural studies.* Anal Biochem, 2006. **357**(2): p. 289-98.
526. Vedadi, M., et al., *Chemical screening methods to identify ligands that promote protein stability, protein crystallization, and structure determination.* Proc Natl Acad Sci U S A, 2006. **103**(43): p. 15835-40.
527. Kohlstaedt, M., et al., *Development of a Thermofluor assay for stability determination of membrane proteins using the Na(+)/H(+) antiporter NhaA and cytochrome c oxidase.* Acta Crystallogr D Biol Crystallogr, 2015. **71**(Pt 5): p. 1112-22.
528. Fan, J., et al., *An efficient strategy for high throughput screening of recombinant integral membrane protein expression and stability.* Protein Expr Purif, 2011. **78**(1): p. 6-13.
529. Liu, W., et al., *LCP-Tm: an assay to measure and understand stability of membrane proteins in a membrane environment.* Biophys J, 2010. **98**(8): p. 1539-48.
530. Alexandrov, A.I., et al., *Microscale fluorescent thermal stability assay for membrane proteins.* Structure, 2008. **16**(3): p. 351-9.
531. Yeh, A.P., A. McMillan, and M.H. Stowell, *Rapid and simple protein-stability screens: application to membrane proteins.* Acta Crystallogr D Biol Crystallogr, 2006. **62**(Pt 4): p. 451-7.
532. Webb, R.L., *Circular Dichroism. Principles and Applications, Second Edition Edited by Nina Berova, Koji Nakanishi, and Robert W. Woody. Wiley-VCH Publishers, New York. 2000. xix + 877 pp. 18.5 × 26 cm. ISBN 0 47133003 5. $195.00.* Journal of Medicinal Chemistry, 2001. **44**(7): p. 1122-1122.
533. Hussain, R., et al., *CDApps: Integrated software for experimental planning and data processing at beamline B23, Diamond Light Source.* Journal of synchrotron radiation, 2015. **22**: p. 465-468.
534. Sreerama, N. and R.W. Woody, *On the analysis of membrane protein circular dichroism spectra.* Protein Sci, 2004. **13**(1): p. 100-12.

535. Siligardi, G. and R. Hussain, *CD spectroscopy: an essential tool for quality control of protein folding.* Methods Mol Biol, 2015. **1261**: p. 255-76.
536. Siligardi, G. and R. Hussain, *Biomolecules interactions and competitions by non-immobilised ligand interaction assay by circular dichroism.* Enantiomer, 1998. **3**(2): p. 77-87.
537. Lorber, B., et al., *Protein analysis by dynamic light scattering: methods and techniques for students.* Biochem Mol Biol Educ, 2012. **40**(6): p. 372-82.
538. Varghese, L.N., et al., *Mechanistic insights into activation and SOCS3-mediated inhibition of myeloproliferative neoplasm-associated JAK2 mutants from biochemical and structural analyses.* Biochem J, 2014. **458**(2): p. 395-405.
539. Inaba, S., et al., *Crystal Structures and Thermodynamic Analysis Reveal Distinct Mechanisms of CD28 Phosphopeptide Binding to the Src Homology 2 (SH2) Domains of Three Adaptor Proteins.* J Biol Chem, 2017. **292**(3): p. 1052-1060.
540. Higo, K., et al., *High Resolution Crystal Structure of the Grb2 SH2 Domain with a Phosphopeptide Derived from CD28.* PLOS ONE, 2013. **8**(9): p. e74482.
541. Zadjali, F., et al., *Structural basis for c-KIT inhibition by the suppressor of cytokine signaling 6 (SOCS6) ubiquitin ligase.* J Biol Chem, 2011. **286**(1): p. 480-90.
542. Condon, R.G., et al., *Development of a Chinese hamster ovary cell line for recombinant adenovirus-mediated gene expression.* Biotechnol Prog, 2003. **19**(1): p. 137-43.
543. Reinhard, L., et al., *Optimization of protein buffer cocktails using Thermofluor.* Acta Crystallogr Sect F Struct Biol Cryst Commun, 2013. **69**(Pt 2): p. 209-14.
544. Kozak, S., et al., *Optimization of protein samples for NMR using thermal shift assays.* J Biomol NMR, 2016. **64**(4): p. 281-9.
545. Seabrook, S.A. and J. Newman, *High-throughput thermal scanning for protein stability: making a good technique more robust.* ACS Comb Sci, 2013. **15**(8): p. 387-92.
546. Chen, K.E., et al., *Molecular Basis for Membrane Recruitment by the PX and C2 Domains of Class II Phosphoinositide 3-Kinase-C2alpha.* Structure, 2018. **26**(12): p. 1612-1625 e4.
547. Hunte, C. and H. Michel, *Crystallisation of membrane proteins mediated by antibody fragments.* Curr Opin Struct Biol, 2002. **12**(4): p. 503-8.
548. Prongay, A.J., et al., *Preparation and crystallization of a human immunodeficiency virus p24-Fab complex.* Proc Natl Acad Sci U S A, 1990. **87**(24): p. 9980-4.
549. Jiang, Y., et al., *X-ray structure of a voltage-dependent K+ channel.* Nature, 2003. **423**(6935): p. 33-41.
550. McKinstry, W.J., et al., *Crystallization of the receptor-binding domain of parathyroid hormone-related protein in complex with a neutralizing monoclonal antibody Fab fragment.* Acta Crystallogr Sect F Struct Biol Cryst Commun, 2009. **65**(Pt 4): p. 336-8.
551. Uysal, S., et al., *Crystal structure of full-length KcsA in its closed conformation.* Proc Natl Acad Sci U S A, 2009. **106**(16): p. 6644-9.
552. Prokop, A. and M.Z. Rosenberg, *Bioreactor for mammalian cell culture.* Adv Biochem Eng Biotechnol, 1989. **39**: p. 29-71.
553. McPherson, A. and J.A. Gavira, *Introduction to protein crystallization.* Acta Crystallogr F Struct Biol Commun, 2014. **70**(Pt 1): p. 2-20.
554. Lorber, B., J.B. Bishop, and L.J. DeLucas, *Purification of octyl beta-D-glucopyranoside and re-estimation of its micellar size.* Biochim Biophys Acta, 1990. **1023**(2): p. 254-65.
555. Chae, P.S., et al., *Maltose-neopentyl glycol (MNG) amphiphiles for solubilization, stabilization and crystallization of membrane proteins.* Nat Methods, 2010. **7**(12): p. 1003-8.
556. Slotboom, D.J., et al., *Static light scattering to characterize membrane proteins in detergent solution.* Methods, 2008. **46**(2): p. 73-82.
557. Strop, P. and A.T. Brunger, *Refractive index-based determination of detergent concentration and its application to the study of membrane proteins.* Protein Sci, 2005. **14**(8): p. 2207-11.
558. Sonoda, Y., et al., *Tricks of the trade used to accelerate high-resolution structure determination of membrane proteins.* FEBS Lett, 2010. **584**(12): p. 2539-47.
559. Parker, J.L. and S. Newstead, *Current trends in alpha-helical membrane protein crystallization: an update.* Protein Sci, 2012. **21**(9): p. 1358-65.

560. Sonoda, Y., et al., *Benchmarking membrane protein detergent stability for improving throughput of high-resolution X-ray structures.* Structure, 2011. **19**(1): p. 17-25.
561. Thiyagarajan, P. and D.M. Tiede, *Detergent micelle structure and micelle-micelle interactions determined by small-angle neutron scattering under solution conditions used for membrane protein crystallization.* The Journal of Physical Chemistry, 1994. **98**(40): p. 10343-10351.
562. Psachoulia, E., P.J. Bond, and M.S. Sansom, *MD simulations of Mistic: conformational stability in detergent micelles and water.* Biochemistry, 2006. **45**(30): p. 9053-8.
563. Durand, G., et al., *New Amphiphiles to Handle Membrane Proteins: "Ménage à Trois" Between Chemistry, Physical Chemistry, and Biochemistry*. 2014.
564. Rosenbaum, D.M., et al., *Structure and function of an irreversible agonist-beta(2) adrenoceptor complex.* Nature, 2011. **469**(7329): p. 236-40.
565. Cho, K.H., et al., *Improved glucose-neopentyl glycol (GNG) amphiphiles for membrane protein solubilization and stabilization.* Chem Asian J, 2014. **9**(2): p. 632-8.
566. Lee, S.C., et al., *Steroid-based facial amphiphiles for stabilization and crystallization of membrane proteins.* Proc Natl Acad Sci U S A, 2013. **110**(13): p. E1203-11.
567. Matar-Merheb, R., et al., *Structuring detergents for extracting and stabilizing functional membrane proteins.* PLoS One, 2011. **6**(3): p. e18036.
568. Fuxreiter, M. and P. Tompa, *Fuzzy complexes: a more stochastic view of protein function.* Adv Exp Med Biol, 2012. **725**: p. 1-14.
569. Tycko, R., *Biomolecular solid state NMR: advances in structural methodology and applications to peptide and protein fibrils.* Annu Rev Phys Chem, 2001. **52**: p. 575-606.
570. McDermott, A.E., *Structural and dynamic studies of proteins by solid-state NMR spectroscopy: rapid movement forward.* Curr Opin Struct Biol, 2004. **14**(5): p. 554-61.
571. Wuthrich, K., *Protein structure determination in solution by NMR spectroscopy.* J Biol Chem, 1990. **265**(36): p. 22059-62.
572. Wagner, G., *An account of NMR in structural biology.* Nat Struct Biol, 1997. **4 Suppl**: p. 841-4.
573. Fu, R. and T.A. Cross, *SOLID-STATE NUCLEAR MAGNETIC RESONANCE INVESTIGATION OF PROTEIN AND POLYPEPTIDE STRUCTURE.* Annual Review of Biophysics and Biomolecular Structure, 1999. **28**(1): p. 235-268.
574. Matthews, S.J., *NMR of proteins and nucleic acids*, in *Nuclear Magnetic Resonance: Volume 36*. 2007, The Royal Society of Chemistry. p. 262-284.
575. Putnam, C.D., et al., *X-ray solution scattering (SAXS) combined with crystallography and computation: defining accurate macromolecular structures, conformations and assemblies in solution.* Q Rev Biophys, 2007. **40**(3): p. 191-285.
576. Rambo, R.P. and J.A. Tainer, *Accurate assessment of mass, models and resolution by small-angle scattering.* Nature, 2013. **496**(7446): p. 477-481.
577. Herzik, M.A., M. Wu, and G.C. Lander, *High-resolution structure determination of sub-100 kDa complexes using conventional cryo-EM.* Nature Communications, 2019. **10**(1): p. 1032.
578. Khoshouei, M., et al., *Cryo-EM structure of haemoglobin at 3.2 Å determined with the Volta phase plate.* Nature communications, 2017. **8**: p. 16099-16099.
579. Fan, X., et al., *Single particle cryo-EM reconstruction of 52 kDa streptavidin at 3.2 Angstrom resolution.* Nature Communications, 2019. **10**(1): p. 2386.
580. Campbell, M.G., et al., *2.8 A resolution reconstruction of the Thermoplasma acidophilum 20S proteasome using cryo-electron microscopy.* Elife, 2015. **4**.
581. Banerjee, S., et al., *2.3 A resolution cryo-EM structure of human p97 and mechanism of allosteric inhibition.* Science, 2016. **351**(6275): p. 871-5.
582. Zhang, X., et al., *An Atomic Structure of the Human Spliceosome.* Cell, 2017. **169**(5): p. 918-929 e14.
583. Greber, B.J., et al., *The cryo-electron microscopy structure of human transcription factor IIH.* Nature, 2017. **549**: p. 414.
584. Hirschi, M., et al., *Cryo-electron microscopy structure of the lysosomal calcium-permeable channel TRPML3.* Nature, 2017. **550**: p. 411.
585. Kamat, V. and A. Rafique, *Extending the throughput of Biacore 4000 biosensor to accelerate kinetic analysis of antibody-antigen interaction.* Anal Biochem, 2017. **530**: p. 75-86.

586. Rich, R.L. and D.G. Myszka, *BIACORE J: a new platform for routine biomolecular interaction analysis.* J Mol Recognit, 2001. **14**(4): p. 223-8.
587. Todd, M.J. and J. Gomez, *Enzyme kinetics determined using calorimetry: a general assay for enzyme activity?* Anal Biochem, 2001. **296**(2): p. 179-87.
588. Williams, B.A. and E.J. Toone, *Calorimetric evaluation of enzyme kinetic parameters.* The Journal of Organic Chemistry, 1993. **58**(13): p. 3507-3510.
589. Lewis, E.A. and K.P. Murphy, *Isothermal titration calorimetry.* Methods Mol Biol, 2005. **305**: p. 1-16.
590. Gaborit, N., et al., *Time-resolved fluorescence resonance energy transfer (TR-FRET) to analyze the disruption of EGFR/HER2 dimers: a new method to evaluate the efficiency of targeted therapy using monoclonal antibodies.* J Biol Chem, 2011. **286**(13): p. 11337-45.
591. Degorce, F., et al., *HTRF: A technology tailored for drug discovery - a review of theoretical aspects and recent applications.* Curr Chem Genomics, 2009. **3**: p. 22-32.
592. Mathis, G., *HTRF(R) Technology.* J Biomol Screen, 1999. **4**(6): p. 309-314.
593. Tefferi, A., *Primary myelofibrosis: 2019 update on diagnosis, risk-stratification and management.* Am J Hematol, 2018. **93**(12): p. 1551-1560.
594. Baxter, E.J., et al., *Acquired mutation of the tyrosine kinase JAK2 in human myeloproliferative disorders.* Lancet, 2005. **365**(9464): p. 1054-61.
595. Yoda, A., et al., *Functional screening identifies CRLF2 in precursor B-cell acute lymphoblastic leukemia.* Proc Natl Acad Sci U S A, 2010. **107**(1): p. 252-7.
596. Chapiro, E., et al., *Activating mutation in the TSLPR gene in B-cell precursor lymphoblastic leukemia.* Leukemia, 2010. **24**(3): p. 642-5.
597. Weijenborg Campos, L., et al., *Oncogenic basic amino acid insertions at the extracellular juxtamembrane region of IL7RA cause receptor hypersensitivity.* Blood, 2019. **133**(11): p. 1259-1263.
598. Ohashi, H., et al., *Two rare MPL gene mutations in patients with essential thrombocythemia.* International journal of hematology, 2009. **90**: p. 431-2.
599. Ma, W., et al., *MPL mutation profile in JAK2 mutation-negative patients with myeloproliferative disorders.* Diagn Mol Pathol, 2011. **20**(1): p. 34-9.
600. Russell, L.J., et al., *Deregulated expression of cytokine receptor gene, CRLF2, is involved in lymphoid transformation in B-cell precursor acute lymphoblastic leukemia.* Blood, 2009. **114**(13): p. 2688-98.
601. Mullighan, C.G., et al., *Rearrangement of CRLF2 in B-progenitor- and Down syndrome-associated acute lymphoblastic leukemia.* Nat Genet, 2009. **41**(11): p. 1243-6.
602. Ensor, H.M., et al., *Demographic, clinical, and outcome features of children with acute lymphoblastic leukemia and CRLF2 deregulation: results from the MRC ALL97 clinical trial.* Blood, 2011. **117**(7): p. 2129-36.
603. Iacobucci, I., et al., *Truncating Erythropoietin Receptor Rearrangements in Acute Lymphoblastic Leukemia.* Cancer Cell, 2016. **29**(2): p. 186-200.
604. Renner, M., D. Choquet, and A. Triller, *Control of the postsynaptic membrane viscosity.* J Neurosci, 2009. **29**(9): p. 2926-37.
605. Kuzu, O.F., M.A. Noory, and G.P. Robertson, *The Role of Cholesterol in Cancer.* Cancer Res, 2016. **76**(8): p. 2063-70.
606. Zidovetzki, R. and I. Levitan, *Use of cyclodextrins to manipulate plasma membrane cholesterol content: evidence, misconceptions and control strategies.* Biochim Biophys Acta, 2007. **1768**(6): p. 1311-24.
607. Shrivastava, S., et al., *Chronic cholesterol depletion using statin impairs the function and dynamics of human serotonin(1A) receptors.* Biochemistry, 2010. **49**(26): p. 5426-35.
608. Zhong, S., et al., *Statin use and mortality in cancer patients: Systematic review and meta-analysis of observational studies.* Cancer Treat Rev, 2015. **41**(6): p. 554-67.
609. Murphy, A.J., et al., *Cholesterol efflux in megakaryocyte progenitors suppresses platelet production and thrombocytosis.* Nature medicine, 2013. **19**(5): p. 586-594.
610. Marmor, M.D. and M. Julius, *Role for lipid rafts in regulating interleukin-2 receptor signaling.* Blood, 2001. **98**(5): p. 1489-97.

611. Tamarit, B., et al., *Correction: Membrane microdomains and cytoskeleton organization shape and regulate the IL-7 receptor signalosome in human CD4 T-cells.* J Biol Chem, 2019. **294**(13): p. 5212-5213.
612. Jiang, J., et al., *14-3-3 regulates the LNK/JAK2 pathway in mouse hematopoietic stem and progenitor cells.* J Clin Invest, 2012. **122**(6): p. 2079-91.
613. Ferrari, M.L., G.A. Gomez, and H.J. Maccioni, *Spatial organization and stoichiometry of N-terminal domain-mediated glycosyltransferase complexes in Golgi membranes determined by fret microscopy.* Neurochem Res, 2012. **37**(6): p. 1325-34.

Appendices

Section A: Hetero-FRET Analysis of TPOR TMD Activating Mutants

Introduction

The initiation of the signal transduction downstream is modulated by conformational changes that occur in the receptor upon cytokine binding. The TMD of various receptors has been shown to play an important role in mediating these changes. In the archetypal GHR, cytokine binding leads to a left-handed subunit rotation of the ECD. Consequently, this induces the dimerisation of the TM N-terminus and separation of the TM C-terminus. This conformational change in the GHR induces the separation of the JAK2 JH1 from the JH2 of the corresponding JAK2, both of which are bound to the Box1-Box2 motifs. *Trans*-phosphorylation occurs, resulting in JAK2 activation. This aim seeks to perform hetero-FRET to determine the structural requirements of the Box1-Box2 motifs for signal transmission in TPOR. In particular, the conformational change (via relative distance changes) that occurs between the Box1-Box2 motifs of the receptor monomers after cytokine binding or in clinical mutants (W515K, T487A, S505N) was investigated. This may reveal the relationship between the conformational changes and the pathogenic signalling.

FRET is a technique that is used to analyse protein conformational changes and to determine protein interactions. Hetero-FRET utilises fluorophore pairs such as the cyan fluorescent protein (CFP) and citrine fluorescent protein, which have a high spectral overlap between the emission peak of the donor and the excitation peak of the acceptor. In principle, in the case where the acceptor (CFP-tagged) and donor molecules (citrine-tagged) are in close proximity (between 1-10nm), energy from the excited donor molecule will be transferred to the acceptor, in a process known as FRET (Figure 84). Increased proximity between the donor and acceptor molecules produces a stronger FRET signal and vice versa.

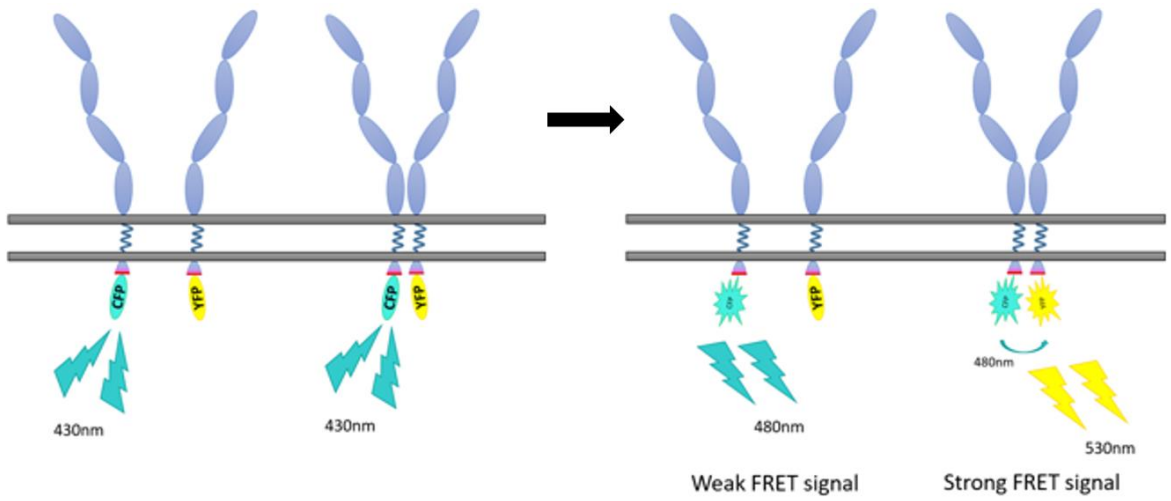

Figure 84: Hetero-FRET of receptor dimers.

Upon excitation of both CFP and Citrine, they emit light of different wavelengths, emission peaks corresponding to both wavelengths will be observed, resulting in a FRET signal. However, when using an excitation wavelength of 480nm, only a CFP emission peak will be observed but if the distance between the acceptor and donor is >10nm, it will result in little to no FRET signal.

Materials and methods

DNA Constructs

The CFP or Citrine fluorescent gene was added to the C-terminus of the Box2 motif (after residue S585 – numberings are based on the original *hMPL* gene without an N-terminal HA-tag) of HA-tagged TPOR (WT, W515K, T487A, S505N) via CPEC essentially as described in Chapter 2, with a short linker separating the receptor and fluorescent gene to provide flexibility.

Transfection

Lenti-X 293T cells were seeded (2×10^5 cells/dish) into 35 mm glass-bottom dishes (Cellvis) and cultured overnight in phenol-red free DMEM supplemented with 10% FBS at 37°C in a humidified 5% CO_2 incubator. Cells were transiently transfected with 50-80 ng of the respective receptor constructs or together with 20-40 ng JAK2 using 1.5 µl Attractene transfection reagent according to manufacturer's instructions (Qiagen). Control plasmids for FRET were also transfected using 30 ng of pmCit-N1 (to calculate acceptor bleed through), pmCFP-N1 (to calculate donor bleed through), or pmCFP-mCit N1 (FRET positive control) [131]. After 10 hours incubation at 37°C, cell starvation was performed for 4-5 hours prior to imaging.

Live Cell Imaging for Hetero-FRET Analysis

Imaging was performed in three channels: donor (cyan), acceptor (citrine), and FRET (magenta) using the spinning disc confocal microscope (SDC) (Nikon) or Inverted LSM 710 BIG confocal microscope (Carl Zeiss GmbH). For the SDC, a 60x oil immersion plan Apochromat objective lens was used. For the inverted confocal microscope, a 63× water immersion plan LD C-Apochromat objective lens with numerical aperture of 1.15 was used. Hetero-FRET was performed essentially as described in [613].

Data Analysis

Description of methods will be based on the images obtained from the inverted confocal microscope as SDC images produced high background. FRET efficiencies were calculated using Matlab Software applying the script generated by Dr Guillermo Gomez. More detailed description of this analysis can be found in [613].

Results

TPOR FRET constructs are functional

TPOR FRET constructs were made by tagging the fluorescent gene (CFP or Citrine) after the Box2 motif. The constructs were truncated directly after the Box2 motif, residue S585, in order to provide a marker of receptor movement where the JAK proteins are. Placing FRET reporters at the C-terminus of the receptor may not show the movements of the JAK bound regions of the receptors because the intracellular domain of cytokine receptors is flexible and intrinsically disordered [231]. As the truncation was made after the Box2 motif, little to no interference with JAK2 binding to the receptor was expected. Subsequently, the constructs were tested for their functionality. The addition of TPO was shown to result in receptor activation of WT and mutant TPOR FRET constructs as demonstrated by the increase in pJAK2 and pERK levels upon stimulation (Figure 85) which suggests that these constructs were functional.

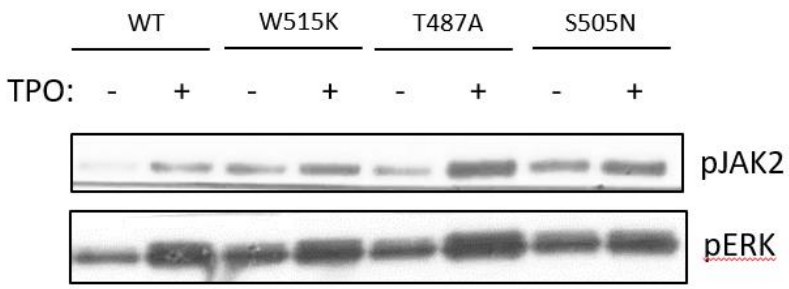

Figure 85: FRET constructs (with Box2 motif) conferred enhanced signalling in the presence of TPO.

HEK293 cells were transiently transfected with JAK2 WT (20 ng) and HA-tagged TPOR WT or mutant TPOR FRET constructs (400 ng). Cells were starved overnight and TPO (final concentration of 50 ng/ml) was added (+) for 10 minutes. Samples in the absence of TPO (-) were used for comparison. Total protein was subjected to SDS-PAGE and immunoblotted with indicated antibodies.

The constructs were subjected to FRET using the SDC microscope (Translational Research Institute, TRI). However, membrane localisation of the FRET constructs was very low, not allowing clear detection using the SDC microscope, in contrast to the observation of strong intra-cytoplasmic expression of the constructs, which may have also masked the presence of the receptors at the surface (Figure 86).

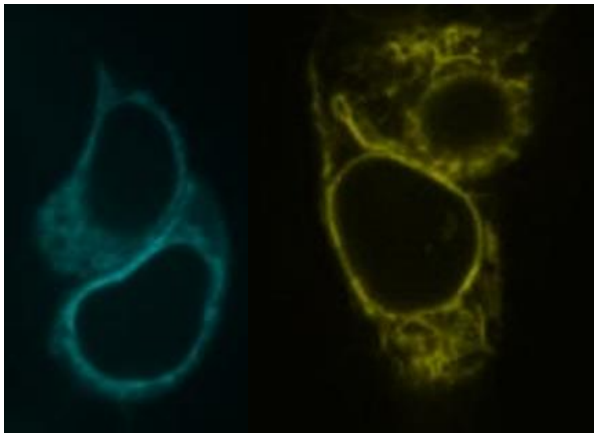

Figure 86: Sub-optimal surface expression of FRET constructs.

Lenti-X 293T cells were seeded in glass bottom dishes and cultured overnight at 37°C. Subsequently, transient transfection was performed with 100ng of the respective constructs. Cells were imaged 15-16 hours after transfection using the SDC microscope. Left: expression of CFP-tagged constructs, right: expression of Citrine-tagged constructs.

Subsequently, expression optimisation was determined empirically by transfecting varying amounts of DNA and utilising other cell lines that may allow for enhanced receptor cell surface expression. The cell lines tested for FRET included the HEK293, Lenti-X 293T, baby hamster kidney (BHK), and COS-7 cells. Co-expression of TPOR with JAK2 was also performed as JAK2 was known to aid in TPOR localisation to the cell surface [115]. Optimal fluorescently-tagged TPOR cell surface expression will facilitate FRET analysis by reducing expression of the construct in the nuclear membrane or the cytoplasm. However, optimal surface expression of the constructs was difficult to obtain even after various efforts.

FRET analysis did not yield reproducible results

Cells expressing the constructs were starved for 4-5 hours before visualisation as starvation may aid in the surface localisation of the receptors by reducing their production and hence reducing aggregation of the protein in the intra-cytoplasmic regions. Upon starving, surface expression of these constructs was improved. However, FRET analysis did not yield interpretable results due to the high background. An alternative confocal microscope, Inverted LSM 710 BIG, was utilised (QBI, UQ). Although cell membrane localisation of the constructs was observed (Figure 87), the analysis of FRET did not yield consistent results between experimental days (results not shown). This could be due to various parameters that may have caused the experimental variation such as cell condition, donor/acceptor expression level, and donor/acceptor fluorescence ratio. Due to the various technical difficulties and time limitation, this aim was not pursued further, and instead, the analysis of fusion constructs by sptPALM was performed.

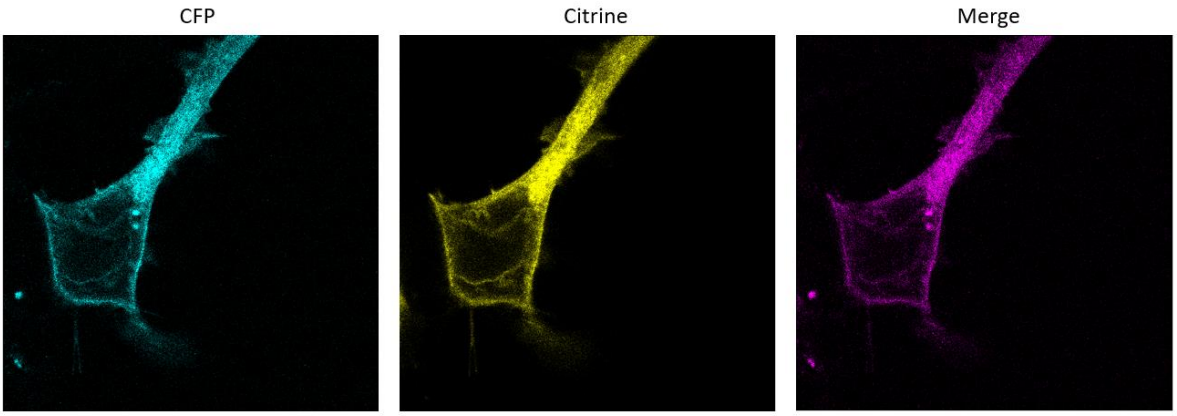

Figure 87: Successful cell surface expression of FRET-tagged TPOR.

Lenti-X 293T cells were seeded in glass bottom dishes and cultured overnight at 37 °C. Subsequently, transient transfection was performed with the respective constructs. After 10 hours of the transfection, cells were starved for 4-5 hours prior to imaging using the Inverted LSM 710 BIG confocal microscope. FRET imaging was performed in the acceptor (left image) and donor (middle image) channel, and merged (right image).

Section B: Replicates and supporting data

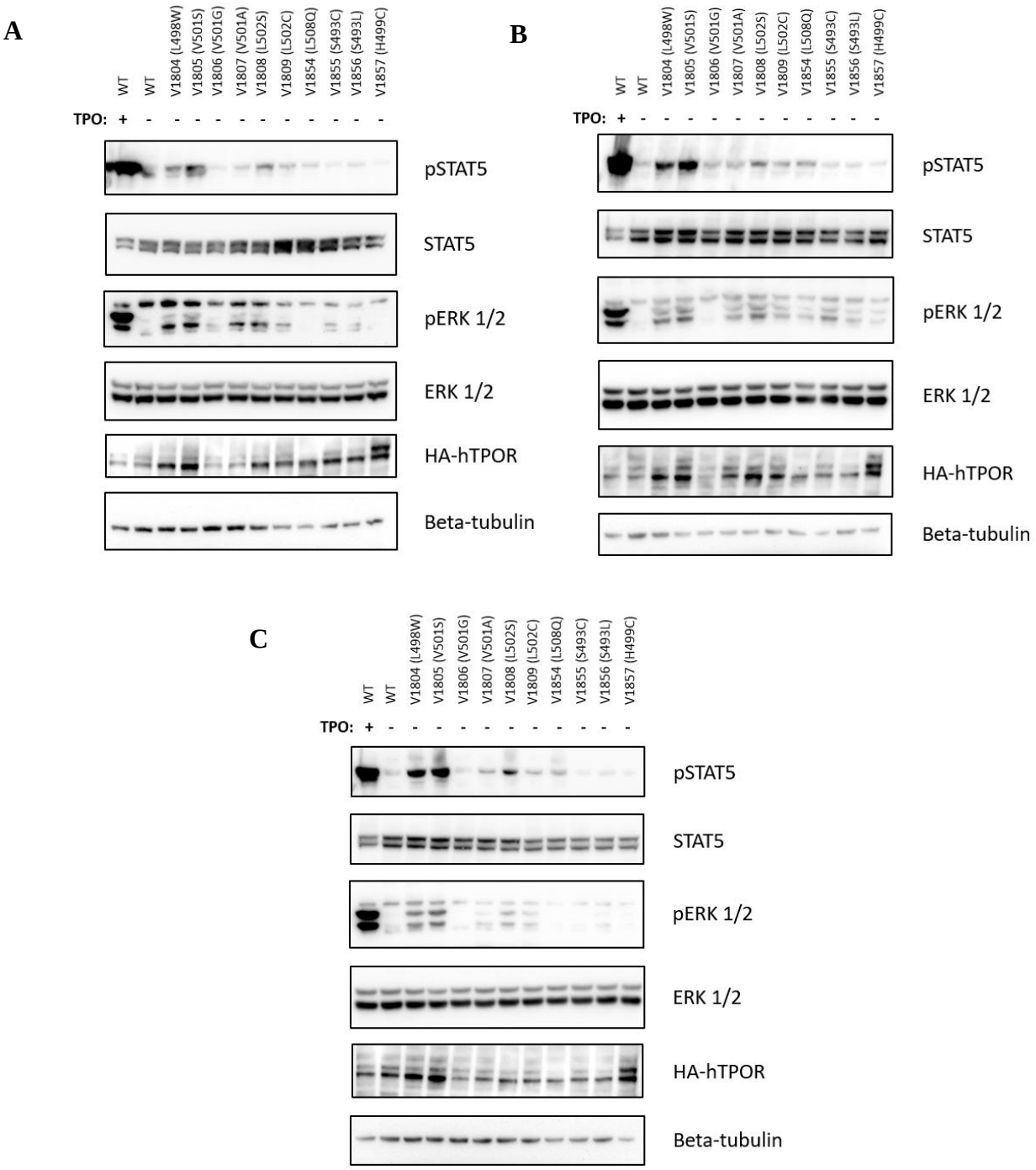

Figure 88: Western data replicates for Figure 18.

A) Batch 1 transduction, B) Batch 2 transduction, C) Batch 3 transduction. Arrangement of mutants is different from Figure 18.

A.

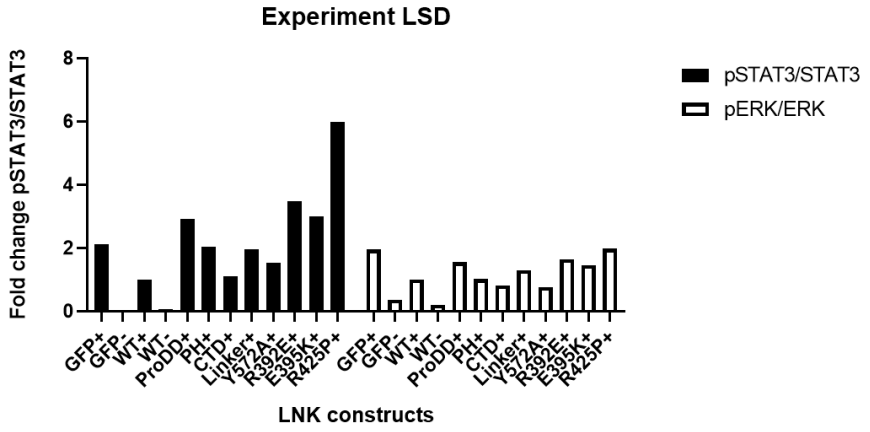

B.

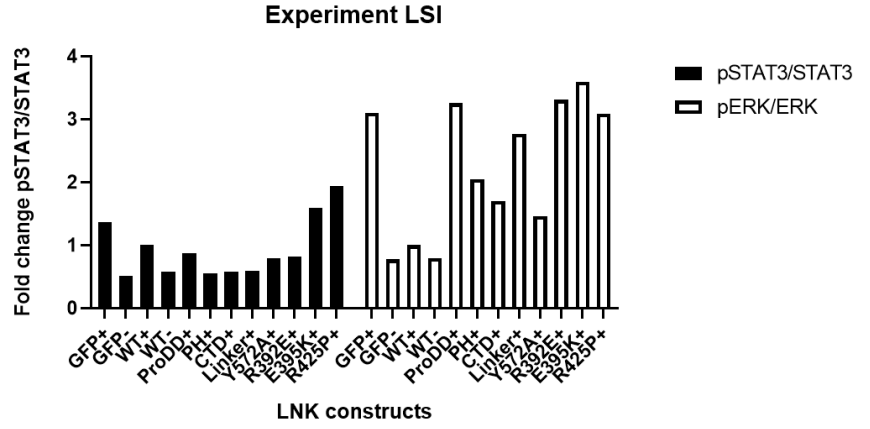

C.

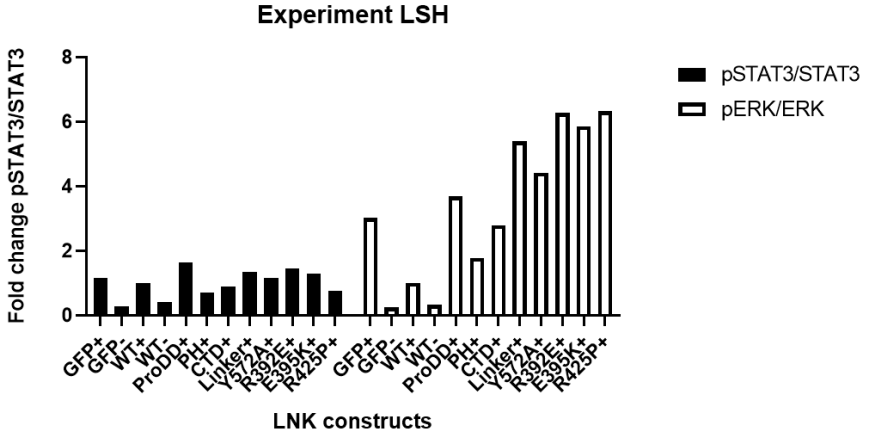

Figure 89: Densitometry immunoblot data for quantitation of pSTAT3 and pERK1/2.

Densitometry data of replicates for Figure 11. Fold change was compared to WT+.

A.

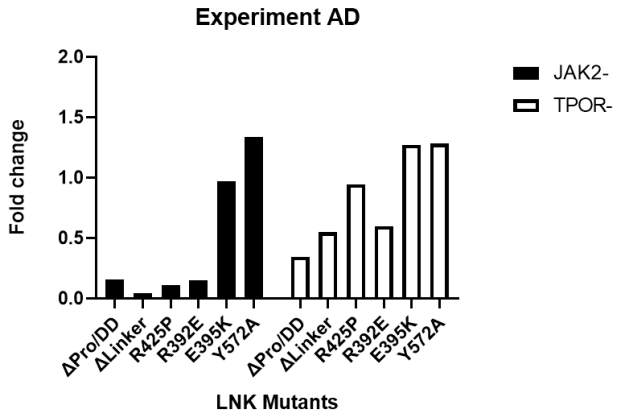

B.

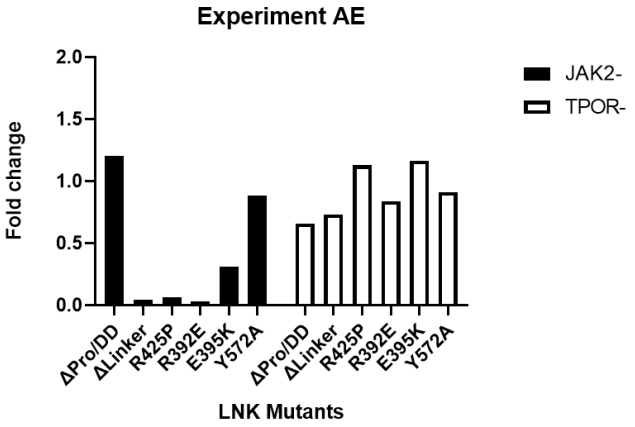

C.

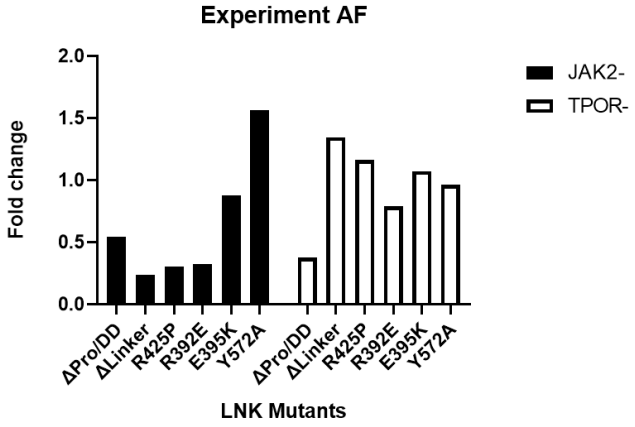

Figure 90: Densitometry immunoblot data for quantitation of JAK2 and TPOR.

Densitometry data of replicates for Figure 17 IP blot. Fold change was compared to WT lane 1 Figure 17 IP blot.

A.

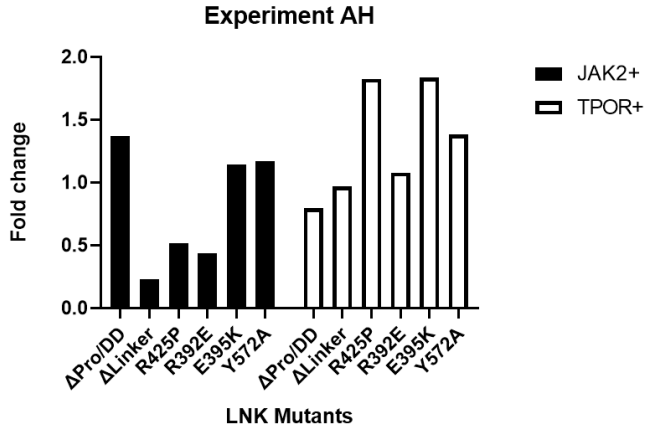

B.

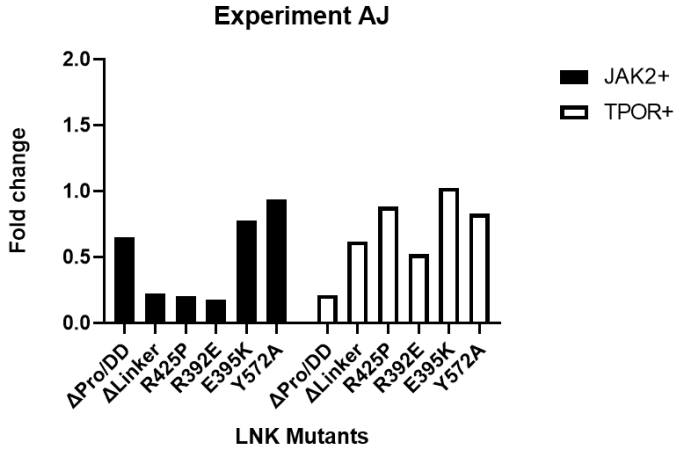

Figure 91: Densitometry immunoblot data for quantitation of JAK2 and TPOR.

Densitometry data of replicates for Figure 18 IP blot. Fold change was compared to WT lane 2 Figure 18 IP blot.

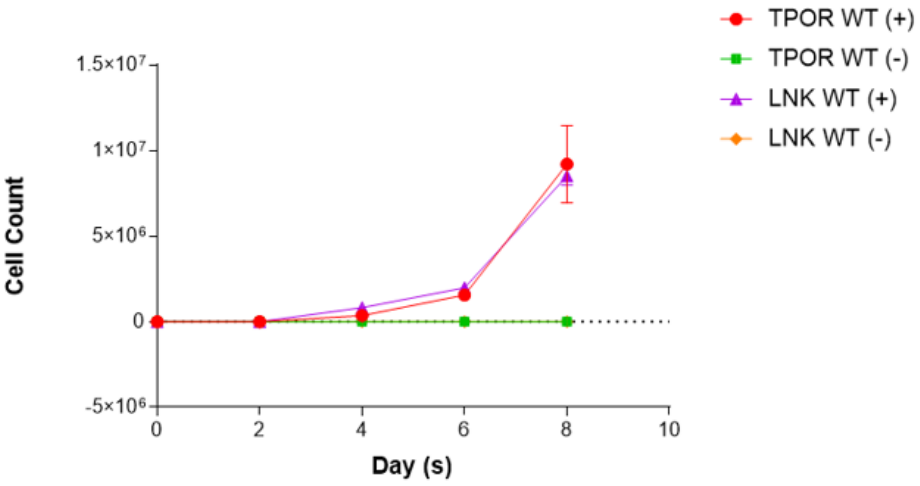

Figure 92: Ba/F3 TPOR WT co-transduced with LNK WT was unable to inhibit cell growth.

Prior to cell seeding, cells were starved for 12-16 hours in RPMI media (no cytokine, 10% FBS). Stably transduced Ba/F3 TPOR WT co-transduced with LNK WT (batch 3) in log growth were plated at a density of 10×10^3 cells/ml per well in duplicates in 12-well plates in IL-3-free and phenol-red free RPMI media (containing 10% FBS). Cells were treated with 10 ng/ml rhTPO or phenol-red free RPMI media (no cytokine, 10% FBS). Viable cells were assayed every other day from day 0 to day 8 using trypan blue exclusion method. Red and green lines represent Ba/F3 TPOR WT, purple and orange lines represent Ba/F3 TPOR WT co-transduced with LNK WT. Image representative of n=2 experiments.

A.

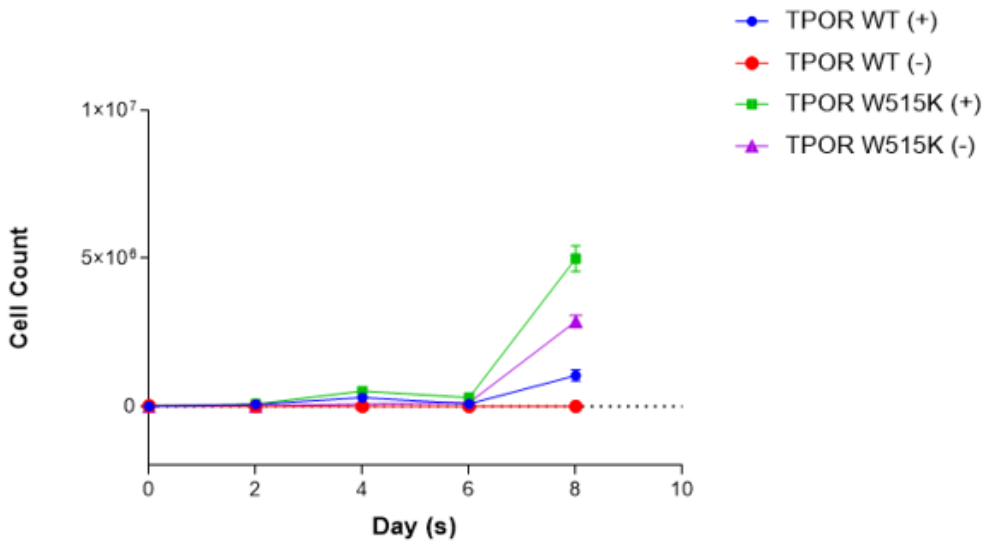

B.

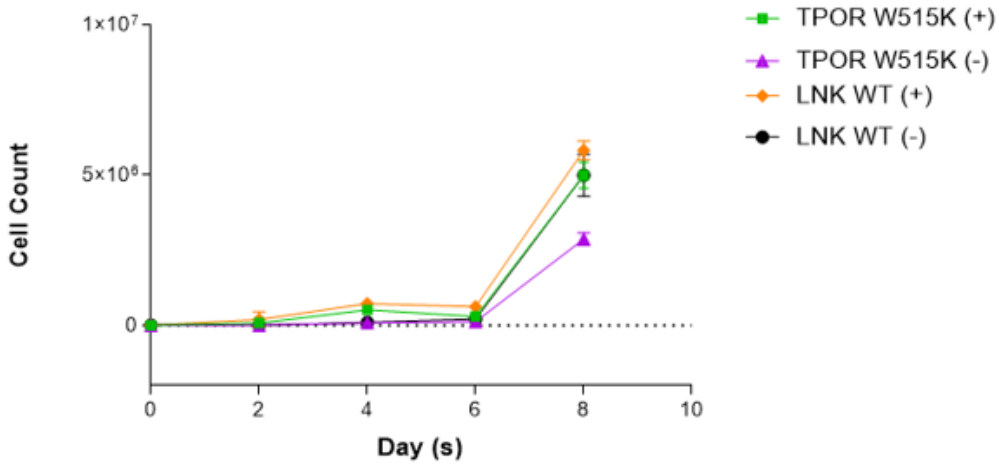

Figure 93: Ba/F3 TPOR W515K co-transduced with LNK WT was unable to inhibit cell growth.

Prior to cell seeding, cells were starved for 12-16 hours in RPMI media (no cytokine, 10% FBS). Stably transduced Ba/F3 TPOR WT co-transduced with LNK WT (batch 3) in log growth were plated at a density of 10×10^3 cells/ml per well in triplicates in 12-well plates in IL-3-free and phenol-red free RPMI media (containing 10% FBS). Cells were treated with 15 ng/ml rhTPO or phenol-red free RPMI media (no cytokine, 10% FBS). Viable cells were assayed every other day from day 0 to day 8 using trypan blue exclusion method. A) Blue and red lines represent Ba/F3 TPOR WT, green and purple lines represent Ba/F3 TPOR W515K. b) Green and purple lines represent Ba/F3 TPOR W515K, orange and black lines represent Ba/F3 TPOR W515K co-transduced with LNK WT. Image representative of n=1 experiment.

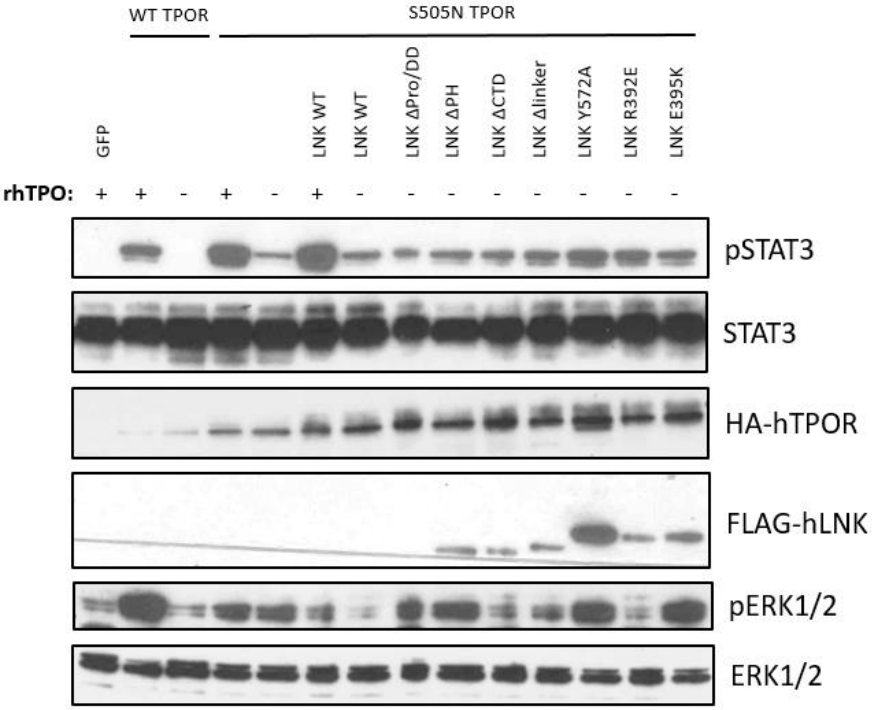

Figure 94: Ba/F3 TPOR S505N co-transduced with LNK WT was unable to inhibit cell signalling in the absence of MG132.

Cells were starved for 12-16 hours in RPMI media containing no FBS and no IL-3. Cells were stimulated with 100 ng/ml rhTPO (Peprotech) for 30 minutes. Total protein was subjected to SDS-PAGE and immunoblotted with indicated antibodies. STAT3 was used as a loading control. Image representative of n=1 experiment.

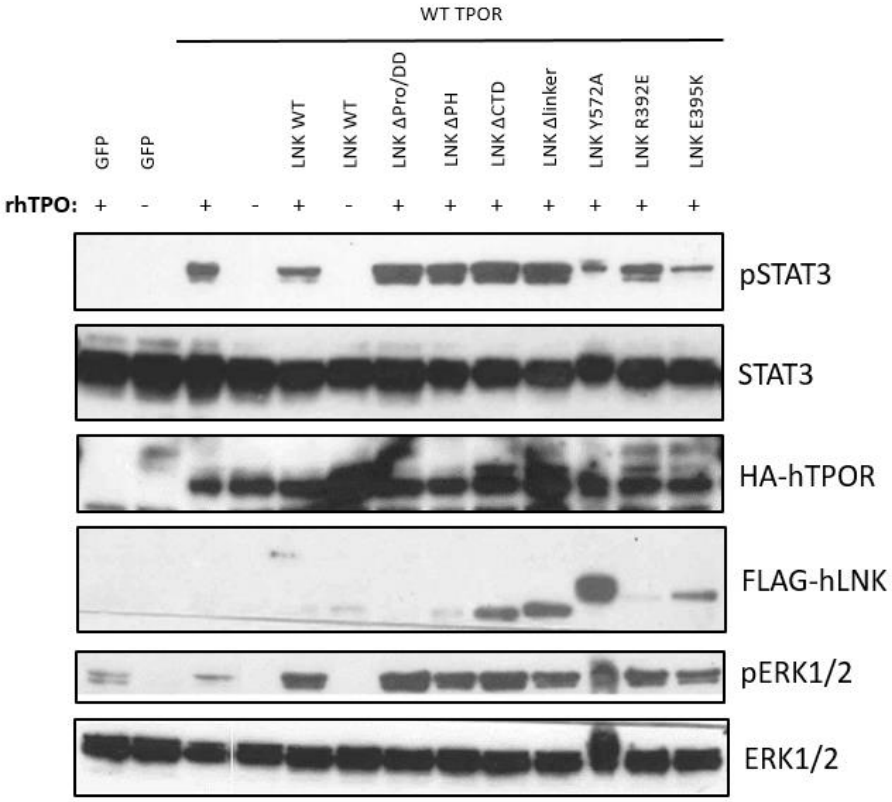

Figure 95: Ba/F3 TPOR WT co-transduced with LNK WT was unable to inhibit cell signalling in the absence of MG132.

Cells were starved for 12-16 hours in RPMI media containing no FBS and no IL-3. Cells were stimulated with 50 ng/ml rhTPO (R&D Systems) for 30 minutes. Total protein was subjected to SDS-PAGE and immunoblotted with indicated antibodies. STAT3 was used as a loading control. Image representative of n=1 experiment.

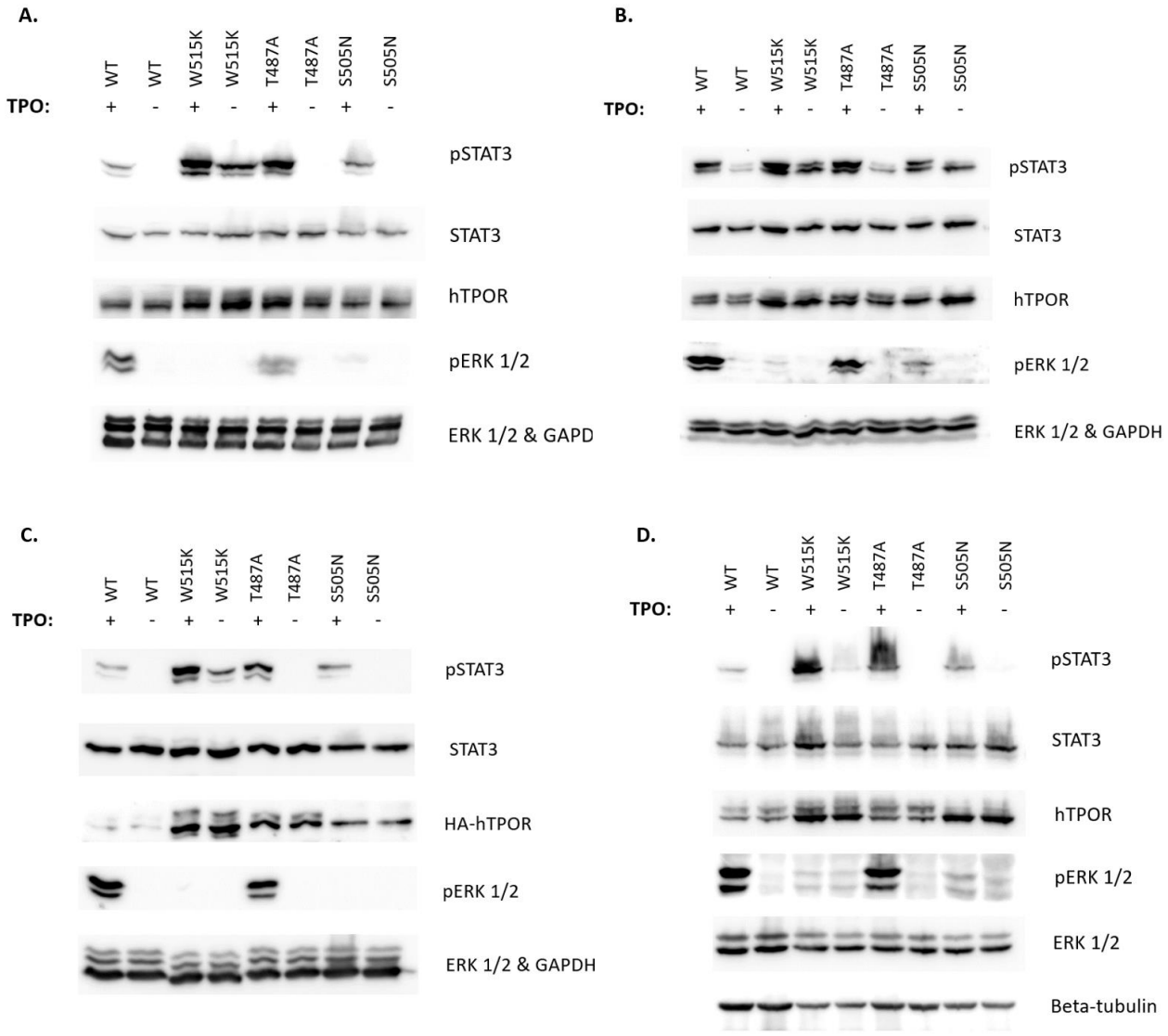

Figure 97: Western data replicates for Figure 12.

A) Batch 1 transduction, B) Batch 2 transduction, C) Batch 3 transduction, D) Batch 4 transduction.

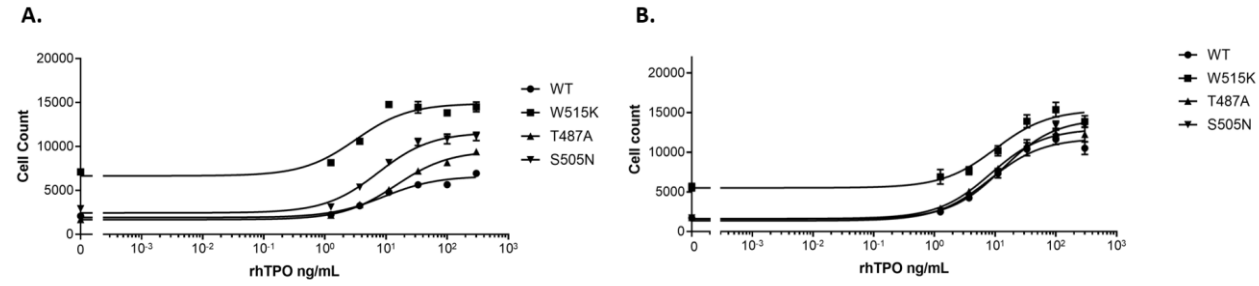

Figure 98: TPO dose-response assay replicates for Figure 15.

A) Batch 1 transduction. B) Batch 3 transduction.

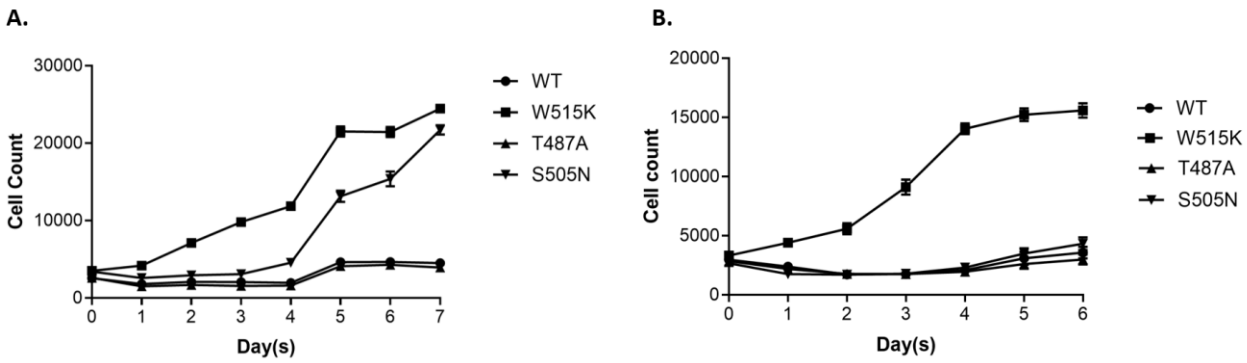

Figure 99: Cytokine-independent assay replicates for Figure 16.

A) Batch 1 transduction. B) Batch 3 transduction.

Section C: List of primers to make constructs

To make constructs for sptPALM:

Primer	**Sequences (5' => 3')**
SP-HA-TPOR Fwd	AGATCCGCTAGCATGCCCTCCTGGGCCCTCTTCA
mEOS2-SP Rvs	CCAGGAGGGCATGCTAGCGGATCTGACGGTTCACTAAAC C
Vec Linker-mEOS2 Fwd	TGGCAGCAGCCTTCGGGCCCGGGATCCGG
ICD-vec linker-mEOS2 Rvs	GGCCCGAAGGCTGCTGCCAATAGCTTAGTGGTAGGT
SP-FRET Vec Rvs	CCGGGCCCGAATCTTGGCTGCTGACTTGGGCCA
Linker-mEOS Fwd	CAGCCAAGATTCGGGCCCGGGATCCGG
mEOS2-HA-TPOR Rvs	GGAACATCATATGGATATCTGGCATTGTCAGGCAATCCA GAATG
mEOS2-HA-TPOR Fwd	CCTGACAATGCCAGATATCCATATGATGTTCCAGATTAC GCAGTCTCCT
FRET Vec Fwd	CAGCAGCCTTAAAGCGGCCGCGACTCTAGATCATAATC
TPOR Rvs	GCGGCCGCTTTAAGGCTGCTGCCAATAGCTTAGTGGT
Box1 TPOR LWASLADLH Fwd	GGCATGCCCTGTGGGCCGCAGCTGCAGACCTGCACCGGG
Box1 TPOR LWASLADLH Rvs	CCCGGTGCAGGTCTGCAGCTGCGGCCCACAGGGCATGCC

To make constructs for FRET:

Primer	**Sequences (5' => 3')**
MPL start fwd (mCFP)	GATCCGCTAGCATGCCCTCCTGGGCCCTCTTCA
pMPL-HA rvs (mCFP)	CCAGGAGGGCATGCTAGCGGATCTGACGGTTCACTAAAC C
p-MPL-HA fwd (mCFP)	GTGGAACCCAGCTCGGGCCCGGGATCCGG
MPL rvs (mCFP)	GGGCCCGAGCTGGGTTCCACTTCTTCACAGGTATCTGA
mCFP/Cit vector Fwd	CCCTGTGTTCCTCCTCGGGCCCGGGATCCGG

hMPL Box2 Rvs	GGCCCGAGGAGGAACACAGGGGCAAAGGAGTC
FLAG-hMPL ECD linker Fwd (homo)	GATGATTACAAGGATGACGACGATAAGGTCTCCTTGCTGGCATCAGACTCAGAGC
Mid-pMX-pGK-puro/GFP Rvs	GGAGACCCTCCCAAGGAACAGCGAG
hMPL ECD linker-FLAG Rvs (homo)	GACCTTATCGTCGTCATCCTTGTAATCATCTTGGCTGCTGACTTGGGCCAG
Mid-pMX-pGK-puro/GFP Fwd	CTCGCTGTTCCTTGGGAGGGTCTCC

To make constructs for Ba/F3 hTPOR stable transduction:

Primer	**Sequences (5' => 3')**
MPL-HA-tag forward	AAGATTATCCATATGATGTTCCAGATTACGCAGTCTCCTTGCTGGCATCAGACTCAGAGC
MPL-HA-tag reverse	GACTGCGTAATCTGGAACATCATATGGATAATCTTGGCTGCTGACTTGGGCCAG
MPL fwd (W515K)	TGCTGCTGAGGAAGCAGTTTCCTGC
MPL rvs (W515K)	GCAGGAAACTGCTTCCTCAGCAGCA
MPL fwd (T487A)	GACCGCCGCCGAGACCGCCTG
MPL rvs (T487A)	CAGGCGGTCTCGGCGGCGGTC
MPL fwd (S505N)	TGGGCCTCAACGCCGTCCTGGG
MPL rvs (S505N)	CCCAGGACGGCGTTGAGGCCCA
MPL-attb1 Fwd	GGGGACAAGTTTGTACAAAAAAGCAGGCTATGCCCTCCTGGGCCCTCTTCA
MPL-attb2 Rvs	GGGGACCACTTTGTACAAGAAAGCTGGGTTCAAGGCTGCTGCCAATAGCTTAGTGG
HA-tag forward	AAGATTATCCATATGATGTTCCAGATTACGCAGTCTCCTTGCTGGCATCAGACTCAGAGC
HA-tag reverse	GACTGCGTAATCTGGAACATCATATGGATAATCTTGGCTGCTGACTTGGGCCAG
Mid-fwd (HA-tag)	CGCTACCAGCGGTGGTTTGTTTGC
Mid-rvs (HA-tag)	GCAAACAAACCACCGCTGGTAGCG

To make hTPOR constructs for co-IP:

Primer	**Sequences (5’ => 3’)**
Fwd Y8F	GCAGTTTCCTGCACACTTCAGGAGACTGAGGCA
Rvs Y8F	TGCCTCAGTCTCCTGAAGTGTGCAGGAAACTGC
Fwd Y29F	CGGGTCCTAGGCCAGTTCCTTAGGGACACTG
Rvs Y29F	CAGTGTCCCTAAGGAACTGGCCTAGGACCCG
Fwd Y78F	GGCCCAGATGGACTTCCGAAGATTGCAGCC
Rvs Y78F	GGCTGCAATCTTCGGAAGTCCATCTGGGCC
Fwd Y113F	CCCACATTGCCAACCATTCCTTCCTACCACTAAGCTATTGG
Rvs Y113F	CCAATAGCTTAGTGGTAGGAAGGAATGGTTGGCAATGTGGG
Fwd Y118F	CCTACCTACCACTAAGCTTTTGGCAGCAGCCTTGA
Rvs Y118F	TCAAGGCTGCTGCCAAAAGCTTAGTGGTAGGTAGG
Fwd Y113F/Y118F	GCCAACCATTCCTTCCTACCACTAAGCTTTTGGCAGCAGC
Rvs Y113F/Y118F	GCTGCTGCCAAAAGCTTAGTGGTAGGAAGGAATGGTTGGC
MPLTrunc7-Fwd	GGCAGTTTCCTGCACACTAAAGGAGACTGAGGCAT
MPLTrunc7-Rvs	ATGCCTCAGTCTCCTTTAGTGTGCAGGAAACTGCC
MPLTrunc28-Fwd	CGGGTCCTAGGCCAGTAACTTAGGGACACTGC
MPLTrunc28-Rvs	GCAGTGTCCCTAAGTTACTGGCCTAGGACCCG
MPLTrunc53-Fwd	GTGAAGAAGTGGAACCCAGCTGACTTGAAATCCTCCCC
MPLTrunc53-Rvs	GGGGAGGATTTCAAGTCAGCTGGGTTCCACTTCTTCAC
MPLTrunc69-Fwd	CTCCTTTGCCCCTGTGATCCTCCCAGGC
MPLTrunc69-Rvs	GCCTGGGAGGATCACAGGGGCAAAGGAG
MPLTrunc83-Fwd	CGAAGATTGCAGCCTTGATGCCTGGGGACC
MPLTrunc83-Rvs	GGTCCCCAGGCATCAAGGCTGCAATCTTCG
MPLTrunc98-Fwd	TGCCCACCCATGGCTTAGTCAGGGTCCT
MPLTrunc98-Rvs	AGGACCCTGACTAAGCCATGGGTGGGCA
MPLTrunc111-Fwd	CTGTACCACCCACATTGCCAACCATTAATACCTACCACTAAGCTATTG
MPLTrunc111-Rvs	CAATAGCTTAGTGGTAGGTATTAATGGTTGGCAATGTGGGTGGTACAG

MPLTrunc116-Fwd	AACCATTCCTACCTACCACTATGATATTGGCAGCAGCCTTGA
MPLTrunc116-Rvs	TCAAGGCTGCTGCCAATATCATAGTGGTAGGTAGGAATGGTT

To make hLNK constructs for Ba/F3 hLNK stable transduction, co-IP assay, and signalling assay:

Primer	**Sequences (5' => 3')**
attb1 Fwd-FLAG-hLNK-WT (corrected)	GGGGACAAGTTTGTACAAAAAAGCAGGCTATGGATTACAAGGATGACGACGATAAGAACG
FLAG-hLNK-attb2 rvs-WT (corrected)	GGGGACCACTTTGTACAAGAAAGCTGGGTTCAGAGAGGTGTGTACTGATTGTCTATGGCCC
attb1 Fwd-FLAG-hLNK(-Pro DD) (corrected)	GGGGACAAGTTTGTACAAAAAAGCAGGCTATGGATTACAAGGATGACGACGATAAGGAGG
FLAG-hLNK-attb2 rvs (-CTD) (corrected 2)	GGGGACCACTTTGTACAAGAAAGCTGGGTTCACACGTAGCTGGAGAGCCGGACA
FLAG-hLNK-attb2 rvs (Y572A)	GGGGACCACTTTGTACAAGAAAGCTGGGTTCAGAGAGGTGTGGCCTGATTGTCTATGG
pDONR221 mid vec CPEC Fwd	CGCTACCAGCGGTGGTTTGTTTGC
pDONR221 mid vec CPEC Rvs	GCAAACAAACCACCGCTGGTAGCG
PH Start Fwd (-Pro-DD) - Corrected	GACGACGATAAGGAGGCGCTGAAGGAGGCGGTG
FLAG start rvs (-Pro-DD) - Corrected	CCTTCAGCGCCTCCTTATCGTCGTCATCCTTGTAATCCATGGTG
SH2 Start Fwd (-PH)	CGCCACCCCGAGGGCTGGAGAGCACAGAAGCA
DD start rvs	CCAGCCCTCGGGGTGGCGGCTCCCGGG
Vector Start Fwd (-CTD) - Corrected	CTCTCCAGCTACGTGTGATAAACCCGCTGATCAGCCTCGA
LNK start rvs (-CTD) - Corrected	AGCGGGTTTATCACACGTAGCTGGAGAGCCGGACATCA
SH2 start fwd (-PH SH2 linker) corrected	CGGAGTGCACAGGCTGGTTCCACGGCCCCATCTCC

PH start rvs (-PH SH2 linker)	GTGGAACCAGCCTGTGCACTCCGAGAGCTCAGC
C-terminus Fwd (Y572A) - Corrected	CCATAGACAATCAGGCCACACCTCTCTGA
C-terminus Rvs (Y572A) Corrected	TCAGAGAGGTGTGGCCTGATTGTCTATGG
SH2 Fwd (R392E)	GTGTTCCTGGTGGAGCAGAGCGAGACGC
SH2 Rvs (R392E)	GCGTCTCGCTCTGCTCCACCAGGAACAC
SH2 Fwd (E395K)	CGGCAGAGCAAGACGCGGCG
SH2 Rvs (E395K)	CGCCGCGTCTTGCTCTGCCG
SH2 Fwd R425P	GGCCAGTGCCCTGTGCAGCAC
SH2 Rvs R425P	GTGCTGCACAGGGCACTGGCC

To make constructs for protein expression and purification (bacterial system):

Primer	**Sequences (5' => 3')**
LNK fwd (pET)	TGCACCATCATCATCACCACAACGGGCCTGCCCTGCAGC
His-tag rvs (pET)	CCGTTGTGGTGATGATGATGGTGCATATGTATATCTCCT
pET fwd (pET)	CAGTACACACCTCTCTGAGGATCCGGCTGCTAACAAAGCCC
LNK rvs (pET)	AGCCGGATCCTCAGAGAGGTGTGTACTGATTGTCTATGGCCC
TEV start fwd (pET11a)	CATCATCACCACGAAAACCTGTACTTCCAAAACGGGCCTG
6His rvs (pET11a)	TTGGAAGTACAGGTTTTCGTGGTGATGATGATGGTGCATATGTATATCTCCT

TEV start fwd (del N22)	ACCATCATCATCACCACGAAAACCTGTACTTCCAACGGGGCTGG
6His rvs (del N22)	AAGTACAGGTTTTCGTGGTGATGATGATGGTGCATATGTATATCTCCT
TEV start fwd (del N37)	ACCATCATCATCACCACGAAAACCTGTACTTCCAACGGGAGCTGG
6His rvs (del N37)	AAGTACAGGTTTTCGTGGTGATGATGATGGTGCATATGTATATCTCCT
pET fwd (del C2)	ACAATCAGTACACATGAGGATCCGGCTGCTAACAAAGCC
LNK rvs (del C2)	CAGCCGGATCCTCATGTGTACTGATTGTCTATGGCCCGCAGG
LNK fwd (pHUE)	CGCGGTGGAAACGGGCCTGCCCTGCAGC
Ub rvs (pHUE)	CAGGCCCGTTTCCACCGCGGAGGCGCA
LNK rvs (pHUE)	GAGCTCGAATTCGGATCAGAGAGGTGTGTACTGATTGTCTATGGCCC
pHUE fwd (pHUE)	CACACCTCTCTGATCCGAATTCGAGCTCGGTACCGTC
LNK fwd del N22 (pHUE)	TCCGCGGTGGACGGGGCTGGAGCGAGTTCTGTG

Ub rvs del N22 (pHUE)	GCCCCGTCCACCGCGGAGGCGCA
LNK fwd del N37 (pHUE)	CCGCGGTGGACGGGAGCTGGCCCGCCA
Ub rvs del N37 (pHUE)	CAGCTCCCGTCCACCGCGGAGGCGCA
pHUE fwd del C2 (pHUE)	AGACAATCAGTACACATAATCCGAATTCGAGCTCGGTACCGTC
LNK rvs del C2 (pHUE)	GAGCTCGAATTCGGATTATGTGTACTGATTGTCTATGGCCCGCAGG

To make constructs for protein expression and purification (bacterial system-codon optimised):

Primer	**Sequences (5' => 3')**
TEV hLNK WT Fwd (TEV-CO)	CATCATCACCACGAGAATCTGTACTTTCAGAACGGTCCGGC
6His pET11a Rvs (TEV-CO)	GTTCTGAAAGTACAGATTCTCGTGGTGATGATGATGGTGCATATGTATATCTCCT
pET11a WT Fwd (TEV-CO)	CACCCCGCTGTAAGGATCCGGCTGCTAACAAAGCCCG
hLNK WT Rvs (TEV-CO)	GCCGGATCCTTACAGCGGGGTGTACTGGTTGTCAATC
hLNK (-N37) Fwd (TEV-CO)	TGTACTTTCAGCGTGAGCTGGCACGCCAGTATTGG
TEV hLNK (-N37) Rvs (TEV-CO)	CGTGCCAGCTCACGCTGAAAGTACAGATTCTCGTGGTGATGATGATG

hLNK (-N22) Fwd (TEV-CO)	TGTACTTTCAGCGTGGTTGGAGCGAGTTTTGCGA
TEV hLNK (-N22) Rvs (TEV-CO)	CTCGCTCCAACCACGCTGAAAGTACAGATTCTCGTGGTGATGATGATG
pET11a Fwd (-C2) (TEV-CO)	CCAGTACACCTAAGGATCCGGCTGCTAACAAAGCCCG
hLNK WT Rvs (-C2) (TEV-CO)	GTTAGCAGCCGGATCCTTAGGTGTACTGGTTGTCAATCGCACGC
hLNK WT Fwd (Ub-CO)	CCGCGGTGGAAACGGTCCGGCACTGCAACCG
6His Ub Rvs (Ub-CO)	CGGACCGTTTCCACCGCGGAGGCGCA
pHUE WT Fwd (Ub-CO)	CCCCGCTGTAACTAGCATAACCCCTTGGGGCCTCTAAAC
hLNK WT Rvs (Ub-CO)	CAAGGGGTTATGCTAGTTACAGCGGGGTGTACTGGTTGTCAATC
hLNK (-N37) Fwd (Ub-CO)	CCGCGGTGGACGTGAGCTGGCACGCCAGTATTGG
6His Ub (-N37) Rvs (Ub-CO)	CCAGCTCACGTCCACCGCGGAGGCGCA
hLNK (-N22) Fwd (Ub-CO)	CCGCGGTGGACGTGGTTGGAGCGAGTTTTGCGA
6His Ub (-N22) Rvs (Ub-CO)	TCCAACCACGTCCACCGCGGAGGCGCA
pHUE (-C2) Fwd (Ub-CO)	CCAGTACACCTAACTAGCATAACCCCTTGGGGCCTCTAAAC
hLNK (-C2) Rvs (Ub-CO)	CCCAAGGGGTTATGCTAGTTAGGTGTACTGGTTGTCAATCGCACGC

To make hJAK2 JH2-JH1 construct for protein expression and purification (mammalian system):

Primer	**Sequences (5’ => 3’)**
TEV-JAK2 Fwd	CGAAAATCTGTACTTCCAAGGCCACAAAATCAGAAATGAAGATTTGATATTTAATGAAAGCCTTGGCC
pD454-SR-6xHis-TEV-JAK2 Rvs	TTCTGATTTTGTGGCCTTGGAAGTACAGATTTTCGTGGTGATGATGATGGTGCAT
JH1-pD454-SR Fwd	TAACATGGCTGGATGAGGTTGAGGTCTCACCCCCTAGCATAACC
pD454-SR-JH1 Rvs	TGAGACCTCAACCTCATCCAGCCATGTTATCCCTTATTTGATCCACTC
6xHis-TEV Fwd	GGGGACAAGTTTGTACAAAAAAGCAGGCTATGCACCATCATCATCACCACGAAAATCTGTAC
JH1 Rvs	GGGGACCACTTTGTACAAGAAAGCTGGGTTCATCCAGCCATGTTATCCCTTATTTGATCCACTC

Section D: List of sequencing primers

Sequencing primers for hMPL:

Primer	**Sequences (5' => 3')**
MPL seq fwd 1	CACCTCTGGGTGAAGAATGTGTTCCTA
MPL seq fwd 2	AACTCCTACTGGCTGCAGCTGCG
MPL seq fwd 3	CCAAACTTGCACTGGAGGGAGATCT
MPL seq fwd 4	CGGGTCCTAGGCCAGTACCTTAGG
MPL seq rvs	TGGCCTTGATGATACTGGGGGG

Sequencing primers for hLNK:

Primer	**Sequences (5' => 3')**
LNK seq 1 fwd	ACTACCGGGACACAGGCCGTG
LNK seq fwd 2	CTCTTCGACCCACCCAAGAGTTCA
LNK seq fwd 3	CTGCAGGGCCCTGATGCTCAT
LNK seq fwd 4	AGATCTTCCACCTGGTGCCTTCG
LNK seq rvs	CTCCTCAGAGCTGCGGGCCT
LNK (-Pro/DD) seq rvs	CTCCTGGATGCTGGAGCAAGCT
LNK seq FLAG	CATGGATTACAAGGATGACGACGATAAG

Sequencing primers for hJAK2:

Primer	**Sequences (5' => 3')**
JAK2 Seq Fwd 1	ACCCTTATTCATGGGAATGTATGTGCC
JAK2 Seq Fwd 2	AATTTCTACAGCAACTTGGCAAGGGTAAT
JAK2 Seq Fwd 3	ATCACTGACAGAGAGCAAGTTTTCTGTGG

Sequencing primers for pHUE and pET11a vectors:

Primer	**Sequences (5’ => 3’)**
pHUE vector seq Fwd primer	GAGCGGATAACAATTCCCCTCTAGAAAT
pET11a vector seq Fwd primer	GAGCGGATAACAATTCCCCTCTAGAAATA

Sequencing primers for codon optimised LNK:

Primer	**Sequences (5’ => 3’)**
Seq Fwd 1 hLNK (CO)	GTCCACCGGCGAAAGCCG
Seq Fwd 2 hLNK (CO)	AGCGCGGTCGTCTGGCG
Seq Fwd 3 hLNK (CO)	AGGCGCGTCCCCGGGT
Seq Fwd 4 hLNK (CO)	GTTGTAGTCAGCCAGCCGCCAG
Seq Fwd Ub (CO)	CTGCACCTGGTGTTGCGCCT
Seq Rvs 1 hLNK (CO)	TAGGCAGGCCCGGTGCG
Seq Rvs 2 hLNK (CO)	AGCCGAGCTCGGGCTGGA

Sequencing primers for phage display:

Primer	**Sequences (5’ => 3’)**
-96 gIII sequencing primer	CCCTCATAGTTAGCGTAACG
-28 gIII sequencing primer	GTATGGGATTTTGCTAAACAAC

Section E: List of Antibodies for Co-IP Assay and Western Analysis

Antibodies	Company	Dilution	Buffer
Akt	Cell Signalling Technology (USA)	1:1 000	5% BSA/TBST
β-actin	Cell Signalling Technology (USA)	1:10 000	5% BSA/TBST
ERK 1/2	Cell Signalling Technology (USA)	1: 1 000	5% BSA/TBST
GAPDH	Cell Signalling Technology (USA)	1: 10 000	5% BSA/TBST
Haemagglutinin (HA)	BioLegend (USA)	1: 6 000	5% BSA/TBST
JAK2	Cell Signalling Technology (USA)	1: 1 000	5% BSA/TBST
pAkt	Cell Signalling Technology (USA)	1: 1 000	5% BSA/TBST
pERK ½	Cell Signalling Technology (USA)	1:2 000	5% BSA/TBST
pJAK2	Cell Signalling Technology (USA)	1:500	5% BSA/TBST
pSrc	Cell Signalling Technology (USA)	1:1 000	5% BSA/TBST
Src	Cell Signalling Technology (USA)	1:1 000	5% BSA/TBST
STAT3	Cell Signalling Technology (USA)	1:1 000	5% BSA/TBST
pSTAT3	Cell Signalling Technology (USA)	1:2 000	5% BSA/TBST
pSTAT5	Cell Signalling Technology (USA)	1:1 000	5% BSA/TBST
STAT5	Cell Signalling Technology (USA)	1:1 000	5% BSA/TBST

β-tubulin	Cell Signalling Technology (USA)	1:10 000	5% BSA/TBST
FLAG	Sigma Aldrich, Merck (USA)	1:8 000	5% BSA/TBST
TPOR/c-Mpl	Merck (USA)	1:1 000	5% BSA/TBST
Anti-6x Histidine	Sigma	1:10 000	5% BSA/TBST
Anti-phosphotyrosine (4G10)	Merck (USA)	1:2 000	5% BSA/TBST
Goat anti-rabbit IgG, HRP-linked	Cell Signalling Technology (USA)	1:10 000	5% BSA/TBST
Horse anti-mouse IgG, HRP-linked	Cell Signalling Technology (USA)	1:10 000	5% BSA/TBST

Section F: Human MPL (hTPOR) full-length cDNA and protein sequence

Human *MPL* (hTPOR) full-length cDNA sequence:

atgccctcctgggccctcttcatggtcacctcctgcctcctcctggcccctcaaaacctggcccaagtcagcagccaagattatccatatgatgttc
cagattacgcagtctccttgctggcatcagactcagagcccctgaagtgtttctcccgaacatttgaggacctcacttgcttctgggatgaggaag
aggcagcgcccagtgggacataccagctgctgtatgcctacccgcgggagaagccccgtgcttgccccctgagttcccagagcatgccccac
tttggaacccgatacgtgtgccagtttccagaccaggaggaagtgcgtctcttctttccgctgcacctctgggtgaagaatgtgttcctaaaccaga
ctcggactcagcgagtcctctttgtggacagtgtaggcctgccggctccccccagtatcatcaaggccatgggtgggagccagccaggggaac
ttcagatcagctgggaggagccagctccagaaatcagtgatttcctgaggtacgaactccgctatggccccagagatcccaagaactccactgg
tcccacggtcatacagctgattgccacagaaacctgctgccctgctctgcagaggcctcactcagcctctgctctggaccagtctccatgtgctca
gcccacaatgccctggcaagatggaccaaagcagacctccccaagtagagaagcttcagctctgacagcagagggtggaagctgcctcatct
caggactccagcctggcaactcctactggctgcagctgcgcagcgaacctgatgggatctccctcggtggctcctggggatcctggtccctccc
tgtgactgtggacctgcctggagatgcagtggcacttggactgcaatgctttaccttggacctgaagaatgttacctgtcaatggcagcaacagg
accatgctagctcccaaggcttcttctaccacagcagggcacggtgctgccccagagacaggtaccccatctgggagaactgcgaagaggaa
gagaaaacaaatccaggactacagaccccacagttctctcgctgccacttcaagtcacgaaatgacagcattattcacatccttgtggaggtgac
cacagccccgggtactgttcacagctacctgggctccccttttctggatccaccaggctgtgcgcctccccaccccaaacttgcactggagggag
atctccagtgggcatctggaattggagtggcagcacccatcgtcctgggcagcccaagagacctgttatcaactccgatacacaggagaaggc
catcaggactggaaggtgctggagccgcctctcggggcccgaggagggaccctggagctgcgcccgcgatctcgctaccgtttacagctgc
gcgccaggctcaacggccccacctaccaaggtccctggagctcgtggtcggacccaactagggtggagaccgccaccgagaccgcctggat
ctccttggtgaccgctctgcatctagtgctgggcctcagcgccgtcctgggcctgctgctgctgaggtggcagtttcctgcacactacaggagac
tgaggcatgccctgtggccctcacttccagacctgcaccgggtcctaggccagtaccttagggacactgcagccctgagcccgcccaaggcc
acagtctcagatacctgtgaagaagtggaacccagcctccttgaaatcctccccaagtcctcagagaggactcctttgcccctgtgttcctcccag
gcccagatggactaccgaagattgcagccttcttgcctggggaccatgcccctgtctgtgtgcccacccatggctgagtcagggtcctgctgtac
cacccacattgccaaccattcctacctaccactaagctattggcagcagccttga

Human thrombopoeitin receptor (hTPOR) amino acid sequence:

MPSWALFMVTSCLLLAPQNLAQVSSQDYPYDVPDYA**VSLLASDSEPLKCFSRTFEDLT**
CFWDEEEAAPSGTYQLLYAYPREKPRACPLSSQSMPHFGTRYVCQFPDQEEVRLFFPL
HLWVKNVFLNQTRTQRVLFVDSVGLPAPPSIIKAMGGSQPGELQISWEEPAPEISDFL
RYELRYGPRDPKNSTGPTVIQLIATETCCPALQRPHSASALDQSPCAQPTMPWQDGPK
QTSPSREASALTAEGGSCLISGLQPGNSYWLQLRSEPDGISLGGSWGSWSLPVTVDLP
GDAVALGLQCFTLDLKNVTCQWQQQDHASSQGFFYHSRARCCPRDRYPIWENCEEE
EKTNPGLQTPQFSRCHFKSRNDSIIHILVEVTTAPGTVHSYLGSPFWIHQAVRLPTPNL
HWREISSGHLELEWQHPSSWAAQETCYQLRYTGEGHQDWKVLEPPLGARGGTLELR
PRSRYRLQLRARLNGPTYQGPWSSWSDPTRVETATETAWISLVTALHLVLGLSAVLGL
LLL*RWQFP**AHYRRLRHALWPSLPDLHRVLGQYLRDTAALSPPKATVSDTCEEVEPSLLEILPKSS*
*ERTPLPLCSSQAQMDYRRLQPSCLGTMPLSVCPPMAESGSCCTTHIANHSYLPLSYWQQP**

Extracellular domain = bold

Signal peptide

HA-tag

Transmembrane

RWQFP

ICD

Section G: Human SH2B3 (LNK) cDNA and protein sequence

Human *SH2B3* (LNK) cDNA sequence:

atggattacaaggatgacgacgataagaacgggcctgccctgcagccctcctcgccctcttccgcgccctcagcctccccggcggcggcccc
gcggggctggagcgagttctgtgagttgcacgccgtagcggcggcccgggagctggcccgccagtactggctgttcgcccgggagcatccg
cagcacgcgccgctgcgcgccgagctggtgtcgctgcagttcaccgacctcttccagcgctacttctgccgcgaggtgcgcgacggacgggc
gccgggccgcgactaccgggacacaggccgtgggcccccagccaaggccgaggcgtccccggagccaggccccggccccgccgcccct
ggcctgcccaaggcccgcagctctgaggagctggccccgccgcggccgcccgggccctgctccttccagcactttcgccgcagcctccgcc
acatcttccgccgccgctcggccggggagctgccagcggcccacaccgctgccgcccccgggacccccggagaggctgctgagaccccc
gcccggcctggcctggccaagaagttcctgccctggagcctggcccgggagccgccacccgaggcgctgaaggaggcggtgctgcgctac
agcctggccgacgaggcctccatggacagcggggcacgctggcagcgcgggaggctggcgctgcgccgggccccgggccccgatggcc
ccgaccgcgtgctggagctcttcgacccacccaagagttcaaggcccaagctacaagcagcttgctccagcatccaggaggtccggtggtgc
acacggcttgagatgcctgacaacctttacacctttgtgctgaaggtgaaggaccggacagacatcatctttgaggtgggagacgagcagcagc
tgaattcatggatggctgagctctcggagtgcacaggccgagggctggagagcacagaagcagagatgcatattccctcagccctagagccta
gcacgtccagctccccaaggggcagcacagattcccttaaccaaggtgcttctcctgggggggctgctggacccggcctgccagaagacggac
catttcctgtcctgctacccctggttccacggccccatctccagagtgaaagcagctcagctggttcagctgcagggccctgatgctcatggagt
gttcctggtgcggcagagcgagacgcggcgtggggaatacgtgctcactttcaactttcaggggatagccaagcacctgcgcctgtcgctgac
agagcggggccagtgccgtgtgcagcacctccactttccctcggtcgtggacatgctccaccacttccagcgctcgcccatcccactcgagtgc
ggcgccgcctgtgatgtccggctctccagctacgtggtagtcgtctcccaaccaccaggttcctgcaacacggtcctcttcccttttctcccttcctc
actgggattcagagtcccttcctcactggggttcagagttgggccttccccaccttagttcttctggctgtccccgggggctcagcccagagggtc
tcccagggcgatcctcacccccgagcagatcttccacctggtgccttcgcccgaagaactggccaacagcctgcagcacctggagcatgag
cctgtgaatcgagcccgggactcggactacgaaatggactcatcctcccggagccacctgcgggccatagacaatcagtacacacctctctga

Human LNK amino acid sequence:

MDYKDDDDKNGPALQPSSPSSAPSASPAAAPRGWSEFCELHAVAAARELARQYWLFARE
HPQHAPLRAELVSLQFTDLFQRYFCREVRDGRAPGRDYRDTGRGPPAKAEASPEPGPGPAA
PGLPKARSSEELAPPRPPGPCSFQHFRRSLRHIFRRRSAGELPAAHTAAAPGTPGEAAETPAR
PGLAKKFLPWSLAREPPPEALKEAVLRYSLADEASMDSGARWQRGRLALRRAPGPDGPDR
VLELFDPPKSSRPKLQAACSSIQEVRWCTRLEMPDNLYTFVLKVKDRTDIIFEVGDEQQLNS
WMAELSECTGRGLESTEAEMHIPSALEPSTSSSPRGSTDSLNQGASPGGLLDPACQKTDHFL
SCYPWFHGPISRVKAAQLVQLQGPDAHGVFLVRQSETRRGEYVLTFNFQGIAKHLRLSLTE
RGQCRVQHLHFPSVVDMLHHFQRSPIPLECGAACDVRLSSYVVVVSQPPGSCNTVLFPFSL
PHWDSESLPHWGSELGLPHLSSSGCPRGLSPEGLPGRSSPPEQIFHLVPSPEELANSLQHLEH
EPVNRARDSDYEMDSSSRSHLRAIDNQYTPL*

FLAG-tag

PH domain

SH2

Section H: Human JAK2 JH2-JH1 cDNA and protein sequence

Human JAK2 JH2-JH1 cDNA sequence:

ATGCACCATCATCATCACCACGAAAATCTGTACTTCCAAGGCCACAAAATCAGAAATG
AAGATTTGATATTTAATGAAAGCCTTGGCCAAGGCACTTTTACAAAGATTTTTAAAGGC
GTACGGAGAGAAGTAGGAGACTACGGTCAACTGCATGAAACAGAAGTTCTTTTAAAAG
TTCTGGATAAAGCACACAGAAACTATTCAGAGTCTTTCTTTGAAGCAGCAAGTATGAT
GAGCAAGCTTTCTCACAAGCATTTGGTTTTAAATTATGGAGTATGTGTCTGTGGAGACG
AGAATATTCTGGTTCAGGAGTTTGTAAAATTTGGATCACTAGATACATATCTGAAAAA
GAATAAAAATTGTATAAATATATTATGGAAACTTGAAGTTGCTAAACAGTTGGCATGG
GCCATGCATTTTCTAGAAGAAAACACCCTTATTCATGGGAATGTATGTGCCAAAAATAT
TCTGCTTATCAGAGAAGAAGACAGGAAGACAGGAAACCCTCCTTTCATCAAACTTAGT
GATCCTGGCATTAGTATTACAGTTTTGCCAAAGGACATTCTTCAGGAGAGAATACCATG
GGTACCACCTGAATGCATTGAAAATCCTAAAAATTTAAATTTGGCAACAGACAAATGG
AGTTTTGGTACAACTCTGTGGGAAATCTGCAGTGGAGGAGATAAACCTCTAAGTGCTC
TGGATTCTCAAAGAAAGCTACAATTTTATGAAGATAGGCATCAGCTTCCTGCACCAAA
GTGGGCAGAATTAGCAAACCTTATAAATAATTGTATGGATTATGAACCAGATTTCAGG
CCTTCTTTCAGAGCCATCATACGAGATCTTAACAGTTTGTTTACTCCAGATTATGAACT
ATTAACAGAAAATGACATGTTACCAAATATGAGGATAGGTGCCCTAGGGTTTTCTGGT
GCCTTTGAAGACCGGGATCCTACACAGTTTGAAGAGAGACATTTGAAATTTCTACAGC
AACTTGGCAAGGGTAATTTTGGGAGTGTGGAGATGTGCCGGTATGACCCTCTACAGGA
CAACACTGGGGAGGTGGTCGCTGTAAAAAAGCTTCAGCATAGTACTGAAGAGCACCTA
AGAGACTTTGAAAGGGAAATTGAAATCCTGAAATCCCTACAGCATGACAACATTGTAA
AGTACAAGGGAGTGTGCTACAGTGCTGGTCGGCGTAATCTAAAGTTAATTATGGAATA
TTTACCATATGGAAGTTTACGAGATTATCTTCAAAAACATAAAGAACGGATAGATCAC
ATAAAACTTCTGCAGTACACATCTCAGATATGCAAGGGTATGGAGTATCTTGGTACAA
AAAGGTATATCCACAGGGATCTGGCAACGAGAAATATATTGGTGGAGAACGAGAACA
GAGTTAAAATTGGAGATTTTGGGTTAACCAAAGTCTTGCCACAAGACAAAGAATACTA
TAAAGTAAAAGAACCTGGTGAAAGTCCCATATTCTGGTATGCTCCAGAATCACTGACA
GAGAGCAAGTTTTCTGTGGCCTCAGATGTTTGGAGCTTTGGAGTGGTTCTGTATGAACT
TTTCACATACATTGAGAAGAGTAAAAGTCCACCAGCGGAATTTATGCGTATGATTGGC
AATGACAAACAAGGACAGATGATCGTGTTCCATTTGATAGAACTTTTGAAGAATAATG
GAAGATTACCAAGACCAGATGGATGCCCAGATGAGATCTATATGATCATGACAGAATG

CTGGAACAATAATGTAAATCAACGCCCCTCCTTTAGGGATCTAGCTCTTCGAGTGGATC
AAATAAGGGATAACATGGCTGGATGA

Human JAK2 JH2-JH1 protein sequence:

M**HHHHHH**ENLYFQGHKIRNEDLIFNESLGQGTFTKIFKGVRREVGDYGQLHETEVLLKVL
DKAHRNYSESFFEAASMMSKLSHKHLVLNYGVCVCGDENILVQEFVKFGSLDTYLKKNK
NCINILWKLEVAKQLAWAMHFLEENTLIHGNVCAKNILLIREEDRKTGNPPFIKLSDPGISIT
VLPKDILQERIPWVPPECIENPKNLNLATDKWSFGTTLWEICSGGDKPLSALDSQRKLQFYE
DRHQLPAPKWAELANLINNCMDYEPDFRPSFRAIIRDLNSLFTPDYELLTENDMLPNMRIG
ALGFSGAFEDRDPTQFEERHLKFLQQLGKGNFGSVEMCRYDPLQDNTGEVVAVKKLQHST
EEHLRDFEREIEILKSLQHDNIVKYKGVCYSAGRRNLKLIMEYLPYGSLRDYLQKHKERIDH
IKLLQYTSQICKGMEYLGTKRYIHRDLATRNILVENENRVKIGDFGLTKVLPQDKEYYKVK
EPGESPIFWYAPESLTESKFSVASDVWSFGVVLYELFTYIEKSKSPPAEFMRMIGNDKQGQ
MIVFHLIELLKNNGRLPRPDGCPDEIYMIMTECWNNNVNQRPSFRDLALRVDQIRDNMAG*

6x Histidine

Tobacco etch virus (TEV) protease cleavage site

Publications

Peer-reviewed paper

- Novel Drivers and Modifiers of MPL-dependent Oncogenic Transformation Identified by Deep Mutational Scanning: https://ashpublications.org/blood/article-lookup/doi/10.1182/blood.2019002561

Review article

- The Growth Hormone Receptor: Mechanism of Receptor Activation, Cell Signaling, and Physiological Aspects: https://www.frontiersin.org/articles/10.3389/fendo.2018.00035/full